U.S. DEPARTMENT OF THE INTERIOR

GEOLOGICAL SURVEY

Seismic structure and stratigraphy of the New England Continental Slope and the evidence for slope instability

Dennis W. O'Leary[1]

Open-File Report 86-118

Prepared in cooperation with
U.S. MINERALS MANAGEMENT SERVICE
(formerly U.S. Bureau of Land Management)
under Memoranda of Understanding
AA551-MU8-24 and AA551-MU9-4

[1]Woods Hole, MA 02543

1986

CONTENTS

ILLUSTRATIONS

ILLUSTRATIONS

ILLUSTRATIONS

ILLUSTRATIONS

TABLE

MAPS

INTRODUCTION

This report culminates a seismic-reflection survey that was designed to study mass-movement phenomena of the sea floor and to determine to what extent and in what ways slope instability is a potential hazard in the process of petroleum exploration and exploitation on the Continental Slope. This objective rests on the assumption that mass movements and surfaces liable to move can be confidently identified in seismic profiles. In fact, most of what is known about submarine mass movement on the U.S. Atlantic Continental Slope is derived from "case history" seismic-profile interpretations. But because most seismic surveys are not designed to study mass wasting in a regional context and because confirmatory observations rarely accompany such studies, most interpretations of mass movement based on seismic-profile data remain ambiguous. Although there is abundant evidence that mass movement has occurred - and can occur - on the Atlantic Continental Slope (e.g., the Grand Banks event of 1929), little is known about the structural extent, frequency of occurrence, and causes of such submarine mass movements..

Two aspects of the problem of slope instability are the subject of this report: identification of mass-movement features, and evaluation of the potential for mass movement. A brief overview of the present state of knowledge of mass movement along the U.S. continental margin, as derived from seismic profile data, is given as the point of departure for the investigation of these topics. A working classification of mass-movement features is then presented to help the reader comprehend the descriptions and interpretations drawn from the seismic-profile analysis. The seismic-profile analysis of mass movement is limited here to describing the profile characteristics of individual features identified in each seismic line. The geological setting of the features is established on the basis of regional stratigraphy, form, and structure interpreted from the seismic-profile data and from other data sources.

The mass-movement features are depicted on the fold-out maps included with this report. It is emphasized that the location of boundaries of mass-movement features between profile lines is inferential and is guided entirely by the configuration of the base map contours. Technical aspects of the data that bear on interpretation are treated in the appendix, which is presented to inform readers of the particular limitations of the seismic-profile analysis and especially as a caveat to uncritical acceptance of my interpretations.

Despite the intentions of the survey, the study provides very limited data on relative ages and on genesis; questions concerning present instability, magnitude, and potential for failure can only be speculated upon at this point. The speculations discussed in this report are intended as points of departure for further work needed to adequately evaluate the potential for mass movement.

The earliest U.S. Geological Survey (USGS)-Bureau of Land Management (BLM) survey made to detect mass-movement features was R/V FAY cruise 003 in 1975. The aim was to use seismic-reflection techniques to locate shallow and intermediate depth faults on Georges Bank and to locate potentially unstable surficial sediment. Accordingly, 2,900 km of minisparker and airgun-generated profiles were gathered, spaced 25 km apart perpendicular to the trend of the slope and extended as far seaward as the 2,000-m isobath (fig. 1). These

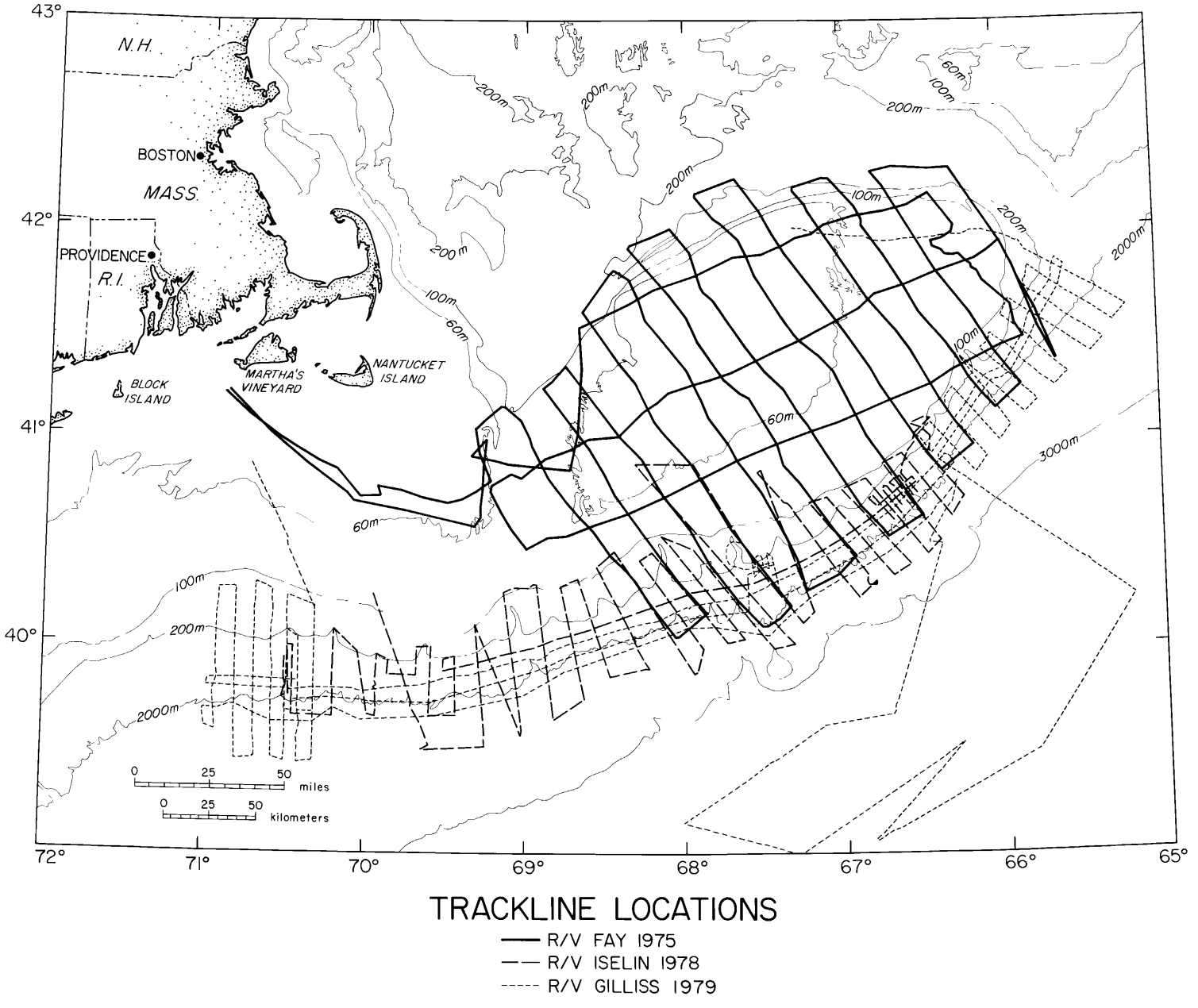

Figure 1. **Trackline map of cruises cited in this report: FAY 003, ISELIN 7-78-2, GILLISS 7903-03.**

profiles provided useful information on structure and stratigraphy (within approximately 350 m below the shelf surface) and their relation to sea-floor morphology on the bank (Lewis and others, 1980). Some of the shelf data from this survey are alluded to in this report; good quality data were not acquired from the slope.

Following this investigation, and in light of the anticipated resource potential of the Continental Slope, it became clear that more detailed surveys directed at the slope were needed. Memoranda of Understanding AA551-MU8-24 and AA551-MU9-4 between USGS and BLM specified the direction and objectives of the subsequent studies. The objectives included identification and mapping of areas of slumping and potential slump hazards on the Continental Slope from the shelf edge (100-200-m water depth) down to the upper rise (3,000 m). The tasks of investigation included the following:

1. To identify and study the effects of processes and mechanisms contributing to sediment instability in offshore lease areas which may lead to the inception of slumping and sliding;

2. To identify, date, and map areas of slumping and potential slump hazards in lease areas and farther offshore in future sale areas;

3. To determine the magnitude and potential of geologic hazards in sale 52 lease areas through historical data review and field surveys.

To fulfill these aims 5,962 km of seismic profile were obtained along the Continental Slope, outer shelf, and upper rise between 65°30'W. and 71°W. by R/V ISELIN cruise 7-78-2 (1978) and R/V GILLISS cruise 7903-03 (1979) (fig. 1).

High-resolution seismic data from ISELIN CI7-78-2 and GILLISS GS-7903-03 are available from the National Geophysical Data Center, Boulder, Colorado (Bailey and Aaron, 1982a,b). The information presented in this report is part of the marine environmental-data acquisition and analysis studies required by the U.S. Bureau of Land Management to implement the Outer Continental Shelf (OCS) Lands Act.

A REVIEW OF MASS-MOVEMENT PHENOMENA INTERPRETED FROM SEISMIC PROFILE DATA FROM THE ATLANTIC CONTINENTAL MARGIN

One of the largest mass movements conjectured to have occurred in the New England region is located along the the Continental Rise off Block Canyon, between 71°00'W. and 71°15'W. (Uchupi, 1967). Uchupi (1967) concluded that here the rise was built of sediment that had been displaced from the adjacent Continental Slope as one or more slumped blocks that possibly extend as far as 30 km beyond the base of the slope. Uchupi's data, unevenly spaced sparker profiles concentrated between 1,000 and 2,400 m depths, show that reflectors of the Continental Rise unconformably onlap the slope; downdip they thin and become progressively more regular. Near the slope, subsurface reflectors dip toward the slope, a feature that Uchupi interpreted as rotated bedding due to slumping. This interpretation was supported by Emery and others (1970) who cited reverse dip as a criterion of sliding, along with faults, hummocks, hyperbolic reflections, and "irregular masses."

MacIlvaine and Ross (1979), on the basis of superior data (10 in^3 airgun (18-300 Hz) and 3.5-kHz records spaced 2 to 5 km on strike, 10 km on dip), also concluded that the bulk of the upper rise sediments west of Alvin Canyon (70°30'W.) is derived from the adjacent slope by mass movement. They identified in the continental rise not only tilted coherent sequences, as Uchupi had observed, but internally coherent blocks ranging in width from 100 m to more than 2 km, apparently derived from directly upslope of their present positions. The 3.5-kHz records showed expanses of surface 1 to 2 km wide between the blocks, characterized by hummocks and abundant hyperbolic echo traces.

Uchupi (1967) had also observed that the sea floor shown in his records forms steep-sided depressions and swales - features which suggested to him that blocks with essentially conformable, undisturbed bedding had been emplaced by "preferential movements of the upper parts of the slump mass toward the south" or, perhaps, that smaller blocks had been superimposed on a larger slumped mass. However, this evidence for block emplacement is strictly topographic; Uchupi described no internal structural discordance except for noting that below 1,400 m, in lines parallel to the slope, the "lower sections" of the inferred slump masses are "chaotic."

Uchupi (1967) further surmised that the broad reentrant between Block and Atlantis Canyons (approximately 71°W., fig. 1) was probably formed by displacement of outer shelf and upper-slope strata, which gave way after the subjacent lower-slope sediments had slumped onto the rise. As evidence, he could cite only "highly disturbed" layering in the upper slope and outer shelf edge.

A variety of slope source areas was cited by MacIlvaine and Ross (1979) for the inferred allochthonous rise sediments near Alvin Canyon. Particularly important are scarps 100 to 200-m high sloping approximately 12° seaward in the 1,000-m depth zone where the slope steepens from about 1.4° to 7.6°. These "detachment scars" represent sites of "large-scale slumping" where, apparently, the "entire Pleistocene section as well as an undetermined amount of Tertiary sediment" has been subject to failure (MacIlvaine and Ross, 1979). Of related origin are numerous steep-sided gullies, tens of meters in relief, that extend downslope from above 600 m depth, their floors mantled by hummocky, acoustically transparent sediment. They coalesce into broad surfaces likewise covered with debris. MacIlvaine and Ross (1979) recorded similar features, smaller in scale, on the steep lower slope where "small-scale slumping" (one to several meters thick, tens of meters across) is thought to have occurred.

Much farther east, from about 69°30'W. to 64°00'W., Uchupi and others (1977) obtained single-channel seismic profiles (airgun generated, filtered between 15-60 Hz, and recorded at a ship speed of 7.5-8.3 km/hr) transverse to the slope, spaced about 25 km apart. They cited at least five slump structures recorded in a single profile across the base of the slope, at about 2,250-m water depth, just east of Nygren Canyon (about 66°30'W., fig. 1) as the only clear indication of slumping in this region. They concluded that the "general scarcity of such structures suggests that the fabric of the upper rise south of Georges Bank is caused primarily by turbidity-current deposition and erosion rather than slumping and gravitational sliding" (p. 1490).

Debris of mass movement has been widely identified on the Continental Rise south of New England. In the vicinity of Hudson Canyon off New York, the entire Tertiary section of the Continental Rise, a mass of sediment more than 3 km thick, several kilometers wide (downslope), and of undetermined lateral extent, is thought to be slump derived (Emery and others, 1970). In places, such as the lower slope and upper rise in the vicinity of Baltimore and Wilmington Canyons, this slumped sediment is reported to have undergone subsequent local displacement (Kelling and Stanley, 1970). Wedge-shaped masses as much as 400 m thick, 8 km long (parallel to the slope), and 10 to 12 km across (downslope) are involved. Because the masses are separated internally by curved surfaces, they are inferred by Kelling and Stanley (1970) to be slump blocks. The slumped masses include slightly imbricated, contorted reflectors.

Mass-movement features on the Continental Slope that are not derived from previously displaced sediment are more widespread and varied. Small-scale primary slump deposits are ubiquitous on the slope south of Hudson Canyon, mostly at depths below 800 m (Knebel and Carson, 1979). They involve the upper 10 to 90 m of sediment, extend downslope from 2 to 8 km, and range in form from thin, homogeneous layers to relatively large, topographically prominent slabs. Mass-movement features of similar variety (thin slides and translated and rotated blocks) in Pleistocene sediment are reported by McGregor and Bennett (1979) on the slope and rise farther south, between Wilmington and Lindenkohl Canyons. Knebel and Carson (1979) infer mass movement on the basis of sea-floor truncation of shallow subbottom reflectors, abrupt changes in slope declivity and/or in bottom roughness, the presence of irregular or discordant internal reflectors, and discordant contacts along a shallow "fairly continuous" basal contact. McGregor and Bennett (1979) identify slides by hummocky topography associated with upslope scarps; translated blocks are identified by broken and rotated internal reflectors and, locally, upturned toes.

Slide debris is reported by Embley (1980) in the uppermost 50 m of sediment on the slope just south of Baltimore Canyon. Piston cores reveal the fragmental texture of the displaced sediment (Embley and Jacobi, 1977). The debris appears to originate from numerous small slides close to the shelf break and is shown in 3.5-kHz profiles as an acoustically transparent, hyperbolae-capped layer offlapping Continental Rise sediments at least as far seaward as 3,100-m water depth.

Blocks that have slid out of place on the Continental Slope are harder to identify than slide debris, especially if internal disruptive features are not visible. McGregor (1977) and McGregor and Bennett (1977) discuss such a block on the slope northeast of Wilmington Canyon. The block, 10 km across and 50 to 300 m thick, is identified mainly on the basis of a strong reflector which is interpreted as both a slip plane and a Pliocene unconformity dipping 7^{o} downslope. This surface cuts out underlying reflectors down the dip, but is indistinguishable from bedding planes along strike. The block itself is stratified Pleistocene sediment; its upslope termination is identified by a "jumbled, irregular surface" and by stratigraphic thinning and a change in slope angle from about 4^{o} on the block to as much as 14^{o} on the scar surface immediately upslope. Despite excellent seismic coverage, the other margins of the block are indistinct. In this case, as in that of Uchupi (1967), the inference of block displacement is made on the basis of morphological features; internal structure ascribable to mass movement is not demonstrable.

The causes and mechanisms of the mass movements that have occurred along the Continental Slope are uncertain. The most widely cited general cause is earthquake shock (Uchupi, 1967; Moore and others, 1976; Embley and Jacobi, 1977; McGregor, 1977; Almagor and Wiseman, 1978), mainly because it is the only cause for which there is historical documentation (e.g., the 1923 slide at Sagami Wan, Japan (Shepard, 1933) and the Grand Banks slump of 1929 (Heezen and Drake, 1964)). Heezen and Drake (1964) established the importance of the earthquake mechanism by concluding, on the basis of a single seismic profile, that a huge slump, more than 400 m deep and 110 km long, was generated by the 1929 Grand Banks earthquake. (The famous turbidity currents were coeval but apparently generated separately). This seemed to be a neat case in point, but on the basis of subsequent seismic records, Moore (1978) argued that the great slump block is actually a complex of smaller features of diverse origin, only some of which were generated by the 1929 earthquake. Moore (1978) points out that different processes working together and successively can so modify structure and morphology that clear-cut genetic mechanisms may not ordinarily be discernable. And this remains the big problem in unravelling the causes of submarine mass movement: identifying the relative contributions of primary and secondary causes and modifying factors. Thus, although earthquakes are viewed as one of the more important triggering mechanisms, numerous other factors probably contribute to slope instability and act as triggering mechanisms also.

A widely held opinion is that upper Continental Slope instability was brought about by rapid sedimentation during Pleistocene low sea-level stands and that mass movement was triggered by depositional oversteepening (Embley and Jacobi, 1977; MacIlvaine and Ross, 1979), overpressurization (Uchupi, 1967), or increased wave-energy input (McGregor, 1977). These factors may have been important for some slides, but evidence is not strong. For example, Knebel and Carson (1979) found no correlation between slope steepness and slumping in the Mid-Atlantic region. MacIlvaine and Ross (1979) indicate that in the New England region some mass movements involve Tertiary as well as Pleistocene sediment. Geotechnical study of cores obtained from the U.S. North and Mid-Atlantic Slope rarely indicates surface instability (Kelling and Stanley, 1970; MacIlvaine and Ross, 1979). One could argue that this is not to be unexpected because the unstable surficial sediment would already have been removed by sliding and that widely spaced core samples are unlikely to hit on what little unstable sediment might remain. On the other hand, Kelling and Stanley (1976) point out that measured values of shear strength on slope sediments commonly indicate a highly stable condition, even in areas where recent mass movement has apparently occurred, and that factors other than inherent cohesion must be involved to cause failure.

For some mass-movement features, such as those on the New England Slope which occur deeper than about 1,000-m water depth, there is no appeal to sedimentation processes which have occurred at or near the shelf edge, or to former very high sedimentation rates. MacIlvaine and Ross (1979) cite a Pleistocene sedimentation rate of only 25 cm/10^3yrs for the U.S. North Atlantic Continental Slope.

Slope oversteepening by current erosion along the lower Continental Slope is a mechanism that might possibly account for mass movement where oversteepening of the upper slope by advanced sedimentation seems out of the question (Embley and Jacobi, 1977). This idea is not enthusiastically

entertained for the U.S. Mid-Atlantic region by McGregor and Bennett (1977) because no erosional scours or channels attributable to bottom currents have been recognized in association with slides. Furthermore, if erosionally oversteepened slopes were destroyed by consequent mass movement (W. P. Dillon, pers. commun., 1984), then no evidence for this mechanism could be adduced in any case. MacIlvaine and Ross (1979) performed experiments on pristine bottom samples from the New England Slope and found that the surface is extremely resistant to current erosion, in part because of biological activity. They concluded that if failure should occur, it would be below the depth of their core penetration (4 to 6 m).

A third means of slope oversteepening is tectonic uplift and/or depression along the Continental Slope (Almagor and Wiseman, 1978; Moore, 1978), but no leveling data exist for the Atlantic Continental Slope, so tectonic steepening remains an undefended hypothesis in this region.

Two other failure mechanisms of interest are overpressurization due to gas generation (Knebel and Carson, 1979; Summerhayes and others, 1979) and ground-water sapping (MacIlvaine and Ross, 1979). Methane buildup in surficial sediment by organic decomposition is referred to by Knebel and Carson (1979), who cite very high methane content in their core samples; physical changes related to a deep clathrate/gas-solution boundary are proposed by Summerhayes and others (1979), but without direct evidence. MacIlvaine and Ross (1979) speculate that large-scale slumping on the New England Slope may have been enhanced during the Pleistocene epoch by excess pore-fluid pressure built up by discharge along aquifers that crop out near the upper/lower slope transition zone. Presumably the updip ends of the aquifers on the exposed Continental Shelf would have received heavy glacial meltwater infiltration.

Most geologists agree that mass-movement features exposed on the Continental Slope are of Pleistocene age. McGregor (1977) and Knebel and Carson (1979) suggest that post-Pleistocene activity may be demonstrated. In some instances radiocarbon and paleontological data support a late-Pleistocene age (McGregor and Bennett, 1977; Summerhayes and others, 1979) but in most cases a circumstantial argument is presented. Thus, Kelling and Stanley (1970), Embley and Jacobi (1977), and Embley (1980) refer to a late-Pleistocene age because in places a veneer of undisturbed sediment is seen draped on slump features. Conversely, in arguing for more recent activity, McGregor and Bennett (1979) cite the lack of sediment accumulation on the slide scar and on the irregular surface at the head of the Wilmington Canyon slide. Probably the most cogent argument against post-Wisconsinan or even late-Wisconsinan failure is presented by MacIlvaine and Ross (1979). They point out that the abundance of cobbles and pebbles of crystalline rock on the New England Continental Rise means there could not have been widespread mass movement there since the period of late Wisconsinan ice rafting.

CONCEPTS OF SUBMARINE MASS MOVEMENT

Submarine and subaerial mass-movement phenomena are referred to by a common terminology. Terms such as slump, slide, debris flow, were originally defined with reference to subaerial features; therefore, application of the terms in marine geology should be based on the same morphological and structural criteria by which they are applied on land. Proper definition of

mass-movement criteria should provide us with a clear idea of what we are out to look for and what exactly we expect to see in order to recognize, say, a slump. The task of recognition would be easy if seismic profiles provided the means for unambiguous identification and if terms had been used consistently in published studies, but this is not the case.

Some order must be brought to the analysis of submarine mass movement, and some conceptual standard must be set against which the validity of identifications on seismic profiles can be judged. For these reasons, I present a classification and description of the various kinds of mass-movement features, suitable for field identification (i.e., visually, in gross aspect) and therefore for identification in seismic profiles. The classification (fig. 2) is designed for this study and is not meant to be universal. The basic concept for this classification is derived from Varnes (1978).

Mass movement

Mass movement is the bulk displacement of a distinctly bounded mass of rock or unconsolidated sediment exposed on a slope or under a dipping unit, down the slope or dip, under the influence of gravity. Although slope depression is the net effect of superficial movement, actual erosion (physical or chemical removal of material effected by the work of a competent medium) does not occur or occurs only incidentally. The collective processes of superficial mass movement in a region over a geologically significant length of time is called mass wasting.

Slides

A slide is a coherent to moderately disaggregated mass of material that moves along one or more surfaces or relatively thin zones of shear deformation that are visible or may reasonably be inferred (Varnes, 1978). Rotational slides or slumps (fig. 3) occur if the displacive movement is rotary (along a concave upward slip surface and around an axis parallel to the strike of the initial slope); if the movement is translational (down an essentially planar surface parallel to the initial slope) a planar slide is indicated (fig. 4). This geometrical distinction is not always clear, particularly where a curved slip surface flattens at depth or a succession of slumps bottoms along a plane of shear resistance (fig. 4, A). Because identification must be made on one or a few seismic profiles, the diagnostic geometry may not be visible. Despite the attribution of a distinctive descriptive term, it is important to appreciate that different kinds of slide mechanisms may contribute to a feature which seems to exemplify only one.

Because slumps involve rotational movement, the component of downslope transport is relatively small and gravitational stability is achieved by in situ slope depression. Thus, slumps are typically characterized in longitudinal profile by a depressed head and an elevated toe (fig. 3). The upslope termination of the depressed surface is defined by at least one more or less distinct scarp from the foot of which the curved slip surface descends beneath the slump. The slip surface is acoustically recorded either as a reflector or as a transparent zone across which stratigraphic reflectors are truncated and/or displaced. If internal structure is preserved and the original surface is largely intact a block slump is indicated (fig. 3, A); if internal deformation is considerable and the depressed surface is concave a

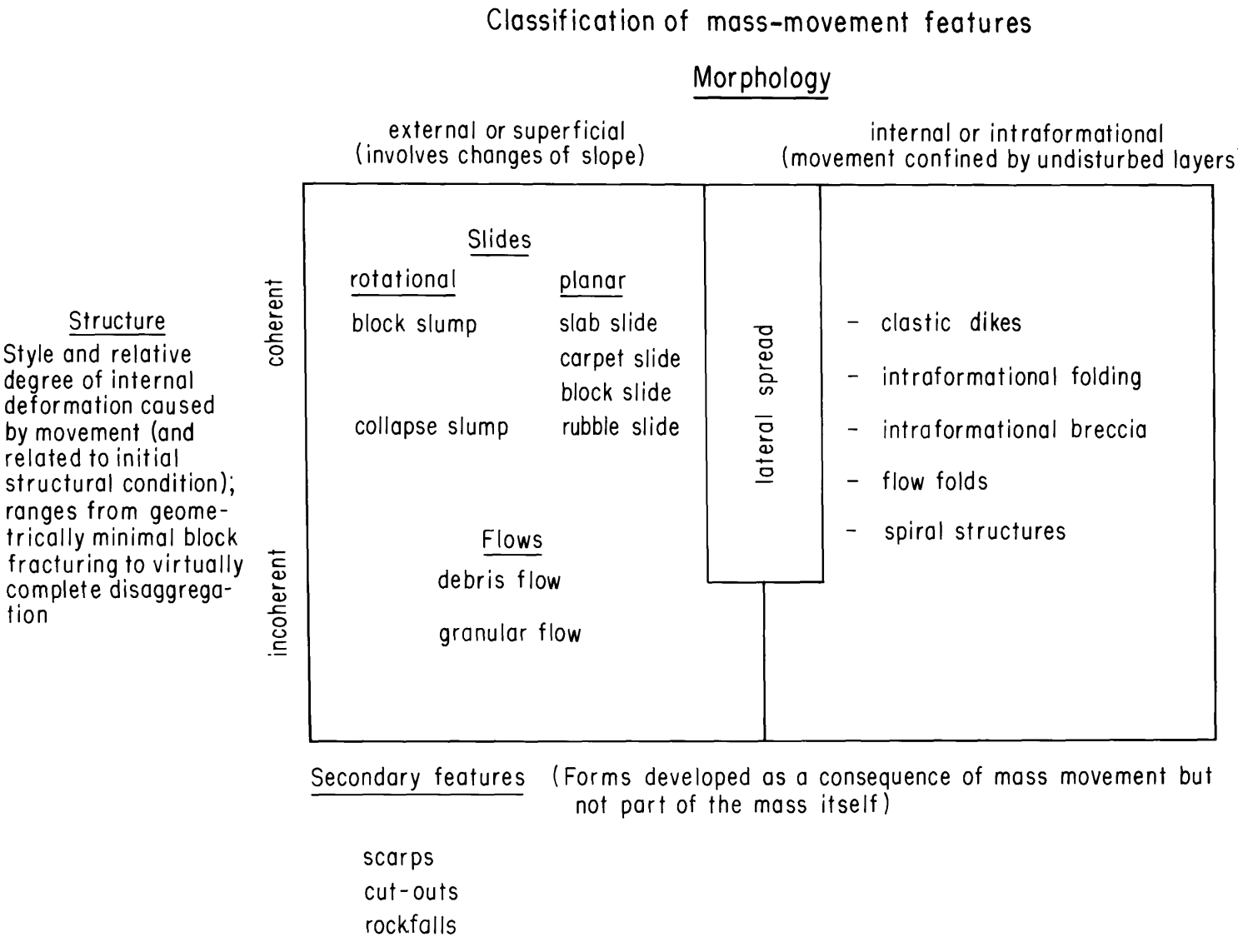

Figure 2. Classification of mass-movement features.

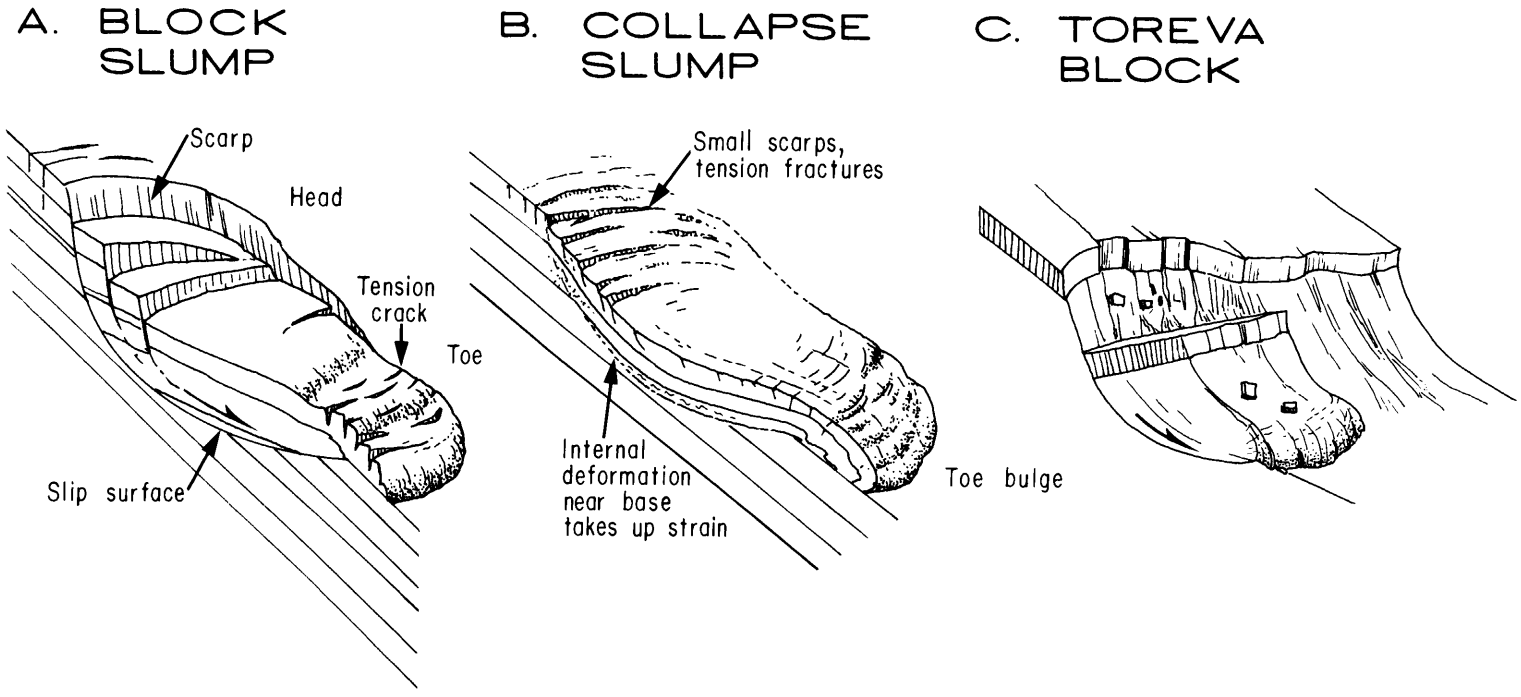

Figure 3. Types of rotational slides.

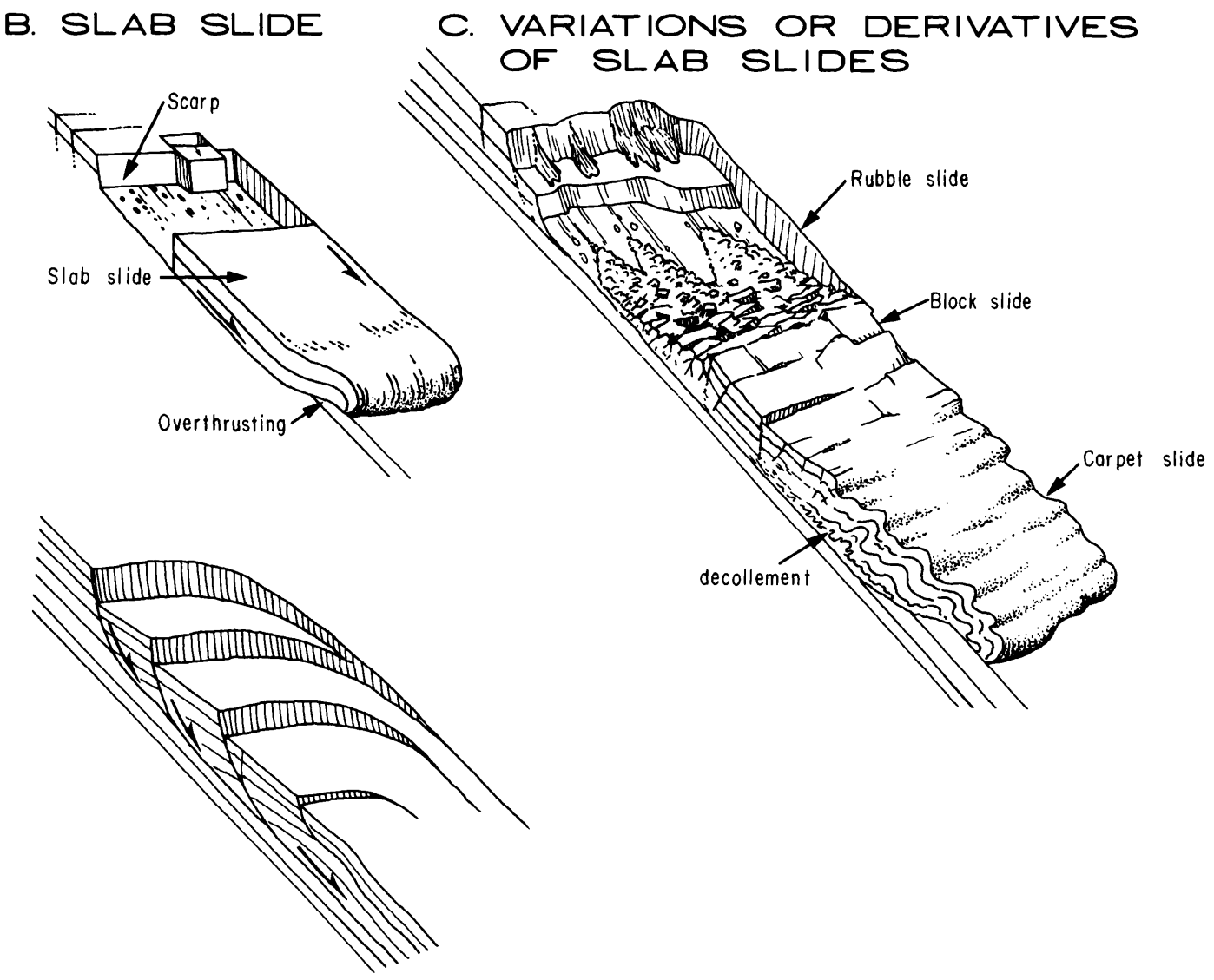

Figure 4. Types of planar slides; 4C illustrates the styles of deformation that may be produced by sliding, not necessarily in the relationships shown.

collapse slump is indicated (fig. 3, B). Internal reflectors in block slumps dip less steeply than do adjacent unslumped reflectors. In some cases (Toreva blocks) the dip direction may be reversed (fig. 3, C). Collapse slumps tend to have pronounced toe bulges. In fact, the toe bulge may constitute the bulk of the slide and take on some of the appearance of a debris flow. The toe bulge of slumps is at the least marked by arching of beds; where collapse has occurred it may display concentric mounding or irregular lobate forms and overthrusting (fig. 3, A, B). Because the headwall scarp represents an unstable free face it is rarely intact except in recent or active slumps. It tends to be reduced by subsequent processes, either additional slumping or some other type of mass movement, or erosion. If the scarp is underlain by cohesive, resistant material, subsequent failure, en masse, may result in Toreva blocks or rockfalls.

The morpho-structural criteria for slumps are clearly seen only in longitudinal (downslope) profiles. In transverse section a slump may not show the characteristic concave slip surface, particularly if the rotated mass is roughly a cylindrical section. If a transverse seismic profile crosses the head or the toe section, mass movement may be difficult to recognize or interpret.

In planar slides the slip surface is a plane across which there is a critical lack of shear strength. This is commonly a bedding plane although low-angle fault planes, extended joint zones, or unconformities may serve (Varnes, 1978). The detached mass separates along a fracture which, because it is a surface of tension, tends to dip at a high angle to the slip plane. The detached mass thus has the form of a parallelepiped. If this form is clearly tabular a slab slide is indicated (fig. 4, B). The slab itself may have existed as a geometric entity only at the time of detachment, however; depending on the nature of the detached mass, downslope transport may cause superficial rumpling or folding, or progressive fragmentation to occur such that first a block slide and then a rubble slide develops (fig. 4, C). Sliding leaves a gap between the detachment scarp and the body of the slide; the gap is accounted for by folding or imbrication in the slide or by the piling up of rubble at the slide toe.

In coherent slab or carpet slides the key seismic features are: (1) a detachment scarp which truncates reflectors above an unbroken conformable horizon which represents the slide plane; (2) structural discordance within the detached mass above a horizon identified as a slide plane, the diagnostic features of which include decollement folding, faulting, and/or acoustically blurred, patchy or transparent zones, especially near the base; (3) relatively high relief on the slide surface caused by disruption. Surface-relief features range from evident block structure and raised folds to small disrupted features represented by irregular hyperbolic echo traces; (4) an elevated toe consisting of relatively incoherent material onlapping autochthonous layers. I emphasize that no single seismic profile is likely to display all of these features, or to show them with unarguable clarity.

Rubble slides are probably the most common type of planar slide. Jacobi (1976) describes an "idealized" slide of this type. It entails, going downslope from the detachment zone, a zone of hummocky slide rubble which grades into a zone of less rugged relief (a blocky terrain, as depicted in fig. 4, C), which grades into a zone of debris flow (fig. 5, A). The slide

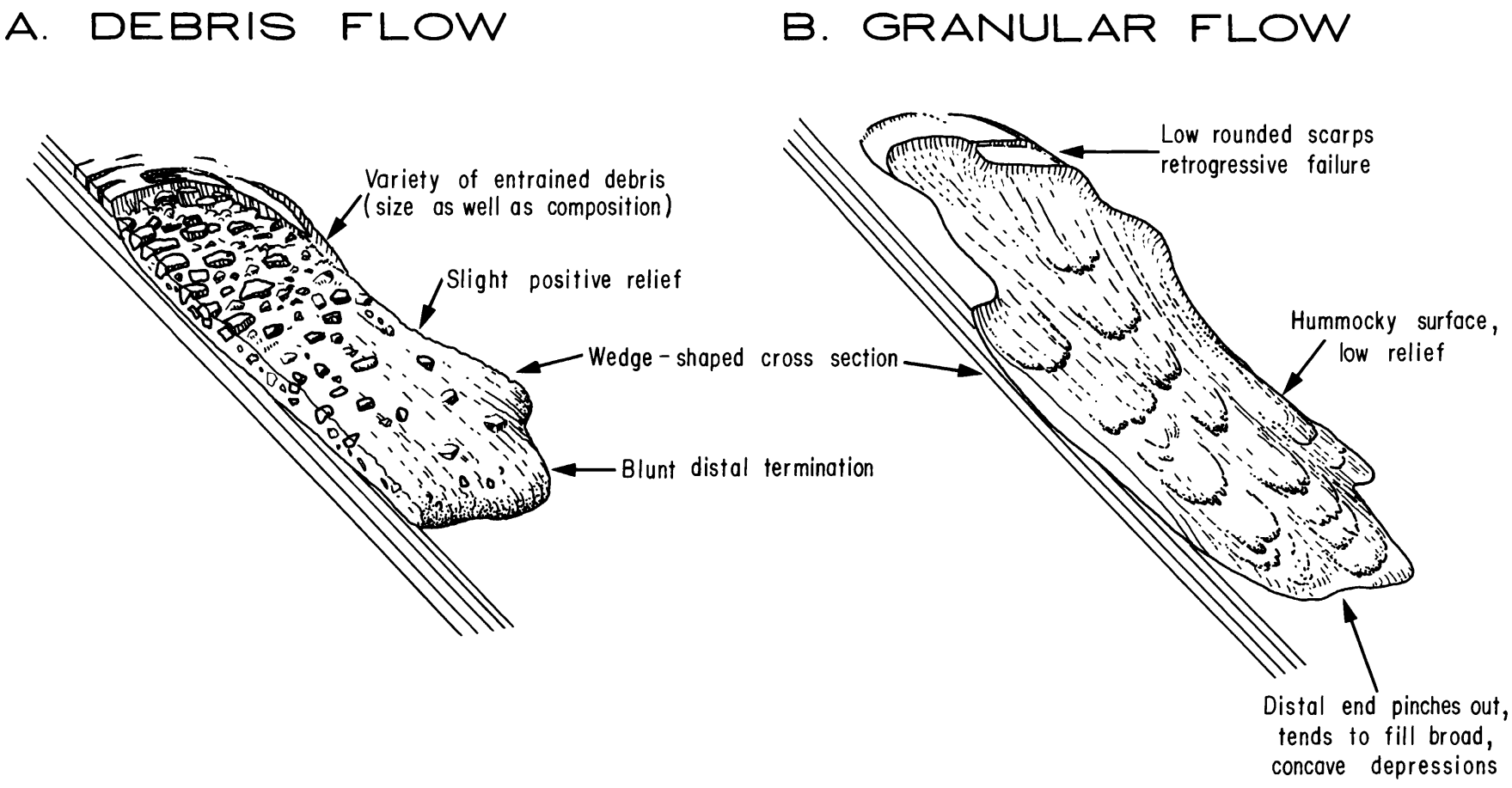

Figure 5. Types of flow.

rubble consists of material which shows acoustically as irregularly spaced high-relief hyperbolae with varied vertex elevations. The distal zone of "debris flow" is a thin wedge of material in which the upper surface is usually slightly elevated and steeply terminated.

One of the key acoustic indicators of rubble slides is the hummocky slide surface. This feature, best seen in high-frequency sparker and 3.5-kHz profiles, is typically raised or depressed with respect to adjacent smooth-surfaced undistorted sediment. Most characteristic is the abrupt contact between these two types of surface, with or without a coincident difference in elevation. The head of the slide is typically depressed; the toe or distal end is typically elevated.

Flows

A flow comprises material so disaggregated that it moves downslope as a fluid, and no internal structure, except possibly local flow folding, is evident. Flow, as a process, is spatially continuous deformation under constant stress (Varnes, 1978). It is similar, then, to creep deformation; creep displacement can disrupt internal structure sufficiently to also result in acoustic transparency (Embley, 1980).

I recognize two kinds of flows based on internal texture and on external form: debris flows (fig. 5, A), in which a "relatively high" percentage of coarse fragments are entrained (Varnes, 1978) and granular flows (fig. 5, B), in which the displaced material is essentially homogeneous. The debris in the former can be derived from preexisting clastic debris or it can originate from initially coherent material contributed to the flow. Nardin and others (1979) and Embley (1980) recognize this type as a "mass flow" deposit.

In general, debris flows have acoustic characteristics similar to those of rubble slides but considerably more subdued (cf., Jacobi, 1976). In seismic-profile they appear as lensoid or mound-shaped units which are acoustically transparent or structureless and which have indistinct surface echoes that range from smooth to irregular to hyperbolic. Core samples from the debris flows on the Continental Slope and Rise off the Spanish Sahara (Embley and Jacobi, 1976) contain clasts of varicolored clay and chalk, pebbles and sand stringers, small folds, and numerous sharp angular contacts. All these features are conducive to internal acoustic scatter, hence "chaotic" internal reflection (Embley and Jacobi, 1976). Debris flows tend to show slight positive relief but without free-standing slopes (i.e., the wedge-shaped or lenticular sections described by Embley, 1980). Irregular or hummocky surfaces may characterize debris flows, especially if a good deal of coarse debris is included. Blunt distal terminations are seen in some debris flows (Nardin and others, 1979), which implies sluggish movement, but Embley (1976) describes flow deposits associated with the Spanish Sahara slide that fill channels which locally display leveed banks. Embley concludes that they must have been very fluid and must have flowed relatively rapidly across the bottom. A cloud of suspended debris generated by turbulence during movement may accompany the flow (Middleton and Hampton, 1976). The suspended sediment settles out upon cessation of transport (Renz and others, 1955) and may drape and partly bury large surface-borne blocks and give the impression of great age.

Granular flows (fig. 5, B) include what Andresen and Bjerrum (1967) refer to as "flow slides" caused by retrogressive failures in noncohesive, well-sorted sand and silt. The term flow slide is unfortunate because failure and transport result from liquefaction and flow not sliding. Because transport along a discrete shear plane or zone is not involved, I call such mass movements "granular flows"; Middleton and Hampton (1976) use the term "grain flow". The term granular is generic; it can be replaced by a more specific modifier such as sand, clay, etc. According to Nardin and others (1979), flows of this type ("fluid-type") produce deposits generally too thin to be resolved acoustically. Woodbury (1977) describes a flow of this type, in the Gulf of Mexico, near Corpus Christi; seismic profiles show that hummocky-surfaced flow material is concentrated in very broadly concave bathymetric depressions. The hummocky surface in places grades up to the level of adjoining undisturbed sediment and in places abuts it at the base of low, rounded scarps.

Acoustic transparency is characteristic of granular flows; they are typically represented by transparent fill in flat or broadly concave depressions, one side of which may be steeper than the other. In the downslope direction the depression is open ended. The depression is typically floored by an acoustically faint bottom over a thin transparent interval with an indeterminate subbottom. Fine, regular hyperbolae may define the bottom especially near the head of the flow. The headwall scarp is ordinarily subdued and low.

Lateral spreads

A lateral spread (fig. 6, A) is basically an intraformational deformation involving plastic flow or liquefaction that breaks its overlying confining layer and releases stress by lateral extension and downslope movement (Varnes, 1978). Translation is distributed over the entire mass by extension rather than by bulk shearing. The coherent upper units may translate, rotate, subside, disintegrate, or even liquefy (Varnes, 1978). Comminution during transport can result in a debris flow. Lithologically, such a deposit could be called a diamicton. Varnes (1978) points out that lateral spreads can be very extensive, especially if liquefaction is the cause of failure, and that the area of failure is not usually clearly delimited.

Lateral spreads show acoustic characteristics similar to those of block slides except that (a) the blocks tend to be more regular in orientation and form, perhaps showing progressive diminution in size downslope, (b) a transparent subjacent layer is evident, (c) detachment scarps are not present; the spread grades into coherent material, (d) the spread surface is rough and broadly depressed; a cut-out section is not present and downslope thickening is usually minor.

A complex mass movement that may be a lateral spread is reported by Moore and others (1976) off the southwest tip of Burma. This feature, the Bassein slide, is a tabular wedge at the base of the Continental Slope and is estimated to be 1 km thick. It comprises two layers: the lower layer is pervasively deformed and overlies undeformed reflectors; the upper layer is a series of stratified blocks (olistoliths: Moore and others, 1976) most of which are bounded by curved planes and are rotated back toward the source. Wedging and forward rotation are also present. The blocks vary in thickness

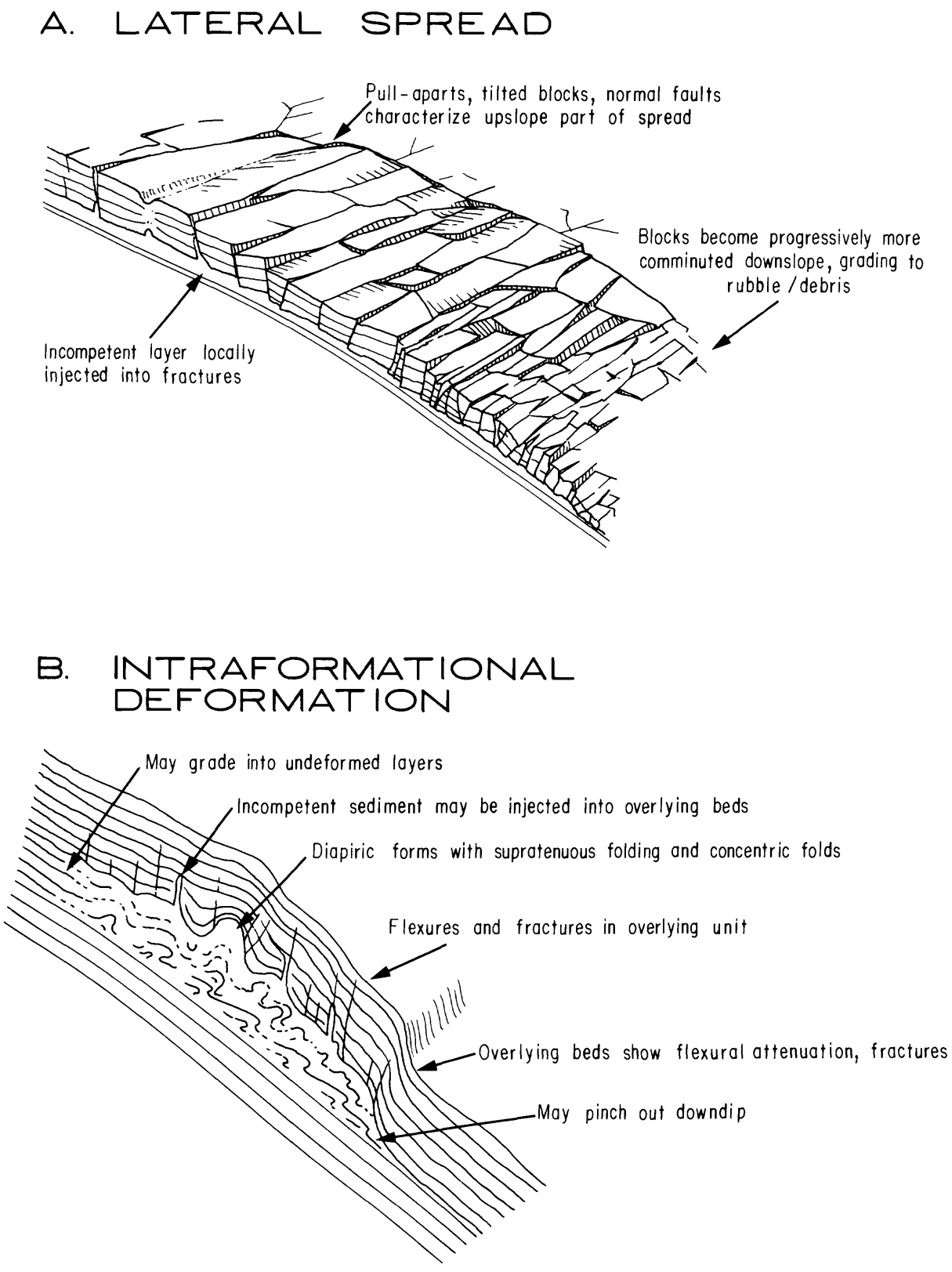

Figure 6. Lateral spread and intraformational deformation.

from a few meters to 360 m and in width from 1 km to 8 km. The surface is blanketed by a sequence of well layered "generally less disturbed" strata from a few tens of meters to 120 m thick. Distal edges of the upper unit define a topographic toe as far as 46 km out from the slope base. The lower unit, interpreted by Moore and others (1976) as a "highly fluid debris flow," extends 3 to 35 km beyond the topographic toe.

Intraformational deformation

Intraformational deformation (fig. 6, B) includes isoclinal or "concertina" folds, intraformational breccia, disharmonic flow folds, and spiral structures (rolled-bed fragments). Such features as intraformational gravitational folding or brecciation between undisturbed strata (Fairbridge, 1946) can be considered as incipient deformation leading to mass movement, which ultimately occurs if the suprajacent confining layer breaks up. If partial fracturing occurs within and above the interval of deformation, clastic dikes may be injected into coherent confining sediment (Baldry, 1938; Brown, 1938).

Intraformational deformation is likely to be detected only by the highest resolution seismic-reflection profilers and then only under optimum survey conditions. The deformed intervals are indicated by acoustic transparency, patchy reflection, rumpling, low-amplitude hyperbolae, and/or transparent vertical gashes.

Secondary features

Scarps, cut-outs, and rockfalls are superficial features that are not directly part of a mass movement but which are formed by it or consequent to it and therefore indicative of mass movement.

Scarps

Submarine scarps vary widely in height and steepness, but all are recognized by truncated reflectors. Scarps steeper than about 20° will produce a hyperbolic echo in seismic profiles so that the actual face will not be recorded. Scarps formed by rotational shear (slumping) curve smoothly into the subsurface and form planes of structural discordance. Such scarps tend to be low angle and are subject to a certain amount of rounding and flattening due to subsequent creep, ravelling, or faunal burrowing. Steeper scarps, especially those associated with planar slides, may be prone to rockfalls, particularly if a caprock crowns the scarp.

Rockfalls

Rockfalls are minor, local features as far as seismic detection goes. As Varnes (1978) describes it, a rockfall is a mass of any size detached from a steep slope or cliff along a surface on which little or no shear displacement occurs, and which descends mostly by free fall, leaping, bounding or rolling. Rockfalls are indicated in seismic profiles by transparent ramplike or steeply peaked accumulations at the bases of scarps.

Cut-outs

Cut-outs seen in seismic profile are essentially rectilinear depressions left by slab slides. They are recognized by steep scarps separated by flat, even bottoms which conform to subsurface reflectors and which are ordinarily coated with a certain amount of generally acoustically transparent locally mounded residual debris. Intersecting cut-outs form intervening promontories that project downslope. The sections of these promontories may be mistaken in transverse seismic profiles for detached blocks resting on a debris-coated surface. Slide cut-outs may be confused with depressions left by granular flows, but flow depressions are usually shallow, and may not show a high-amplitude bottom echo or steep sidewalls. The subbottom record of a flow depression is usually transparent or nearly so.

GENERAL SHALLOW STRATIGRAPHY AND FORM OF THE NEW ENGLAND CONTINENTAL MARGIN

The shallow seismic stratigraphy (within 0.8 s acoustic penetration) of the New England continental margin is divisible into five major units referred to in this report as the surficial layer, the foreset unit, the upper-slope unit, the lower-slope unit, and the layered rise unit. Boreholes, dredge samples, and submersible observations described in the text establish some geological identity for the units.

An outline of the units is presented here in order to provide the regional stratigraphic context for the history of mass movement along the New England Continental Slope and to introduce the stratigraphic designations that are cited farther on in the text. Although much of the stratigraphic section described here is exposed along the Continental Slope, the upper units are best seen, in seismic profile, beneath the outer shelf. Therefore, some reference to the shelf will be made here. Likewise, the deeper part of the section is best seen in profiles that cross the upper Continental Rise, so the rise will also be discussed.

Surficial layer

A surficial layer 20- to 40-m thick caps the Continental Shelf (cf., Garrison, 1970; Lewis and others, 1980; fig. 7). It is typically nearly acoustically homogeneous, but in places it shows weak internal layering, especially near its base. Internal structure includes foreset bedding, uneven laminate bedding, vague lensing, and channeling. The layer has been widely sampled (Hathaway and others, 1979; Bothner and others, 1980), and everywhere it consists of sand: in places fine and silty; elsewhere, particularly toward the east end of Georges Bank, coarse, gravelly, and shelly.

The surficial layer is a composite outwash sheet of late Wisconsinan age. The head of ice in Great South Channel must have been located close to 40°30'N., as indicated by the FAY data (Lewis and others, 1980). Bothner and Spiker (1980) describe till from core samples nearly 6 m long from the margins of Great South Channel, (approximately 40°55'N.) which gave radiocarbon dates of at least 20,000 years B.P. AMCOR hole 6014, in 70 m water, obtained till or till-like sediment from the surficial layer at a distance of only 35 km from the head of Lydonia Canyon (Hathaway and others, 1976).

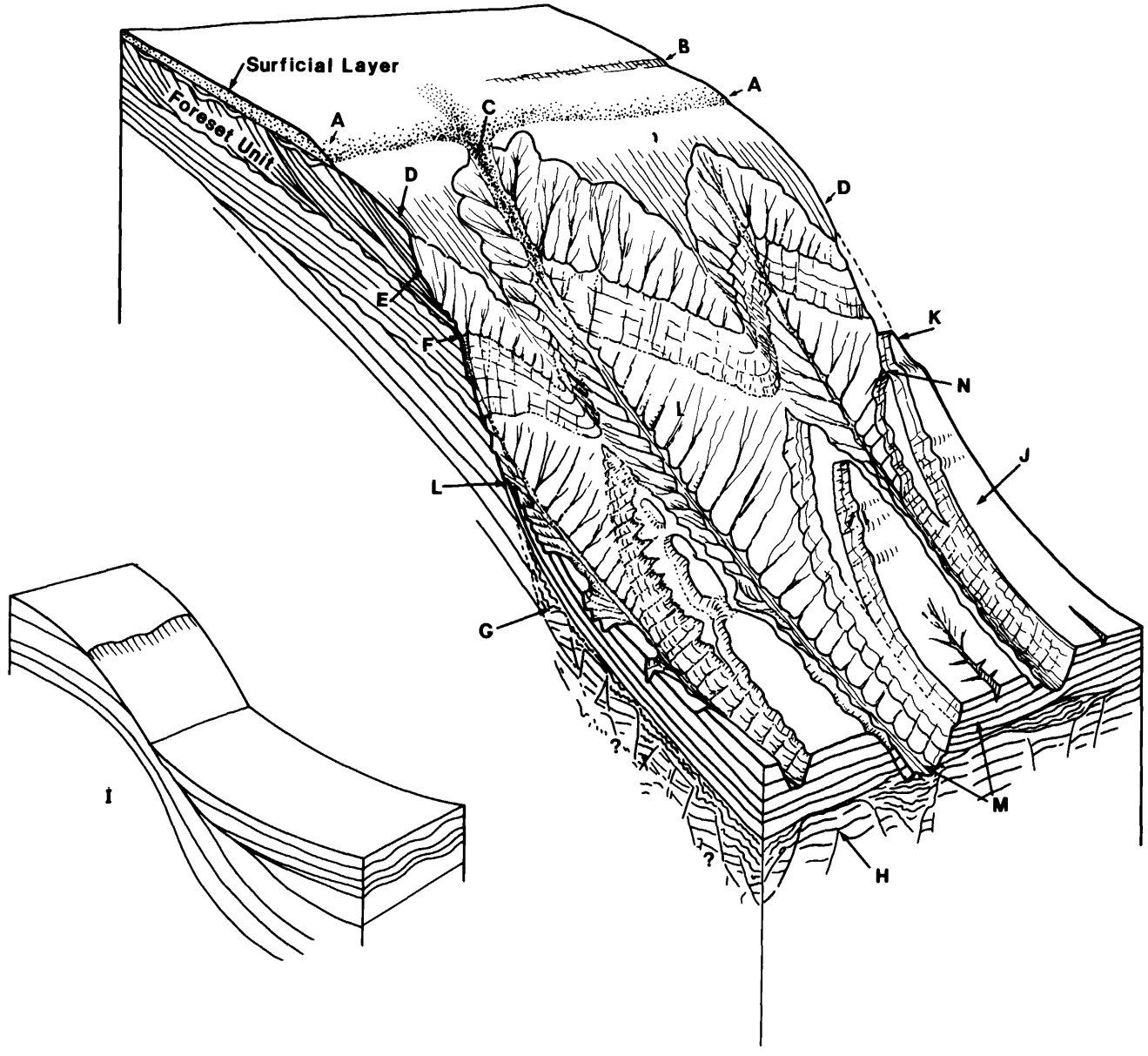

Figure 7. Block diagram shows generalized structural and stratigraphic relationships along the Continental Slope off Georges Bank. Interpretations are based on seismic profiles discussed and illustrated in text.

Along most of the outer shelf, mostly landward of the 160-m isobath, the surficial layer is terminated as a foreset ramp (fig. 7, A) 30 to 40 m in relief, with a slope of 0.5° to 1.8° (Hoskins, 1967). The ramp crest, which is generally considered to represent the shelf break, lies from 105 to 140 m below sea level. Variations in form and elevation of the ramp must reflect local differences in deposition during rising sea level, as well as complex beach genesis. The ramp crest elevations are in general accord with a late Pleistocene lowstand estimate of about -120 m (Curray, 1965) to -135 m (Emery and Uchupi, 1972).

On the shelf the uppermost part of the surficial layer is greatly modified by wave and current action (Twichell, 1981). Near the shelf edge the surface is marked by broad swales and longitudinal culminations which probably indicate wave/current erosion and redeposition. A variety of bermlike forms (fig. 7, B) along the outer margin of the layer suggest submerged beach profiles. Radiocarbon dates from the distal margin of the surficial layer approximate an age of 10,000 year B.P. (Bothner and others, 1980). These dates must reflect marine redeposition because latest ice in the Gulf of Maine was present not much later than 15,000 years ago (J. P. Schafer, oral commun., 1981). The surficial layer may be cut out in those canyon heads that extend shoreward of the 140-m isobath, but seismic evidence suggests that the layer is draped down in the heads (fig. 7, C) and simply did not accumulate to any appreciable thickness on the steep side walls.

The surficial layer is everywhere laid down on a beveled surface underlain by seaward-dipping layers of the foreset unit (cf., Garrison, 1970). This is probably a wave-cut surface as it is regionally nearly flat and is locally eroded to slightly different levels. The beveled foreset unit was subjected to a period of subaerial erosion represented by irregular depressions and channel fills cut as deep as 80 m along the outer shelf. Around the heads of some shelf-indenting canyons there are exceptionally deep filled channels, on the order of 150 m deep (based on i.v. = 1,700 m/s, see appendix). The large filled channels are evidently graded to the canyon heads, but they do not seem to be part of a shelf-wide channel network - at least such is not indicated in the profile data. My impression is that they represent blind canyons eroded headward in response to local rapid lowering of base level to the present 350-m isobath.

A glacial foreland bulge along the outer shelf during the time of maximum Wisconsinan or pre-Wisconsinan ice advance (Quinlan and Beaumont, 1981) could account for the high relief called for by the deep channels. A relatively narrow uplifted strip would account for deep local incision graded to elevated canyon heads, downslope incision along the shelf brow above 250-m depth (implied in most seismic profiles), and lack of a deep channel network farther landward on the shelf (however, note Knott and Hoskins' (1968) description of deep channel cuts along the northern margin of Georges Bank). A relative sea-level fall of 350 m is not supported, to my knowledge, by evidence other than channel incision. The deep channels would probably have been filled during the preculminating outwash phase as the foreland bulge subsided and sea level rose.

Foreset unit

The foreset unit (fig. 7) is chiefly a complex succession of continuous, sharply defined concave reflectors that converge downdip toward the Continental Slope. The concave reflectors represent truncated deltaic foreset beds laid down in a succession of prograded groups, each separated by a convex erosional surface. Typical rates of reflector-dip flattening indicate that individual depositional groups range in thickness from about 200 to 250 m.

The foreset unit forms a complex prograded wedge on a broadly uneven but smoothly sloping surface the average dip of which, west of Martha's Vineyard (fig. 8), is estimated at about 4.8 m/km (Garrison, 1970). Foreset beds thin across Georges Bank and are generally not present within the area circumscribed by the 40-m isobath. Beneath the shelf break, the unit attains a maximum thickness of about 450 m (cf., Stetson, 1936).

Throughout the survey area the foreset unit forms the convex constructional brow of the slope (fig. 7, D) at about 180-m depth. The brow is nearly everywhere acoustically opaque and is constructed of firm clayey sediment (e.g., Ryan and others, 1978; Slater, 1982). This is probably sublittoral sediment deposited during the transgression that planed the top of the unit. With depth the convex surface becomes progressively more deeply incised and inclined to bedding.

West of the "mid-bank divide" of Lewis and others (1980), the foreset unit has a regional westward dip component; east of the divide the unit has an easterly dip component. On this basis Lewis and others (1980) inferred two depositionally distinct units of different age, but Lewis now believes (R. S. Lewis, pers. commun., 1982) that the units are coeval and Pleistocene.

Nondeltaic homoclinal intervals are interbedded with the foresets, and west of Great South Channel the entire unit is nearly homoclinal (fig. 9). Here the unit comprises two slightly nonconformable subunits, the younger offlapping the older. Both subunits are built of graded beds (acoustically transparent bottoms) which show internal deformation and increased acoustic definition and lamination downdip.

The change in stratigraphic character west of 69°30'W., from steeply foreset to nearly homoclinal bedding, corresponds with the presence of a smooth transition of shelf to upper slope. The upper slope surface extends to depths of at least 750 m, at an average inclination of about 1.4° (MacIlvaine and Ross, 1979) and without significant break. Locally in this region the foreset unit continues as an unconformable blanket, at least 90 m thick, out across the lower slope and onto the Continental Rise (fig. 9, A). East of Great South Channel the unit is typically abruptly truncated below 200 m by a distinctive steep, concave segment of the upper slope (fig. 7, E).

The foreset unit was penetrated by AMCOR holes 6012 to 6017 (Hathaway and others, 1979) which showed the sediment to be dominantly dark-gray clay and silt with interlayers of fine sand. Indurated sediment is present low in the unit. Paleontological evidence (Hathaway and others, 1976) shows that the bulk of the foreset unit is pre-Wisconsinan Pleistocene. The Pleistocene foreset groups represent successive outwash sequences derived mainly from upland regolith (Kaye, 1967a,b; Feininger, 1971) and coastal-plain sediment

that originally occupied the Gulf of Maine and coastal lowlands farther west. The later foreset groups are derived, in part, from earlier drift sequences and from Tertiary strata torn from the top of Georges Bank and Great South Channel by ice. The lithologic character of the foreset unit indicates its Coastal Plain/Tertiary regolith provenance: the high quartz/feldspar ratios and the clay compositions (Poppe, 1981), the mixed fossil assemblage, and the fact that Fay 003 profiles (Lewis and others, 1980) clearly show the juxtaposition beneath the bank of deformed and nondeformed foresets with distorted and uplifted older strata.

Toward the base of some AMCOR holes Miocene or probable Miocene sediment was encountered (Hathaway and others, 1976). This included glauconitic, plastic silty clay beneath Georges Bank and dark olive-gray, plastic, slightly silty clay beneath the upper slope. ASP holes 17 and 18 (Manheim and Hall, 1976) show that the foreset unit at depths on the slope below 1,200 m consists of gray silty clay of Pleistocene age grading down to hard green-gray, glauconitic silty-sandy clay throughout an interval about 150 m thick. The glauconitic lower part of this section may be Miocene. Samples of latest Miocene or earliest Pliocene age were obtained along the slope (Stetson, 1949) nearly 100 m above the base of the foreset unit, as determined from seismic profiles; Miocene strata probably form a more or less indurated basal interval of the foreset unit along most of the upper slope. In this report, the basal part of the foreset unit is presumed to include the Miocene section.

Upper-slope unit

The contact between the foreset unit and the underlying upper-slope unit is erosional and very shallowly progradational along the outer shelf, but relief is low and in many places the units appear conformable. In most seismic profiles the upper-slope unit is distinguished by its bold, contrasty reflectors. Downdip the reflectors are fairly continuous and parallel; on strike they are irregularly warped and flexed and show lensing and pinching on a scale of kilometers. The upper-slope unit ranges in thickness from 200 to 400 m along the upper slope, although in places it is markedly thicker. Thickness varies with relief of the basal contact. The regional dip of the upper-slope unit is at least 1.25 m/km.

The upper-slope unit includes two acoustically distinct members. The upper member is relatively thin and is characterized by continuous, strong, parallel reflectors in which broad lensing and pinching are present. A weakly reflective basal layer fills shallow depressions in the top of the lower member, which is off-lapped at a very low angle. The lower member is thicker, and shows more internal deformation and lateral facies changes. It is markedly unconformable on the lower-slope unit and, in places, appears to be partly faulted down into keystone depressions.

All along the upper slope the unit is ordinarily exposed by truncation between 400-900-m water depths. East of Hydrographer Canyon (fig. 8) the truncated interval is marked by a steep (8^{o}-9^{o}) concave face. The top of the slope face typically is marked by an inflection or, where extensive lateral erosion has occurred, by a distinct bench apparently capped by dissected basal remnants of the foreset unit (fig. 7, F). Smaller benches mark the outcrop interval of the upper-slope unit to depths as great as 970 m, but most are present above 750 m.

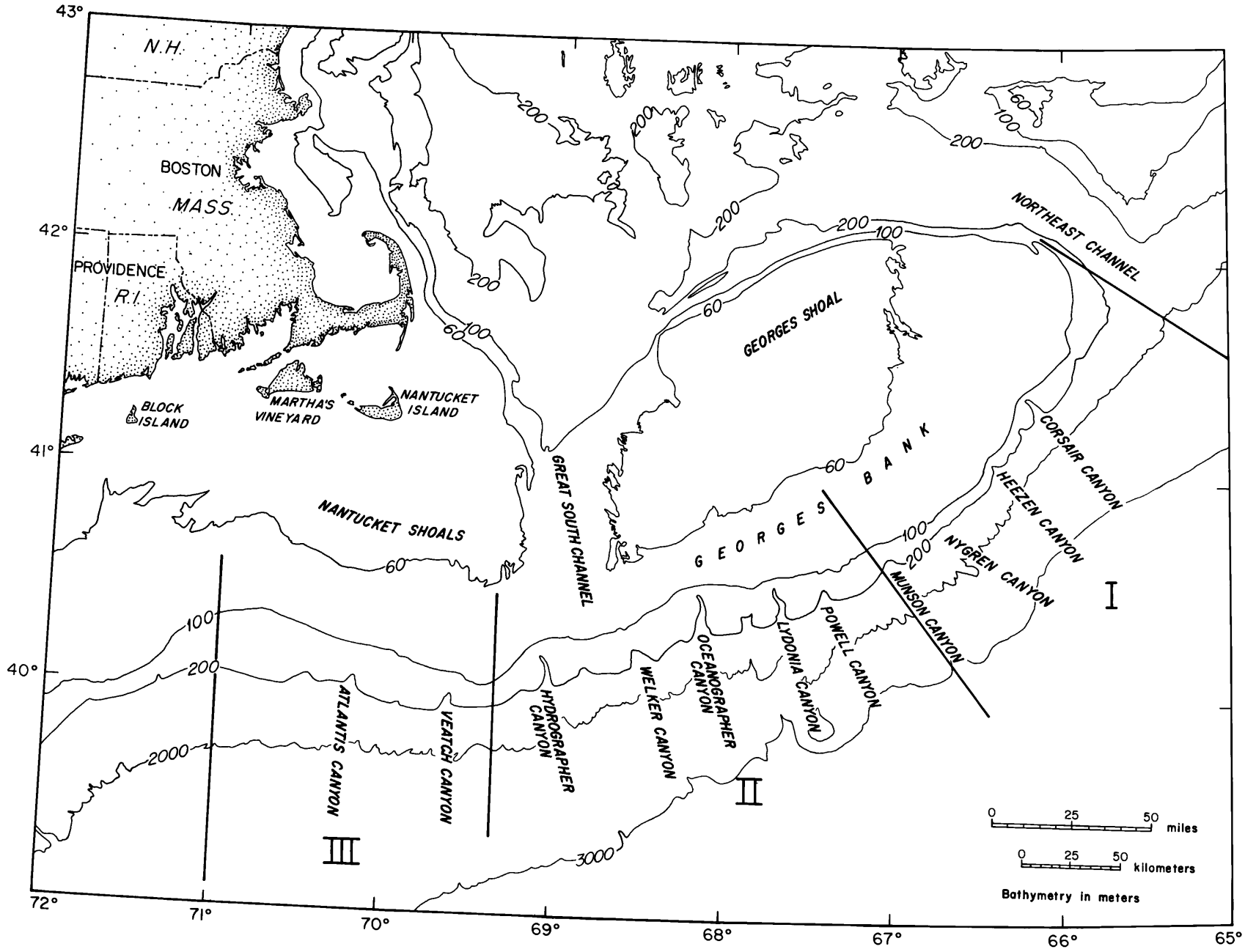

Figure 8. Major geographic features of the North Atlantic continental margin and division of the slope into sectors I-III.

West of Hydrographer Canyon (fig. 8) the upper-slope unit and the upper-slope surface are nearly conformable down to the 750-m to 900-m isobaths where the unit is generally truncated by scarps. In places, the unit extends virtually unbroken (though thinned) across the slope (fig. 9, B), attaining a regional dip of about 7^{o}.

At the east end of Georges Bank the upper-slope unit consists of lower middle Eocene siltsone, which crops out to depths of 1,538 m in Corsair Canyon (fig. 8) (Ryan and others, 1978). From "Heezen Canyon" (Ryan and others, 1978; fig. 8) on west, chalky sediment of late middle Eocene age, which evidently represents the upper member, is a characteristic part of the upper-slope unit. The calcareous section varies laterally from a true chalk to a calcareous clay or glauconitic marl. Toward the west end of the survey area the entire unit becomes more monotonous and marly.

The Eocene section may be overlain by thin upper Oligocene sediment (Poag, 1982). Upper Oligocene buff-colored calcareous clay and brown glauconitic sandy clay were dredged from Oceanographer Canyon (Gibson and others, 1968).

Lower-slope unit

The lower-slope unit is poorly rendered in the seismic profiles because of its depth and the steep, rugged terrain it underlies along its zone of outcrop below approximately 900 m on the slope. It crops out along a steep (7^{o}-8^{o}) middle- to lower-slope segment in which transverse incision has produced landforms of high relief and irregularity. Along much of the slope the surface of truncation is mantled by a seaward-thickening wedge or ramp of rubble in which large tilted blocks are, in places, apparent (figs. 7, G; 9, C).

Beneath the outer shelf, the lower-slope unit is separated from the upper-slope unit by an erosional unconformity. Downdip, the unconformity is barely discernable in most records and is marked by a very shallow truncation of older beds; in profiles along strike the contact is marked by an irregular rising and falling surface of considerable relief, broadly similar in profile to the present slope surface, particularly along the lower slope/upper rise. In places where erosional relief is low, the contact appears nearly conformable.

The lower-slope unit evidently includes a number of deformed and eroded Upper Cretaceous stratigraphic subunits. Each of the subunits shows generally weak, parallel layering. The upper two subunits appear to drape-fill broad troughs cut in the lowermost subunit (fig. 7, H). In places the uppermost subunit comes close to conformity with the upper-slope unit, though it is everywhere distinguished from it by weaker, finer reflectors.

West of Veatch Canyon (fig. 8) the upper levels of the lower-slope unit are more regularly layered and internal relief is somewhat diminished. In places the horizontal beds beneath the shelf pass under the slope and splay or prograde seaward across a distinct benchlike form (fig. 9, D), and apparently fill transverse depressions along the lower slope, which feed into the lower slope wedge.

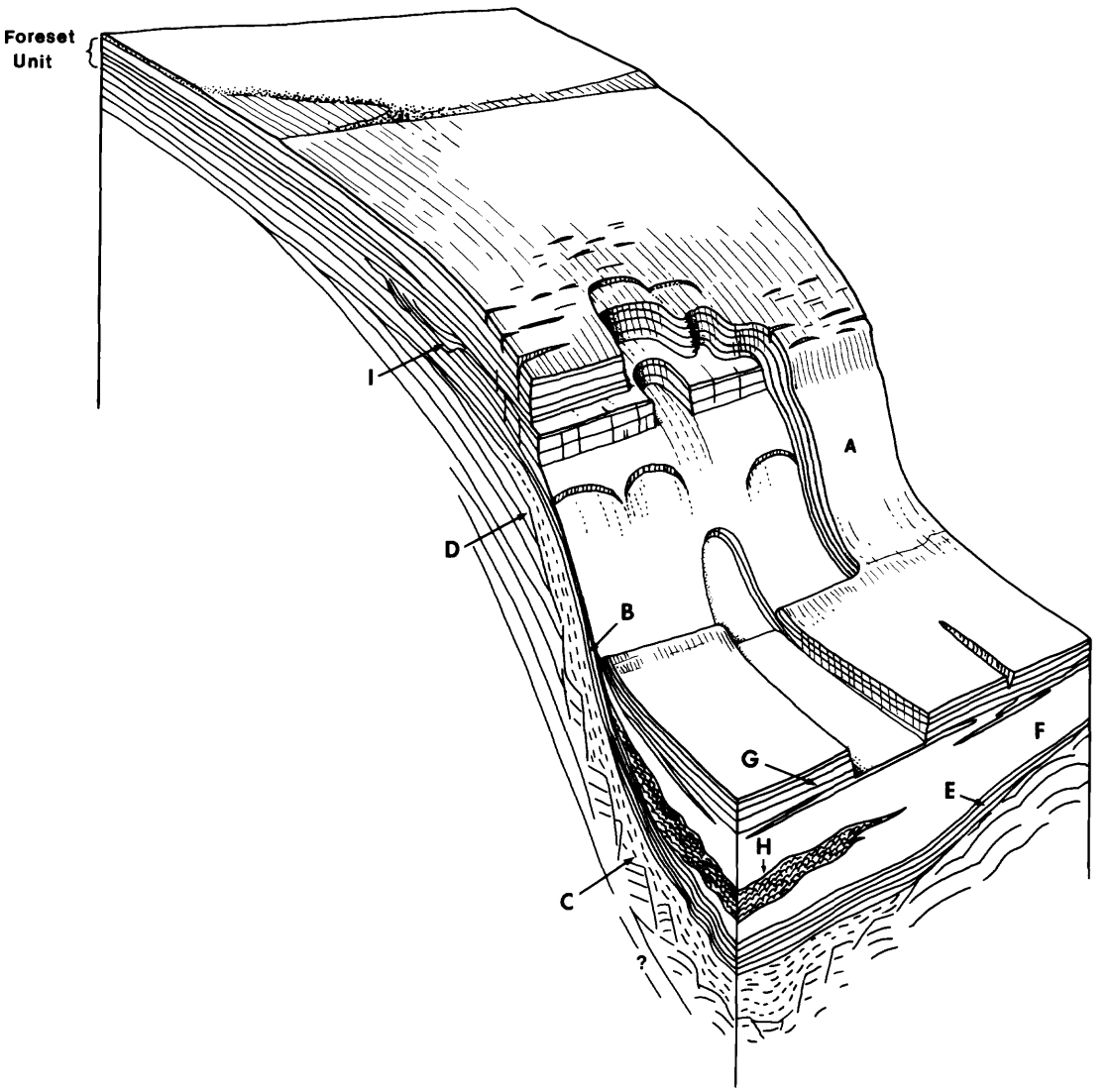

Figure 9. Block diagram shows generalized structural and stratigraphic relationships along the Continental Slope in sector III. Interpretations are based on seismic profiles discussed and illustrated in text.

Sediment of the lower-slope unit has been sampled in submarine canyons all along the New England Slope. It generally consists of fine-grained, dominantly calcareous graywacke -- thin-bedded to massive gray clayey siltstone, marl, and fine-grained sandstone ranging in age from Maestrichtian to Coniacian. Maestrichtian sediment probably forms the uppermost layered-fill subunit that is most conformable with the overlying upper-slope unit.

Layered rise unit

The layered-rise unit is a thick and complex interval of well-layered strata that extends across the Continental Rise and onlaps the slope such that, typically, progressively younger beds lie unconformably on progressively older ones as the slope steepens going updip (fig. 7, I).

Toward the east end of the survey area the unit extends well up onto the lower slope, as high as 1,100-m water depth, as a relatively thin (240-350 m thick) monoclinal succession (fig. 7, J). The updip end of the monoclinal succession is deeply and abruptly eroded so that, in profile, much of the lower slope is a cuesta (fig. 7, K). Only where the monoclinal interval is completely eroded away is a distinct slope/rise contact formed by the exposed deeper onlapping layers of the layered rise unit (fig. 7, L).

Along strike the unit is preserved in flat-topped mesalike forms separated by flat-bottomed troughs, some of which represent canyons that extend across the slope (fig. 7, M).

In a few places reflectors of the layered rise unit can be projected updip in conformity with truncated reflectors of the upper-slope unit and the lower part of the foreset unit. The projection implies original stratigraphic continuity such that the lower part of the layered rise unit must include middle Eocene strata. Approximately 120 m of Pleistocene section forms the top of the unit. In places, much of the capping Pleistocene interval is draped across the cuesta face (fig. 7, N), which means the cuesta is as old as pre-Pleistocene or perhaps pre-middle Pleistocene.

The layered rise unit thins across the relatively elevated, dissected terrain between Powell and Oceanographer Canyons (fig. 8). The lower intervals pinch out against it from the east, are intermittently present across it, and reappear as continuous reflectors west of Dogbody Canyon (69°00'W.). From this point west the layered rise unit thickens greatly, mainly by the addition of a parallel, finely layered interval at its base that onlaps from the west (fig. 9, E). This is overlain by a dominantly transparent interval, at least 170 m thick (fig. 9, F), which is capped by a well layered but severely eroded Pleistocene(?) section originally 170 m or more thick (fig. 9, G). Here the layered rise unit onlaps the lower slope at a relatively steep angle, creating a distinct constructional slope-rise contact.

On strike, beds of the layered rise unit intertongue or change facies up and down the section, whereas downdip they are very persistent and uniform. This suggests that at least some of the unit is derived from local sources along the slope. This characteristic is particularly evident toward the west end of the area where an opaque fanlike lentil (fig. 9, H), apparently derived from slope sources, occupies the lower part of the transparent interval.

SHALLOW SEISMIC STRATIGRAPHY, STRUCTURE, AND SURFICIAL FEATURES OF THE NEW ENGLAND CONTINENTAL SLOPE

The Gilliss and Iselin seismic data comprise about 5,962 km of profile with a spatial resolution of better than 300 m along track. It is convenient to discuss these data in three groups, each covering a more or less physiographically distinct sector of the New England Continental Slope. The sectors numbered I, II, III from east to west (fig. 8), are discussed below. Sector I, the eastern sector, is about 180 km long; it extends from Northeast Channel (fig. 8) to 67°00'W. Sector II, the central sector, is about 200 km long; it extends from 67°00'W. to 69°20'W. Sector III, the western sector, is about 175 km long; it extends from 69°20'W. to 71°00'W. Numbered seismic profiles referred to in each sector are prefixed G (Gilliss), I (Iselin), or F (Fay). The G and I lines are shown on the 1:250,000 maps accompanying this text. The maps, listed A through G (back pocket), show the geological features which are discussed and illustrated in the following descriptions of the sectors; the maps are identified in figure 10, which also shows the area of the slope included in lease sale 52.

Sector I: Northeast Channel to Munson Canyon (67°00'W.):

Lines G1 to G16, G24, G25, G34, G35; I15 to I39, maps A, B, C

General physiography

In this sector the Continental Shelf falls off to deep water along a broadly convex profile. In general, the shelf break lies between 120 and 160 m depth. Toward the eastern end of the sector, the break is represented by a gentle declivity at 150–165 m depths. This marks the upper edge of a flat, seaward-tilted surface or facet, which varies in width from line to line and which is missing in lines G1, G4, and G9. The seaward end of the facet is abruptly terminated by the steep surface of the upper slope (fig. 11). Where the slope is embayed into the shelf, cutting out the facet, the point of truncation marks the shelf break; where the slope face has not been cut back so far, the point of truncation is in deeper water, as deep as 400 m, and a relatively broad facet is preserved behind it (fig. 11). The facet is evidently a constructional surface of the foreset unit.

The broadly concave profile of the Continental Slope in this sector can be roughly subdivided on the basis of form into four levels (fig. 12). From top to bottom these are: (1) a concave recess that extends from the shelf break, or seaward edge of the facet, to a shoulder or bench (C^1) at depths from 360 to 690 m (greater depths to the west); (2) an irregular steeper surface from C^1 to an inflection or notch (C^2) located at depths that range from 750 to 1,050 m; (3) a broadly irregular, concave segment (locally marked by a distinct, steep shoulder (S) that extends from C^2 to either a cuestaform scarp or the onlap of the layered rise unit, between 1,200 to 2,300 m; (4) a flattened segment underlain by slope-conformable reflectors, which extends down to a more or less distinct inflection marking the rise between 2,325 and 2,700 m.

West of 66°30'W. the lower slope flattens at shallower depths and forms a broad, flattened or slightly convex profile at about 1,900-m depth across which the layered rise unit is broken into large tabular blocks separated by flat-floored troughs (fig. 13), in contrast to the dominantly ridge-and-gully

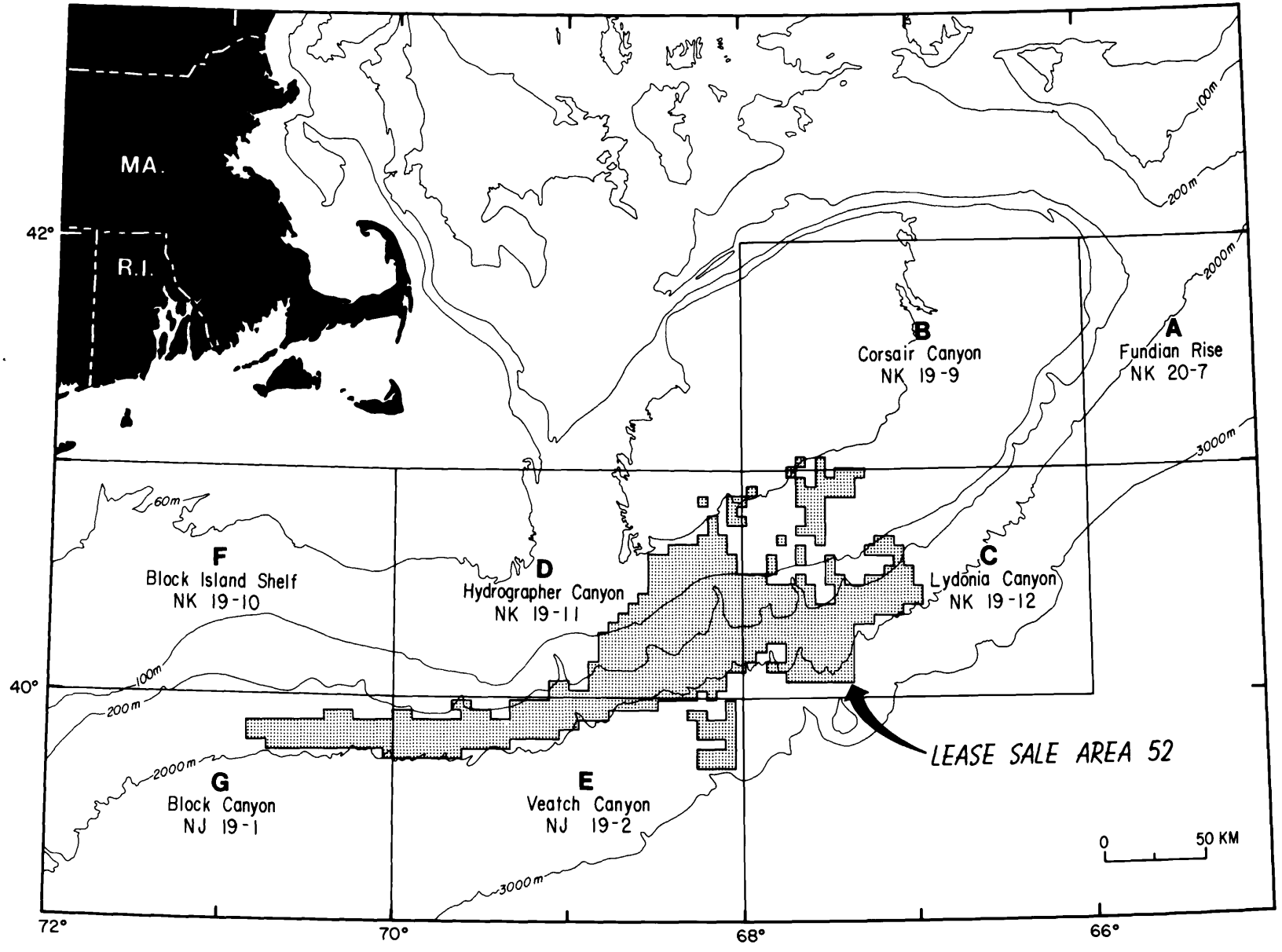

Figure 10. Map areas A-G accompanying text at 1:250,000 scale; North Atlantic lease sale area 52.

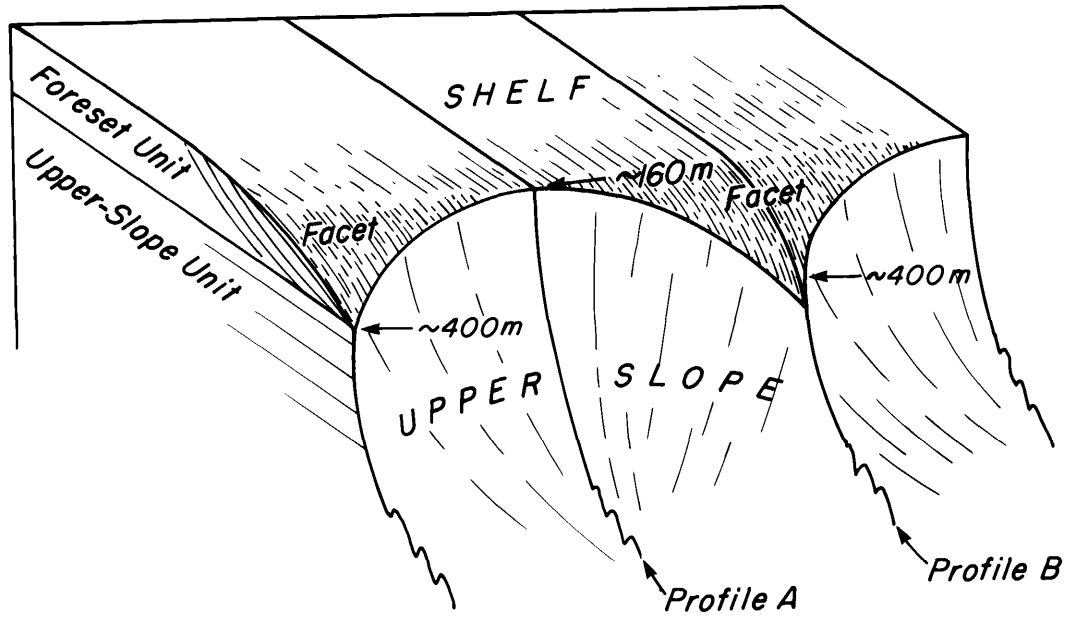

Figure 11. General relationship of upper slope and shelf surfaces: the facet shown in some seismic profiles (profile B) is a constructional part of the outer shelf. Elsewhere (profile A), the truncating upper slope has been cut back at the expense of the facet surface, which originally formed much of the slope.

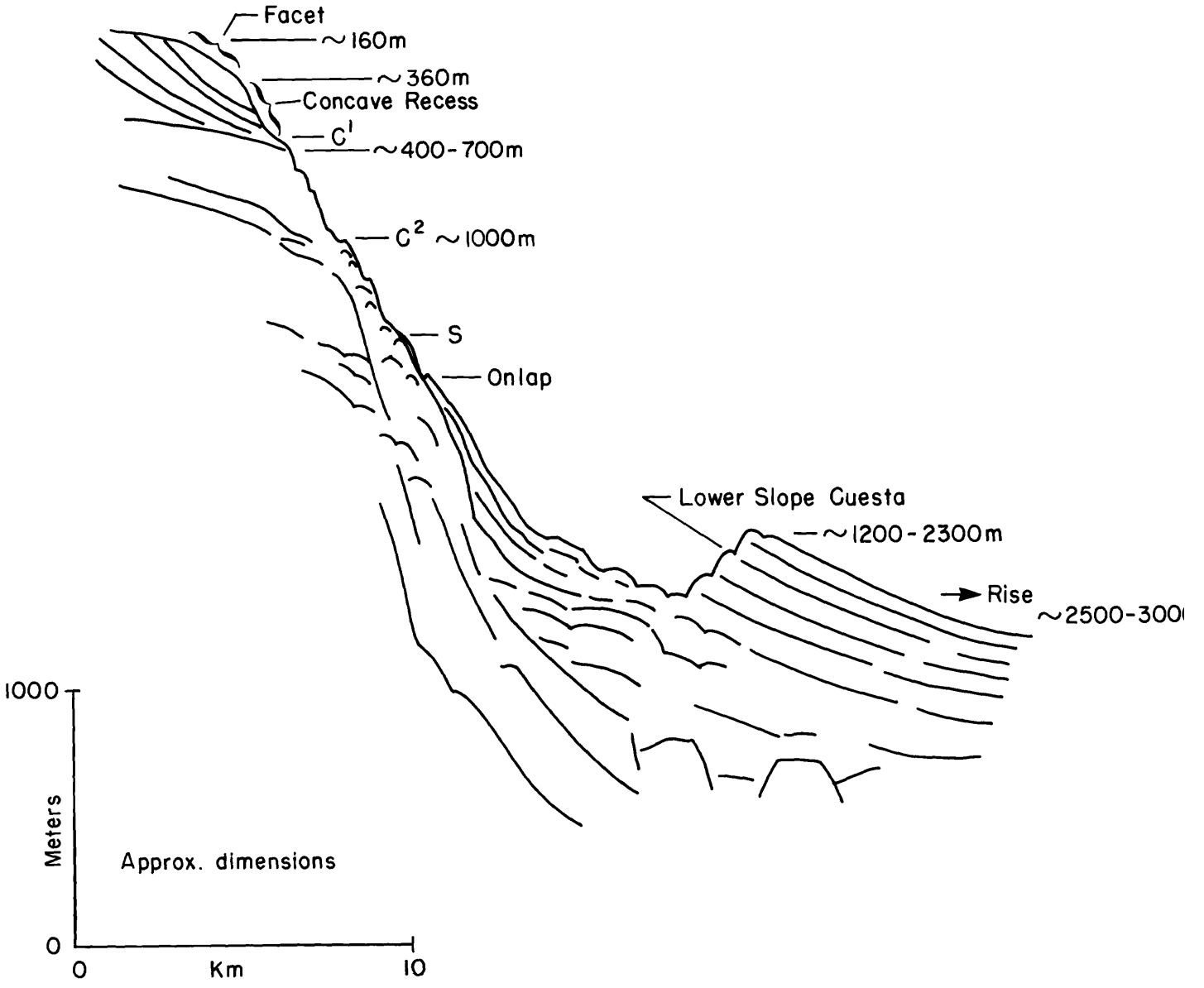

Figure 12. General form of the Continental Slope in sector I (based on GILLISS airgun line 8).

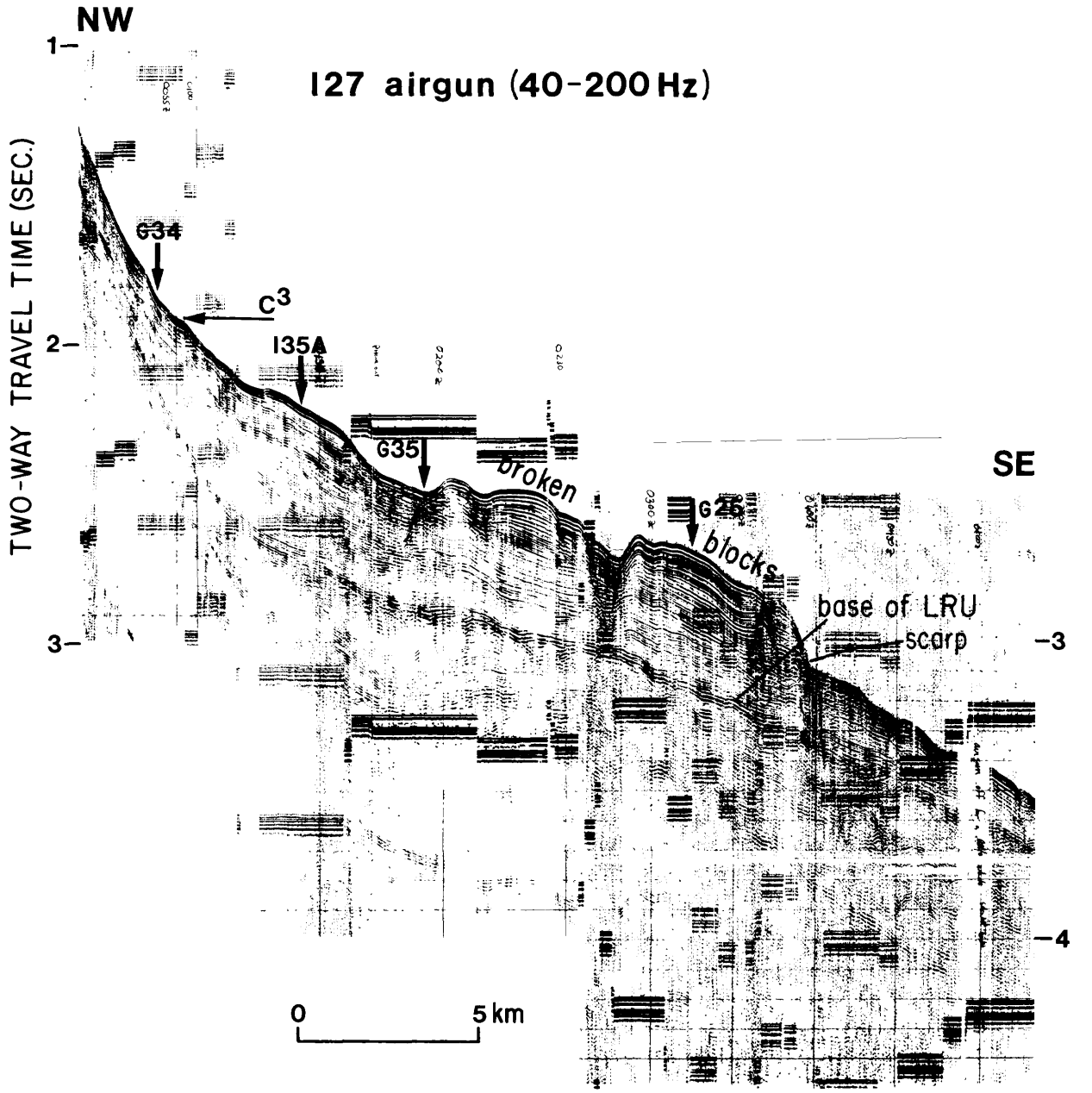

Figure 13. Profile I27 (airgun) shows broken, onlapping strata of the layered rise unit (LRU). Vertical exaggeration ~ 11:1.

terrain of the midslope and of the lower slope farther east. Strikelines suggest that the tabular blocks of layered rise strata form flatirons (fig. 7).

On strike, the middle to upper slope is irregularly and deeply incised. The lower slope is marked by relatively deep, steep downslope incisions of great continuity and regularity, the most notable of which are Corsair and Nygren Canyons. Incisions over most of the slope seem to form a rill-like pattern.

Form and stratigraphy

In this sector the surficial layer is generally smooth and flat out to depths of 116-120 m. Beyond these depths the surficial layer is pinched across a smooth seaward facing ramp 2-3 km wide to a depth of 160-180 m (fig. 14). The ramp represents the prograded distal margin of the surficial layer. Along the east rim of Munson Canyon (map C), at about 135-m depth, the surficial layer is 75 m thick. It seems to pinch out at about 337 m depth on the very uneven upper wall of the canyon just below the rim. East of Corsair Canyon the morphological expression of the surficial layer is obscure; it may extend past the shelf break and pinch out on the slope at depths below 200 m.

On strike, the surficial layer is flat and evenly bedded. It unconformably overlies the foreset unit and a thin, irregular, transparent interval of channel fill (fig. 15) cut into the foreset unit along unconformity A of Lewis and others (1980). The channel fill ranges from a few meters to 40 m thick, but locally channels as deep as 100 m are cut below the shelf surface. Lewis and others (1980) included the cut-and-fill interval with the veneer for a total thickness of as much as 80 m.

In this sector reflectors of the foreset unit vary greatly in apparent dip from group to group, becoming generally steeper toward the slope. Dips are generally east-southeast. Steeply downdip-converging reflectors are interlayered with less steeply inclined, continuous homoclinal intervals which probably represent marine deposits. Some steep reflectors are closely layered and jumbled (fig. 15), which perhaps indicates rapid deposition and contemporaneous deformation. The updip ends of all the foreset layers have been beveled, though topset flattening, visible in some Fay lines, indicates that not more than a few tens of meters can have been eroded. Some seismic lines show that the outermost foreset group is beveled back from the shelf break to a berm located near the 95-m isobath. At the eastern end of the sector the unit apparently extends to considerable depth across the slope, as Ryan and others (1980) reported pre-Wisconsinan Pleistocene subhorizontally bedded "sandy mudstone" cropping out in "Heezen Canyon" as deep as 1,070 m.

The concave recess that forms the upper slope along much of this sector probably represents the profile of a series of reentrants cut into the foreset unit along the upper slope (fig. 11). In places the bench (C^1, figs. 12, 14) is underlain by parallel-layered, continuous reflectors of the relatively resistant upper-slope unit capped by a thinned, eroded selvage of the offlapping foreset unit (fig. 14). Elsewhere, the recess is cut entirely within the foreset unit (fig. 16).

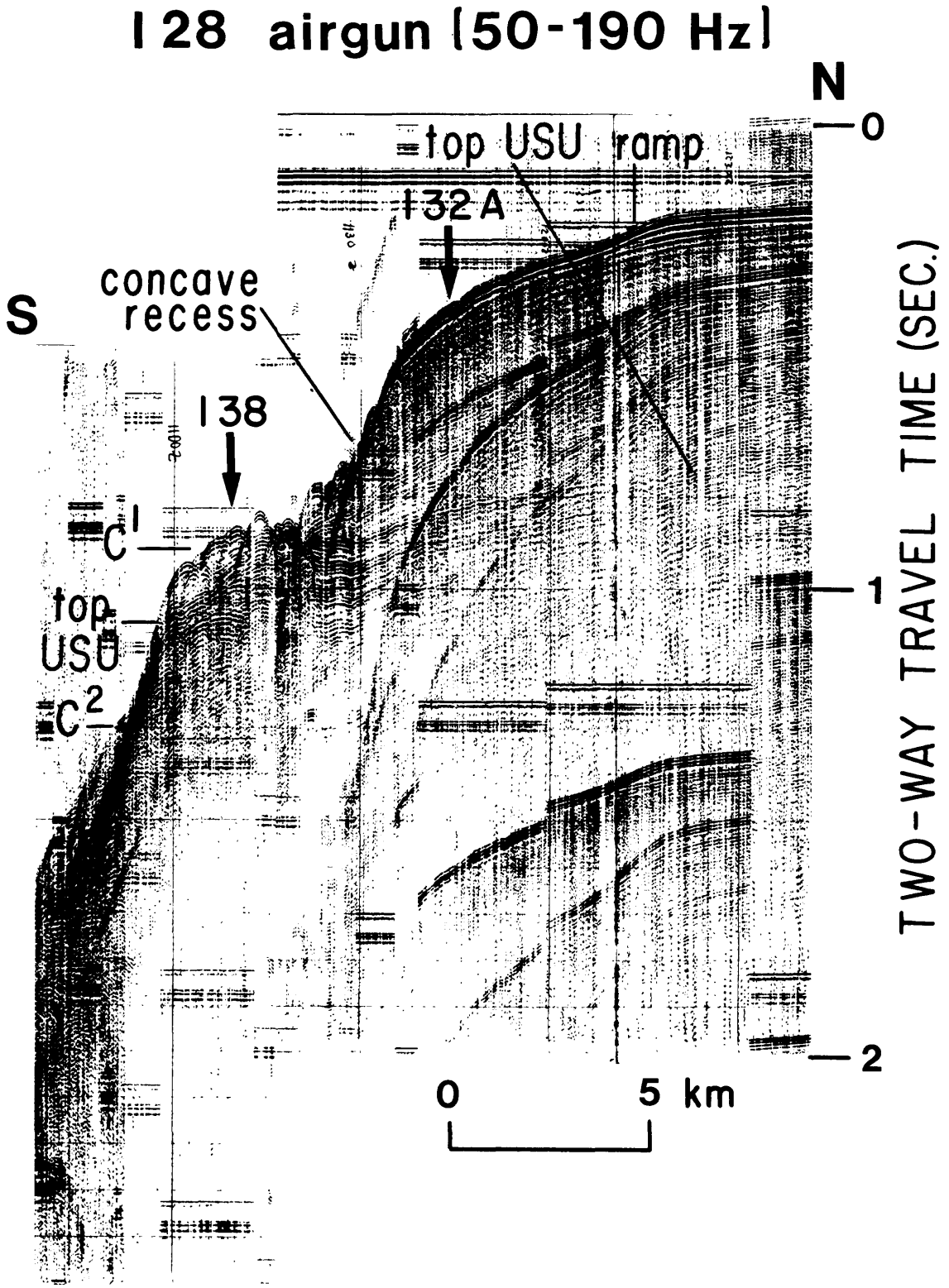

Figure 14. Profile I28 (airgun) shows ramp marking shelf break, and concave recess in the upper slope that forms upper reach of Nygren Canyon; USU = upper-slope unit. Vertical exaggeration ~ 16:1.

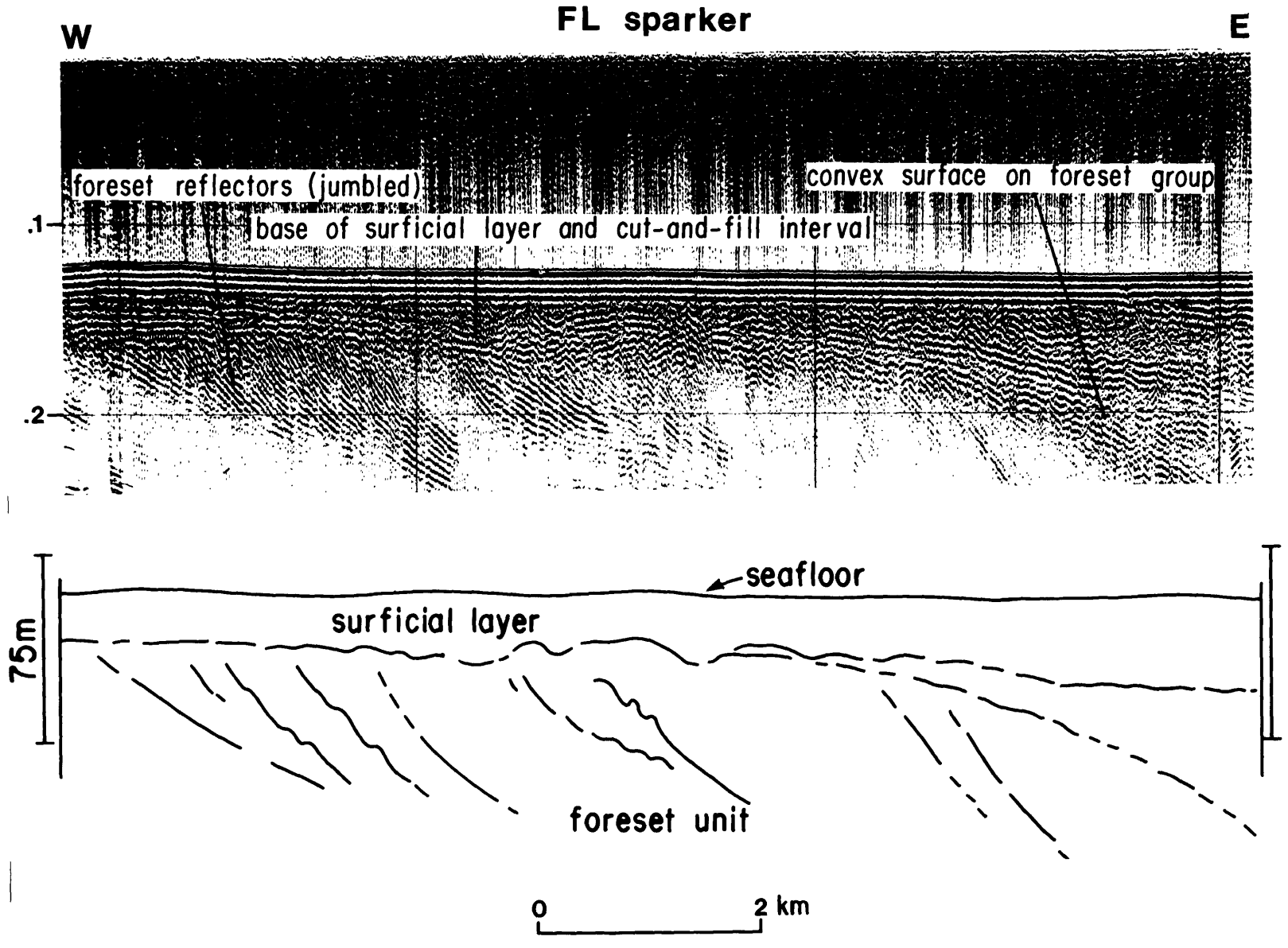

Figure 15. FAY sparker line L on outer shelf of Georges Bank shows convex form of earlier foreset package overlain by later foreset package, both capped by surficial layer from 20 to 40 m thick.

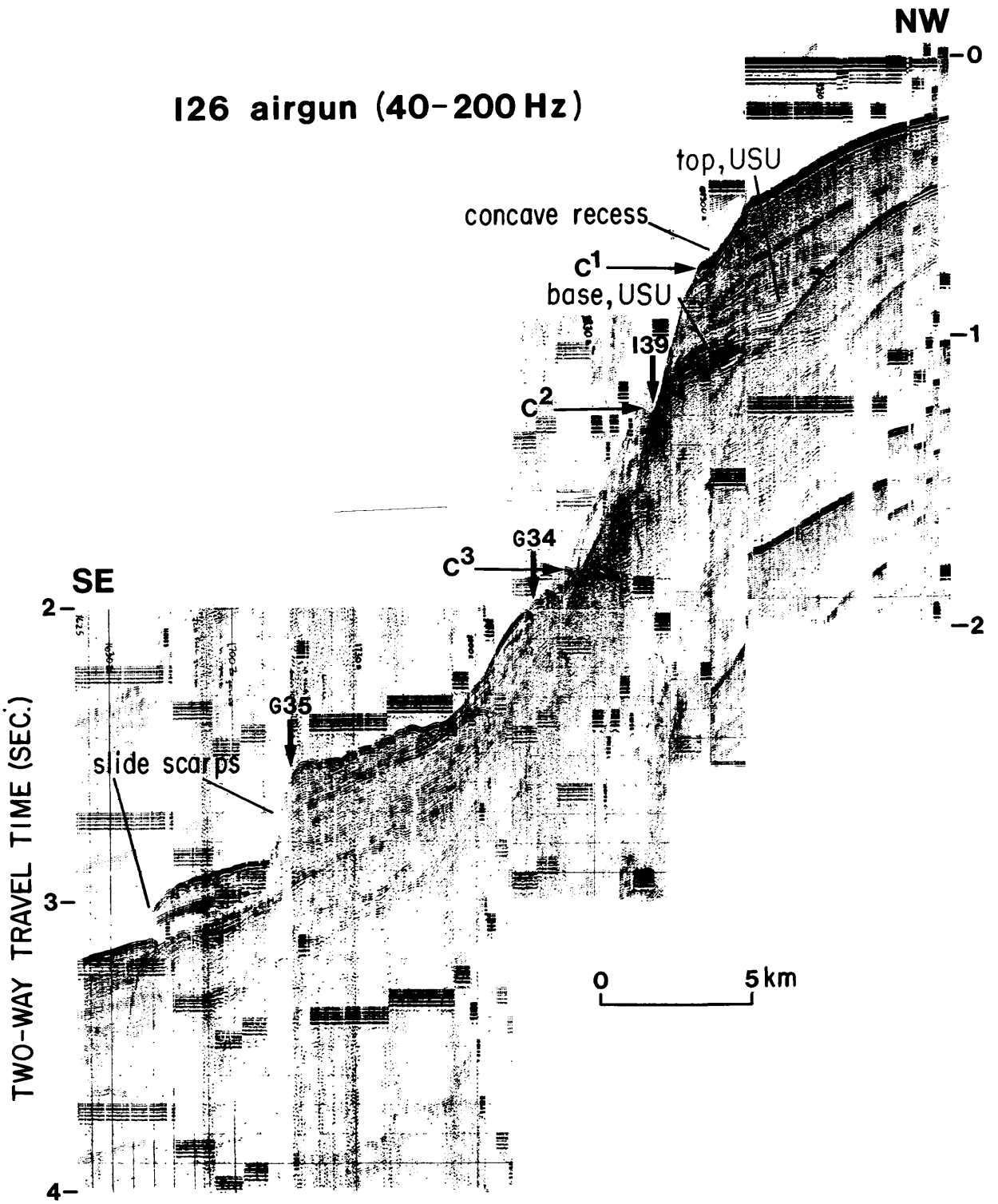

Figure 16. Profile I26 (airgun) shows layered rise unit on lower slope cut by two seaward-facing scarps. Note concave recess at top of slope; USU = upper-slope unit. Vertical exaggeration ~13:1.

A prominent reflector present 340-470 m beneath the shelf break marks the top of the essentially parallel-layered upper-slope unit (fig. 14). Projection of the top of the inferred Tertiary section (equivalent to the upper-slope unit) in lines FJ and FK (Lewis and others, 1980) shows that it should crop out on the slope no higher than 325 m depth. The lower intervals of the upper-slope unit thin or converge slightly downdip to a depth of approximately 900 m (C^2), but in places (line G35A), the upper-slope unit is present as low on the slope as 1,500 m.

In general, the upper-slope unit crops out within the steep, nearly rectilinear slope interval between inflections C^1 and C^2 (fig. 16), a vertical distance of about 450 m. Toward the western end of the sector the unit or its interval of projected outcrop thins to about 345 m.

Dillon and Zimmerman (1970) reported the observed wall of Corsair Canyon, from 488-700 m depths, (i.e. below point C^1, above point C^2) to consist of a series of small cliffs and talus slopes, and that the cliffs expose layers 5-10 cm thick of semi-indurated, buff-brown sandstone and siltstone dipping apparently 10^o to 15^o seaward. Below 1,168 m in the canyon, similar strata were sampled by Ryan and others (1978) and were found to be of Eocene age. Ryan and others (1978) described the Eocene section as dominantly non-calcareous, brown, silty mudstone. In "Heezen Canyon" Ryan and others (1978) recovered Eocene rock in place at 1,165 m, over Lower Cretaceous strata.

In some profiles (e.g. line G1, fig. 17) the inferred Tertiary section truncated along the upper-slope can be projected to reflectors of the layered rise unit truncated at the up-slope facing cuesta scarp on the lower slope. This implies not only that the upper-slope unit originally extended down across the lower slope, but that the nearly 325 m of Pleistocene and possibly Miocene strata beneath the shelf break are represented on the lower slope by only about 120 m of well-layered correlative sediment.

Along the slope, the basal layers of the upper-slope unit lie upon a broadly irregular (eroded?) contact (x) (fig. 18), which is underlain by reflectors scarcely different from those above but which show steeper local dips (fig. 19).

Horizon x seems to mark an angular unconformity below and downdip from which strata are locally much broken and distorted (fig. 20). Most of the incisions shown in line G15 are cut to this horizon; only Corsair and Nygren Canyons and a trough along line I29 (fig. 21) penetrate it deeply, probably by as much as 225 m. Horizon x may represent either the Tertiary-Cretaceous contact, or a lithologic contact within the Tertiary section. Beneath the lower slope, horizon x marks the base of the layered rise unit (figs. 13, 20). Beneath the contact the lower-slope unit is characterized in places by variously tilted, discontinuous reflectors (fig. 20). There may be three or more chaotic units stacked beneath the layered rise unit (fig. 13); the uppermost is represented by isolated wedges or troughlike fillings capped by the unconformity (fig. 21: at I32, I34). The distorted, broken horizons of the lower-slope unit beneath the unconformity apparently converge or project upslope toward C^2 (figs. 13, 20).

In general, inflection C^2 marks the level below which Cretaceous strata crop out; it is represented by a narrow, rough-surfaced bench or by pronounced

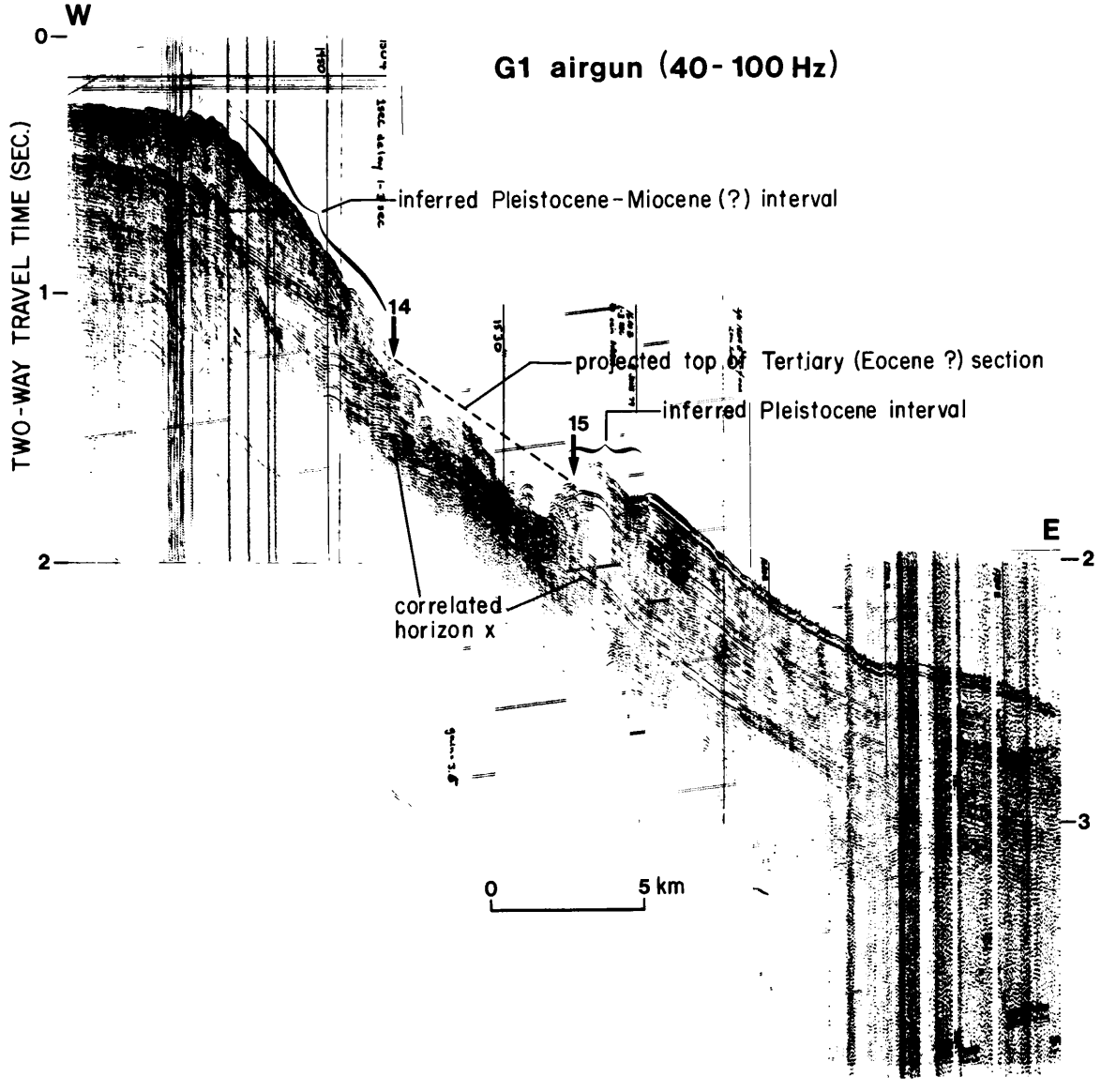

Figure 17. Profile G1 (airgun) showing inferred slope stratigraphy. Vertical exaggeration ~ 11:1.

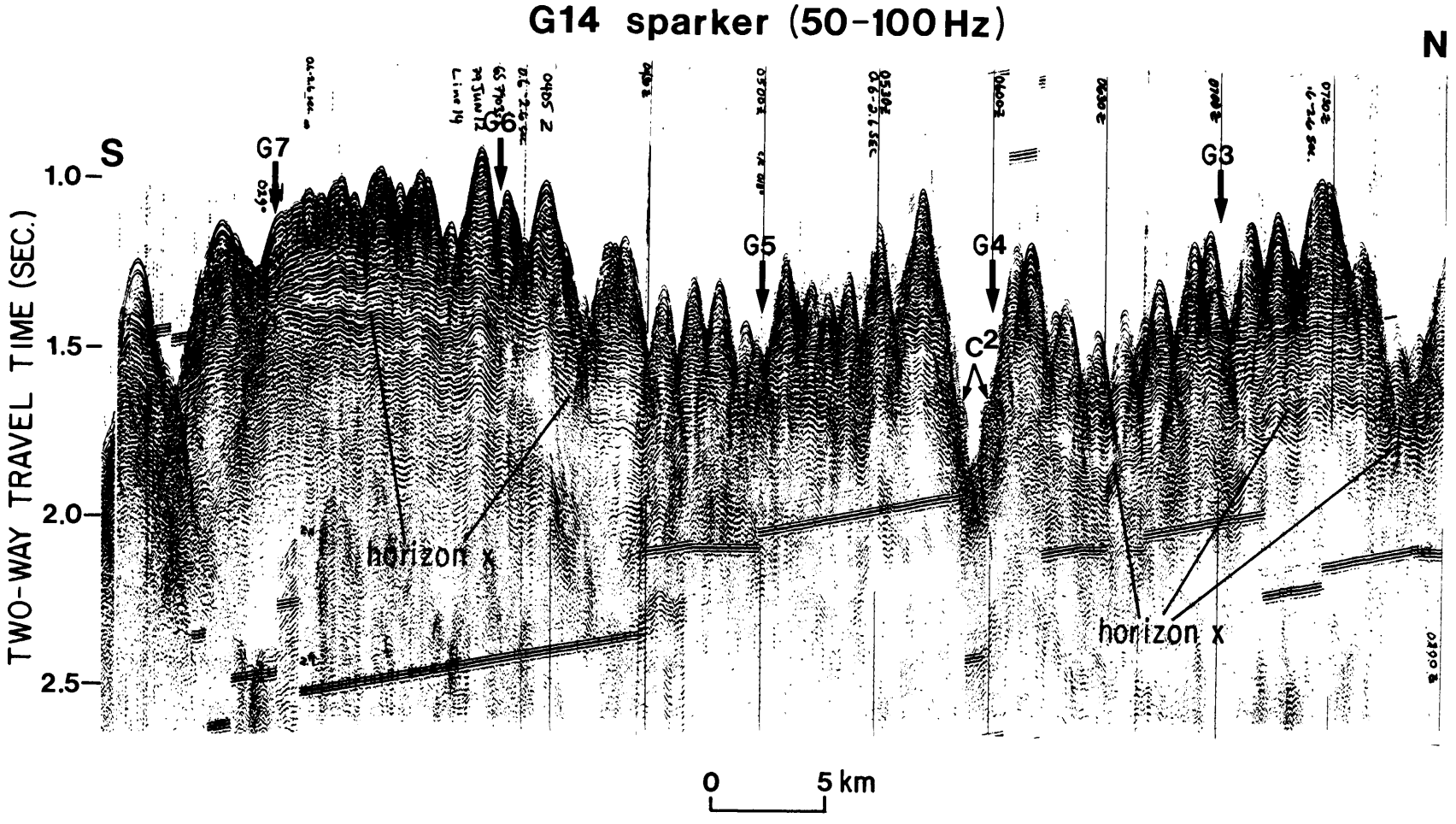

Figure 18. Profile G14 (sparker) shows transverse incision along midslope (about 950 m depth), position of horizon x and overlying upper-slope unit; position of inflection C^2 essentially marks top of lower-slope unit. Vertical exaggeration ~ 19:1.

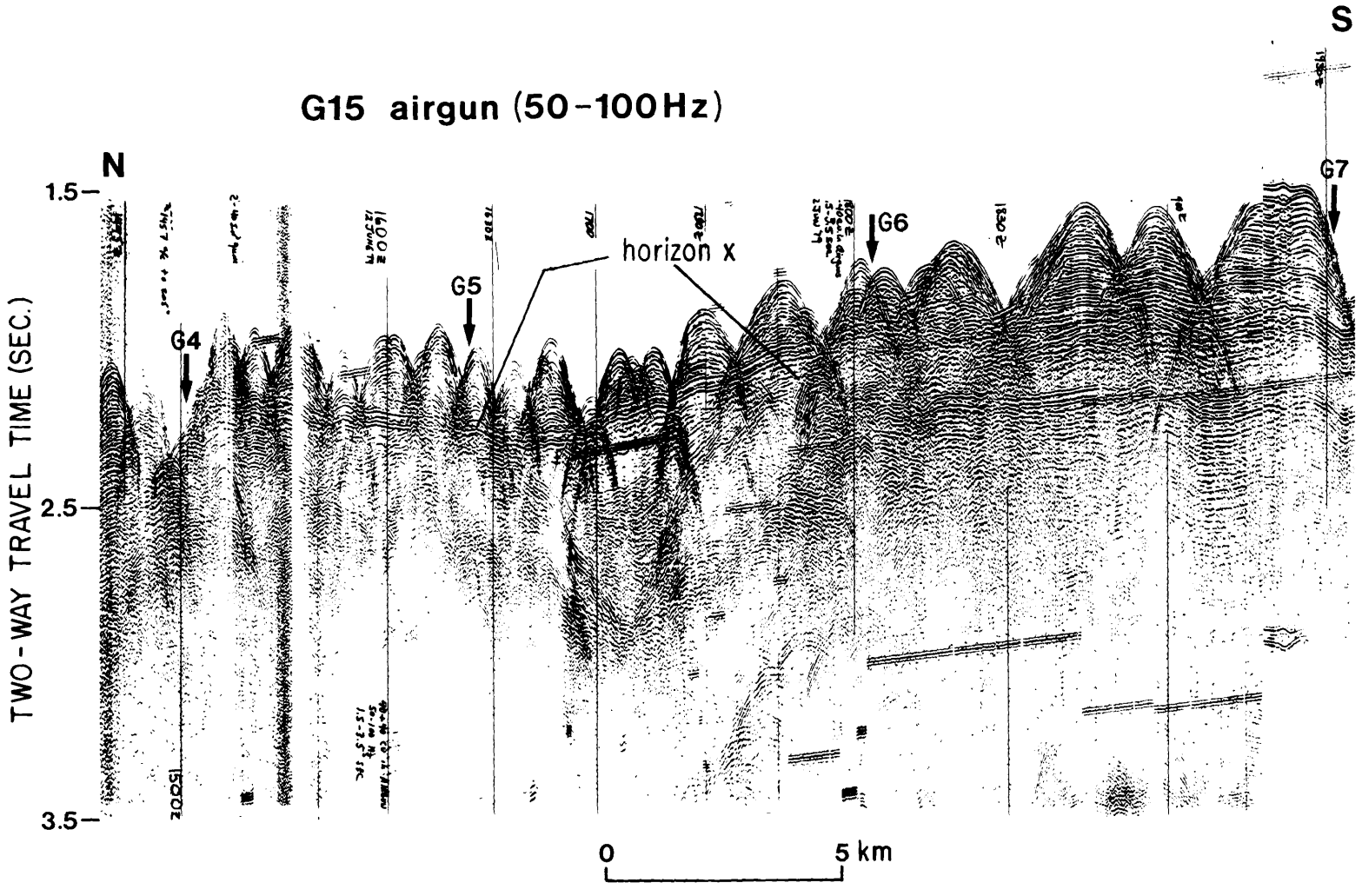

Figure 19. Profile G15 (airgun) shows horizon x along strike beneath midslope (from approximately 1,200-1,500 m depths). Note trough and disrupted reflectors in the lower-slope unit. Vertical exaggeration ~ 9:1.

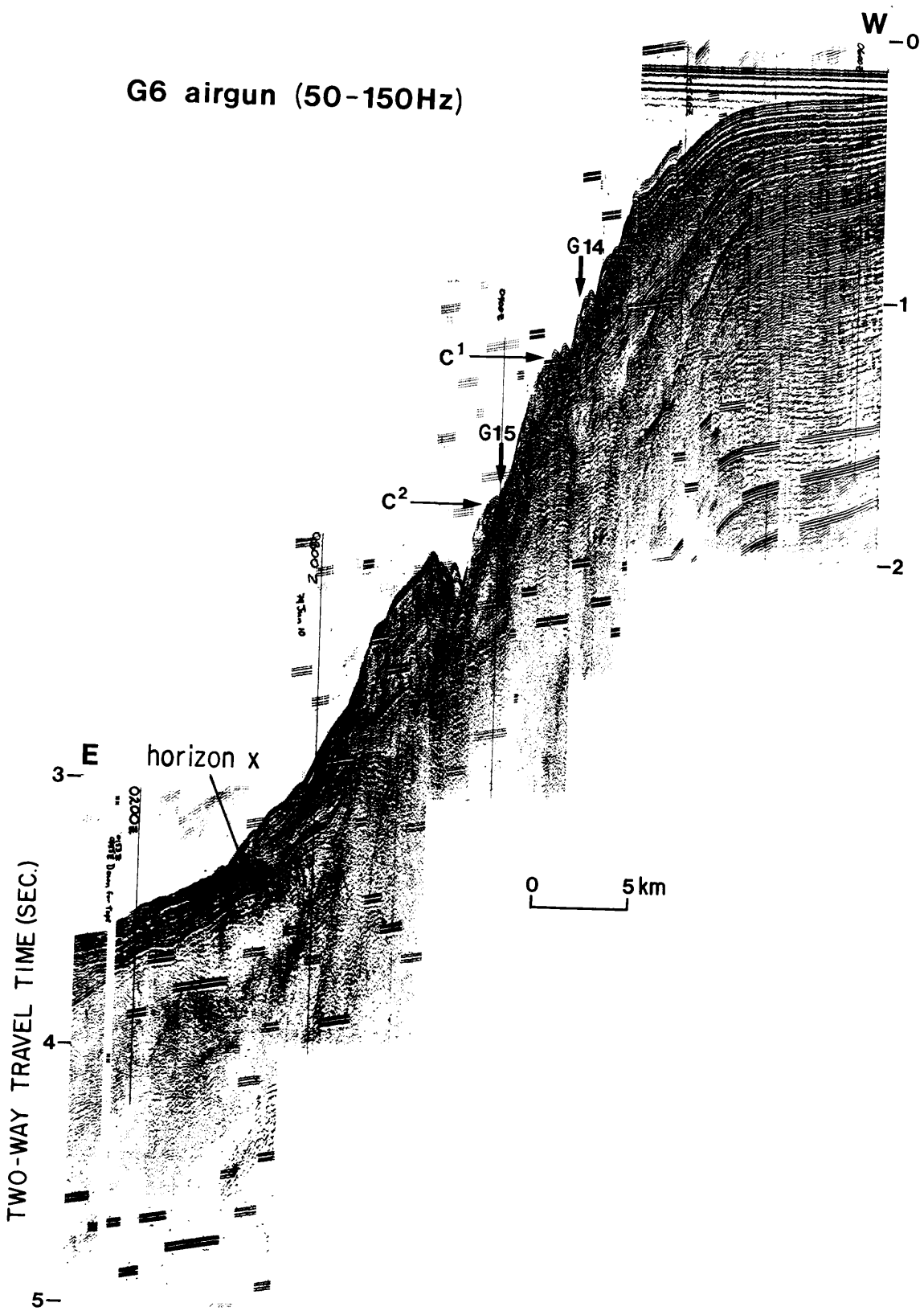

Figure 20. Profile G6 (airgun) shows deformation beneath lower slope (cf. fig. 19). Vertical exaggeration 19:1.

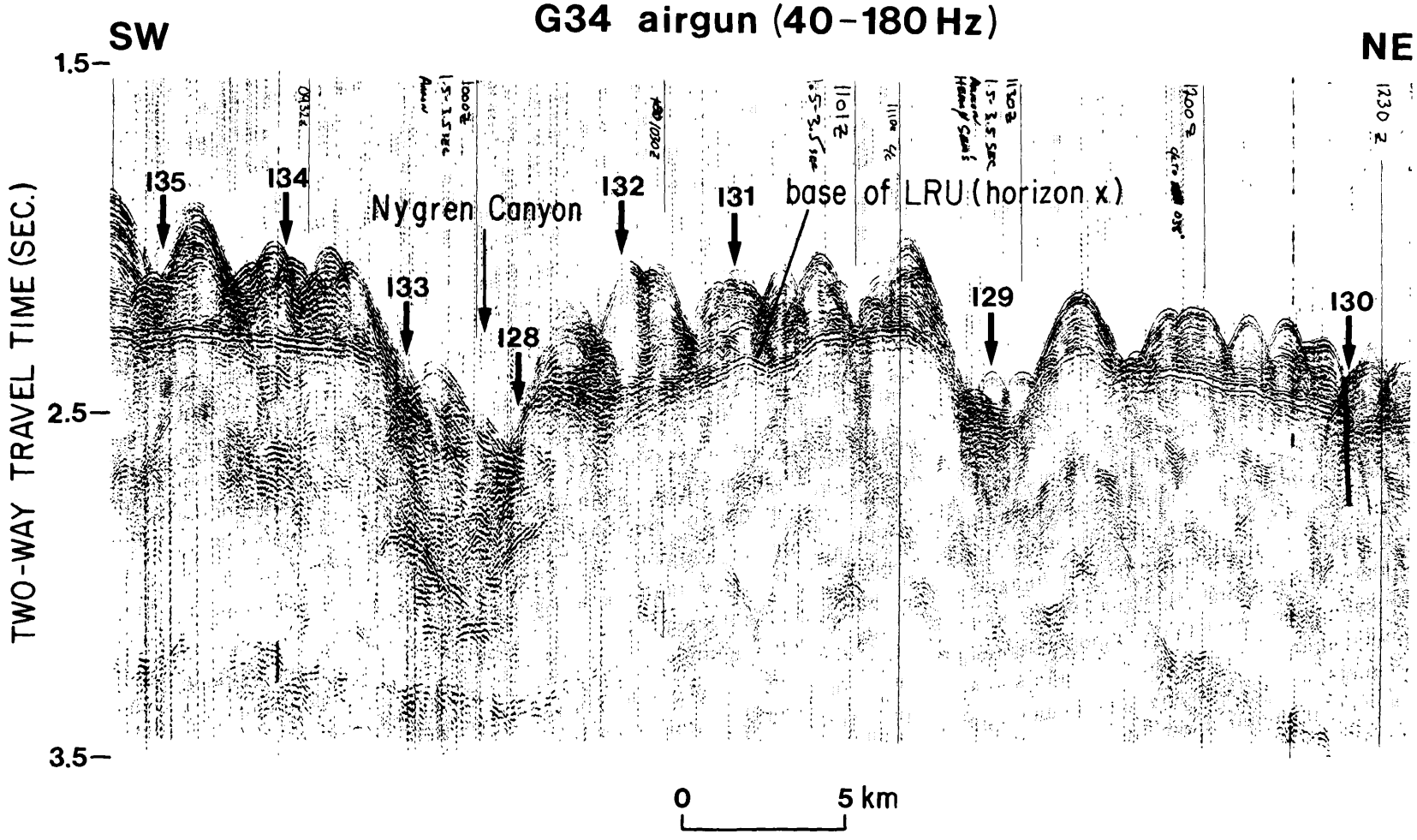

Figure 21. Profile G34 (airgun) shows eroded layered rise unit unconformably on lower-slope unit; unconformity is penetrated by Nygren Canyon at 1130Z (I29); inferred fault shown at I30. Vertical exaggeration ~ 14:1.

hyperbolic echoes that originate between 860 m and 1,050 m depths. Line I26 (fig. 16) shows that the hyperbolae at C^2 are side echoes and that the steep, rectilinear slope profile above C^2 actually extends down to 1,140 m across (or beneath) the hyperbolic echo trace originating above C^2. This suggests that in some profiles C^2 may represent the eroded updip end of layered rise sediment which partly buries the rectilinear slope surface (and consequently obscures the deeper reflectors of the upper-slope unit) to depths as shallow as 860 m. Deep incision in the slope below this point greatly obscures the seismic stratigraphy along strike.

The slope segment between points C^2 and C^3 has been eroded into ridgelike and, less commonly, buttelike (i.e., flat-surfaced or broadly convex) forms oriented upslope and downslope. Nested hyperbolae along steep, smooth ridge slopes indicate that the deep downslope incisions are fringed by closely spaced but relatively shallow extended lateral gullies, especially in the deep, steeply incised basin of Nygren Canyon (map C).

The onlapping layered rise unit is well shown in dip line G16 (fig. 22), where it is seen to have a thickness of about 240 m at its upper extent. Where best preserved, the layered rise unit approaches 340-m thickness. The very low-angle truncated reflections seen in some lines suggest two nearly conformable subunits. West of line I27 there is increasing evidence for tonguing members low in the layered rise unit. The unit becomes progressively more conformable with depth, and on the rise below 4,000 m, it is a relatively thin (153 m) conformable unit in many places scarcely distinguishable from underlying layers. West of 66°20'W. the layered rise unit abruptly thickens and flattens between 1,800 m and 1,950 m depths (figs. 13, 16)

Structure and mass movement

Profile G1 (fig. 17) shows that the Continental Slope in sector I is the eroded dip slope of a monocline constructed, presumably, of Cenozoic strata. In places the monoclinal structure seems to be greatly deformed, mostly seaward of inflection C^2. Two generations of deformation seem to be present. Above the unconformity that marks the base of the layered rise unit, beds are warped, broken, collapsed and, in places, thinned and apparently cut out downdip (fig. 13). Earlier block rotation and/or translation beneath (or within the lower levels of) the layered rise unit has almost totally obliterated the deeper stratigraphic continuity in some lines (fig. 20).

The confused structure seen in the dip lines is not as evident in the relatively undistorted strike lines. Conversely, the relatively smooth-surfaced dip profiles contrast with the deeply notched surfaces of the strike lines. These features imply that major mass-movement features are aligned downslope; and on strike they are relatively restricted in their lateral dimensions. Nevertheless, discrete mass-movement features are difficult to discern on the distorted lower slope.

The individual mass movements that are identifiable seem to have involved decollement deformation. For example, sparker line G9 (fig. 23; cf. fig. 3, B) shows an incipient collapse slump. About 90 m of evenly laminated reflectors lie on a thin, transparent to diffuse layer showing weak internal hyperbolae. This, in turn, lies on a thin interval of very fine, continuous, parallel reflectors which overlie an interval of bolder, more contrasty

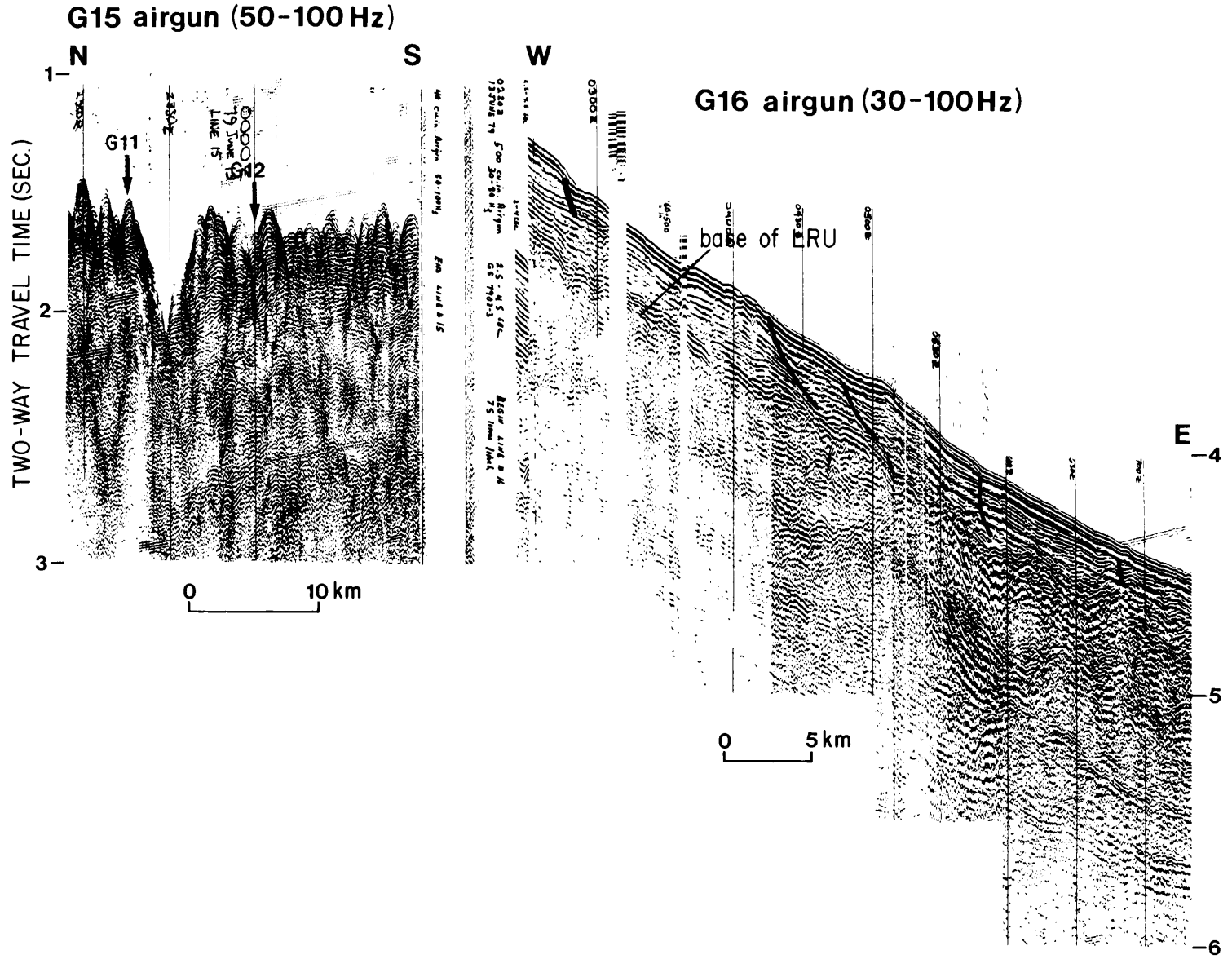

Figure 22. Profile G15-G16 (airgun) shows closely incised midslope surface along strike (G15) and smooth downslope surface (G16). Heavy curved lines indicate inferred listric faults above deformed strata.

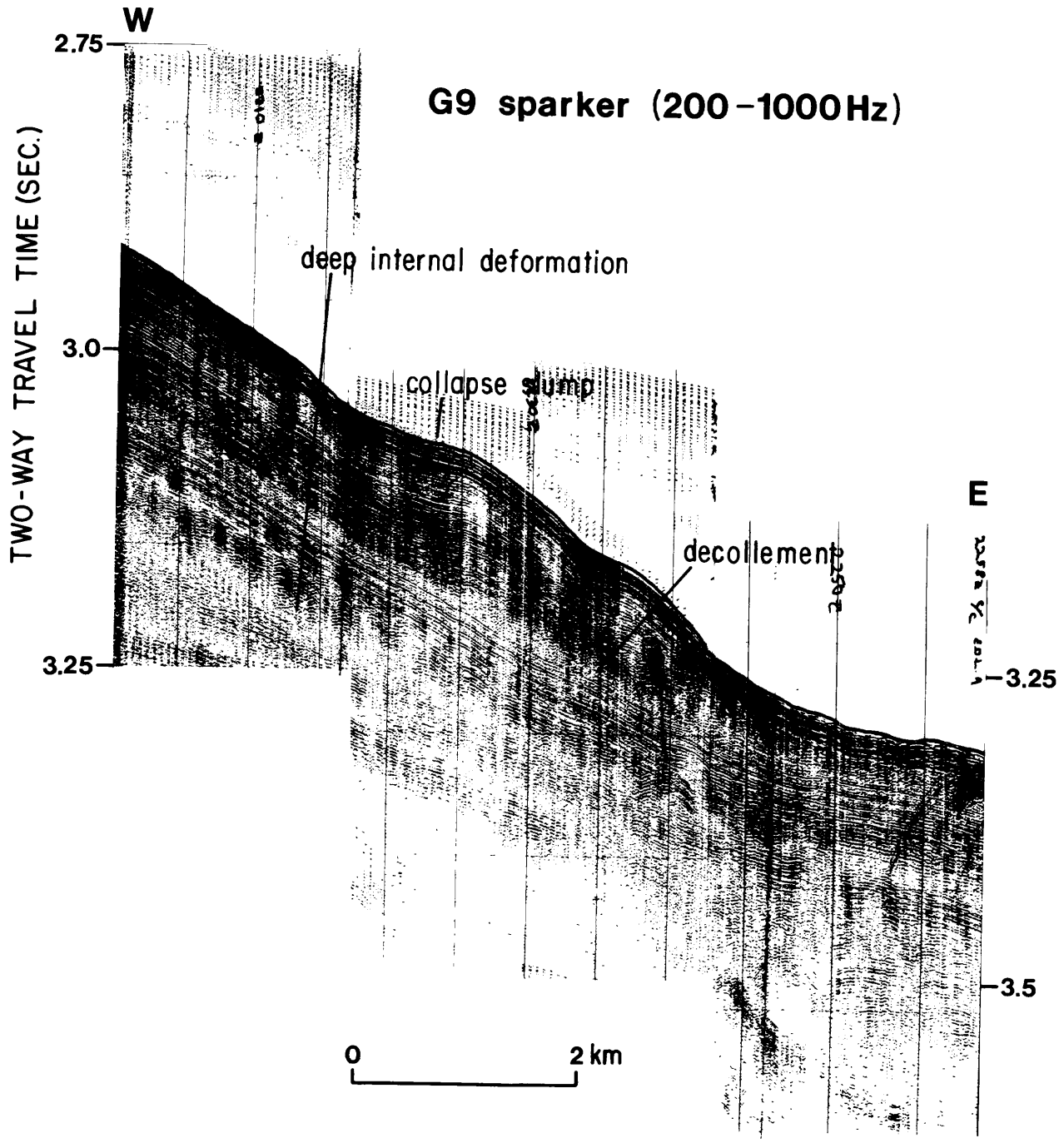

Figure 23. Profile G9 (sparker) shows decollement structure in layered rise unit. Mass movement incorporates features of carpet slide and collapse slump. Vertical exaggeration ~ 15:1.

hyperbolae. The 90-m capping unit is bulged and rumpled downdip and pinches out updip on the transparent layer across a concave slope at 2,250 m depth. The separation of structure implies that the hyperbolae indicate internal deformation, possibly tight folds in the top of the incompetent transparent unit or displacement along the contact in the overlying unit, which is probably flexed and fractured from top to bottom here. The underlying layered unit shows no such deformation.

In contrast, the uppermost 125 m of sediment on the lower slope crossed by line G1 (fig. 24) is expressed as isolated acoustically transparent masses overlying weakly layered material. The masses possibly represent remnants of slab slides. If the surface irregularities that generate the hyperbolae shown in figure 24 are caused by displacive structure (e.g., wedging, graben) rather than simply by erosional incision, the masses are probably allochthonous. Sea-floor observations are required.

Elsewhere in the eastern third of this sector, the upper levels of the inferred pre-Wisconsinan Pleistocene strata of the lower slope are disturbed by sliding, listric faulting, and internal deformation (e.g., figs. 22, 25).

The largest mass-movement feature in the sector is located between Nygren and Munson Canyons at a depth of 1,900 m (fig. 16). It involves the entire 350-m thickness of layered rise unit for a lateral extent of approximately 20 km, and a downslope extent of at least 35 km. The slide complex comprises a relatively deep, steep-sided trough (fig. 26, map C) floored with rubble that covers the unconformity at the base of the layered rise unit. Relief along the edge of the central trough is as great as 325 m.

Line I26 (figs. 16, 27) passes along the axis of the slide trough. It shows a layer of rubble about 70 m thick lying at three levels (fig. 27), the lowest of which (A) is the trough floor. Reflectors beneath the middle level (B) appear to correlate with reflectors in the upper 136 m of section beneath the upper level (C) (fig. 27). This implies that a thick rubble slide formed first, and that it was transected as material below 136 m in the section failed, leading the more competent upper part of the section, including the rubble slide, to subside as one or more large blocks. The great mass of removed material is probably spread out over the deeper rise as a fan-shaped blanket of progressively comminuted debris, part of which is represented by the rubble at level (A).

The trough is bordered upslope (fig. 16) and to either side (fig. 26) by a zone 5- to 10-km wide characterized by large, broken, slightly back-tilted blocks (or slabs) locally covered with surficial rubble. The blocks have apparently slid toward the trough axis consequent to the main slide, and in doing so generated peripheral rubble slides.

The east margin of the complex is bordered by a large fractured slab of layered rise strata, that extends eastward to Nygren Canyon (fig. 28). The slab is arched and broken over a culmination of the unconformity. On the east side of the culmination the deeper layers of the slab are structurally distorted; they seem to indicate slight translation toward Nygren Canyon (fig. 28). On the west side of the culmination a segment of the slab 7-km across and 250-m thick has slid on a dipping layer low in the section down toward the slide trough (fig. 26). Surficial debris partly fills depressions in the slid mass.

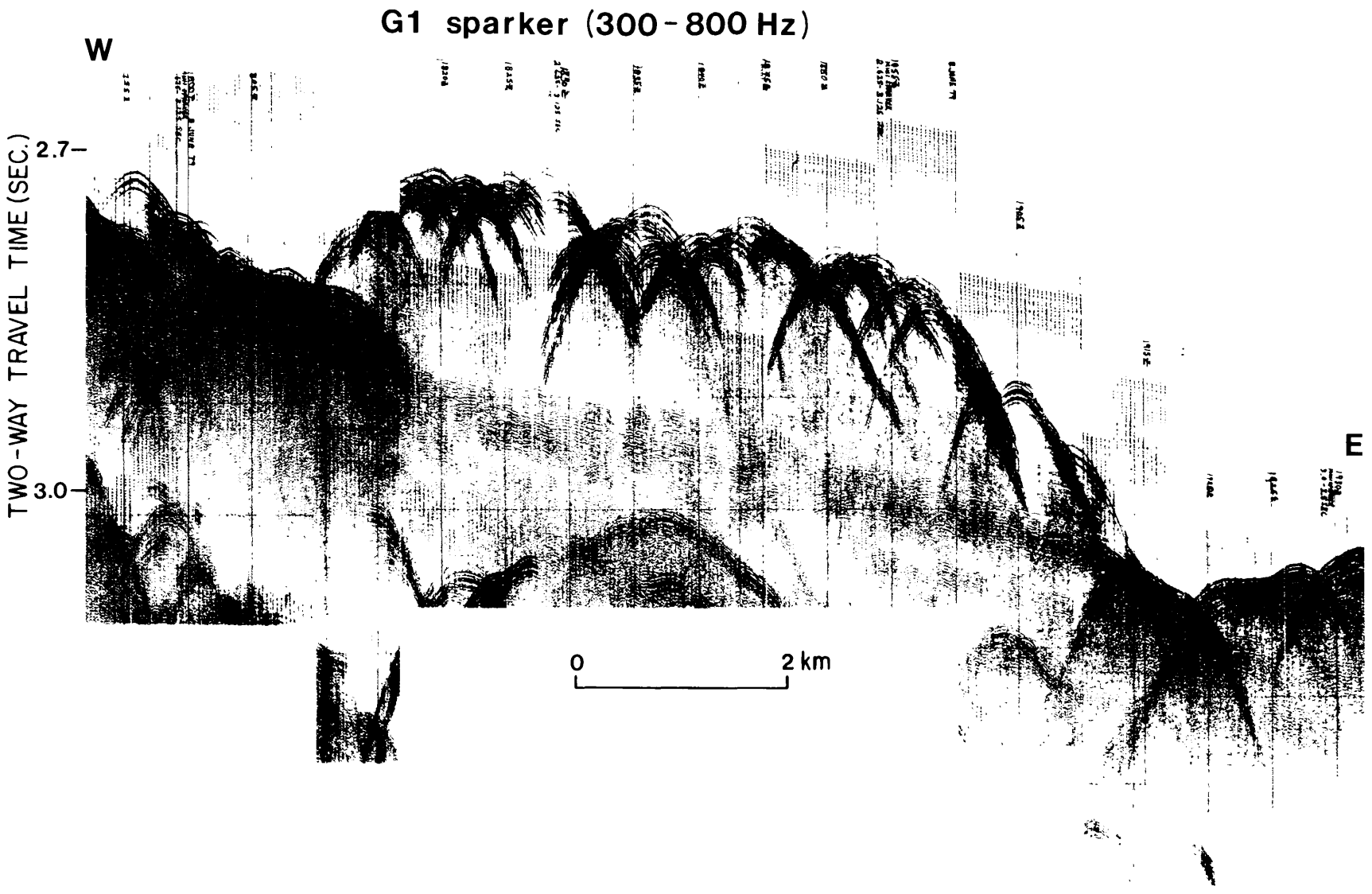

Figure 24. Profile G1 (sparker) shows large, isolated, possibly fractured, block of sediment (Pleistocene?) on weakly reflecting stepped surface. Possibly a block slide. Vertical exaggeration ~ 16:1.

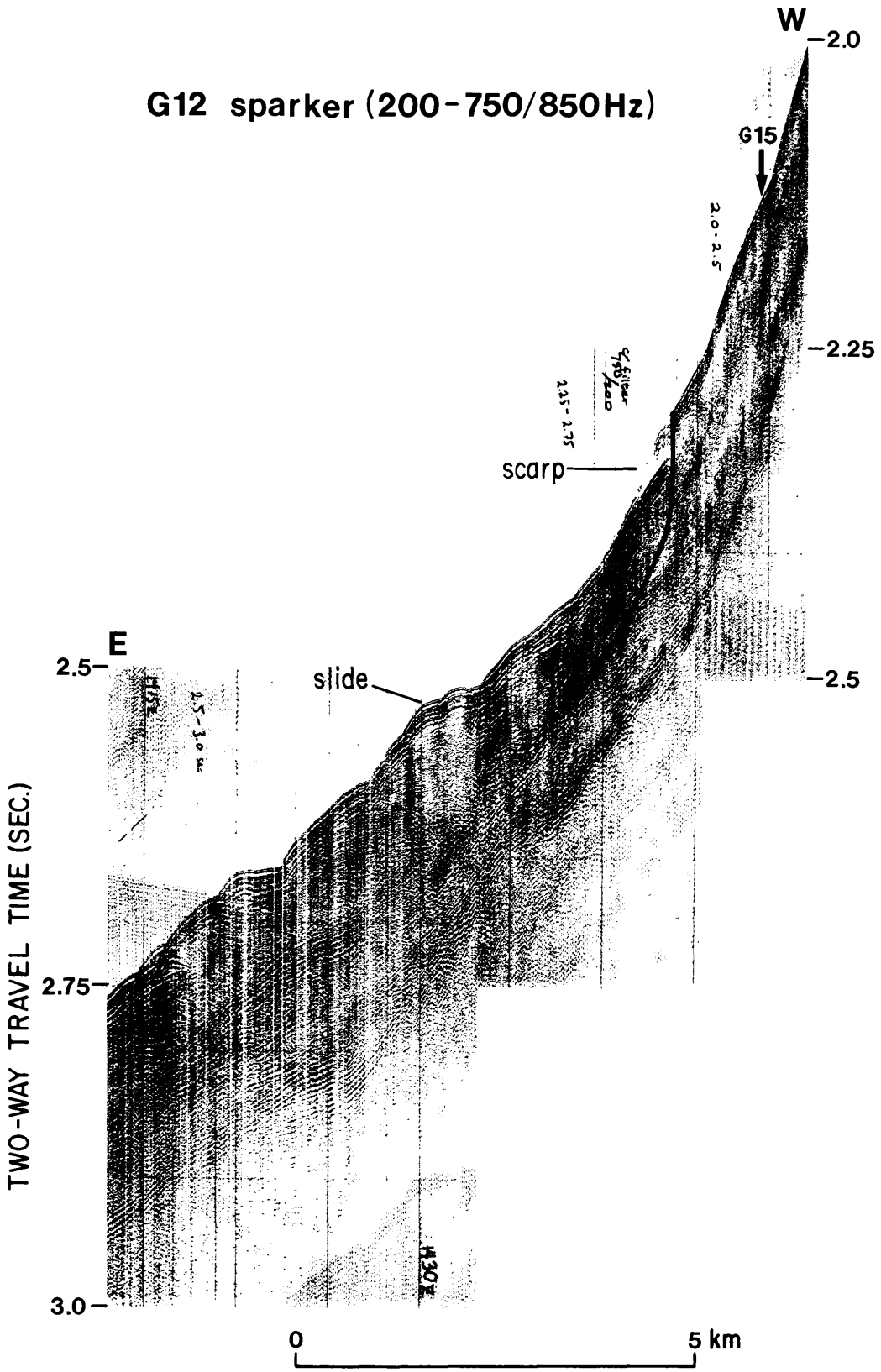

Figure 25. Profile G12 (sparker) shows inferred collapse slump and rubble slide/carpet slide on lower slope. Heavy line indicates inferred slip plane. Vertical exaggeration ~ 21:1.

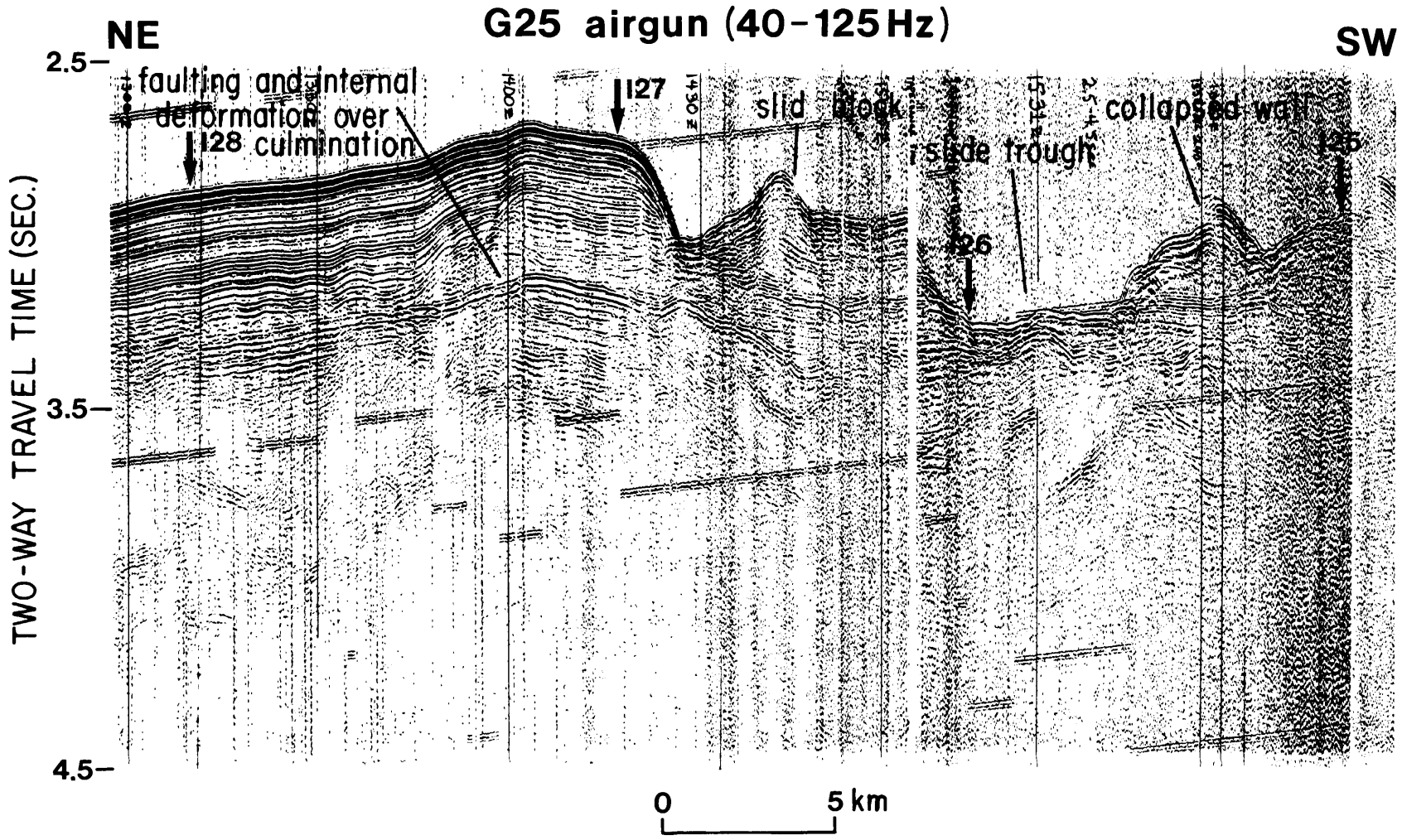

Figure 26. Profile G25 (airgun) shows section across slide trough between Munson and Nygren Canyons at approximately 2,350 m depth. Vertical exaggeration ~ 13:1.

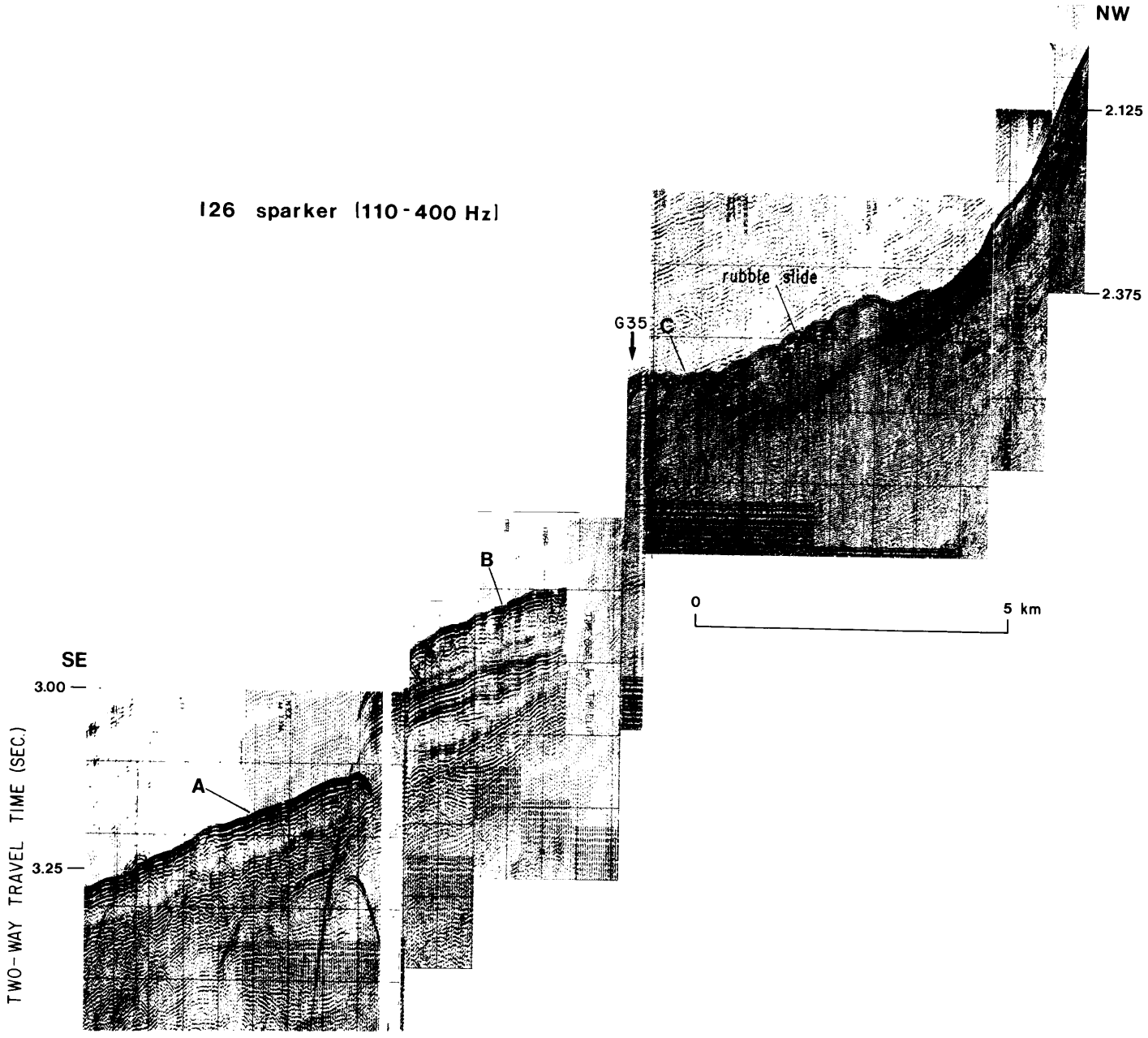

Figure 27. Profile I26 (sparker) shows three levels (A, B, C) of collapse, plus truncated rubble slide on uppermost level C. Vertical exaggeration ~ 16:1.

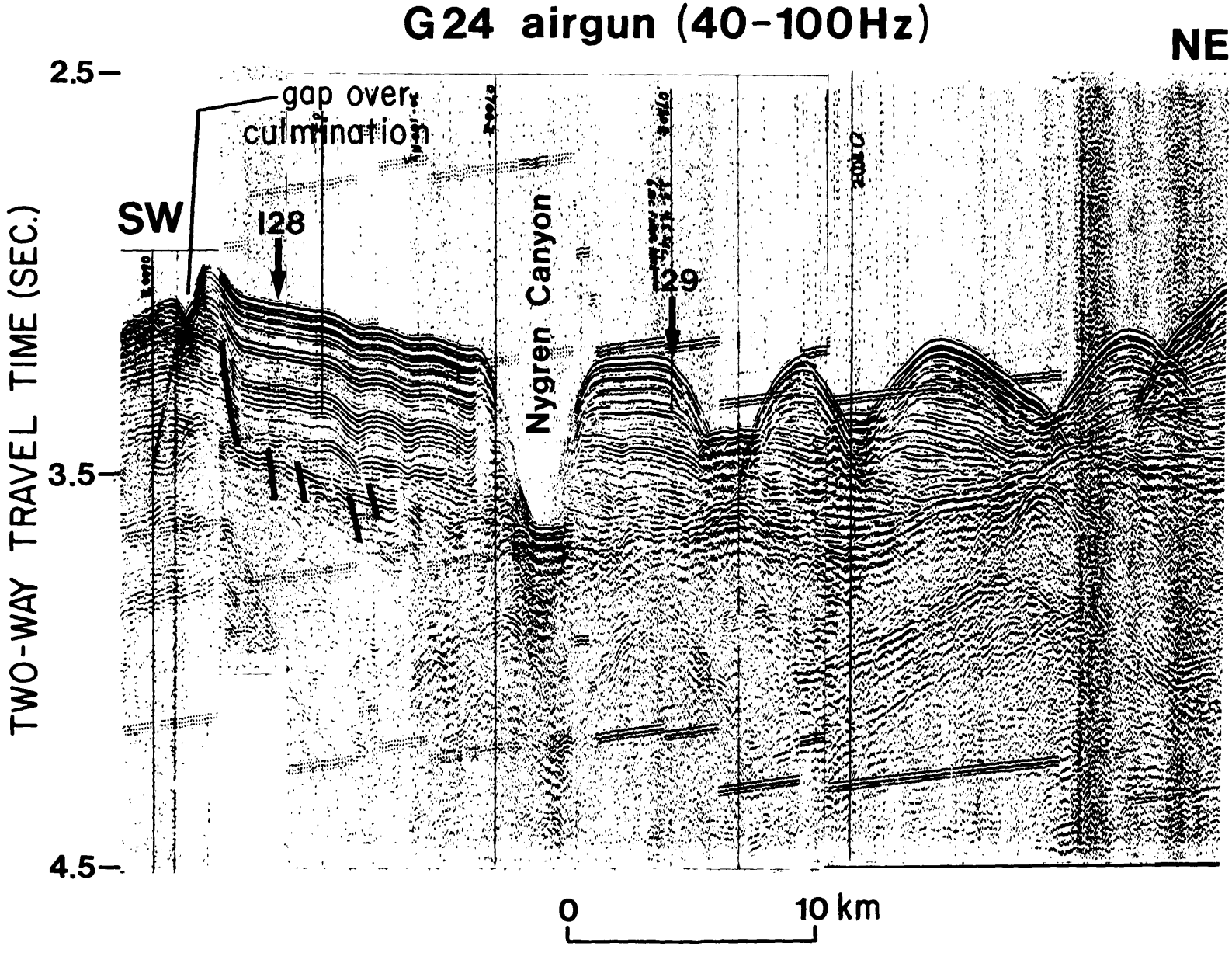

Figure 28. Profile G24 (airgun) shows separated or broken blocks of the layered rise unit near Nygren Canyon at approximately 2,500 m depth. Heavy lines indicate inferred faults. Vertical exaggeration ~ 22:1.

Lines I27A (fig. 29) and I25A (fig. 30) show the collapsed eastern and western border zones of the slide complex, respectively. They both show downfaulting and collapse of layered rise strata over and adjacent to culminations in the underlying lower-slope unit. Figure 32 shows that vertical fracturing and internal deformation have contributed to or resulted from collapse of the borders.

Collapse of the layered rise unit extends at least as far west as the ridge crest that borders the eastern flank of Munson Canyon (fig. 31). This implies that collapse postdates formation of the canyon. It is reasonable to assume that this collapse is related to, or at least contemporaneous with, the main slide complex crossed by line I26 (fig. 16). An examination of map C raises the possibility that the ridge crest flanking Munson Canyon was breached by collapse (fig. 32) and that sliding has affected the east wall of the canyon and partly filled the canyon (fig. 31). Navigational uncertainty (see appendix) precludes a definite interpretation here.

Along the outer shelf and upper slope in sector I, evidence of mass movement is highly questionable. Where the surficial layer descends over the rim of Munson Canyon, small slope breaks and changes in profile form suggest the effects of creep. These features probably could not be detected on the ground or at true scale. Faulting in the upper-slope unit is indicated by offset reflectors, abrupt reversals of dip, and wipeouts at inflections (fig. 33). BGR multichannel line 204 (fig. 34) shows that deeper faulting of a similar style occurs between Corsair and Georges Canyons. Its relevance to mass movement is uncertain. Beds of the foreset unit are displaced in what appear to be Toreva blocks bordering some of the incisions along the upslope margin of the basin of Nygren Canyon (fig. 35).

Sector II: Munson Canyon to 69°15'W.:
Lines I8 to I24, I39; G25, G34 to G45, maps C, D, E

General physiography

In sector II the transition from a conformable outer shelf to a truncational upper slope starts at a gradual convex rolloff between about 180-225 m depths, below which units dip more steeply and thin appreciably before being incised and truncated across an increasingly steepened upper slope, below depths ranging from 425 to 600 m.

The slope profile shows the same inflections seen to the northeast in sector I, but they are here more accentuated. Benchlike forms controlled by parallel layers of the upper-slope unit are present on the slope as deep as 970 m, but most are found above 750 m. A steep, rugged midslope extends from 750-950 m down to a lower slope contact which varies in form from an inflection to a cuesta marking the truncated updip end of the layered rise unit at 950-1,900 m. The point also marks a pronounced updip steepening of more deeply buried reflectors. The slope-rise transition is not seen in some profiles but is abrupt and as shallow as 1,900 m in others. It generally is present between 2,000-m and 2,475-m depths; at about these depths the layered rise unit thickens and becomes more nearly conformable with underlying strata.

For the most part, the lower slope is smoothly concave except in lines I21 and I23 (map C) where broad, flat inflections are seen between

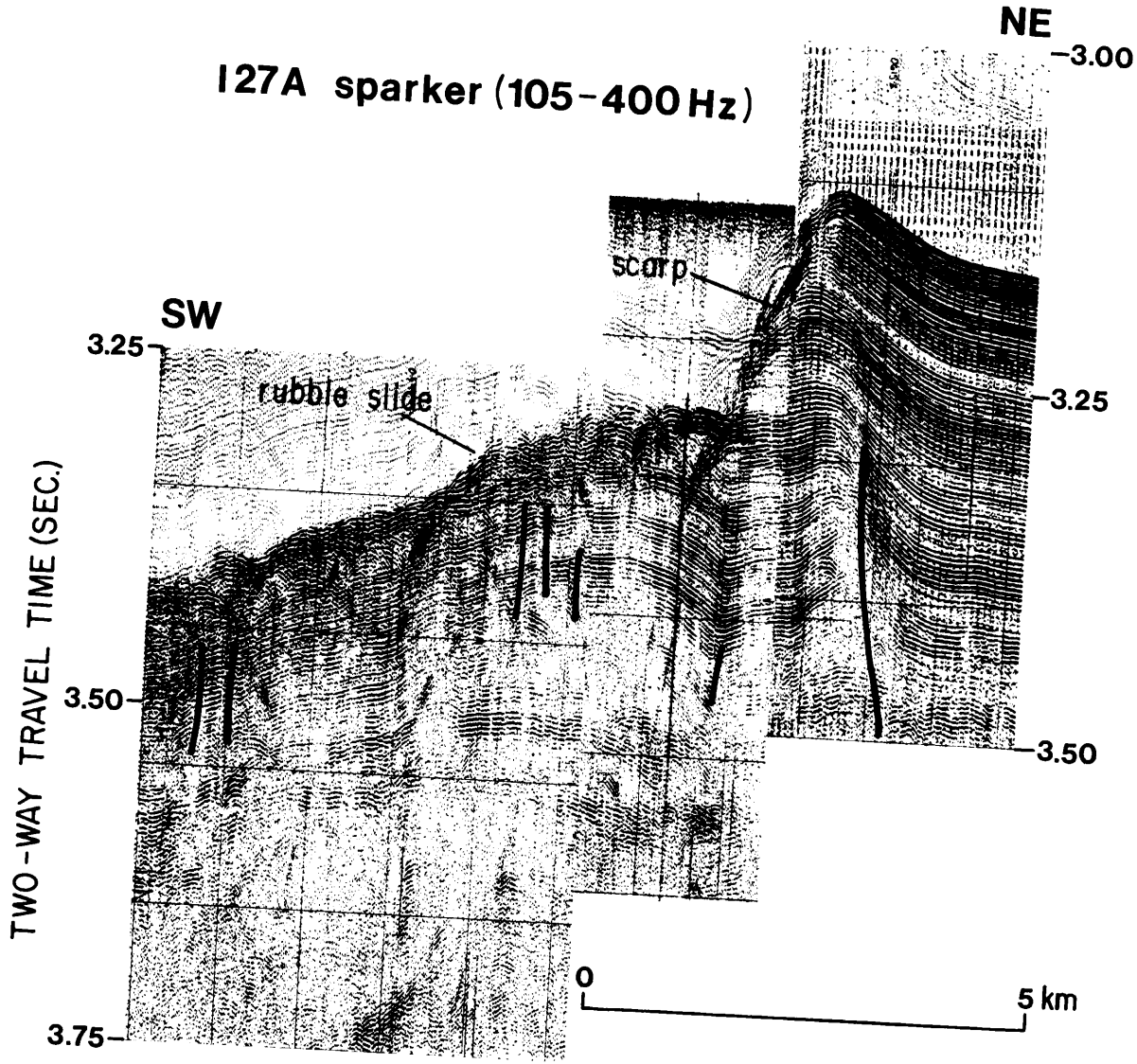

Figure 29. Profile I27A (sparker) shows collapsed east margin of slide complex at approximately 2,500 m depth; heavy lines indicate inferred faults. Vertical exaggeration ~ 21:1.

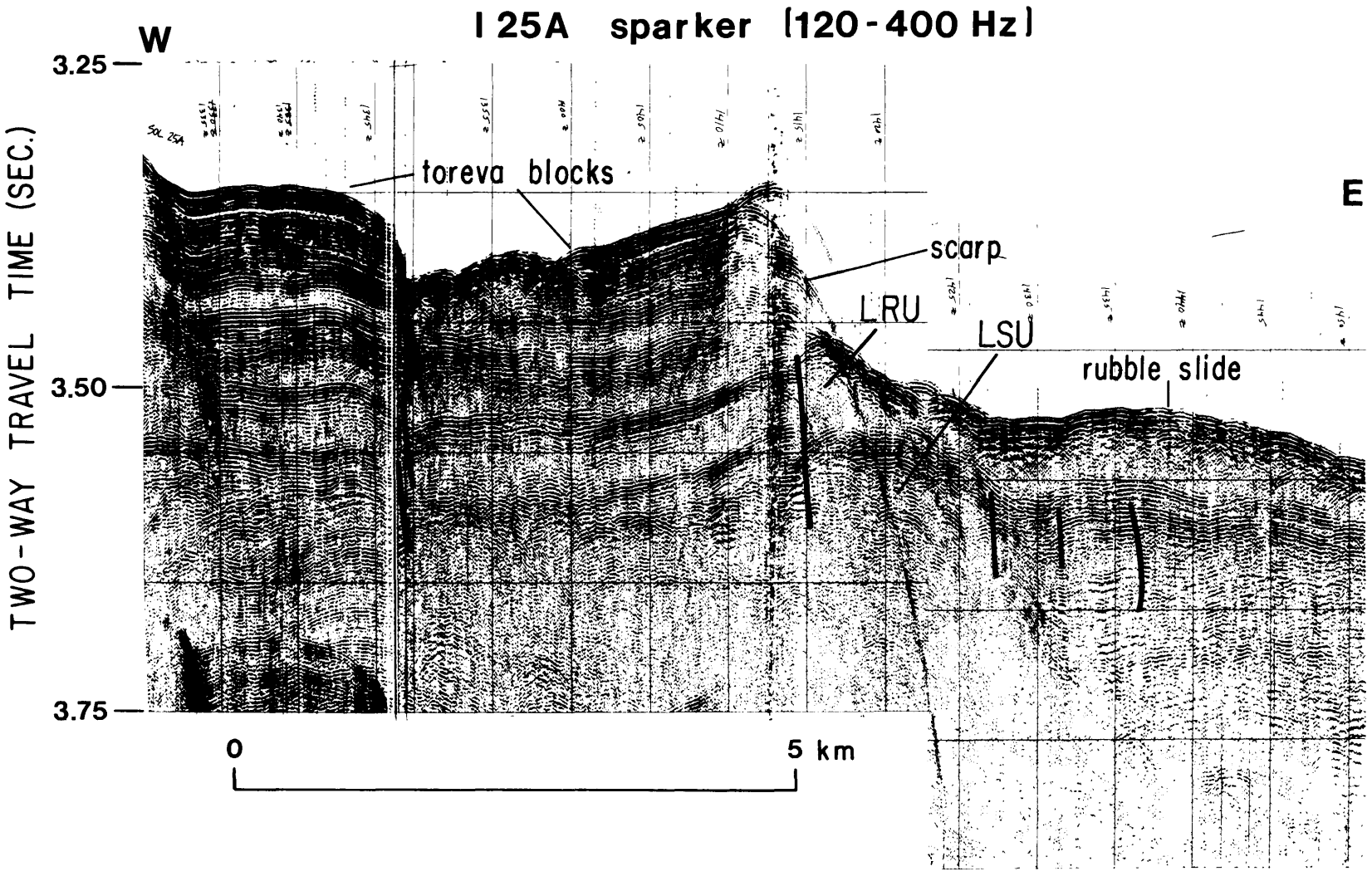

Figure 30. Profile I25A (sparker) shows collapsed, downfaulted western margin of slide complex at about 2,500 m depth. Collapse has occurred across a culmination in the lower-slope unit (LSU), probably because of failure of an incompetent layer at the base of the layered rise unit (LRU); heavy lines indicate inferred faults. Vertical exaggeration ~ 16:1.

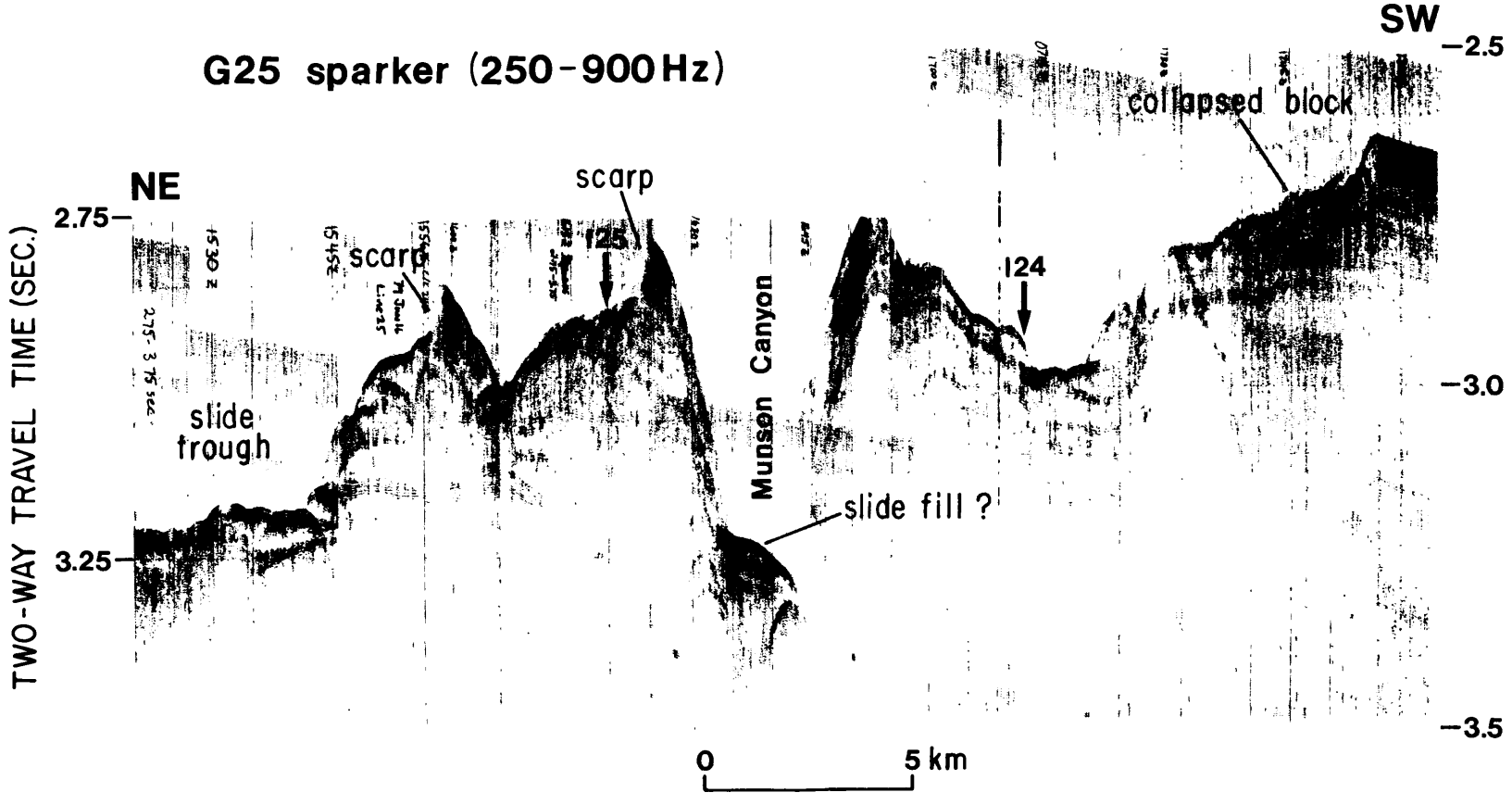

Figure 31. Profile G25 (sparker) across western margin of slide trough shows collapse along east flank of Munson Canyon (at I25) at about 2,250 m depth. Vertical exaggeration ~ 22:1.

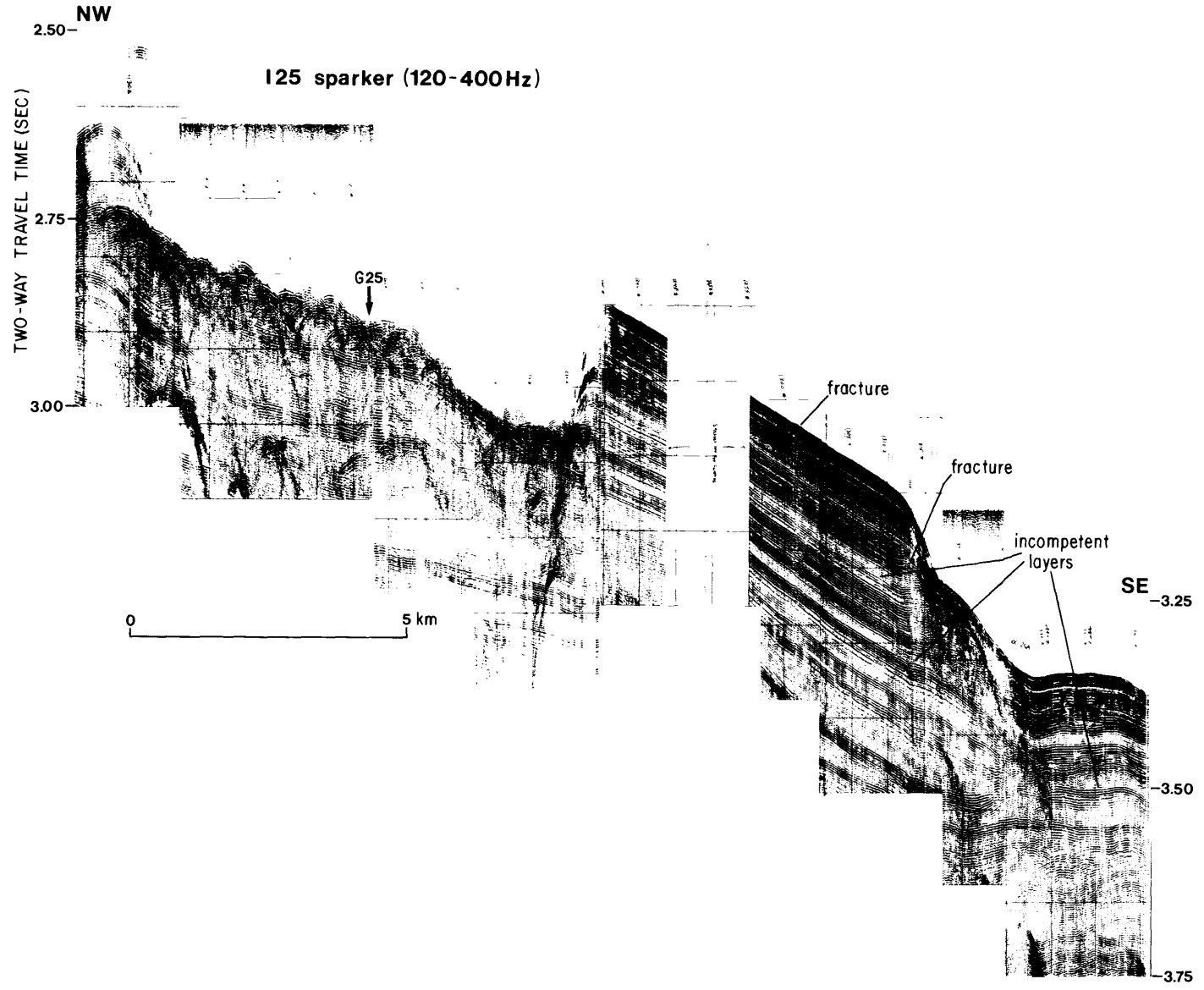

Figure 32. Profile I25 (sparker) along or near crest bordering east side of Munson Canyon at approximately 2,250 m depth. Slide extends into or away from canyon, or both. Southeast end of profile shows collapsed part of layered rise unit. Note subtle distortions in incompetent nearly transparent layers. Unit is cut by vertical fractures which may have initiated distortion leading to collapse. Vertical exaggeration ~ 18:1.

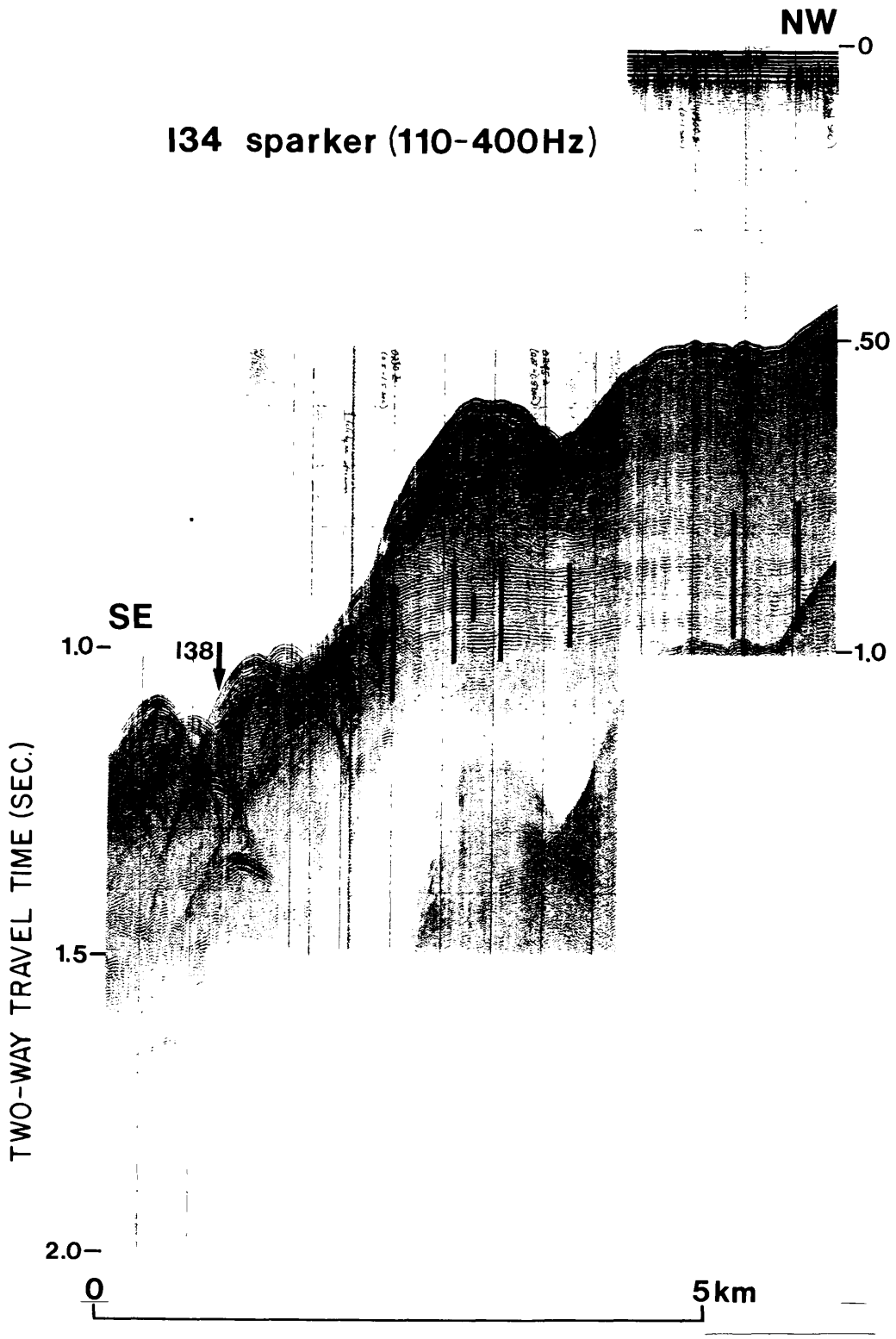

Figure 33. Profile I34 (sparker) shows faulted(?) (heavy lines) upper-slope unit. Vertical exaggeration ~ 7:1.

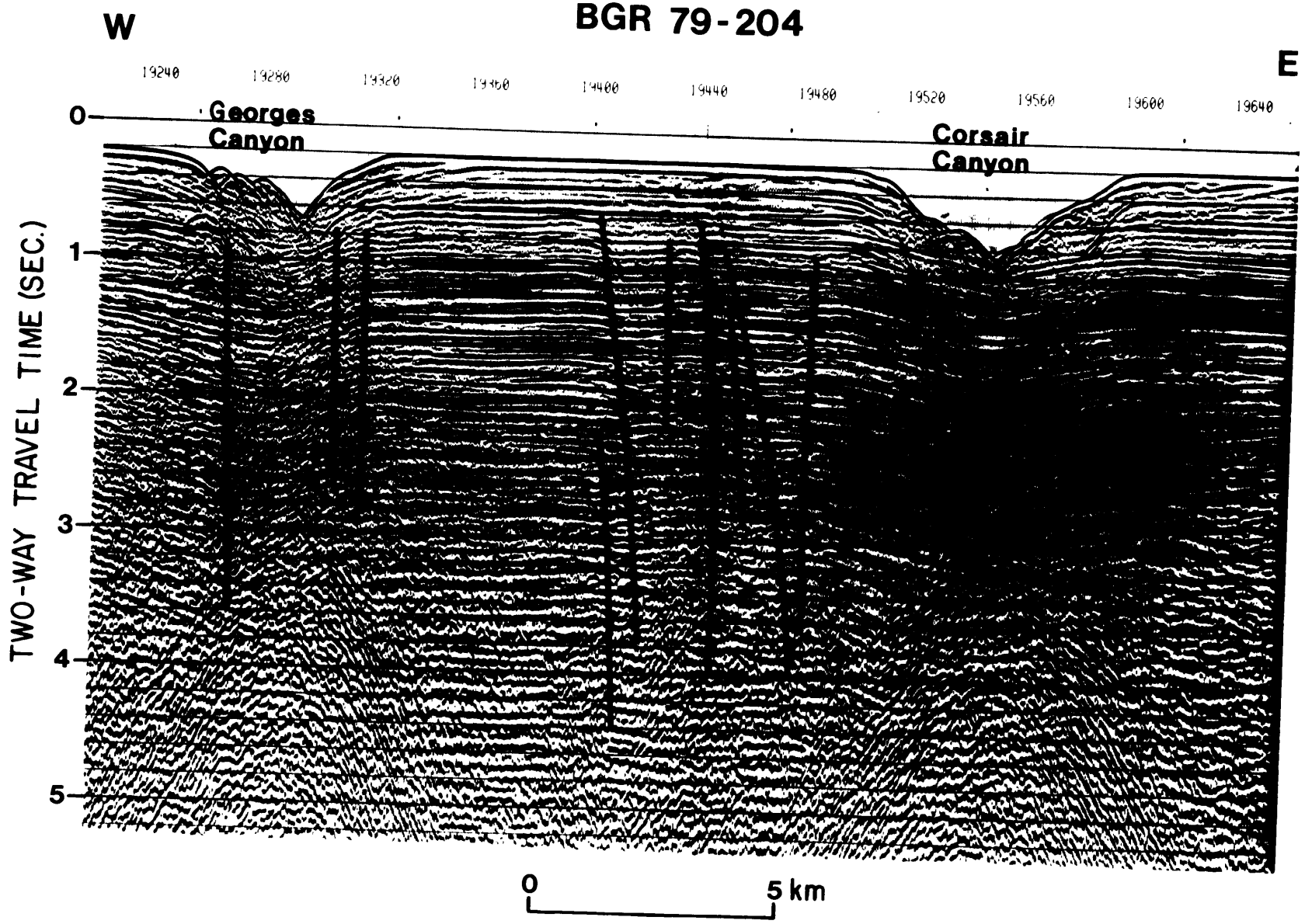

Figure 34. BGR line 204, multichannel seismic profile, shows transverse faults beneath outer shelf west of Corsair Canyon, between 150-200 m water depth.

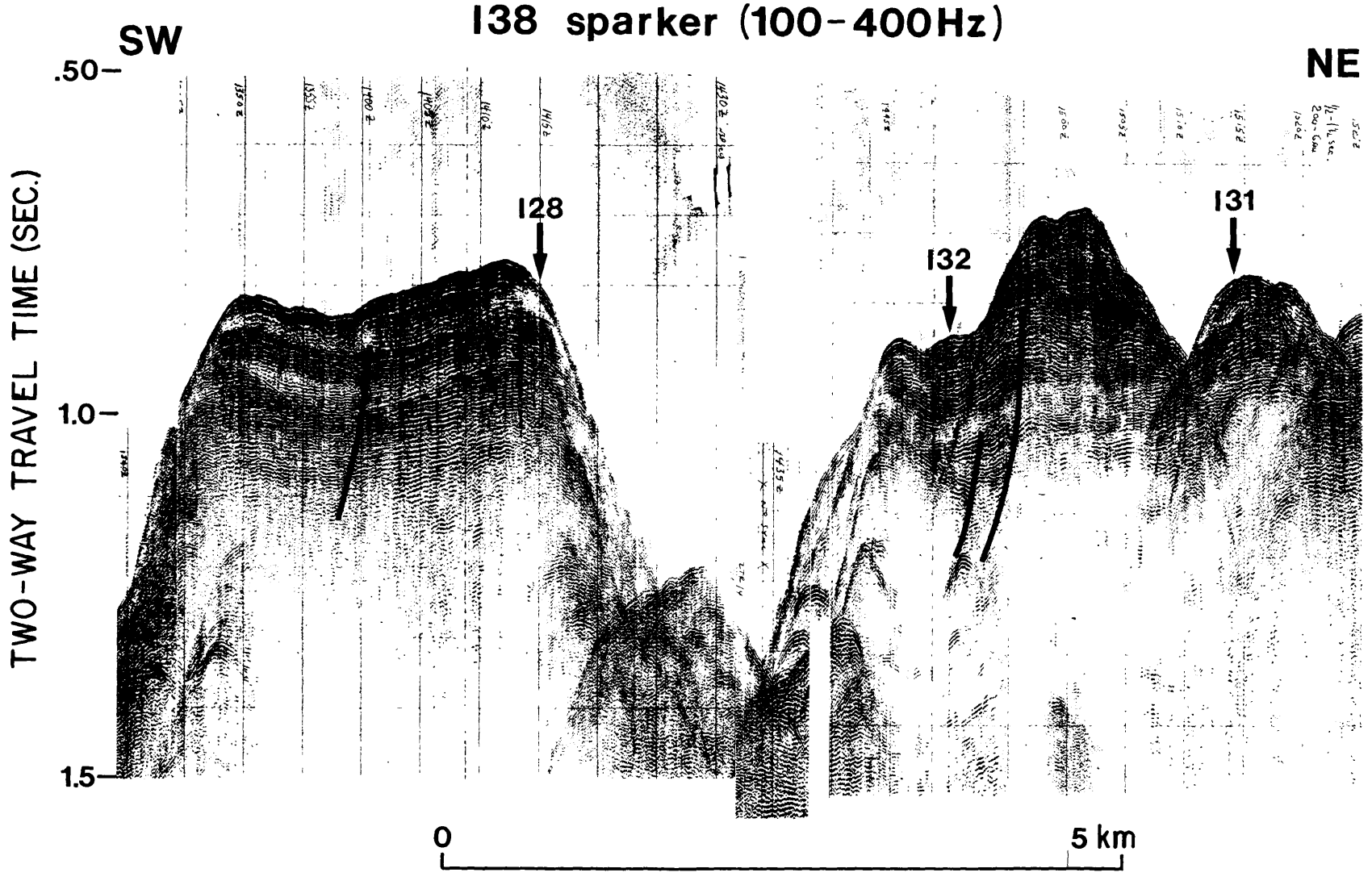

Figure 35. Profile I38 (sparker) shows Toreva blocks along incisions leading to Nygren Canyon. Trackline along upper slope at water depths between 500-700 m. Heavy lines indicate inferred slip planes. Vertical exaggeration ~ 7:1.

1,650 m and 1,800 m depths, as in sector I. Around these depths the layered rise unit flattens, thickens, and overlies a small trough or basinal form aligned along the slope. This feature is also seen in profile I17, at 2,175-m depth, where it is cut by Gilbert Canyon.

Toward the western end of the sector the middle to lower slope is cut by deep transverse incisions separated by long ridgelike or buttelike elevations. The incisions coalesce downslope to become broad troughlike forms; the intervening ridges become subdued and narrowed. Among these incisions are the largest shelf-indenting canyons along the northern U.S. continental margin: Lydonia, Hydrographer, and Oceanographer Canyons (fig. 8). Other formidable canyons are present that do not indent the shelf or do so only slightly, such as Munson, Powell, Jigger, Welker, Dogbody, and Gilbert Canyons. Local slopes associated with these canyons dominate the forms in this sector. The canyons themselves vary greatly in physiographic character: Welker Canyon is a distinct midslope trough; Dogbody Canyon is a ramified basin, similar to Nygren Canyon in sector I. Hydrographer Canyon is a simple, shallow, steep-walled notch cut into an older surface; it shows no evidence of colateral terrain or convergent slopes. With increased slope depth the canyon forms and relief become less pronounced.

Form and stratigraphy

Here, as in sector I, the surficial layer lies in broad eroded swales or on a beveled contact which probably represents a wave-cut surface. Presumed scouring and resedimentation along the distal end of the surficial layer complicates the upper part toward the west. Internal structure includes unusual cut-outs and dip reversals, probably related to late Pleistocene outwash transport through Great South Channel.

AMCOR hole 6014 (Hathaway and others, 1976) penetrated the surficial layer at a position crossed by line I21 (map C). Samples obtained from the upper 16.5 m of sediment suggest coarse channel deposits. Below this depth to the base of the layer at 35 m, sandy to silty clay including shell fragments was encountered.

In general, the distal margin of the surficial layer is expressed by a ramp (fig. 36) that descends from a depth of about 108 m to 145-150 m. West of line I23 (map C) the ramped front of the surficial layer appears to be displaced 17 km landward [illegible] from the position seen east of the line. The bathymetry on map C [illegible] he impression that the ramp has been scoured back [illegible] rents). West of Lydonia Canyon the ramp is less [illegible] layer is perhaps thinned by erosion (fig. 36); in [illegible] forms a very gradually thinned wedge that is [illegible] lf or upper-slope brow.

[illegible] unit, the westward component of dip gradually [illegible] itional packages occupy thinner intervals updip [illegible] ward the western end of the sector, the foreset [illegible] e (fig. 36). Below about 195- to 225-m water [illegible] ntially a relict depositional surface of the [illegible] eepens it typically becomes more irregular and [illegible] and at about 345-m depth the surface is rather

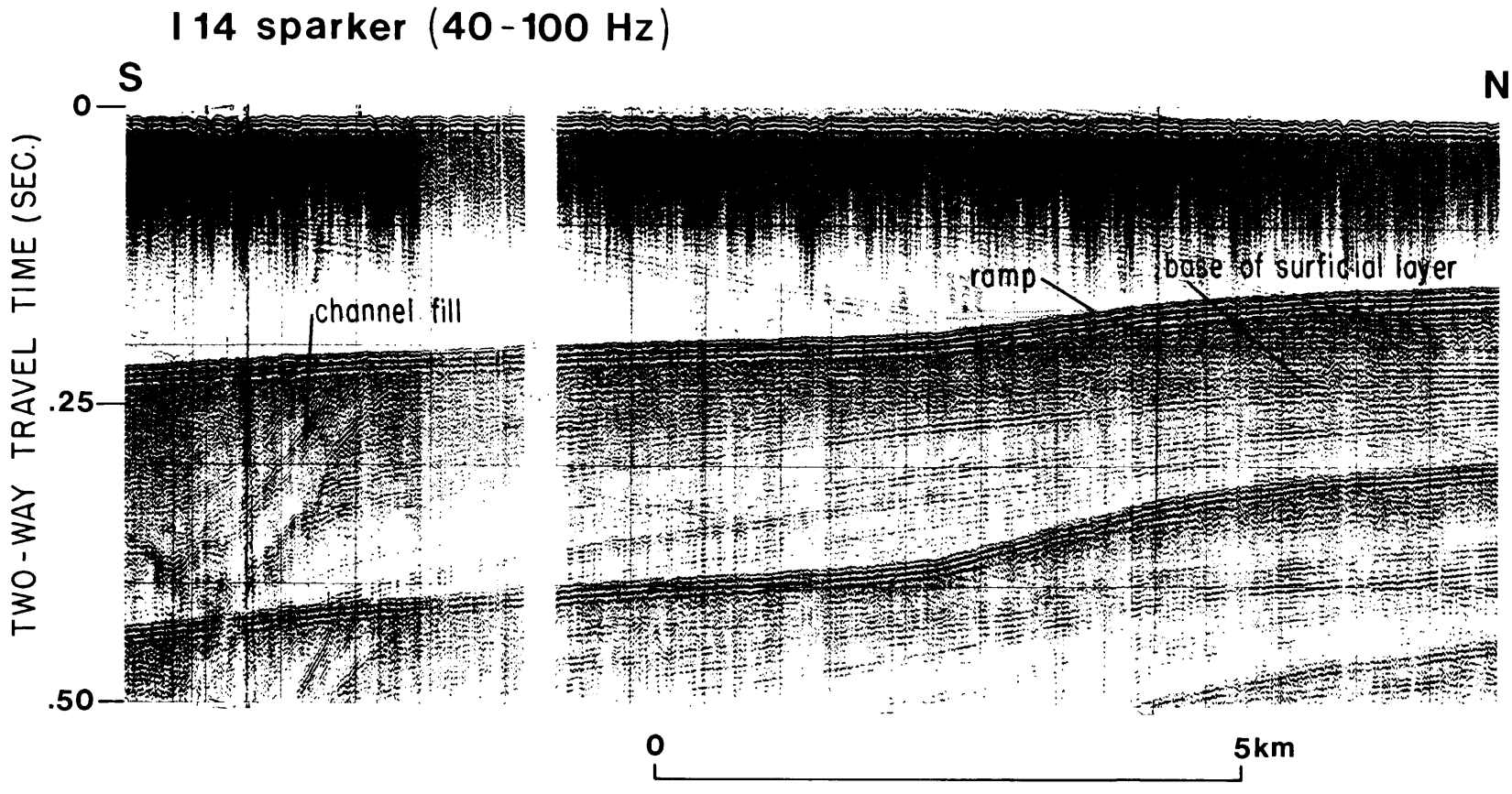

Figure 36. Profile I14 (sparker) shows beveled surficial layer unconformable on beveled homoclinal layers of the foreset unit, and filled channel in foreset unit.

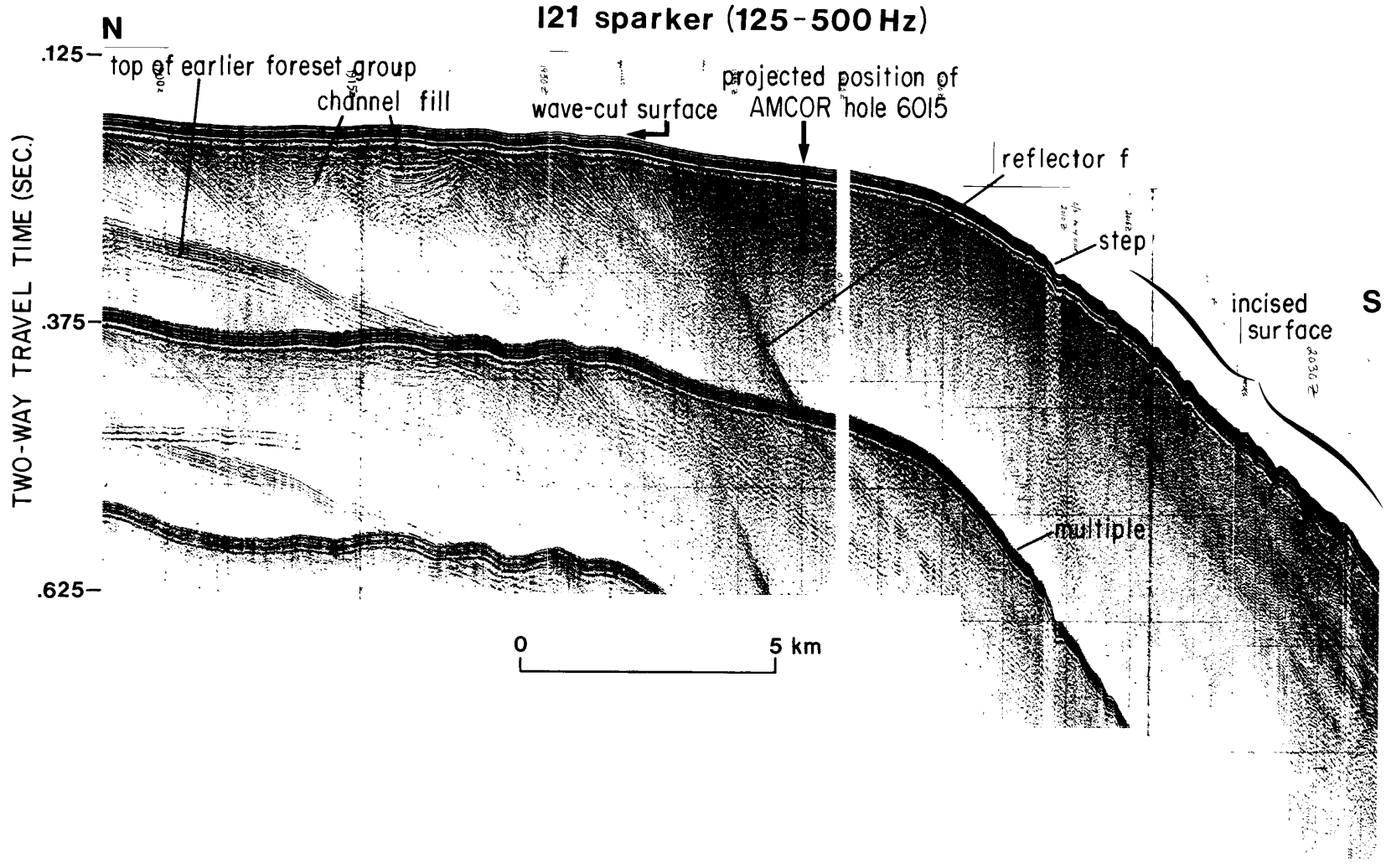

Figure 37. Profile I21 (sparker) shows "festoon" foreset package underlying outer shelf brow. Note that updip ends of beds are beveled by the descending incised slope surface. Vertical exaggeration ~ 14:1.

AMCOR hole 6014 (Hathaway and others, 1976) penetrated 67 m into one of the lower depositional groups of the foreset unit. The sediment, which is as old as early Pleistocene (Hathaway and others, 1976), includes very dark-gray, fine-grained, silty quartzose sand, fine-grained calcareous sandstone, micaceous sand, and coarse pebbly sand with large shell fragments. The hole may penetrate the extreme updip end of a horizon that is marked downdip by a prominent reflector 225 m beneath the 145-m isobath. Above this reflector are perhaps three foreset packages cut by channel fills.

Filled channels in the foreset unit are numerous between Lydonia and Oceanographer Canyons (figs. 36, 37, 38). The head of Gilbert Canyon is flanked by complex cut-and-fill structures. Channel fill at least 150-m thick underlies the swale that forms the northeast reentrant at the head of Gilbert Canyon (fig. 39). Perhaps two generations of channel fill are shown in figure 39, as the smooth, rounded bottom and shoulders of the swale are draped, not incised, whereas the channel fill to the north is apparently beveled by the same (i.e., drape) surface.

Line I17 (fig. 40) shows that the northwest side of Oceanographer Canyon, at about 140 m depth, is partly filled by sediment draped down off the shelf. As with Gilbert Canyon (fig. 39), the surface of the Oceanographer Canyon fill extends smoothly over the channel fill located beneath the shelf to the northwest. However, here internal stratification suggests that the fills are of the same generation, and most likely represent the basal part of the surficial layer (cf. fig. 36). At the head of Heeltapper Canyon (line I15) a 425-m-deep channel is cut in the foreset unit and the underlying upper-slope unit (fig. 41; cf. fig. 40).

In the western part of sector II the slope brow is underlain by a distinctive foreset interval (f, fig. 37) with an apparent dip of 2^{o}-3^{o}. It seems to crosscut or offlap older, less steeply dipping strata of the foreset unit, and it extends as an unconformable interval across the slope and onto the rise (fig. 42). It may be younger than or coeval (at least the lower part) with the beveled channel fills. AMCOR hole 6015 (Hathaway and others, 1976; map C; fig. 37) penetrated 62 m into this interval. Sediment is mainly dark-gray silty clay, dark-gray to dark-brown very fine sand, and olive-gray silty clay. Nannofossils indicate a pre-Wisconsinan Pleistocene age, and the unit contains many reworked Late Cretaceous nannofossils (Hathaway and others, 1976). Line I21 indicates that the downdip base of this interval should crop out between 525 and 750 m on the slope. Within this depth range in Oceanographer Canyon (at 690 m), Valentine and others (1980) recorded pre-Wisconsinan Pleistocene blue-gray clay and silty clay containing Emiliani huxleyi and Gephyrocapsa sp.

In this sector, the top of the upper-slope unit is marked by a thin, persistent, well-layered interval (a-b, fig. 43) that seems to be more resistant than the overlying foreset unit. A thicker interval (b-c) of continuous, parallel reflectors lies conformably beneath a-b (fig. 43).

A projection of inferred Miocene and Eocene horizons from apparent dips recorded in Fay lines T and P (Lewis and others, 1980) to the east of Dogbody Canyon suggests that the top of the Eocene lies no shallower than 480 m beneath the 200-m isobath (assuming Vi = 2,000 m/s). Thus, the top of the well-layered interval (a-b) of the upper-slope unit, which everywhere in this sector is at about this level, is inferred to be Eocene.

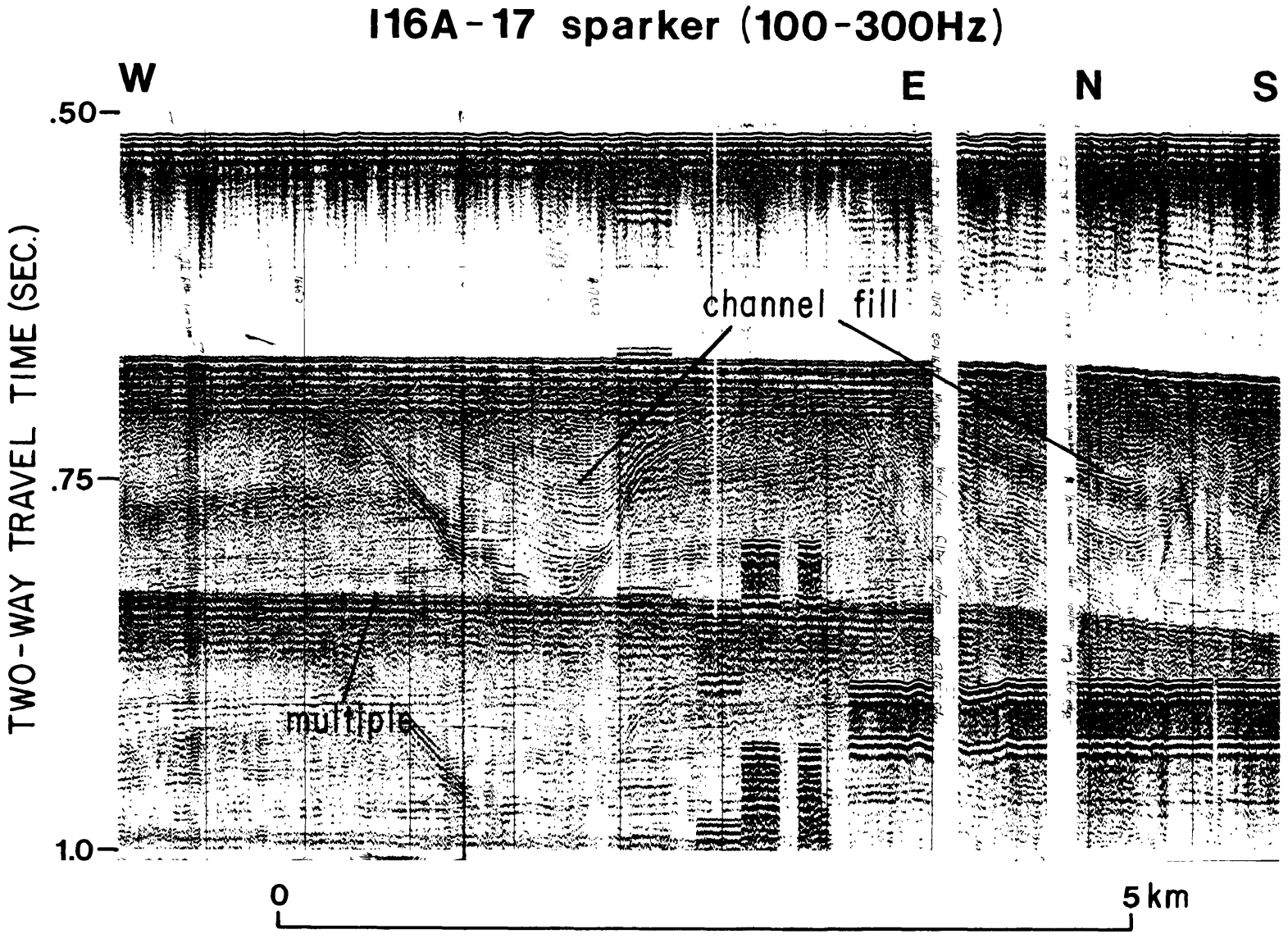

Figure 38. Profile I16A-17 (sparker) shows filled channels in the foreset unit.

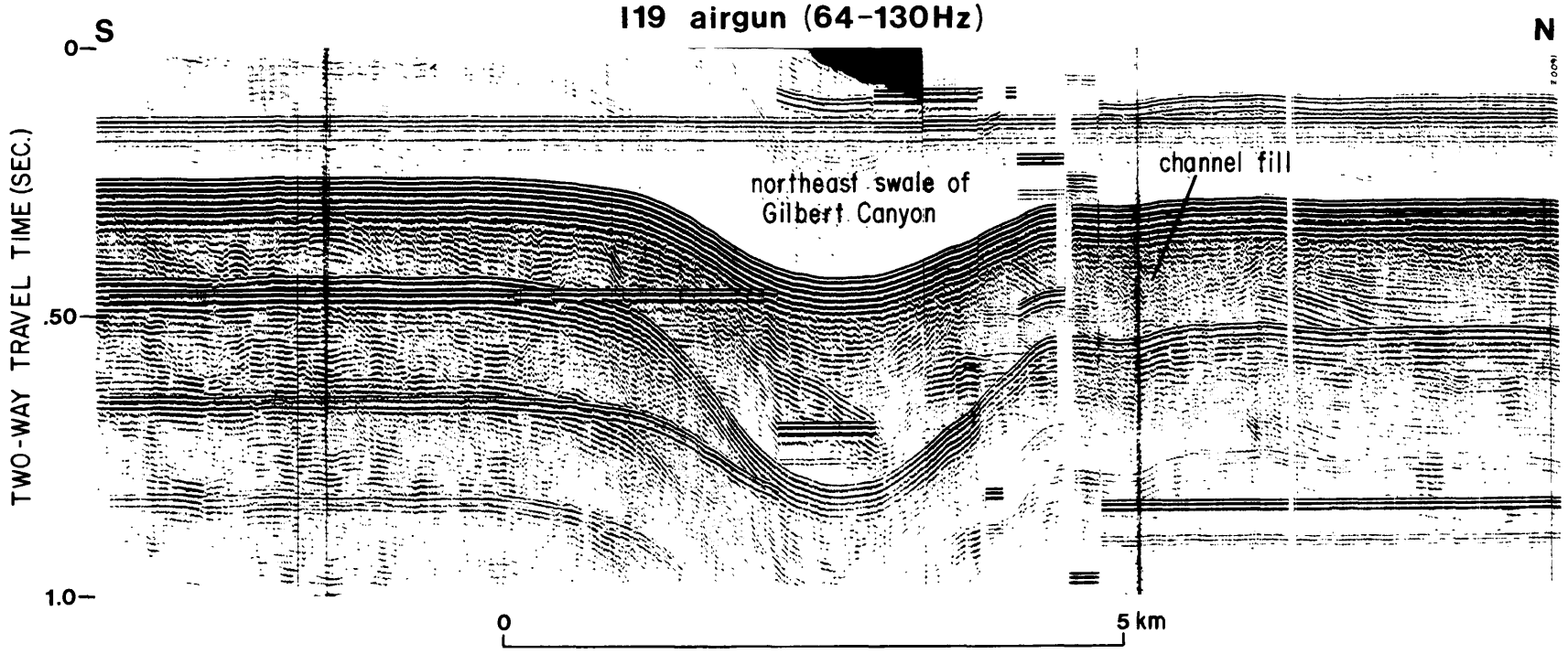

Figure 39. Profile I19 (airgun) shows draped, partly filled northeast swale at head of Gilbert Canyon and adjacent beveled channel fill to north.

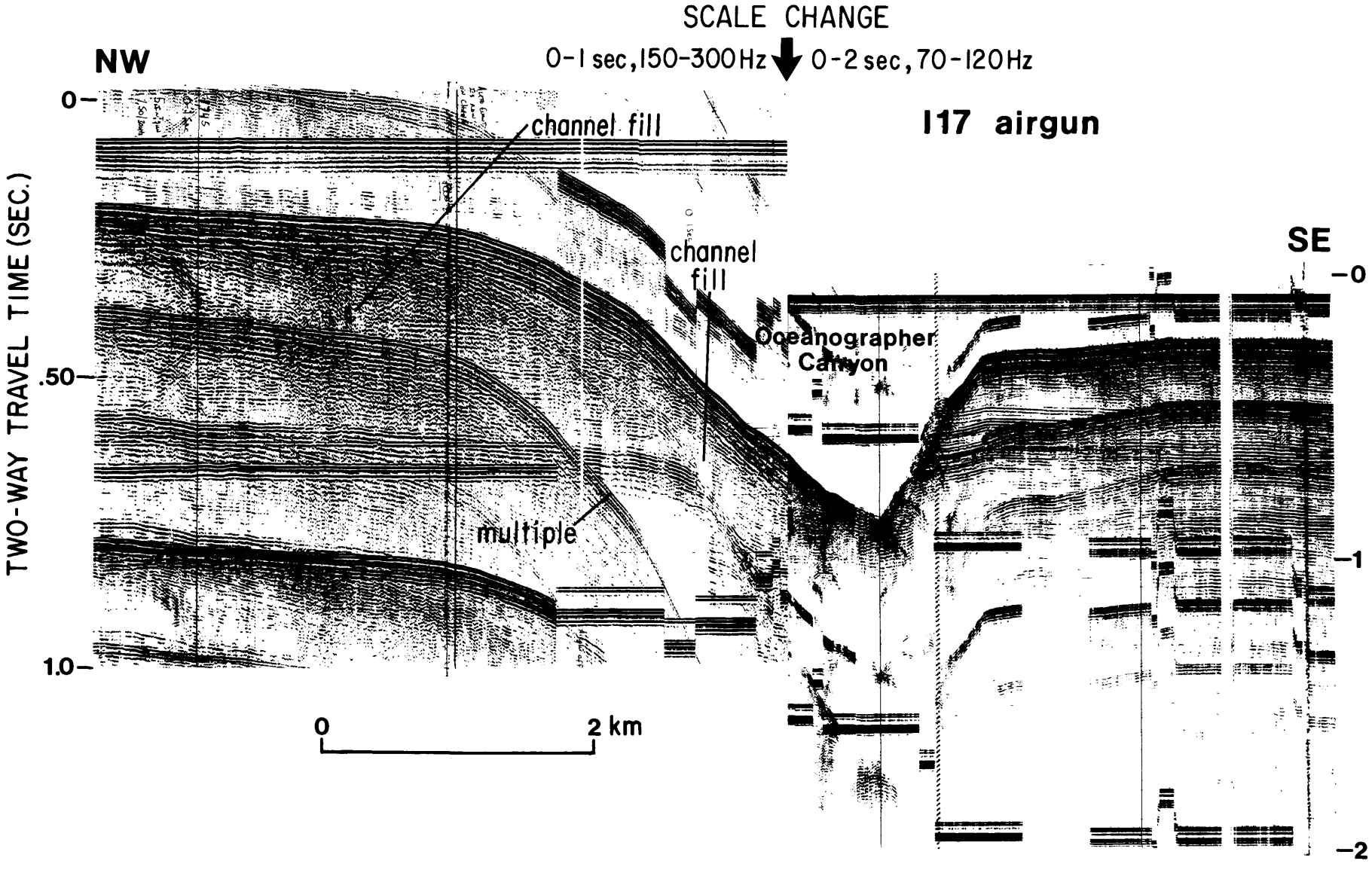

Figure 40. Profile I17 (airgun) shows sediment infilling northwest side of Oceanographer Canyon at around 140 m depth on outer shelf.

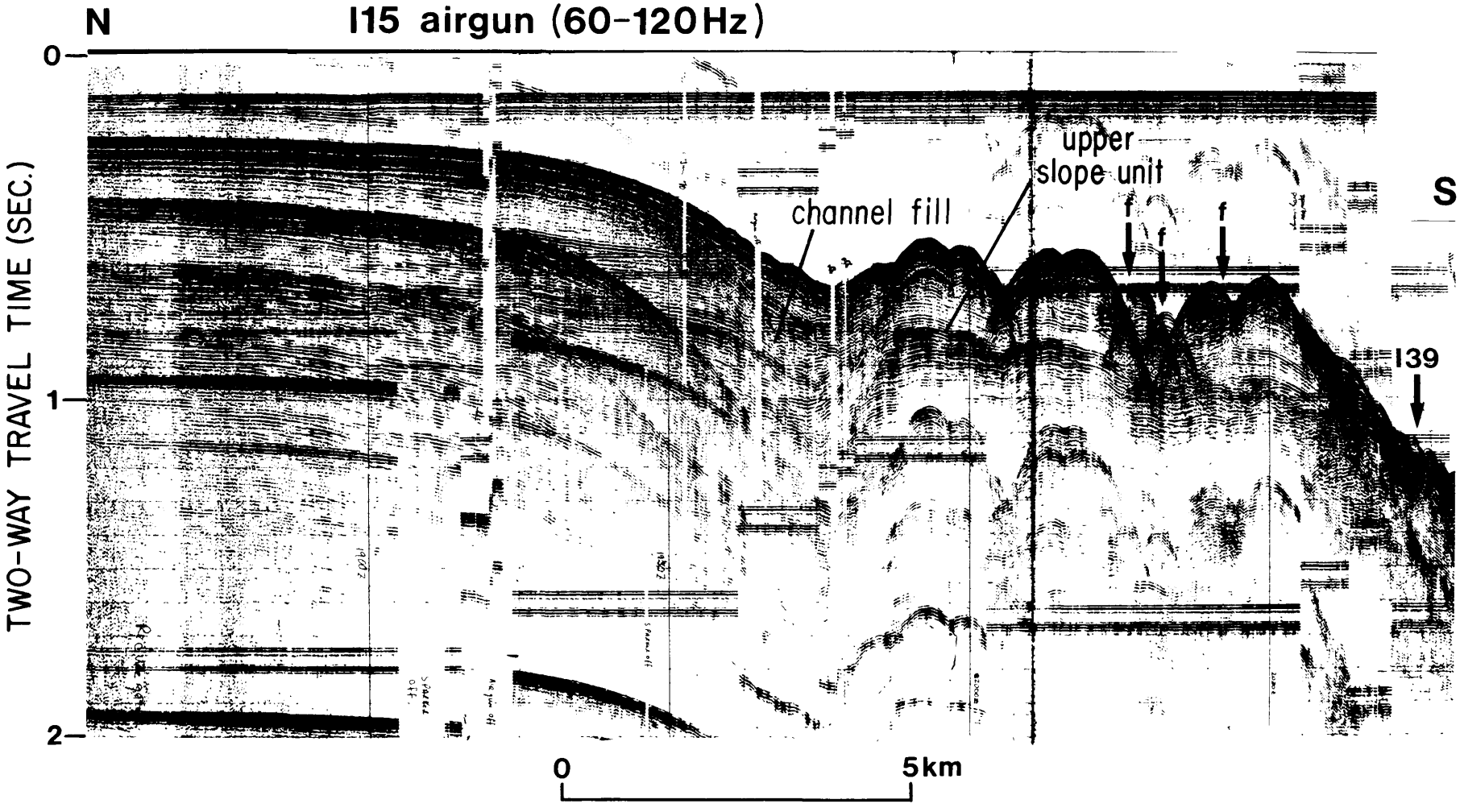

Figure 41. Profile I15 (airgun) shows filled channel cut in foreset and upper-slope unit; f indicates inferred fault traces. Vertical exaggeration ~ 7:1.

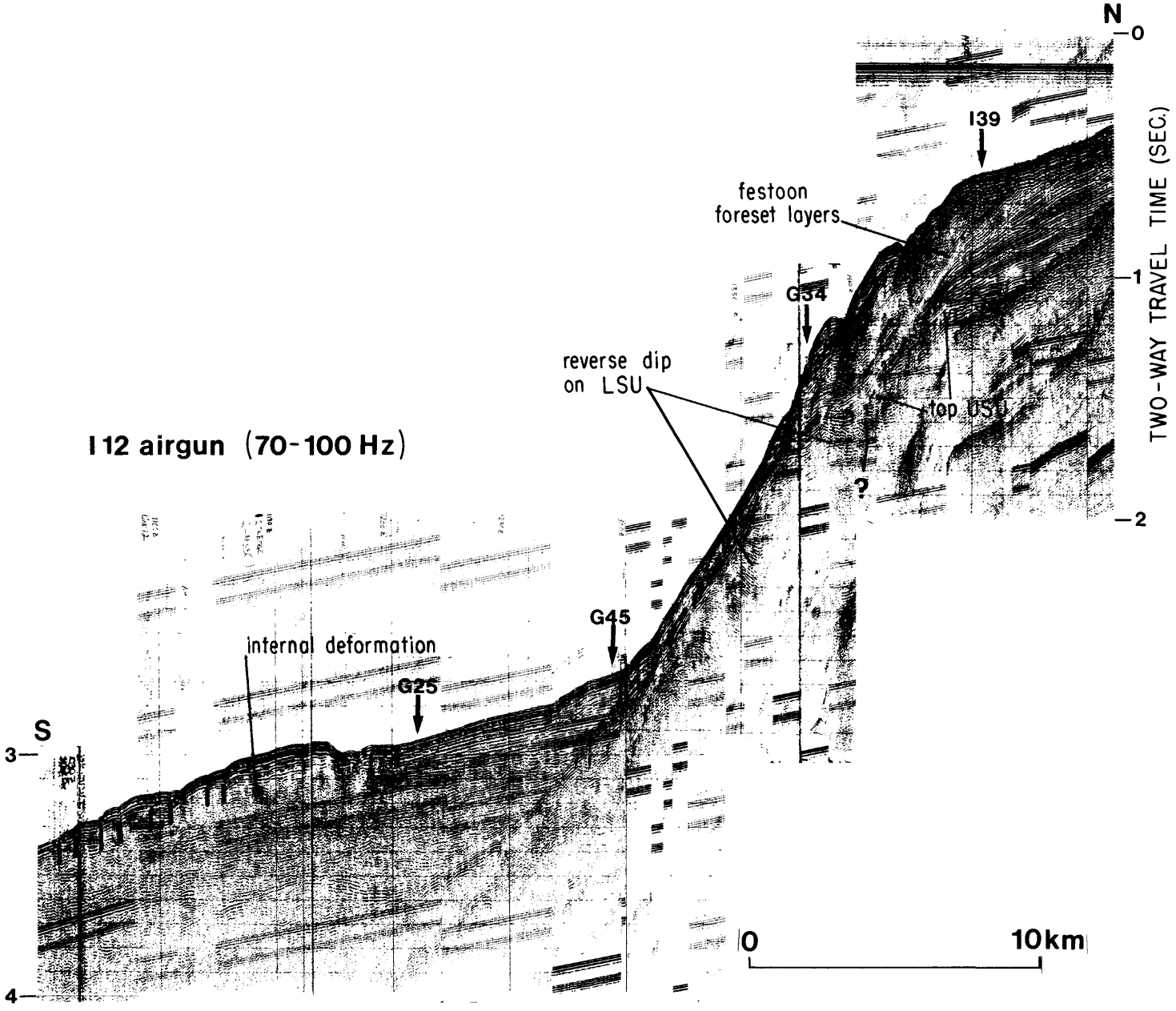

Figure 42. Profile I12 (airgun) shows steep-bedded "festoon" foreset package extending downslope and onto rise east of Dogbody Canyon. Vertical exaggeration ~ 11:1.

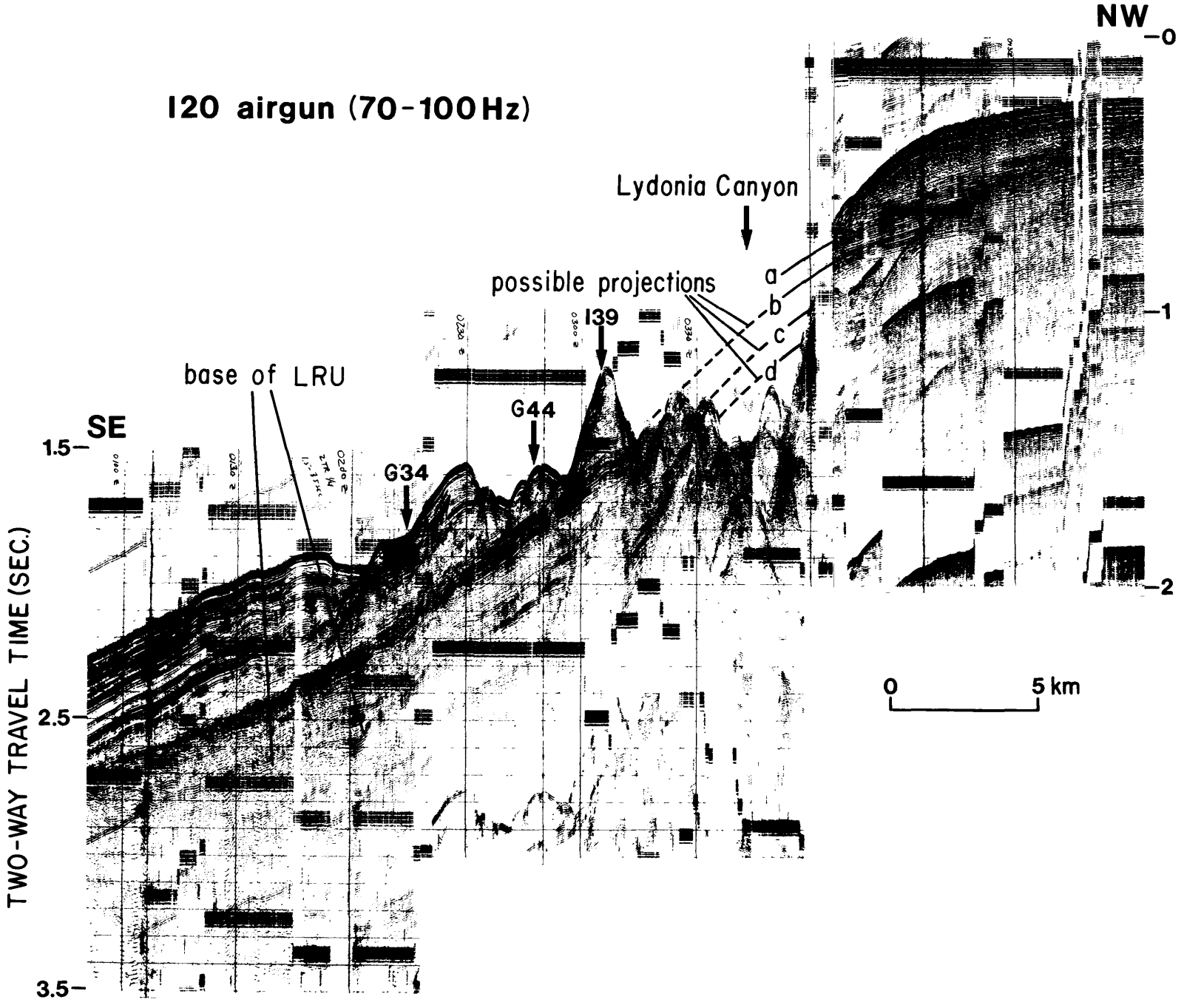

Figure 43. Profile I20 (airgun) crosses Lydonia Canyon oblique to the southeast. Vertical exaggeration ~ 25:1.

On strike, the upper-slope unit is irregularly layered and pinches and swells (fig. 44). It is apparently draped over a surface of considerable relief underlain by the lower-slope unit. The upper interval, a-b, is locally unconformable on the lower interval b-c, which thickens, pinches out, fills or is faulted down in swales and depressions (figs. 44, 45).

The lower-slope unit comprises two intervals: c-d, an acoustically transparent to chaotic interval that fills deep gaps in d, an otherwise flat-surfaced interval of parallel reflectors (figs. 44, 45). The layered lower interval d extends to depths beyond penetration of our system. Where it abuts the slope it is largely covered by onlapping layered rise strata (fig. 46), but it is probably exposed in canyons (e.g., Lydonia Canyon, fig. 47). Powell Canyon seems to be cut through a large filled depression in the lower-slope unit (fig. 44). Interval b-c of the upper-slope unit appears to be draped down, perhaps partly faulted down, into the depression also (fig. 44).

Between Lydonia and Jigger Canyons, interval d of the lower-slope unit appears to be brought up or pinched out across or against relatively elevated, perhaps truncated, older units (fig. 47). This tilt (accentuated by a course change during the survey) implies that the upper-slope unit rests on progressively older beds west of Lydonia Canyon. Between Gilbert and Oceanographer Canyons, an apparently deep section is exposed.

Ryan and others (1978) collected calcareous or dolomitic arenaceous rocks in Oceanographer Canyon below 1,517 m, which they infer to be Early Cretaceous in age on the basis of seismic-profile interpretation and lithologic similarity to their Neocomian(?) samples from "Heezen Canyon". In Lydonia Canyon, on the other hand, beds of the upper-slope unit crop out to depths of at least 1,245 m.

Generally, the layered rise unit shows more internal distortion and is stratigraphically more complex in this sector than it is to the east in sector I. It is markedly unconformable on the deeply broken and disturbed lower-slope unit (fig. 48). Figure 48 also shows the lateral stratigraphic and structural complexity of the layered rise unit. Lateral facies transitions, intertonguing, pinchouts, thick basal fills in the high-relief surface of the lower-slope unit, and abrupt structural distortions all contribute to a very complex layered rise unit in this sector. Generally, reflectors of the layered rise unit conform to the underlying contact well up on the slope. Only locally does the layered rise unit seem to onlap a slope surface of considerable relief (fig. 49), particularly toward the west.

The layered rise unit is everywhere unevenly eroded and so varies greatly in thickness. Probably the best-preserved section of the layered rise unit is seen in line I20 (fig. 43), where the unit is at least 560-m thick. Its continuity with the upper-slope unit and the foreset unit is shown in figure 49. In line I20 (fig. 43; cf. fig. 14, sector I) the lower part of the thick, well-preserved layered rise section may correlate with interval b-c of the upper-slope unit.

Toward the east, the layered rise unit includes a number of acoustic subunits stratigraphically above the correlative upper-slope unit interval b-c. These subunits, which together are about 400-m thick (fig. 43), probably include mostly Miocene through Pleistocene sediment.

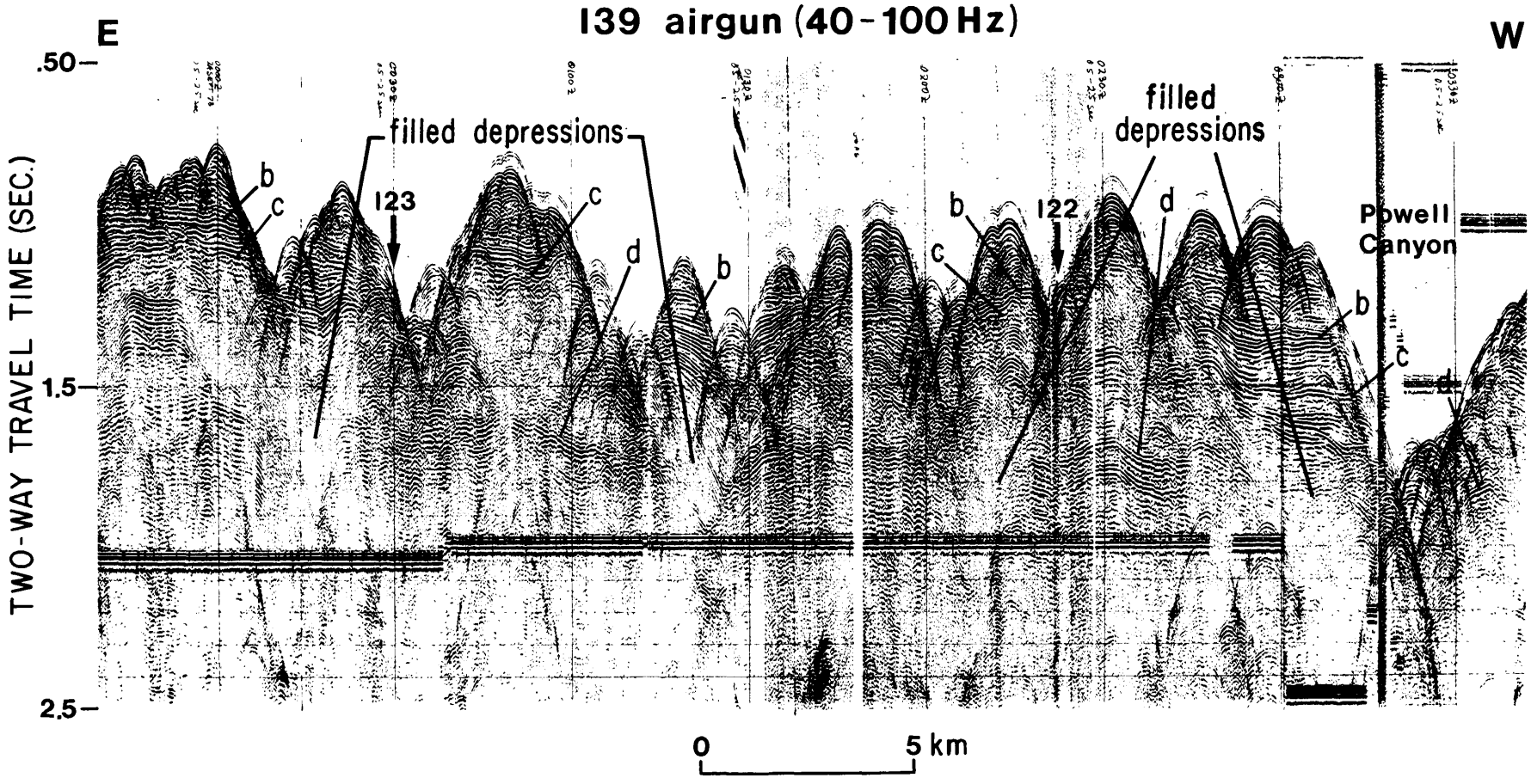

Figure 44. Profile I39 (airgun) along slope between approximately 700 m and 1,000 m depth. Bottom of Powell Canyon is at about 1,450 m. Note filled depression at 0130. Vertical exaggeration ~ 10:1.

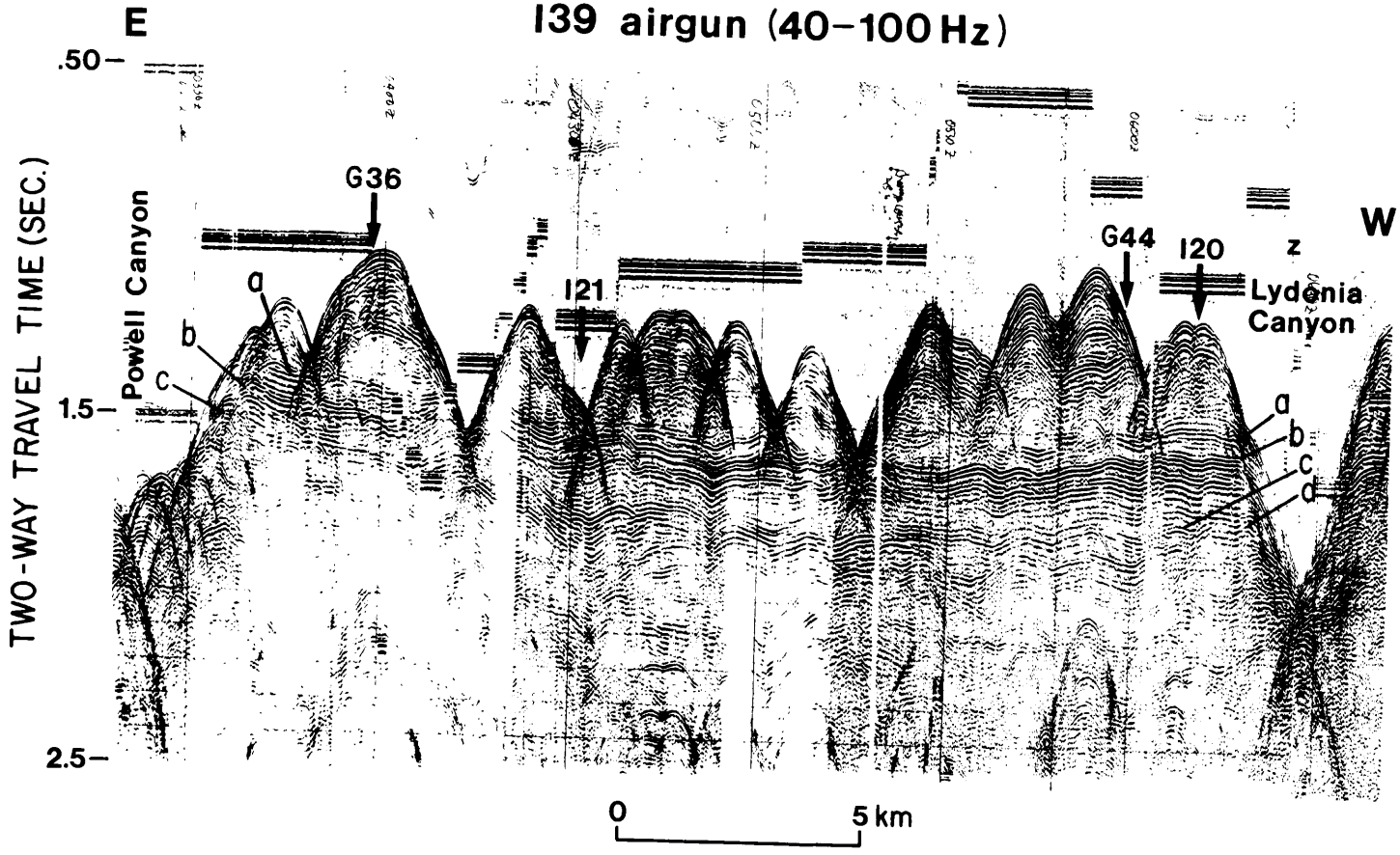

Figure 45. Profile I39 (airgun) along slope between Powell and Lydonia Canyons; approximately 1,000 m depth. Vertical exaggeration ~ 10:1.

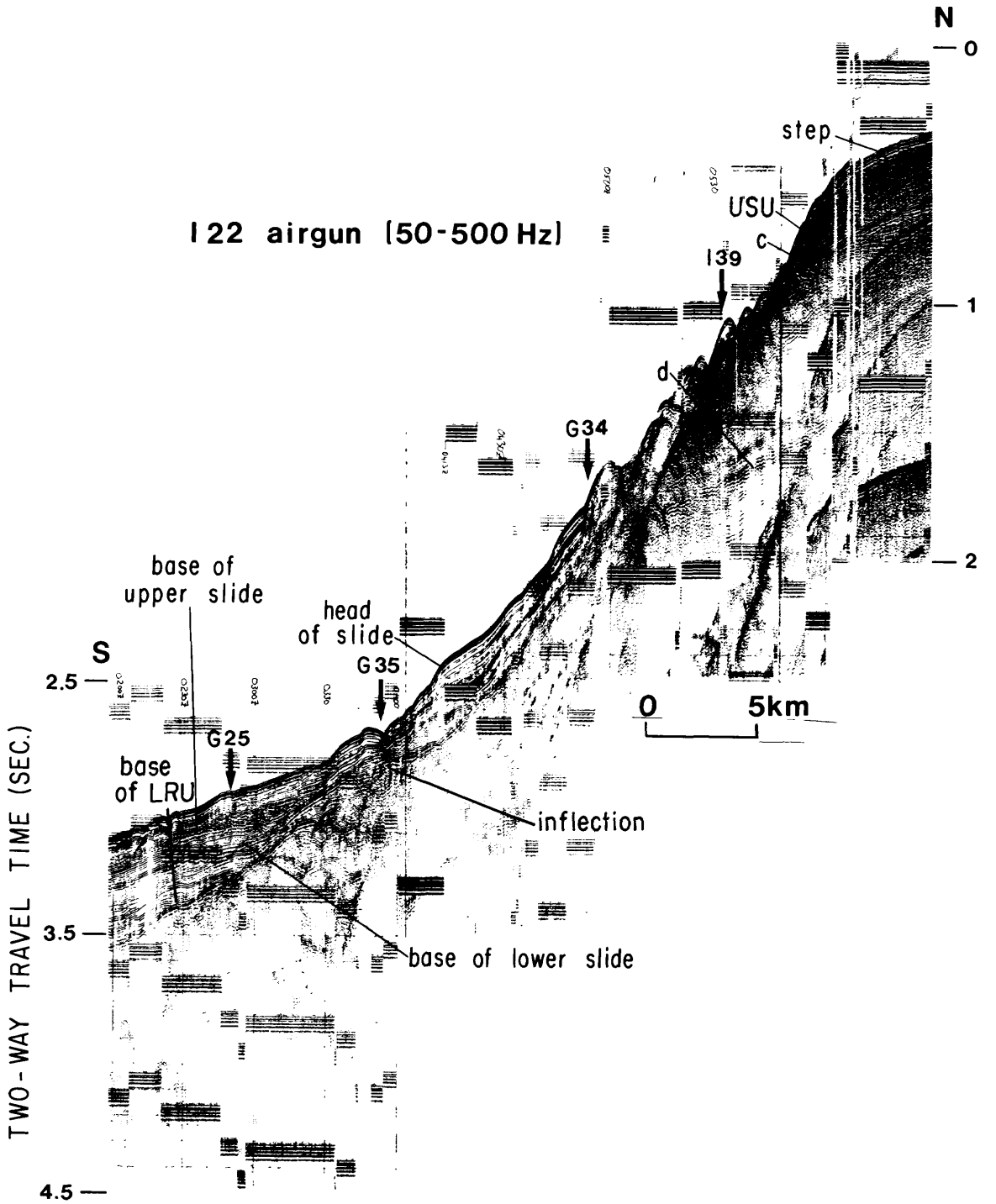

Figure 46. Profile I22 (airgun) parallel to and east of Powell Canyon; note that labeled horizons differ in depth from those shown in figure 43 (cf. figs. 45, 47). Vertical exaggeration ~ 15:1.

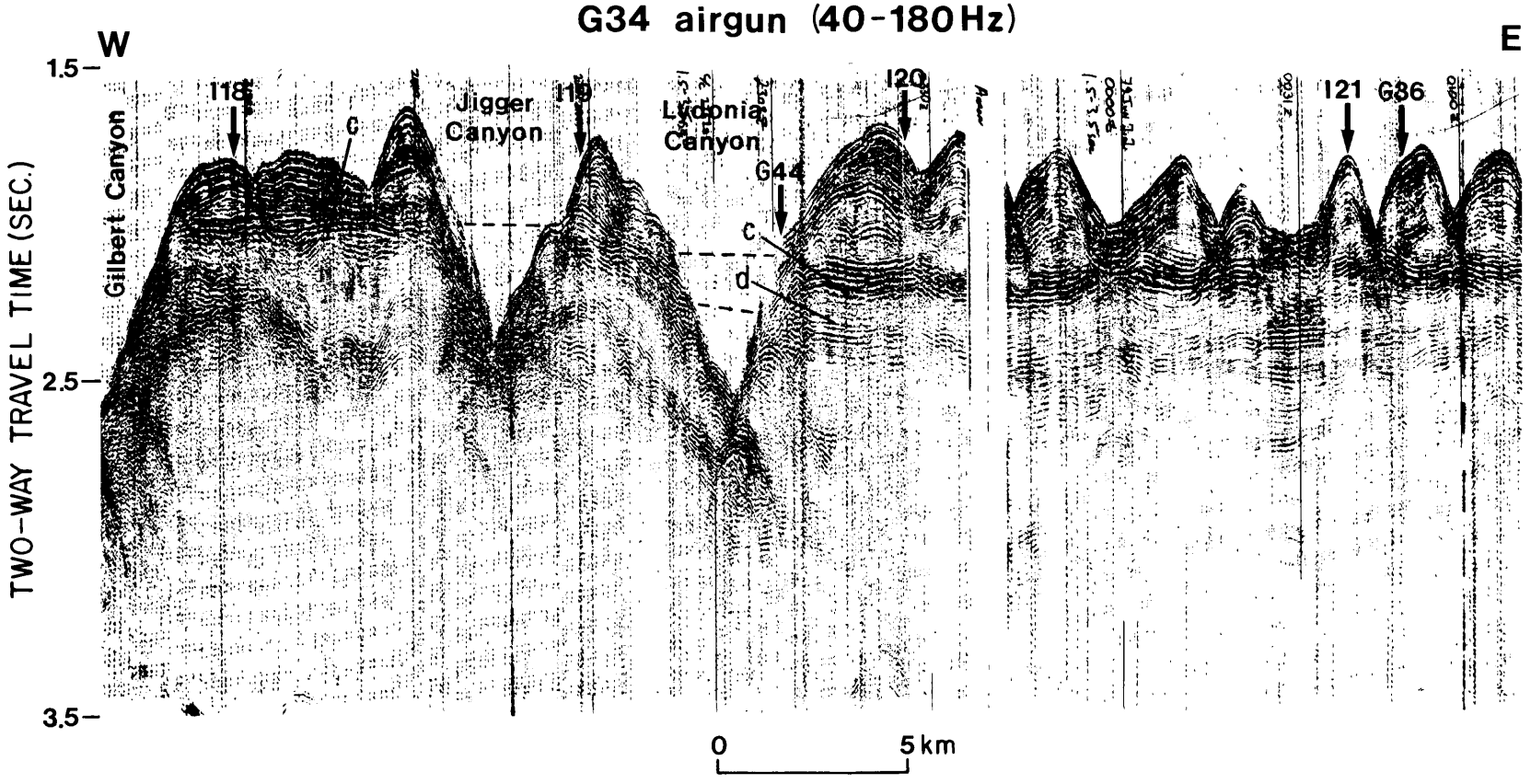

Figure 47. Profile G34 (airgun) along slope at depths from about 1,250 m to 1,500 m. Bottom of Lydonia Canyon is at about 2,050 m. Vertical exaggeration ~ 11:1.

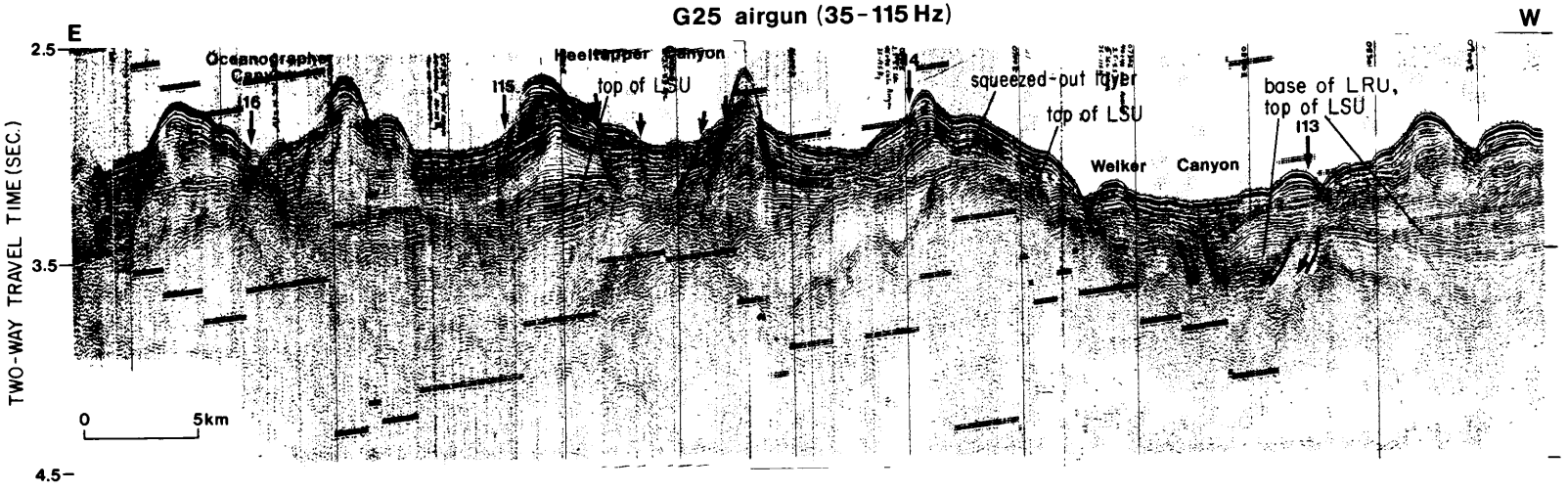

Figure 48. Profile G25 (airgun) along the lower slope between approximately 2,200 m and 2,750 m depths. Arrows show margins of an inferred graben and possible faults. Vertical exaggeration ~ 13:1.

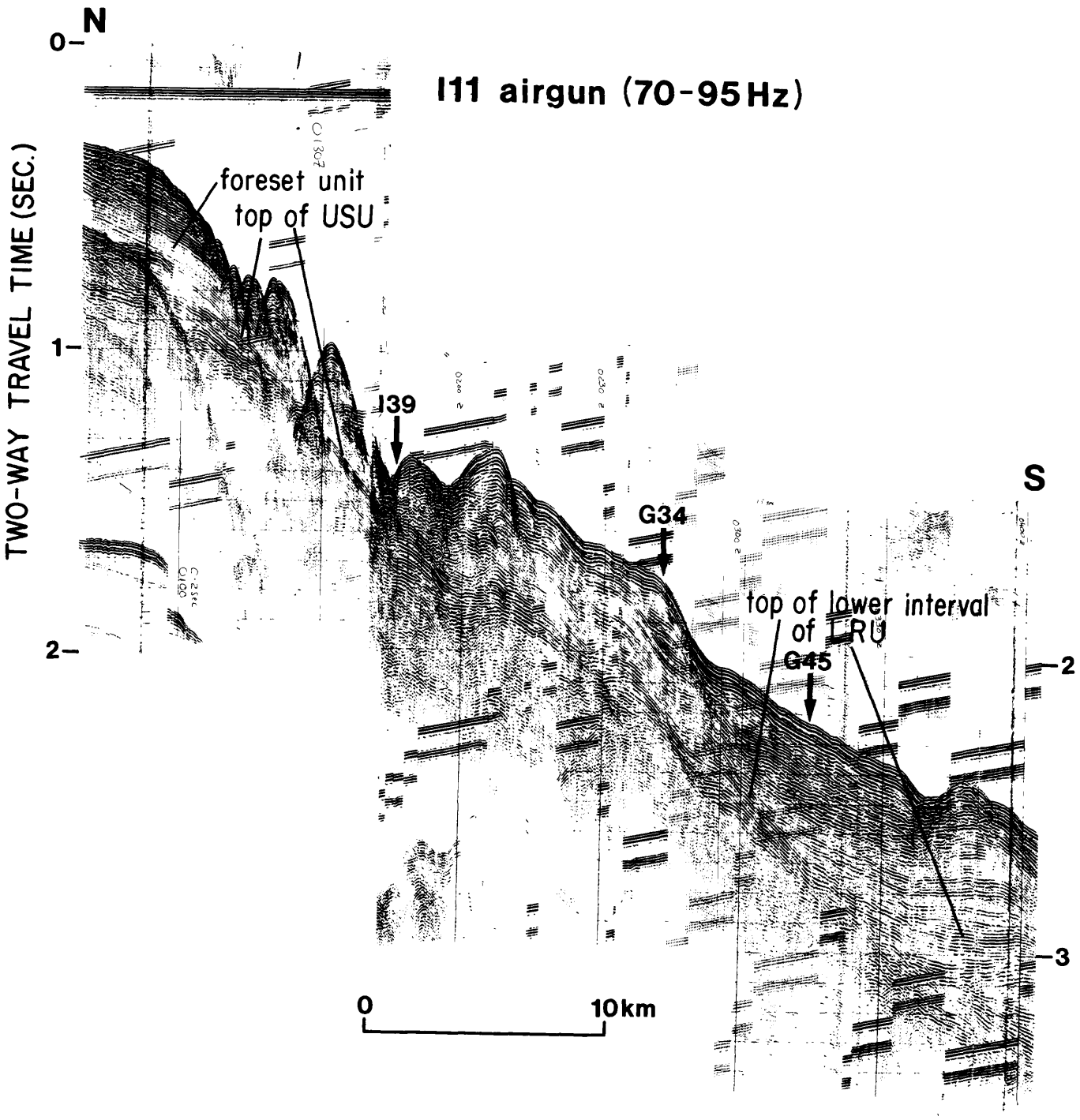

Figure 49. Profile I11 (airgun) shows continuity of upper-slope unit (USU) across the slope with layered rise unit (LRU) (cf. fig. 42). Vertical exaggeration ~ 17:1.

West of Dogbody Canyon, a steepening of the lower-slope unconformity brings deeper levels of the layered rise unit closer to the slope. On strike, the unit thickens appreciably by the addition of successively deeper strata that lap onto the lower-slope unit from the west (fig. 50). The upper part of the layered rise unit likewise thickens and is bathymetrically higher; its surface relief diminishes and becomes more regular to the west.

Structure and mass movement

There is some suggestion of faulting, or at least of local collapse, associated with channel fills intersected by the canyon heads, particularly in the buried trough between Gilbert and Lydonia Canyons. Where they are intersected by the canyon walls, contours along the canyon walls show concavities or shallow reentrants, as though the cut fill has slid or spilled down into the canyons.

Sparker line I10 (fig. 51) passes below the rim of the western headwall of Hydrographer Canyon (cf. map D). The rounded steplike forms shown in the profile represent broad, eroded salients transverse to the canyon axis. One of these forms is cut out by a 65-m deep excavation depicted in the profile as a keystone-shaped gap because of high vertical exaggeration (~21:1). Because the excavation truncates the convex surface formed by the salients, it represents a younger landform; and because the convergent sideslopes of the excavation are evidently scarps, the excavation is probably the result of a slide. The inferred slide has cut out part of the foreset unit along an orientation close to strike; there is thus a suggestion of fracture control here, if not of displaced channel fill.

Obscure steplike forms along the slope brow (such as those upslope from I39, line I8, fig. 52), might represent sliding associated with creep, especially in light of deformation or erosion farther downslope, but they could also represent wave-cut benches.

A 15-m high scarp at 240-m depth marks the back slope of a 6.5-km-wide slide or flow depression along line G39 (fig. 53). A broad concave surface represents the scar along strike (fig. 54). Projection of the profile of the intact surface across the concave slide scar indicates that about 70 m of foreset sediment have been removed. Two kilometers downslope, on line G43 just below the 475-m bench level, the scar is represented by deep, irregular incisions underlain by shadowy, perhaps debris choked troughs (fig. 55). Farther down, in line G39A (fig. 53), steep chutes are indicated. Line G44 indicates that the sediment prone to sliding is downlapped on well-layered, downwarped sediment of the upper-slope unit and is internally deformed (fig. 56).

Block displacement down to canyon axes along part of the upper slope is perhaps indicated in line I39 (fig. 57). The uneven, back-tilted surfaces (and subjacent layering) on otherwise convex buttelike forms suggest Toreva blocks.

Between Powell and Munson Canyons the middle-to-lower slope is excavated by broad, irregular embayments which owe much of their form to mass wasting. The embayments resemble filled troughs in cross section (fig. 58). The trough walls are draped with sediment that has locally slid down, along with

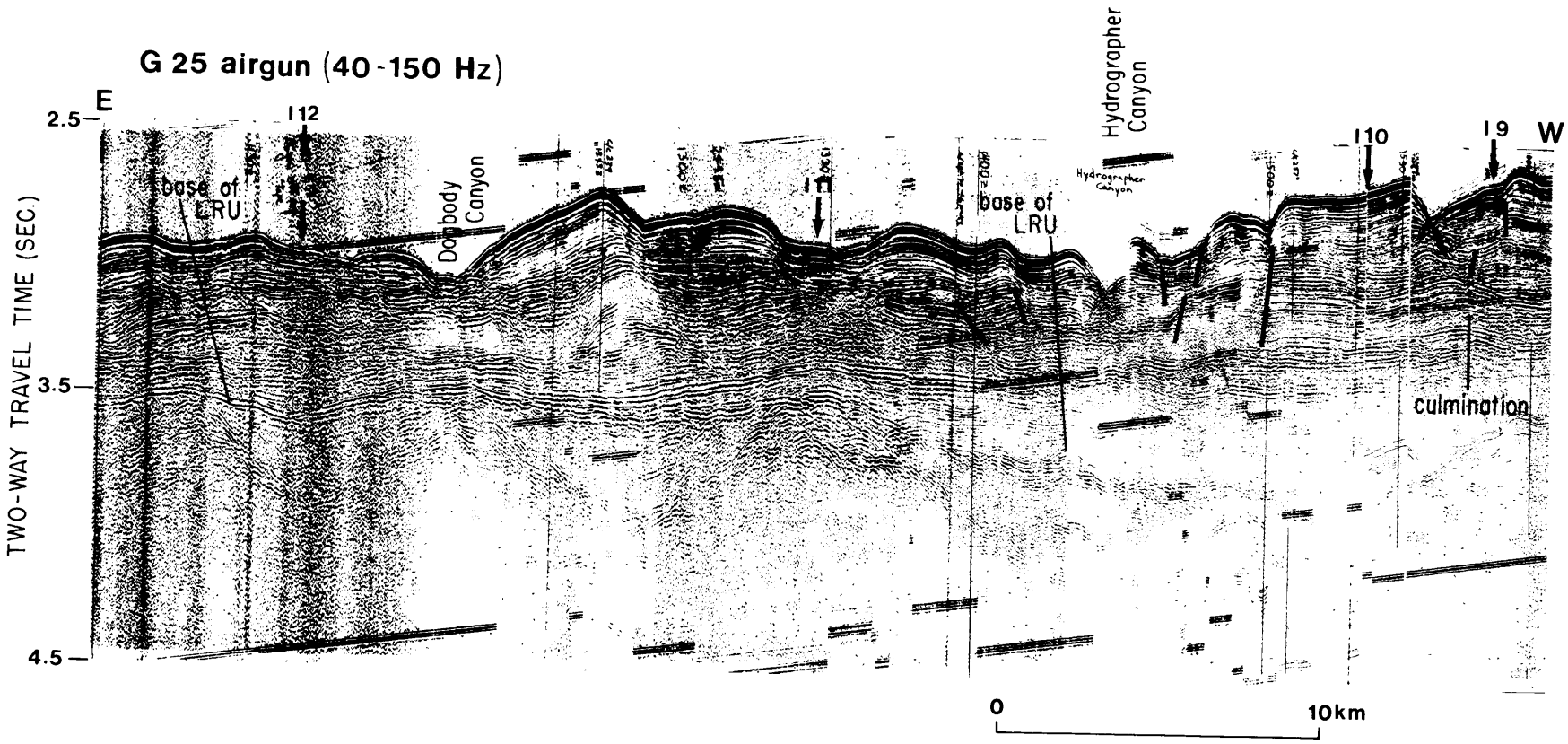

Figure 50. Profile G25 (airgun) along slope between approximately 2,000 m and 2,350 m depths shows onlap in layered rise unit from west of Dogbody Canyon. Heavy lines indicate inferred faults. Vertical exaggeration ~ 11:1.

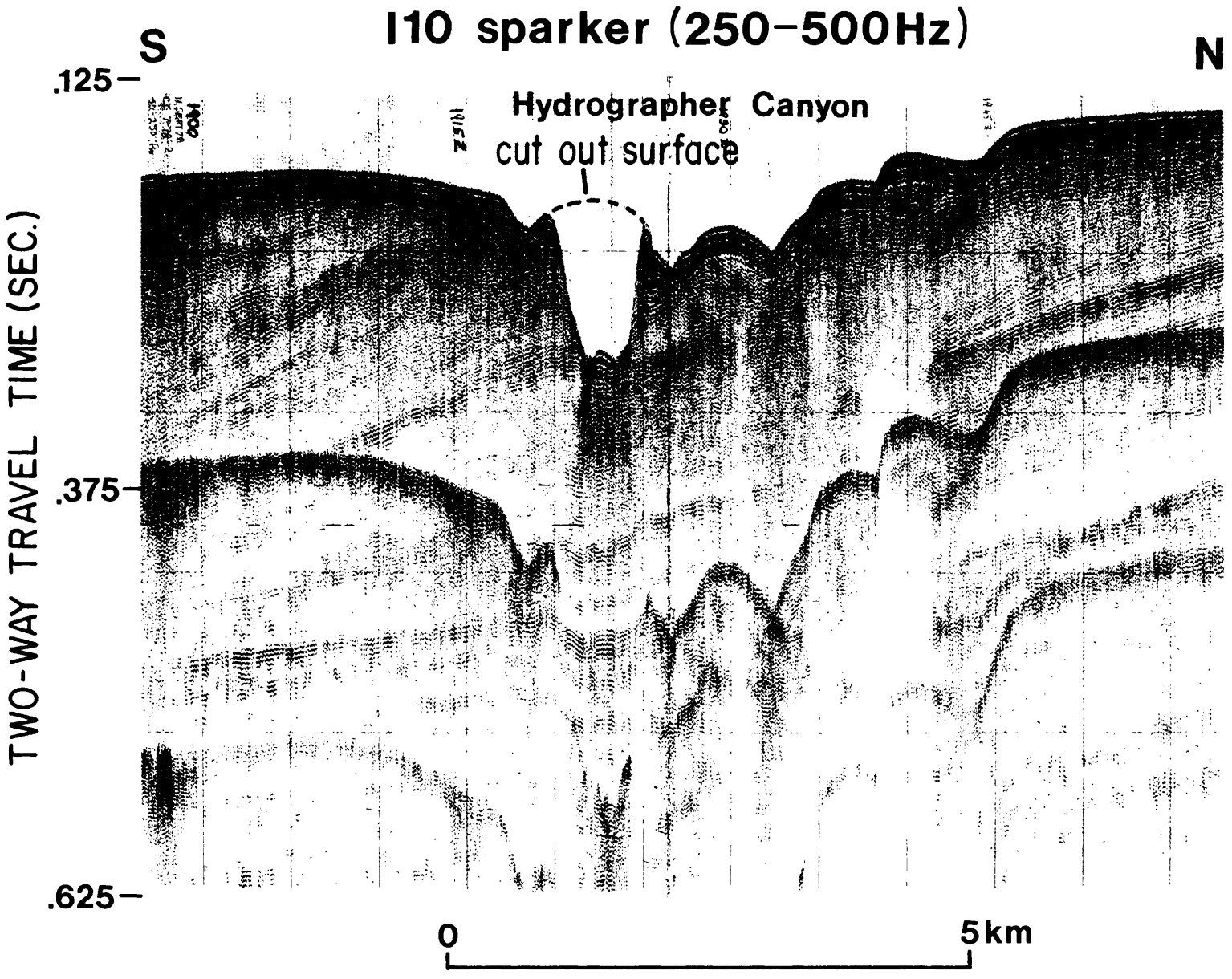

Figure 51. Profile I10 (sparker) shows terraces along the side of Hydrographer Canyon. Note keystone-shaped gap cut through convex surface. Vertical exaggeration ~ 21:1.

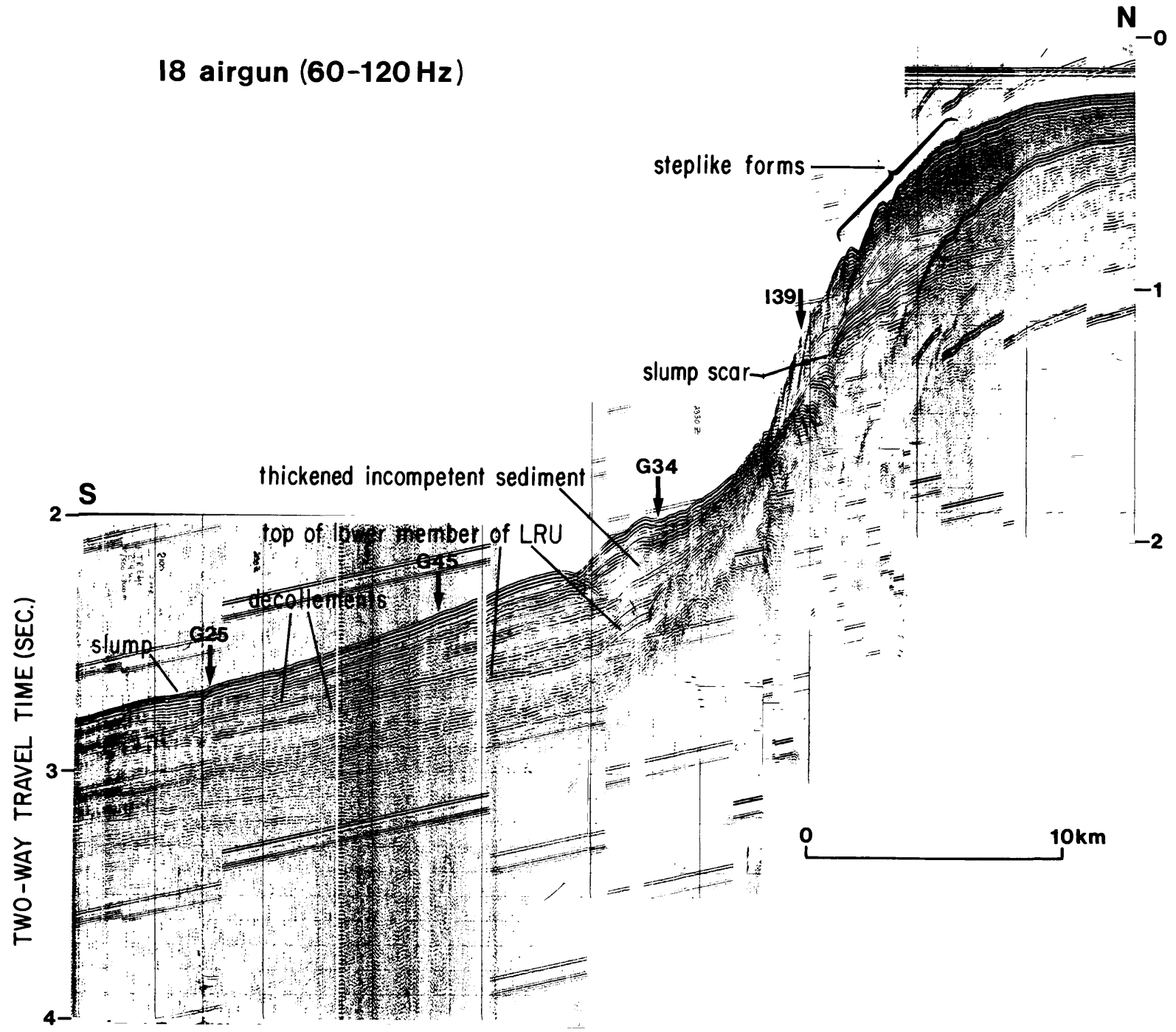

Figure 52. Profile I8 (airgun) shows details of layered rise unit (LRU), and concave, truncated middle slope inferred to be a slump scar. Vertical exaggeration ~ 13:1.

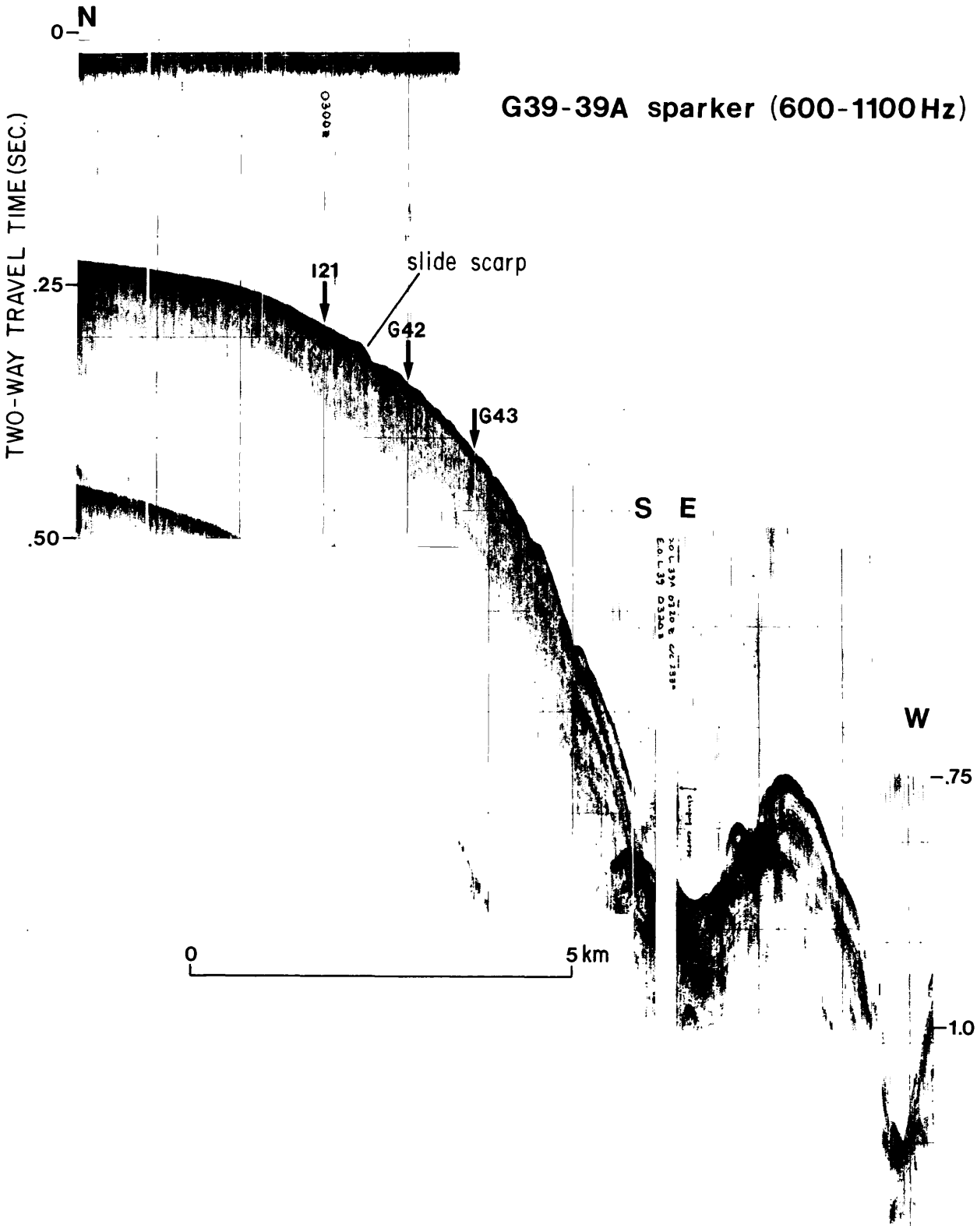

Figure 53. Profile G39-39A (sparker) shows scarp and rough downslope surface indicative of slide in foreset unit along outer shelf brow. Vertical exaggeration ~ 18:1.

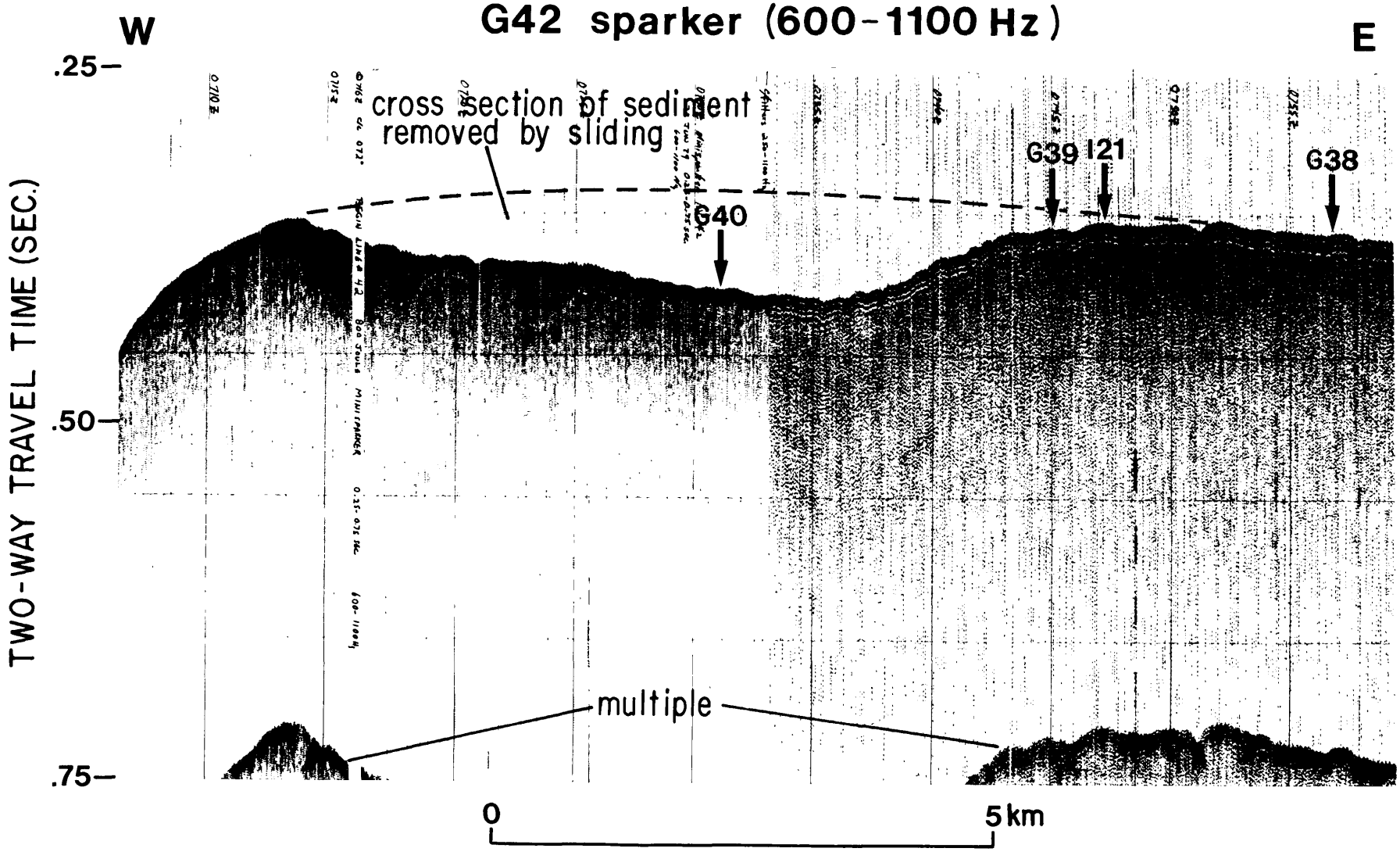

Figure 54. Profile G42 (sparker) shows concave slide depression along outer shelf brow. Convex slope falls off to west into Lydonia Canyon. Vertical exaggeration ~ 19:1.

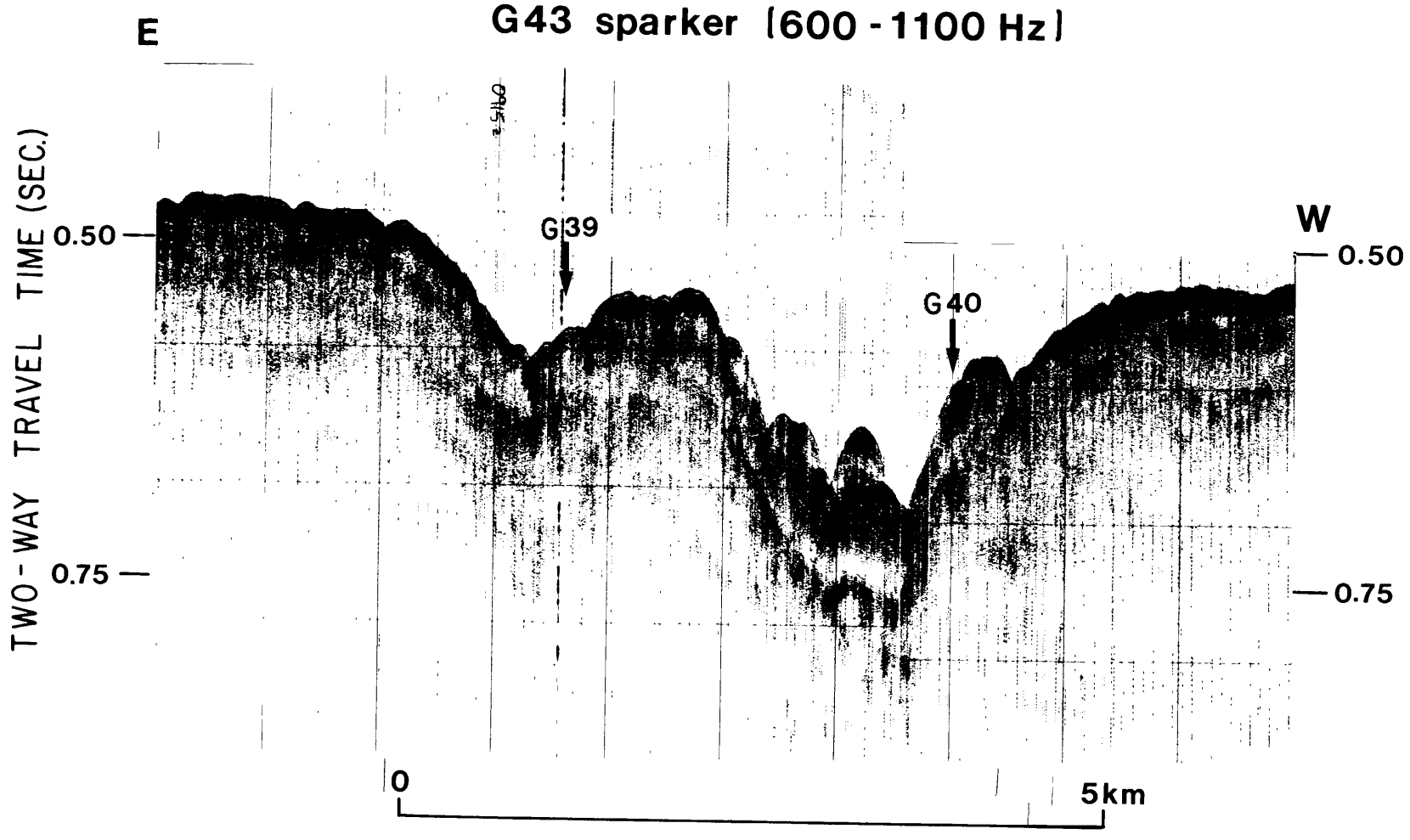

Figure 55. Profile G43 (sparker) along slope at approximately 500 m depth shows incisions downslope from slide depression illustrated in figure 54. Vertical exaggeration ~ 13:1.

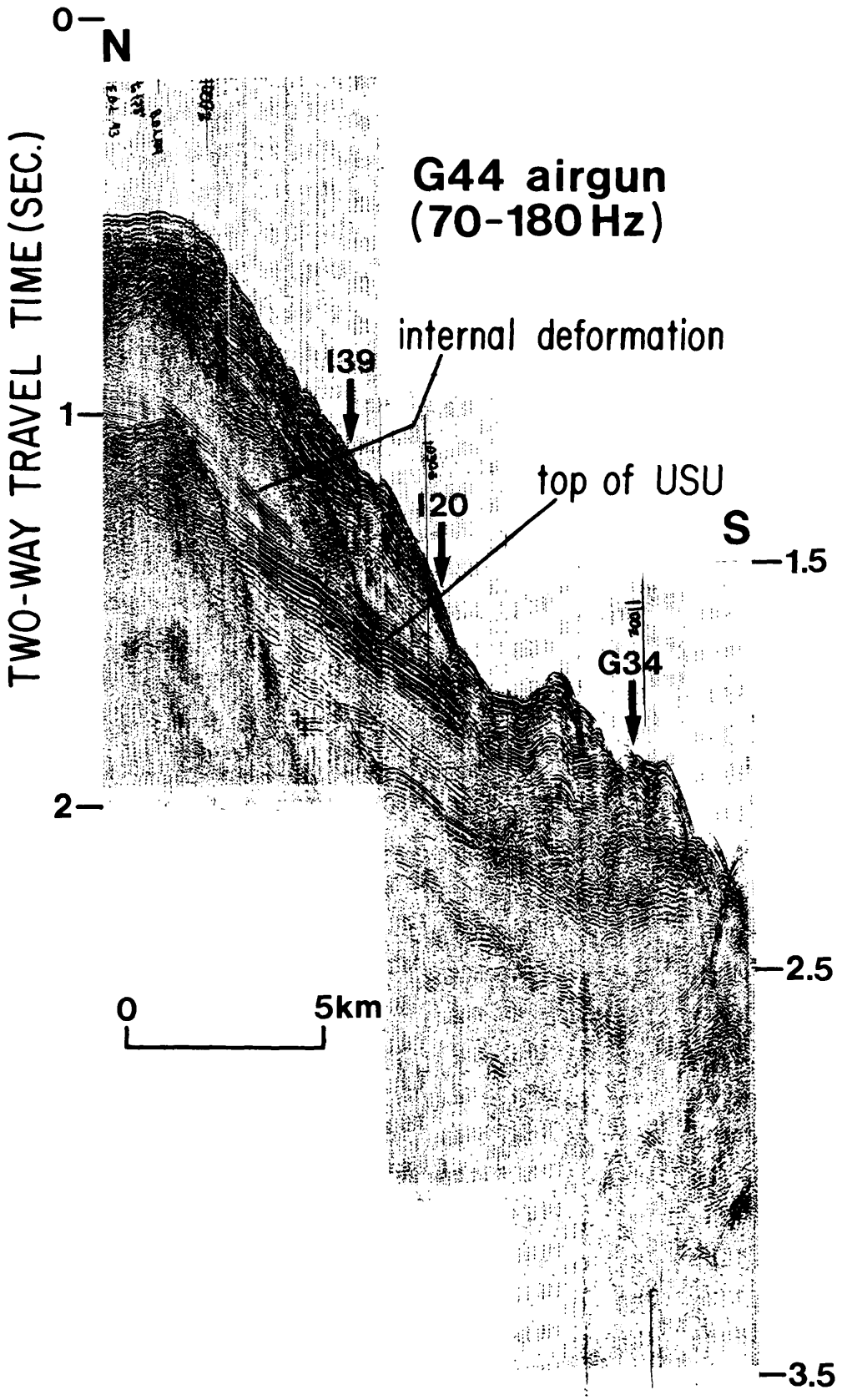

Figure 56. Profile G44 (airgun) shows internal deformation in downlapping foreset unit below about 500 m depth. Deformation downslope from about 1045Z is related to east wall of Lydonia Canyon. Vertical exaggeration ~ 13:1.

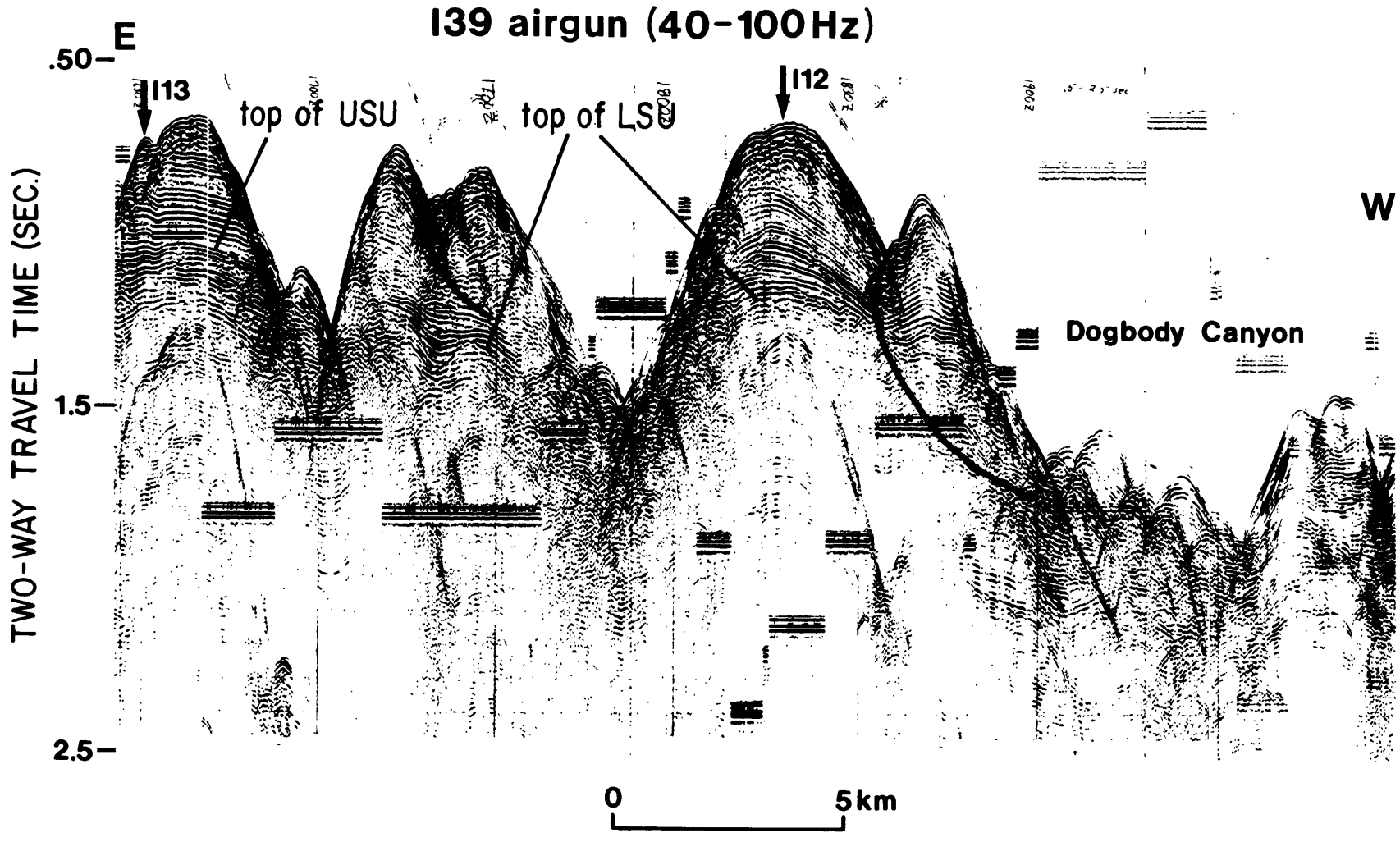

Figure 57. Profile I39 (airgun) along upper slope from about 500 m depth to about 1,600 m in axis of Dogbody Canyon. Heavy lines indicate traces of inferred Toreva block slip planes. Vertical exaggeration ∿ 10:1.

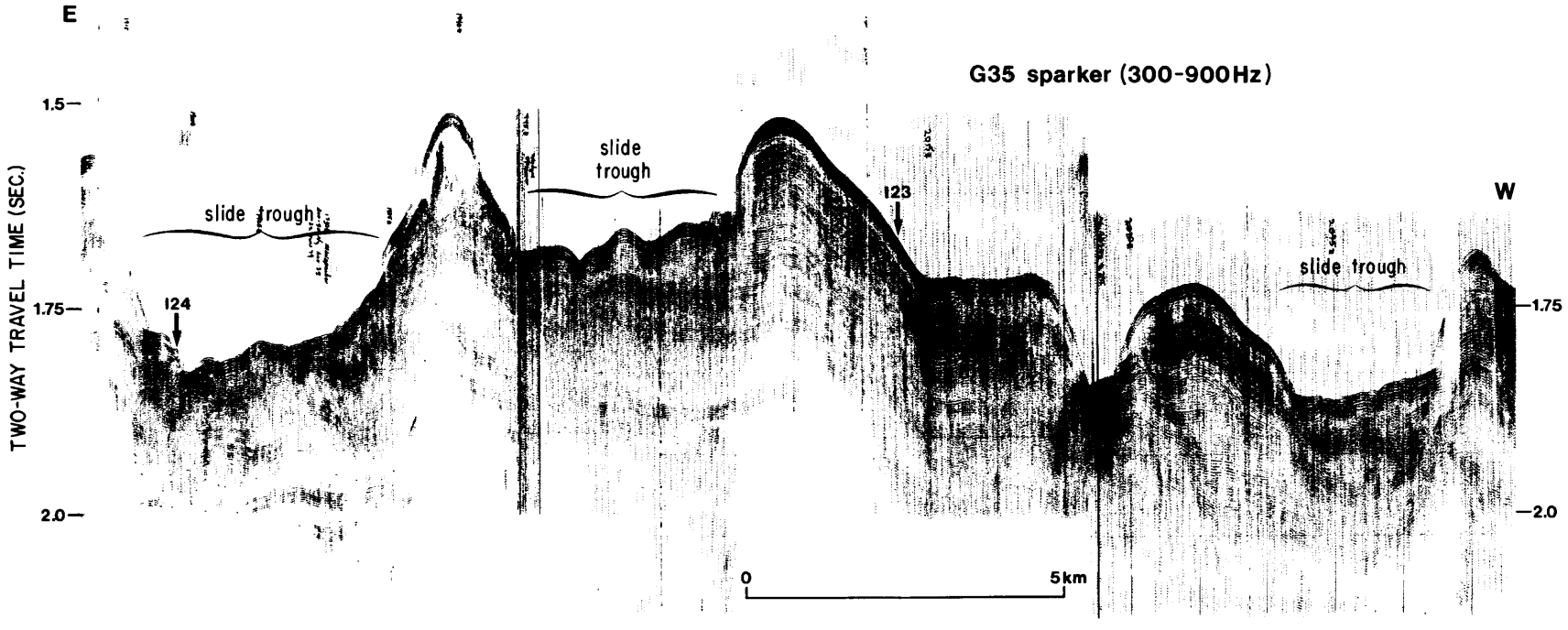

Figure 58. Profile G35 (sparker) along slope west of Munson Canyon from approximately 1,850 m to 2,000 m depths. Vertical exaggeration ~ 18:1.

variously tilted blocks (fig. 59). Low on the slope (about 2,200-m depth), the west wall of the easternmost trough shown in figure 58 is spectacularly collapsed over a vertical extent of 225 m (fig. 60). Approximately 12 km farther downslope, the collapsed west wall has about 375-m relief (fig. 61). Only about 45-50 m of rubble lies on broken, downwarped reflectors within the trough here. Disharmonic folds at the base of the intact layered rise section and especially beneath the trough floor (fig. 61) suggest that internal deformation of weak layers has led to collapse. The steep upper part of the scarp may be controlled by a fracture plane in relatively competent strata (fig. 61). Note on the same figure that strong deeper reflectors extend beyond the inferred fracture out under the collapsed section and control the lower scarp profile which is underlain by a slight structural culmination.

Just east of Powell Canyon, at about 2,200-m depth, a large mass of layered rise sediment at least 5 km across is structurally detached (fig. 62). In cross section (fig. 62) the concave sea floor above the mass indicates volumetric loss, probably by downslope translation, extending well beyond the 2,250-m isobath (map C). Two levels of detachment are indicated (not shown in figure): one 95 m beneath the sea floor, the other at about 200 m. Structural thickening and thinning downslope (fig. 46) suggest that the upper level is a carpet slide that has overridden the deeper slide. A buried slope inflection seems to have controlled detachment. The higher carpet slide seems to have come from above the inflection, at 0410, line I22 (fig. 46, cf. fig. 4c)

Line I20 (fig. 63) apparently passes along the side of a similar slide (shown in cross section in fig. 62). Two levels of slide-distorted sediment are seen downslope from slip planes at 2356-2349 (fig. 63) over a slight subsurface culmination. Internal deformation has led to thickening of incompetent layers between competent ones. The surficial deformation located between 2321 and 2345 (fig. 63) is a separate collapse slump; most of the toe has slid out of the plane of the profile into the trough crossed by line G25 (fig. 62).

The broad slope down to Jigger Canyon shown in line G25 (fig. 64) is deformed by slumping. A slump toe forms the east side of the 65-m deep trough of Jigger Canyon. Line I19 (map C) suggests that this deformed surface is bounded upslope by fault blocks from which it extends seaward at least 11 km.

Deep, disharmonic structures are evident beneath the broad trough of Welker Canyon and under the west wall shown in figure 59. Large blocks of the layered rise section are tilted on an incompetent layer that extends down under Welker Canyon and which may represent the transparent layer deformed upslope to the east (figs. 48, 59).

In the thickened rise strata west of Welker Canyon a succession of incompetent layers controls extreme internal deformation, probable block faulting, and surface mounding and collapse on the rise. The shallowest such layer in this region is only 10 m below the surface (fig. 65).

West of Hydrographer Canyon slabs of strata are rotated slightly to the east on an incompetent layer about 300 m deep. The deep, incompetent layer that underlies the tilted slabs is terminated along an inferred tension fracture at 1500, line G25 (fig. 50). To the west, the same stratigraphic

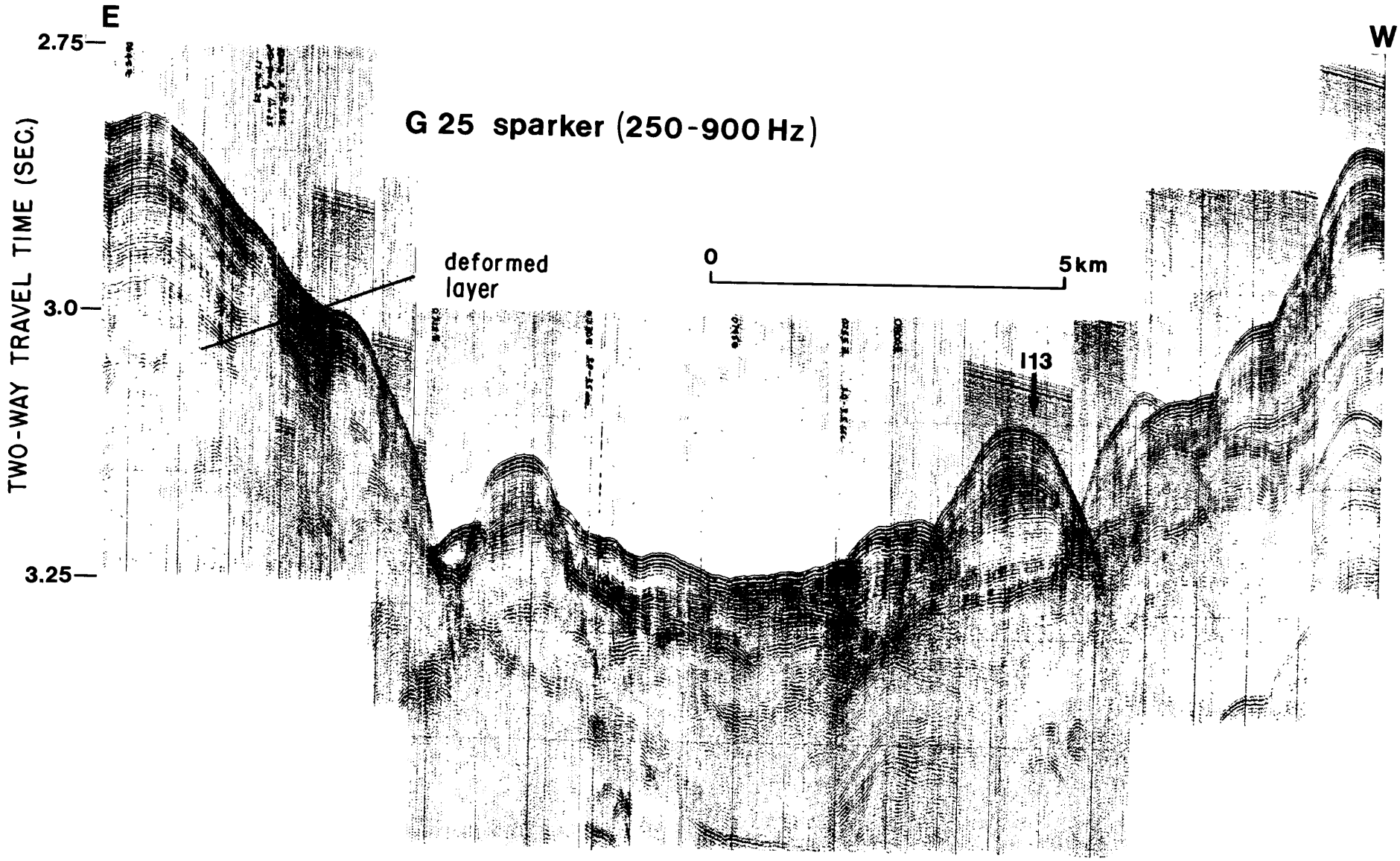

Figure 59. Profile G25 (sparker) crosses trough of Welker Canyon at about 2,400 m depth. Note confused internal structure and deformed layer (cf. fig. 48). Vertical exaggeration ~ 21:1.

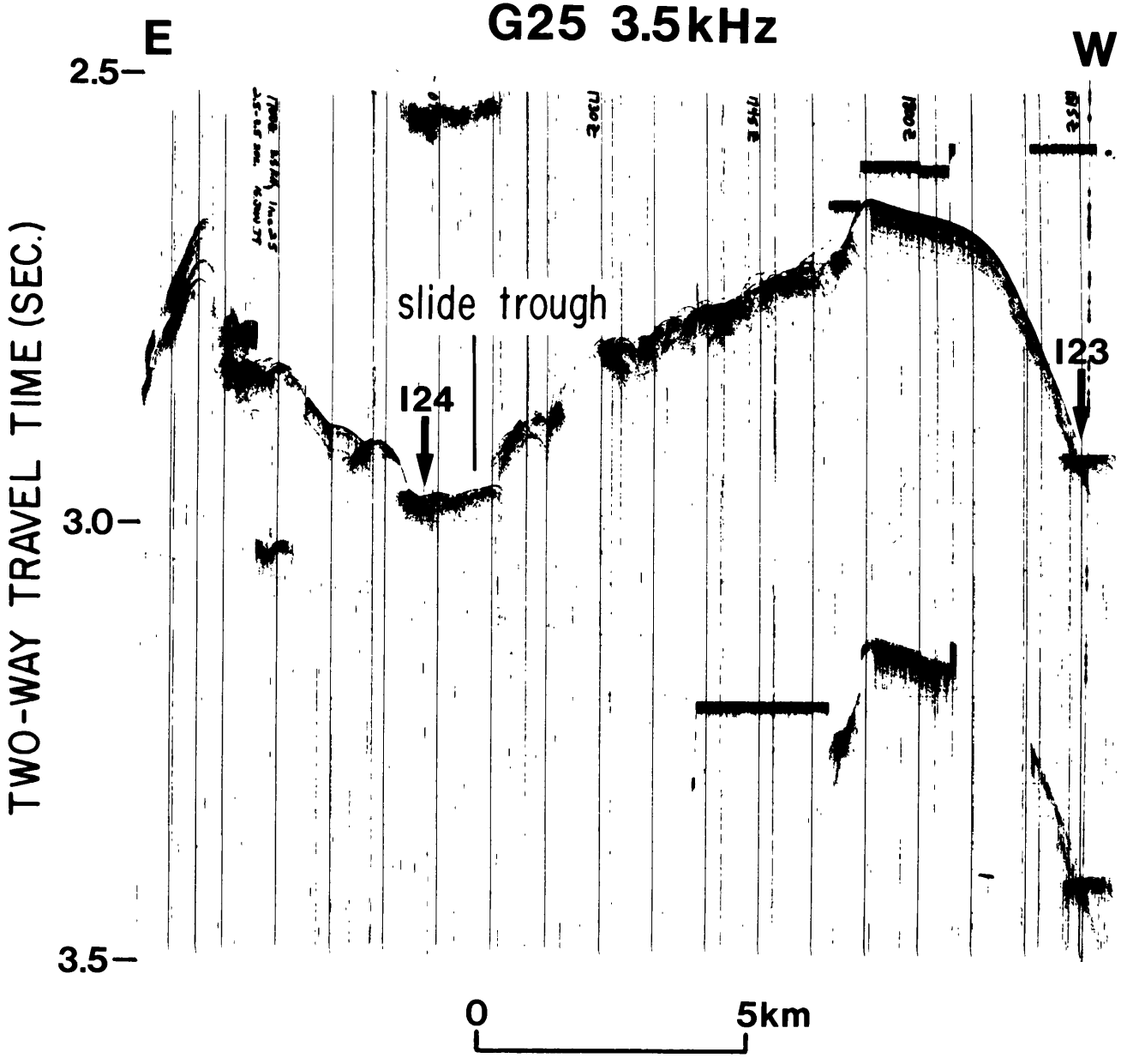

Figure 60. Profile G25 (3.5 kHz) shows collapsed west wall of slide trough. Vertical exaggeration ~ 22:1.

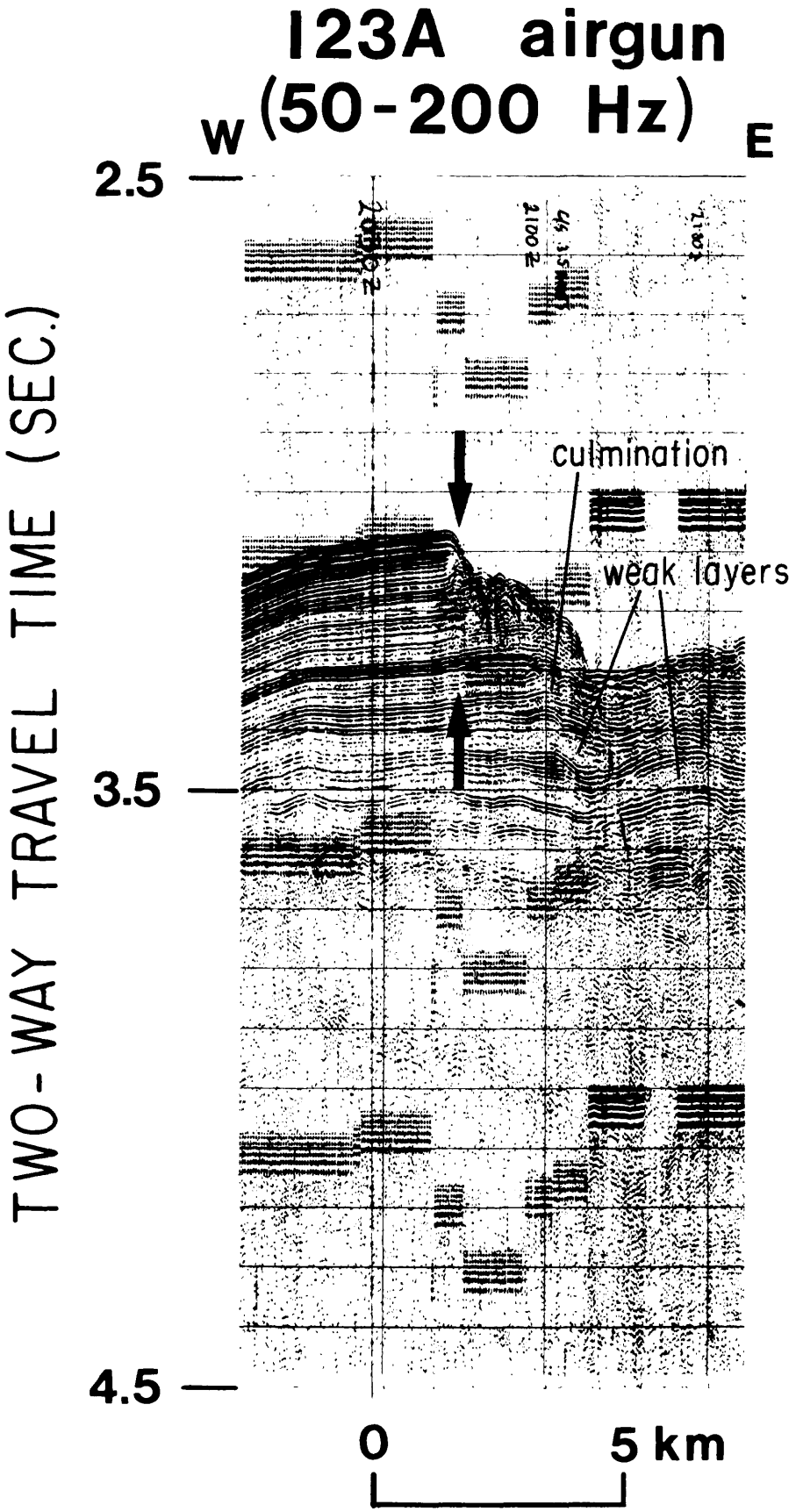

Figure 61. Profile I23A (airgun) shows collapsed west wall of trough at 2,300 m depth. Arrows indicate inferred fracture trace. Vertical exaggeration ~ 16:1.

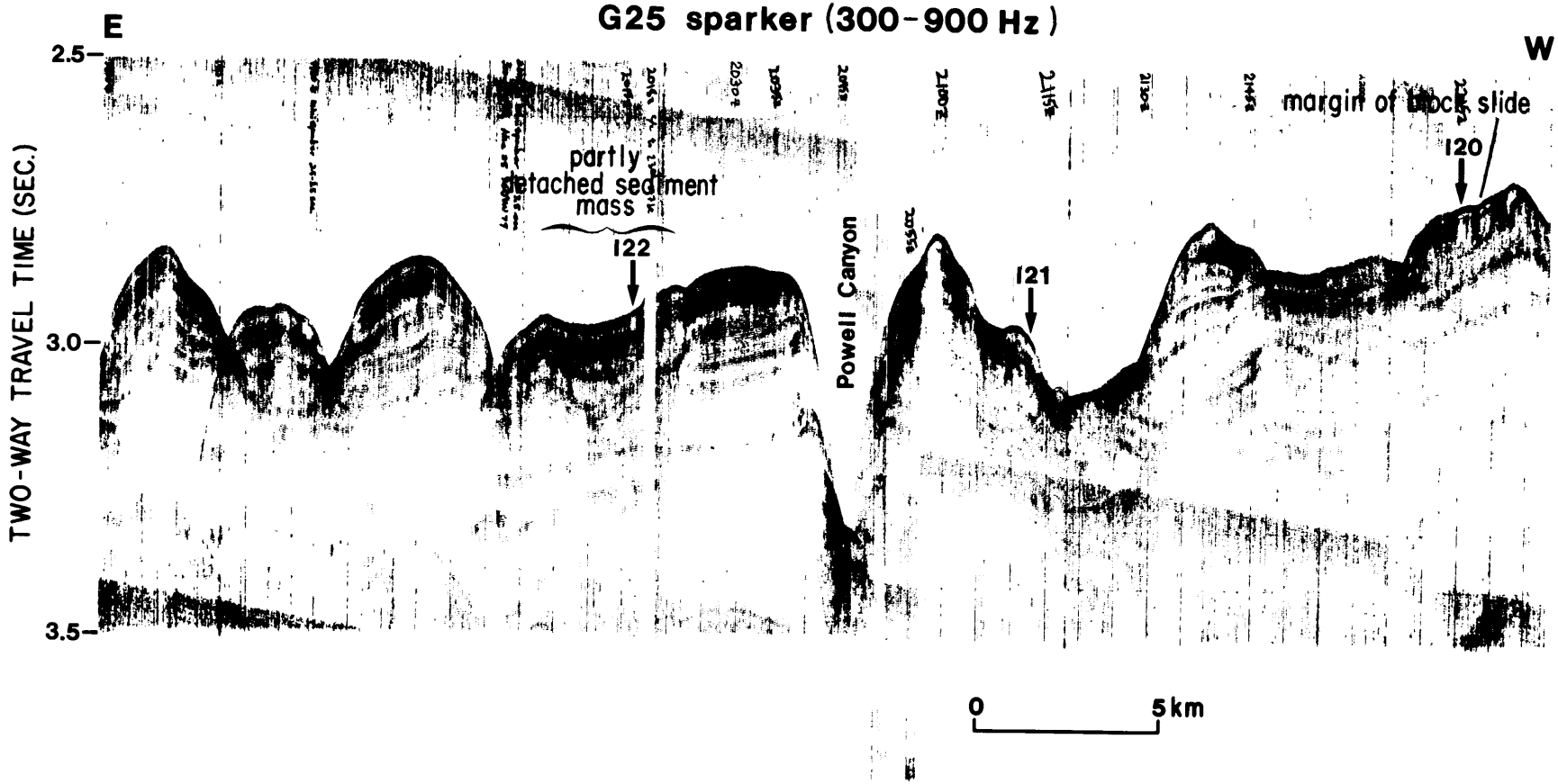

Figure 62. Profile G25 (sparker) along lower slope between approximately 2,150 m and 2,250 m depths. Bottom of Powell Canyon is about 2,350 m. Vertical exaggeration ~ 21:1.

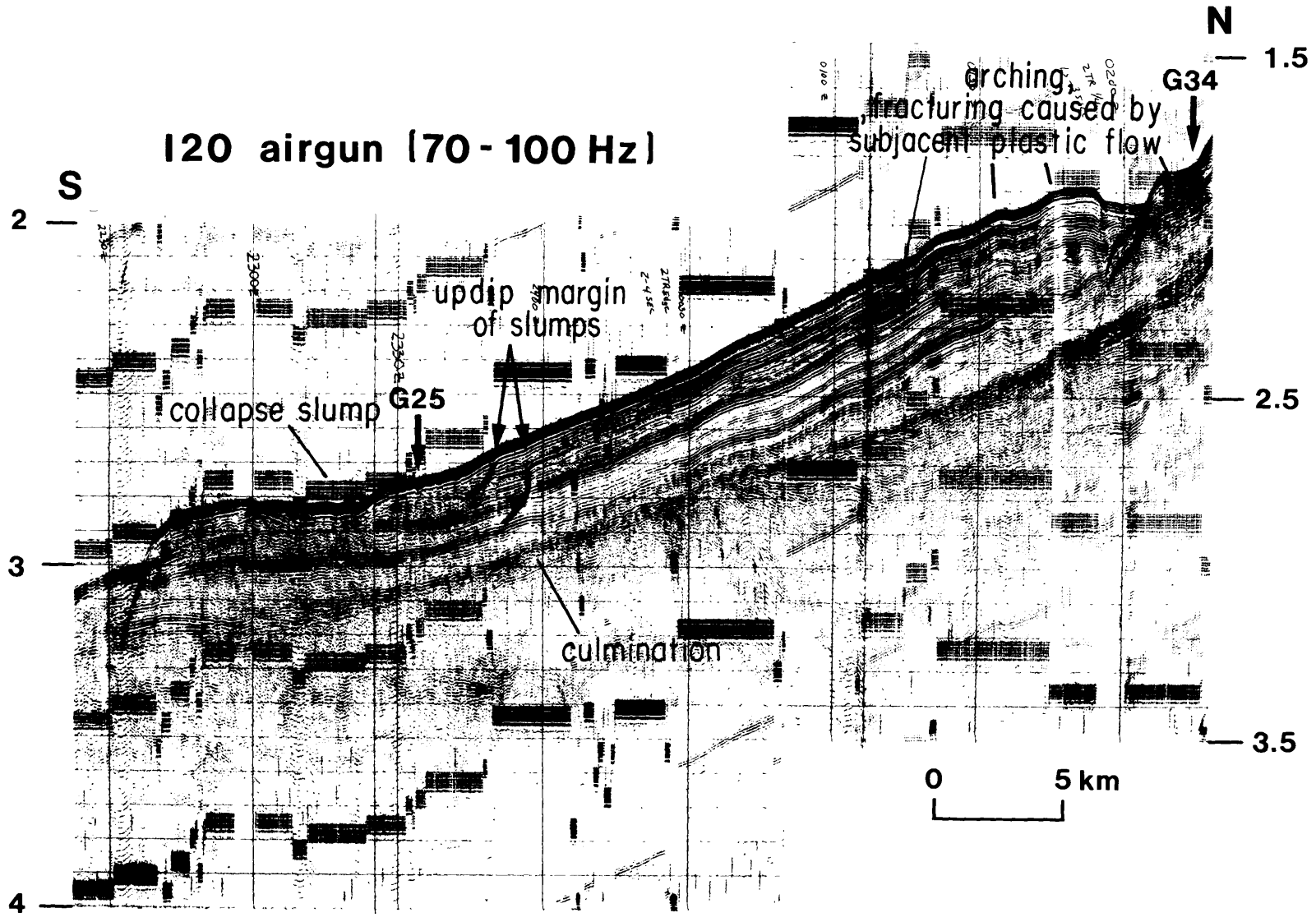

Figure 63. Profile I20 (airgun) shows internal and surficial deformation related to transverse trough shown in figure 62. Trough margin shown here at about 2240Z. Heavy curved lines indicate slip planes. Vertical exaggeration ~ 18:1.

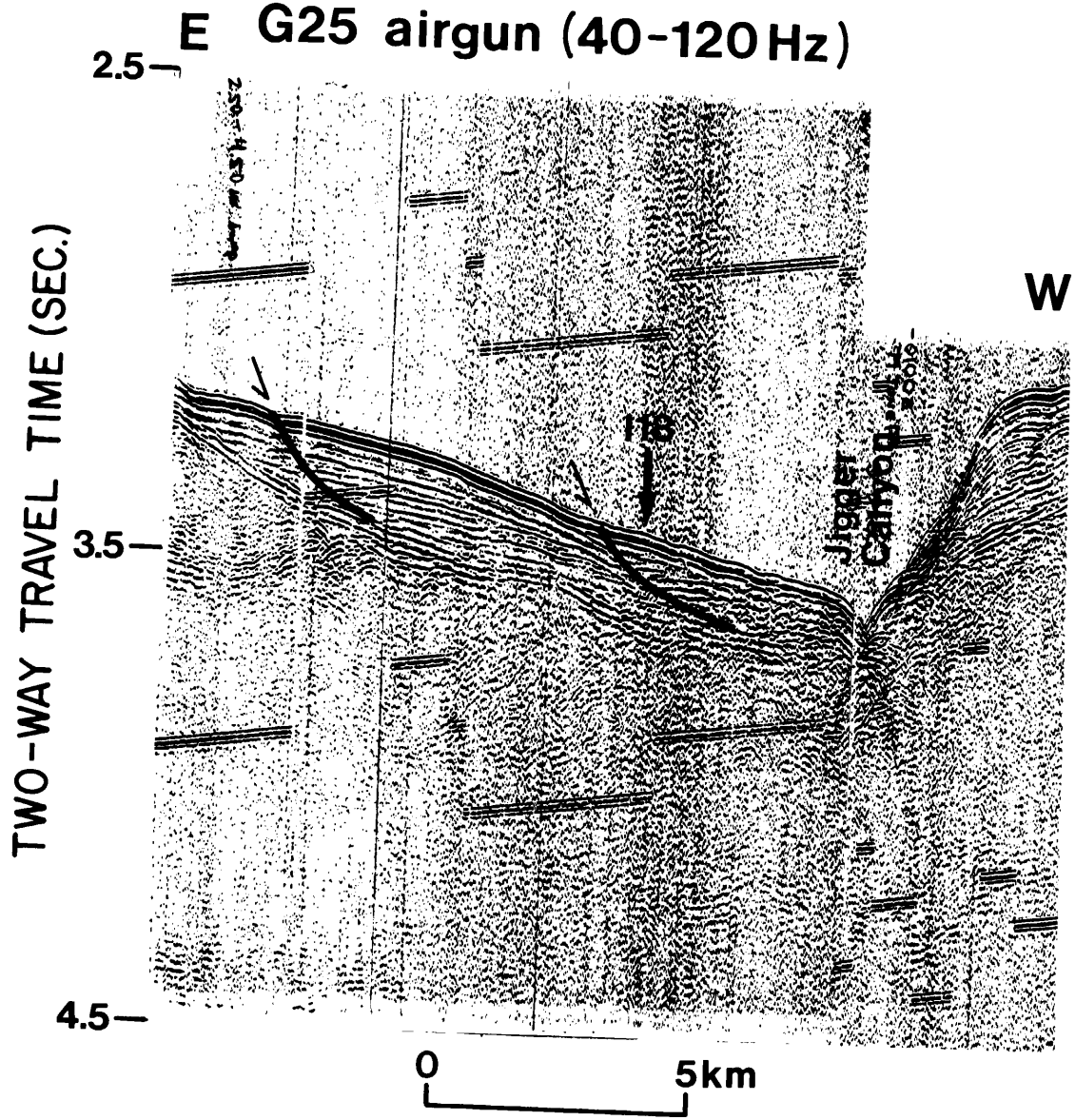

Figure 64. Profile G25 (airgun) along lower slope from 2,300 m to 2,650 m depths shows translation of layered rise sediment toward Jigger Canyon. Arrows indicate heads of slumps. Vertical exaggeration ~ 12:1.

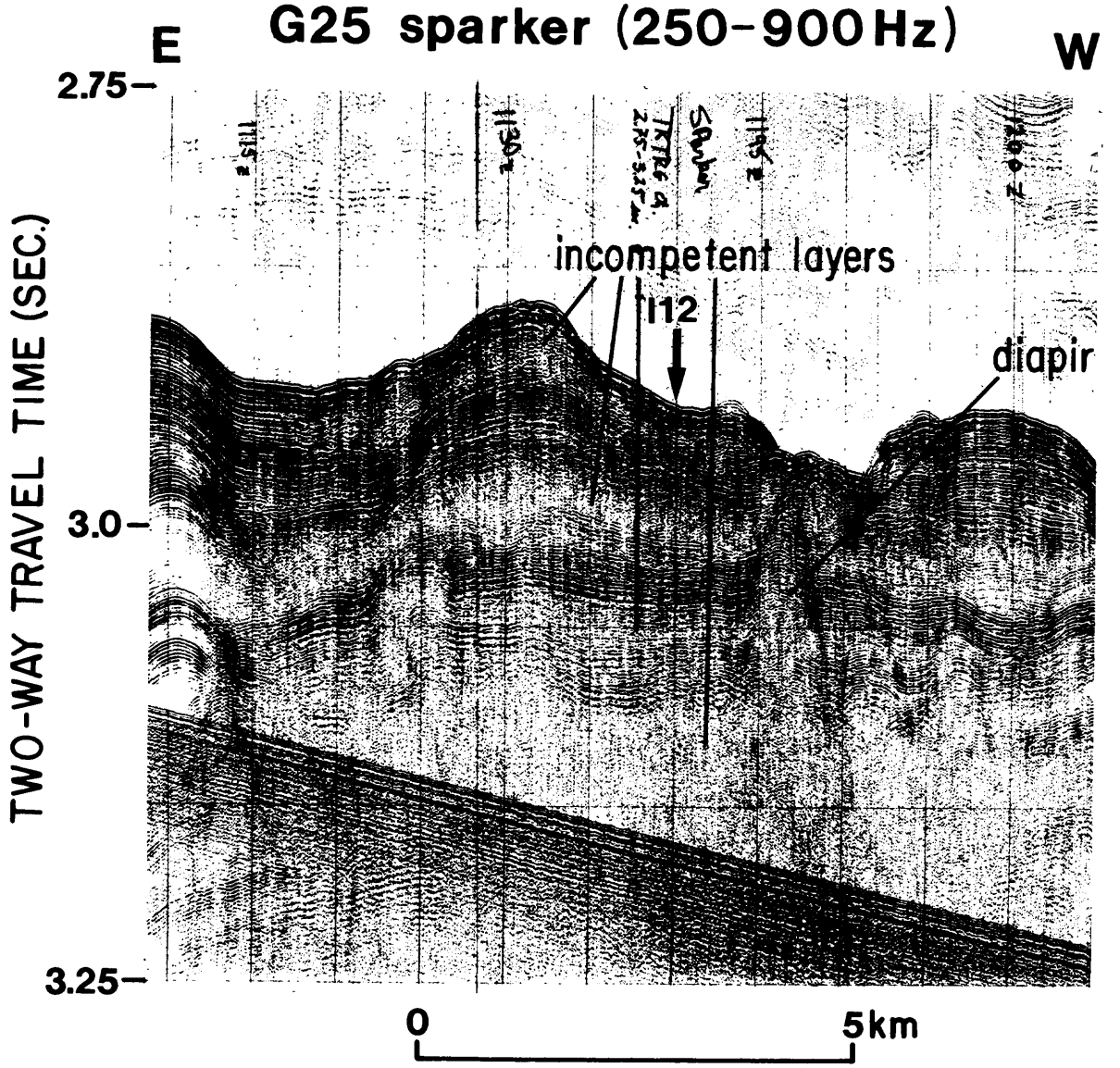

Figure 65. Profile G25 (sparker) shows deformation associated with incompetent layers along lower slope at about 2,250 m depth, east side of Dogbody Canyon (cf. fig. 50). Vertical exaggeration ~ 27:1.

interval is represented by thin, weak, parallel reflectors. Here, slight culminations in transparent layers higher in the section, especially one 220 m deep, control notchlike forms that may have formed along zones of tensile fractures (fig. 66). A mound at 1715, line G25 (fig. 66), represents a culmination away from which adjacent surfaces have subsided due, presumably, to internal collapse and layer-parallel extension.

Depressed blocks associated with culminations of deformed sediment in the layered rise unit are common. A good example is shown in figure 67 (cf. fig. 48). It is crossed obliquely by line I9 (fig. 68). Here the structure is represented as a slump having 60-m displacement at 0840. The toe abuts a sediment-filled notch; map E indicates that a 14-km-long trough oriented north-northeast probably corresponds to this feature.

Downdip structural incompetency and internal disruption are also common in the layered rise unit farther seaward on the upper rise. In places, incompetent material breaches layered sediment close to the sea floor (line I12, fig. 42). Downdip from 1130 (fig. 42) the rise surface is perhaps step-faulted over a section in which internal layering is almost totally obliterated.

A rare slump on the rise is shown in line I8 (fig. 69, cf. fig. 52). The slip plane (arrow) shows 13 m of displacement; it extends down 90 m to the base of an incompetent layer. Overlying sediment is dropped down, partly pinching out the incompetent layer and causing it to bulge downslope at 2057.

Sector III: 69°15'W. to 71°00'W.:
Lines I1-I7, I39; G25-G34, G45-G48, maps D, E, F, G

General physiography

In this sector the shelf generally rolls off to a smooth, broadly convex upper slope that steepens progressively with depth and conforms to bedding of underlying strata, including the upper-slope unit. Toward the west, the shelf break is marked by an abrupt, slight lip at 105-140 m depths. The break fairs out onto the upper slope, a rectilinear to very slightly convex, incised, conformable surface which extends, with an average inclination of 1.4°, to about 750-m depth.

West of 69°40'W., the upper slope is typically terminated seaward, at 720-970-m depths, by one or more prominent scarps. East of 69°20'W., the profile of the upper slope, from 400-m to about 600-m depths, is very uneven. On some lines a broad, incised bench is recorded at about 525-m depth; in others a relatively simple concave depression is represented.

From about 1,000-m depth, along most of the sector, the lower slope descends smoothly, with an average inclination of 7.6° (MacIlvaine and Ross, 1979), down to an abrupt contact with the Continental Rise between 1,900 and 2,200-m depths. The brow of the lower slope also marks the outcrop of an important stratigraphic contact below which lies the lower-slope unit; the lower-slope profile exhibits hyperbolic echoes, broad mounded surface forms, and complex subsurface structures typical of the lower-slope unit.

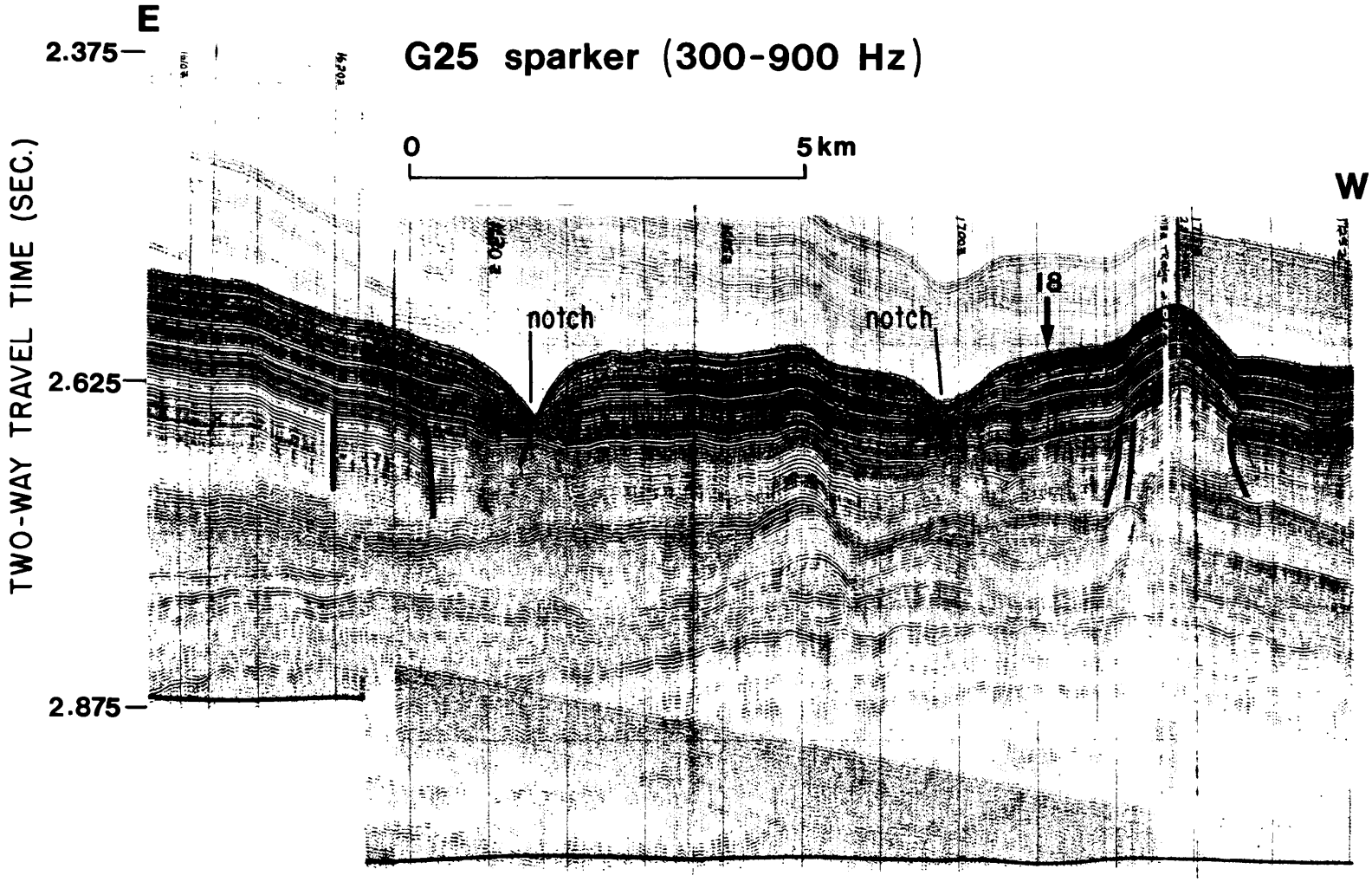

Figure 66. Profile G25 (sparker) along lower slope at about 2,000 m depth shows internal deformation in the layered rise unit. Heavy lines indicate inferred faults. Vertical exaggeration ~ 22:1.

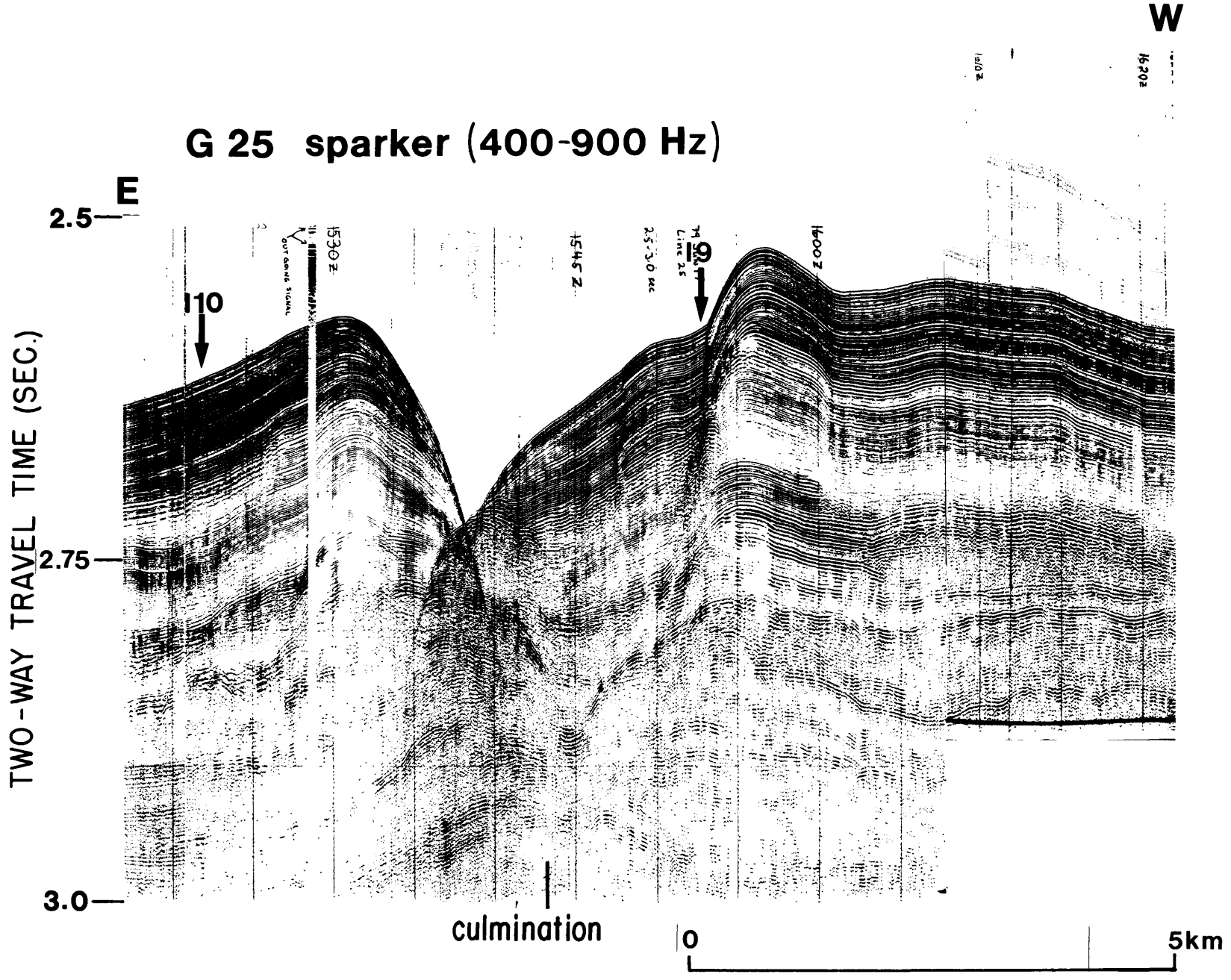

Figure 67. Profile G25 (sparker) along lower slope at about 2,000 m depth shows transverse graben over culmination west of Hydrographer Canyon (cf. fig. 50). Vertical exaggeration ~ 19:1.

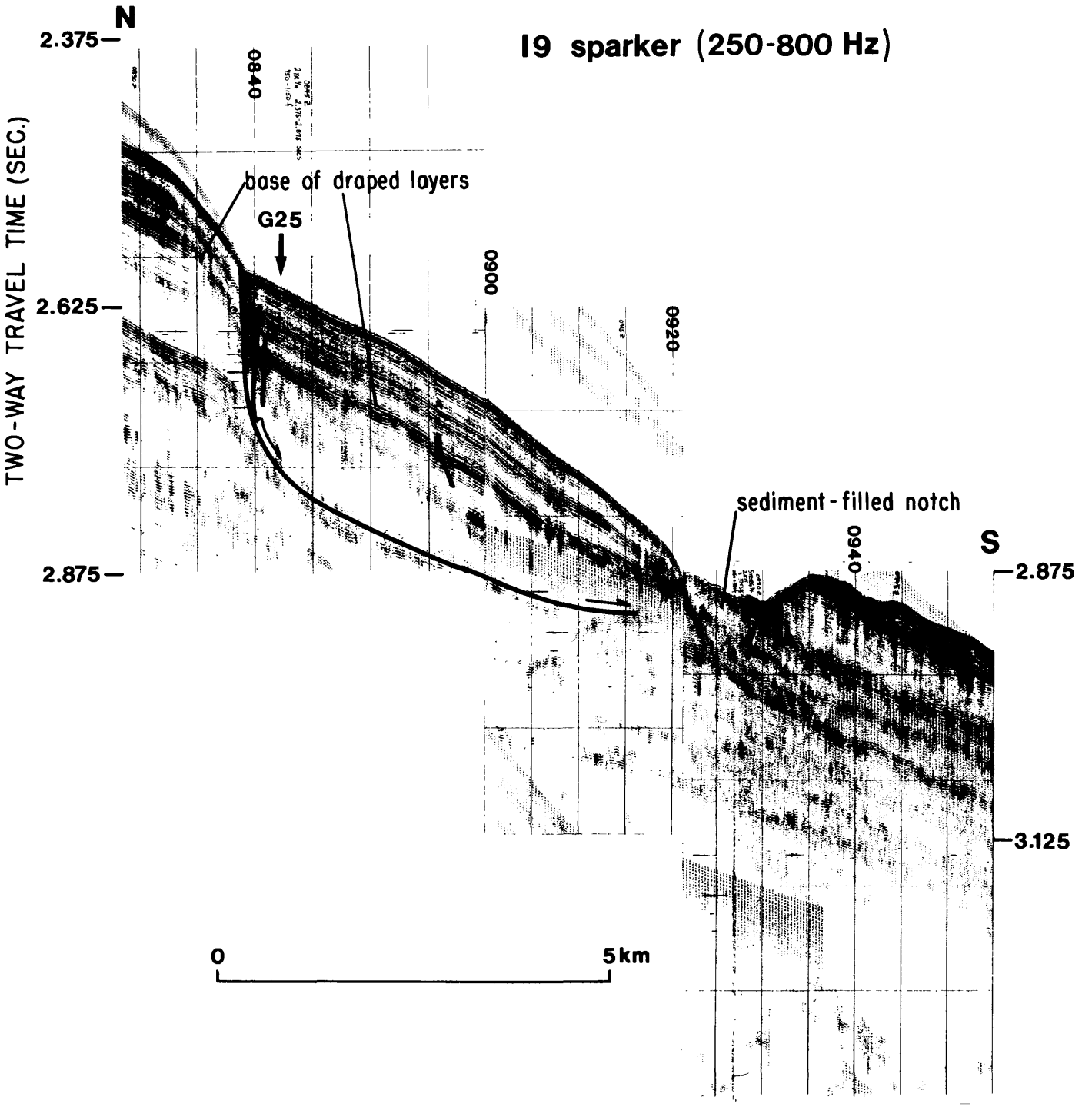

Figure 68. Profile I9 (sparker) shows block displacement along listric fault. Note that structure has been draped and reactivated (cf. fig. 67). Vertical exaggeration ~ 18:1.

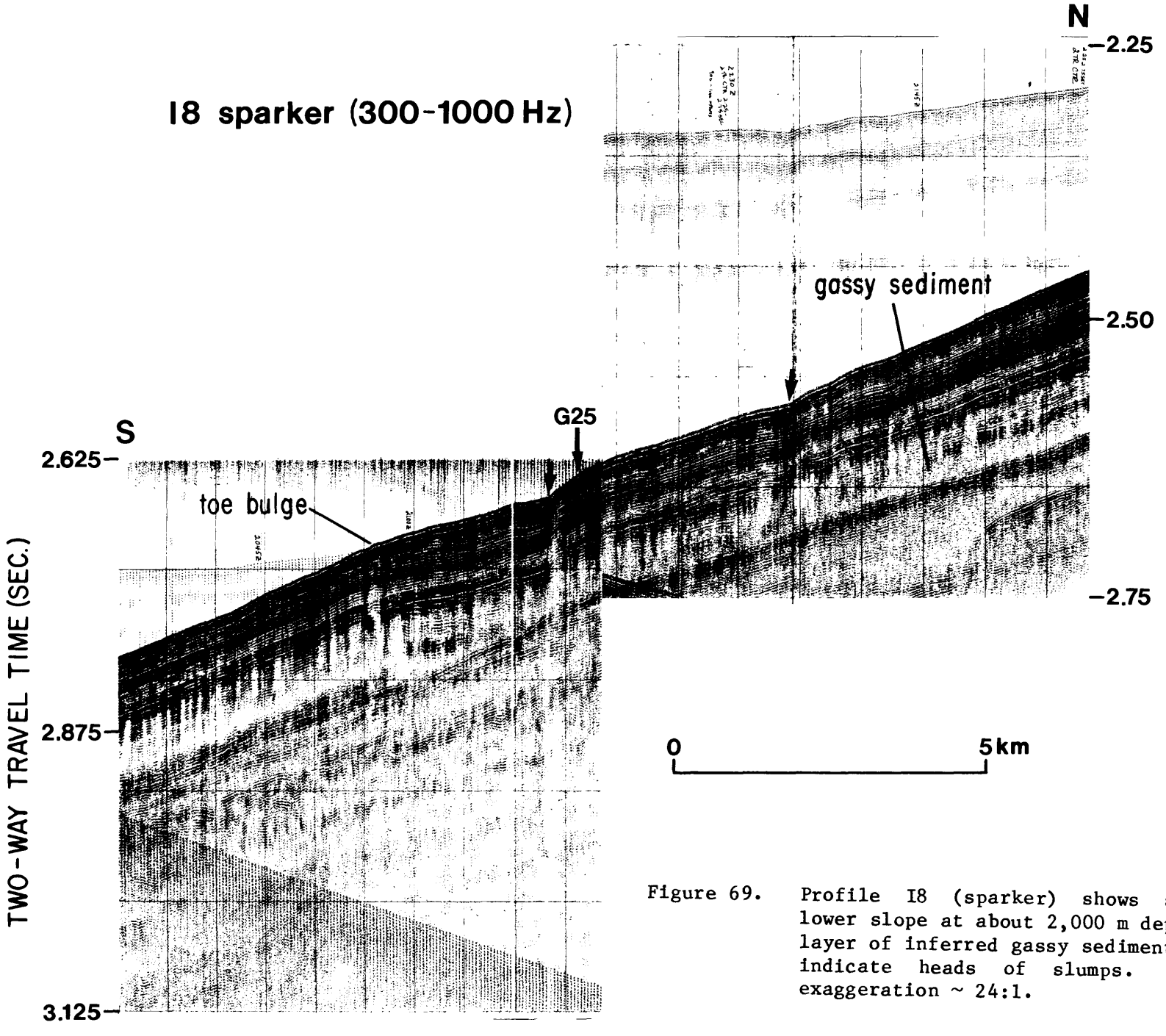

Figure 69. Profile I8 (sparker) shows slumps on lower slope at about 2,000 m depth. Note layer of inferred gassy sediment. Arrows indicate heads of slumps. Vertical exaggeration ~ 24:1.

The rise surface is typically flat and conformable and is underlain by acoustically well-discriminated strata. Beneath the rise onlap, the buried lower-slope surface flattens with depth and becomes conformable with the layered rise unit.

Toward the west and below 1,500-m depth the lower slope is abruptly flattened to a 1.5° gradient (MacIlvaine and Ross, 1979). Below this break, the nearly rectilinear to slightly convex surface is underlain by a wedge of chaotic material that thickens seaward and is onlapped by the rise at depths between 2,300 m and 2,400 m.

The slope in sector III is cut by numerous relatively small complex erosional forms (MacIlvaine and Ross, 1979) and by four canyons: Veatch Canyon, a relatively wide, shelf-indenting canyon; Nantucket Canyon, a complex depression formed of coalescent gullies; and Alvin and Atlantis Canyons, which are morphologically similar to Veatch.

At the midslope level (approximately 1,500-m depth) the canyons are distinct, notchlike gorges with relief of about 300-350 m; among the steep, transverse landforms of the rise, the canyons have 40 m or less of relief and are scarcely discernable.

Form and stratigraphy

East of 70°00'W. the surficial layer is seen only in line I5, where it is recorded as a very attenuated opaque wedge that pinches out at about 135-m water depth. Its maximum thickness is about 35 m. Broad, irregular, concave surface forms suggest that the layer has been thinned by current scour, an interpretation supported by bathymetric forms shown in map E. Other seismic lines in this part of the sector do not extend far enough up on the shelf to record the presence of the surficial layer, but the 1:250,000 scale bathymetry of the base map suggests it is present near the shelf break east of Veatch Canyon and that it has been scoured back west of the canyon. The canyon itself may intersect the surficial layer.

In places where the surficial layer is absent, a wedge of sediment with a relief of about 30 m forms the shelf break (fig. 70); it is underlain by acoustically nearly opaque sediment and thin onlapping layers, features that imply a strand-line environment. The wedge may represent a wave-built spit derived from surficial sediment farther east as well as sediment cut from the foreset unit by wave planation.

In this sector the foreset unit is represented beneath the outer shelf by acoustically nearly opaque sediment within which sparse, vague, shallow-dipping reflectors are seen (fig. 70). Under the shelf break the unit attains a maximum thickness of about 425-460 m. Seaward of the shelf break strata become progressively better defined and form a homoclinal sequence to which the upper-slope surface conforms. Truncated layers of the unit are well exposed in the head of Veatch Canyon (Slater, 1982). J. S. Schlee (pers. commun., 1982) reported gray, compact, silty clay substrate in Veatch Canyon to depths of at least 495 m.

The foreset unit was penetrated by AMCOR hole 6012 (Hathaway and others, 1976) on the upper slope near Block Canyon, approximately 38 km west of line

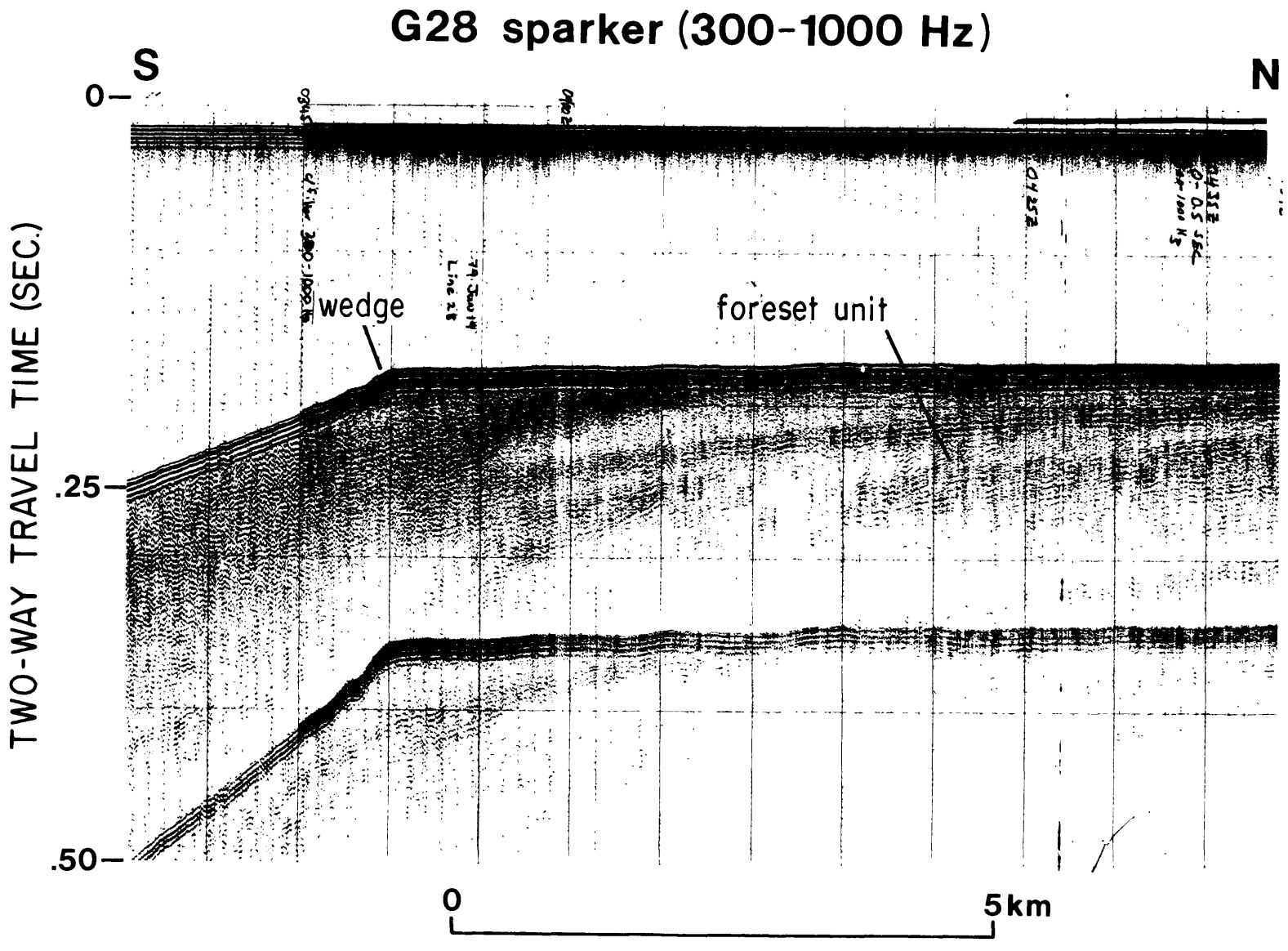

Figure 70. Profile G28 (sparker) shows wave-planed foreset strata and wedge representing the shelf break. Vertical exaggeration ~ 19:1.

G26 (map G). Nearly 304 m of mainly sticky-to-plastic, slightly silty, dark-gray clay of Pleistocene age was logged. The sediment was gassy below 90 m. The hole bottomed in dark-olive-gray, slightly plastic clay of possibly Miocene age.

At elevations above the 1,000-m isobath the foreset unit comprises at least two nonconformable subunits (fig. 71): a finely laminated lower subunit, which extends across the slope on truncated underlying beds, and a draped, finely laminated upper subunit. Fine reflectors within both subunits dip shallowly west.

Beneath the outer shelf the upper subunit of the foreset unit is represented by a few nearly opaque layers that together are about 30 m thick. These dip progressively seaward and thicken to about 150 m beneath the shelf break. Under the shelf the upper subunit lies unconformably on truncated, more steeply dipping beds of the lower foreset subunit; seaward of the shelf-break layers of both subunits are very nearly conformable, but with increasing water depth the upper subunit thins and offlaps the lower subunit, and three or four distinct layered intervals become increasingly more sharply defined (fig. 72), suggesting a facies transition to thinner, more parallel layers (or possibly a transition from gassy(?), internally deformed sediment). The layers have a distinctive acoustic grading, from sharply bounded, nearly opaque upper parts down to diffuse, relatively thick, transparent lower parts. Each layer is paraconformable on the lower one (fig. 72); the irregular contacts indicate that deformation and/or erosion occurred between successive episodes of deposition. A great deal of local fine-scale wipeout in the intervals below distorted reflectors implies that internal deformation has occurred.

The scarps along the upper-slope brow truncate all or most of the upper foreset subunit (fig. 72). Much of the lower subunit continues, thinned, down across the lower slope in marked unconformity on the lower-slope unit (fig. 73). The foreset unit is 60-90 m thick as far down on the slope as 1,500-1,600 m where it includes well layered strata similar to those described on the upper slope. In general, the foreset drape is very thin toward the east end of the sector, and it is probably discontinuous.

ASP hole 18, below 1,000 m on the west side of Veatch Canyon, encountered 92 m of Pleistocene silty sand on lower Maestrichtian sediment (Valentine, 1981; Poag, 1982). Approximately the same thickness of inferred Pleistocene dark-gray, sandy-silty compact clay and soft-to-hard dark-greenish-gray glauconitic silt and clay was encountered at ASP hole 17 (Manheim and Hall, 1976) on the east side of Veatch Canyon below 1,200 m.

The upper-slope unit is fairly uniform in thickness (about 400 m) along the upper slope; it comprises two nonconformable, acoustically poorly discriminated subunits. The upper subunit is a relatively thin interval of strong, continuous, relatively closely spaced parallel reflectors (fig. 74) which show attenuated lensing and pinching on strike, and thin, nearly transparent lentils, especially toward the east end of the sector. At the base of the upper subunit a weakly reflective layer fills hollows in the surface of the lower subunit (fig. 74). The basal contact cuts across reflectors of the lower subunit downdip (figs. 74, 75). The upper subunit is in many places gradational, or at least conformable, with the overlying foreset unit (fig. 75).

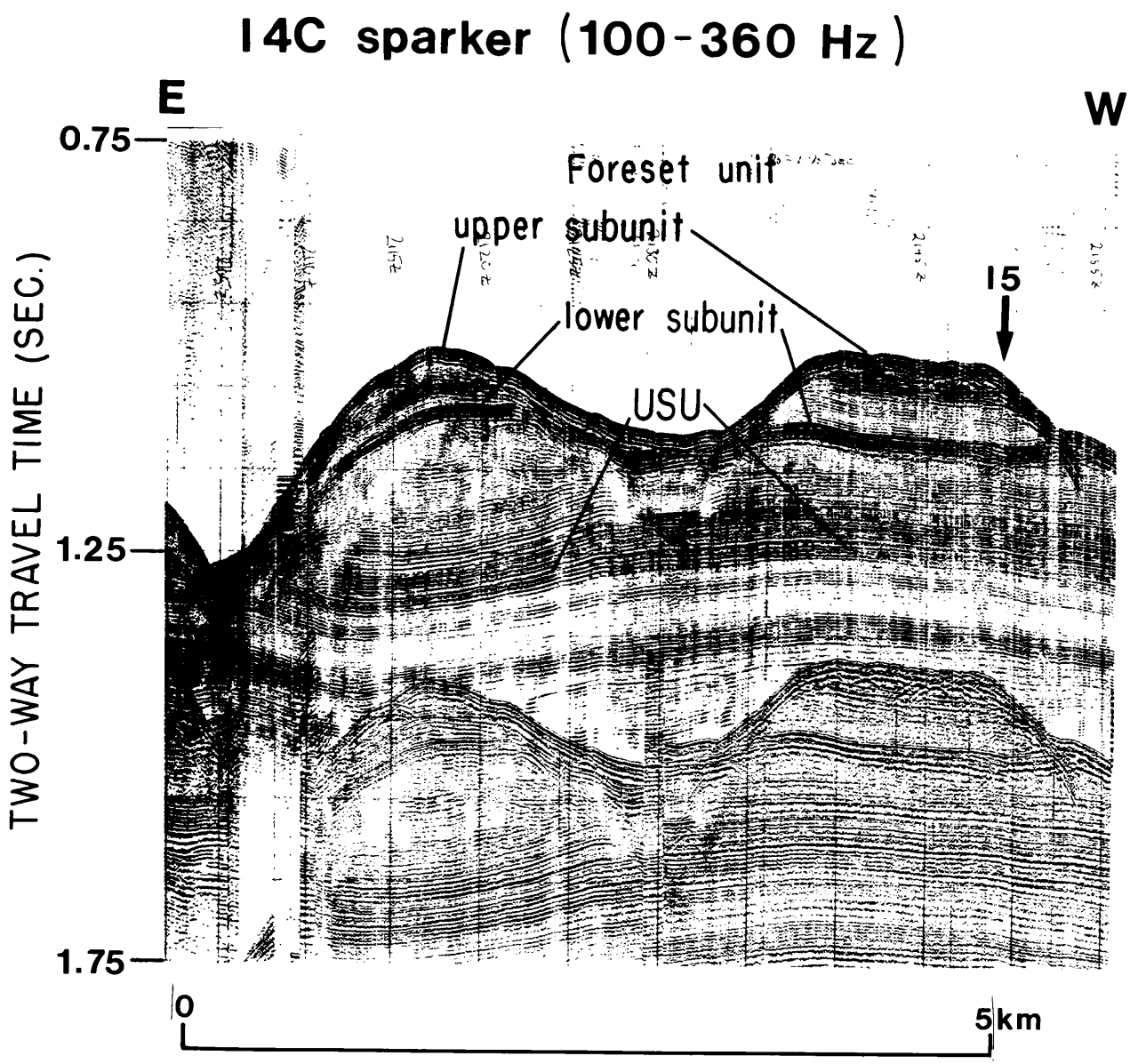

Figure 71. Profile I4c (sparker) along upper slope at about 750 m depth, between Veatch and Nantucket Canyons, shows stratigraphic-structural relationships of the foreset and upper-slope (USU) units along strike. Vertical exaggeration ~ 7:1.

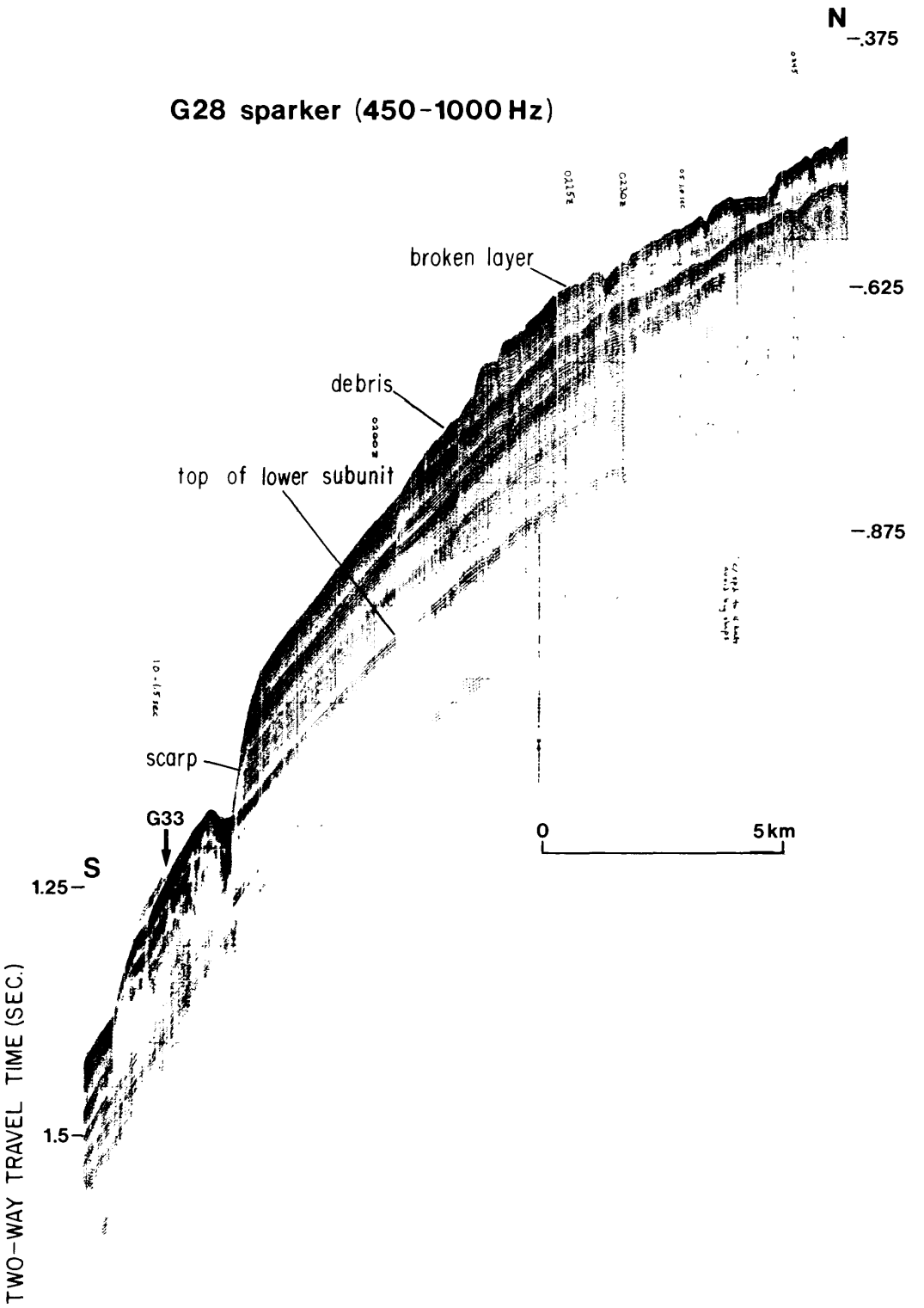

Figure 72. Profile G28 (sparker) shows mass-movement features and increasing definition of reflectors in foreset unit with depth on slope. Vertical exaggeration ~ 28:1.

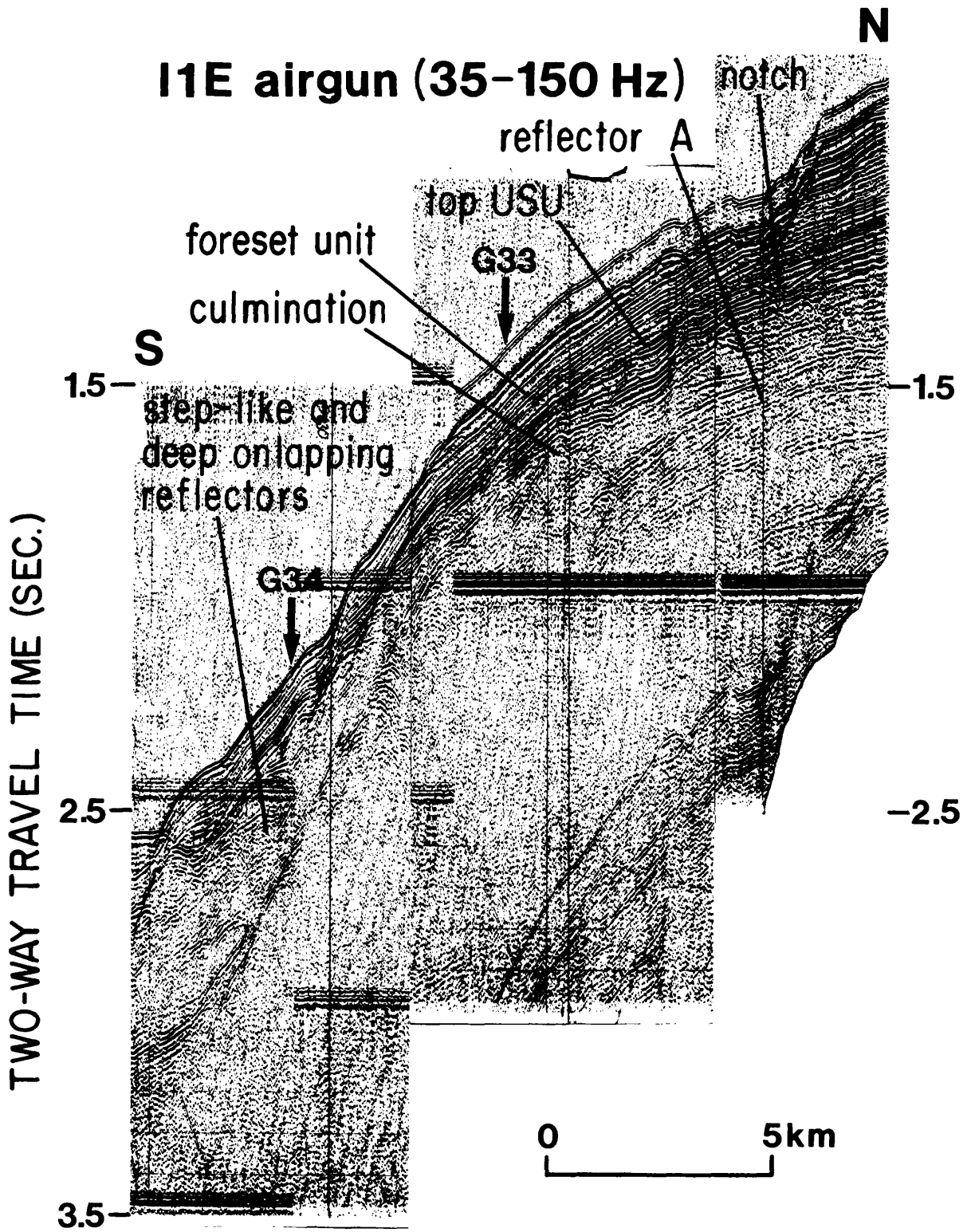

Figure 73. Profile I1E (airgun) shows structure along east side of Alvin Canyon. Vertical exaggeration ~ 12:1.

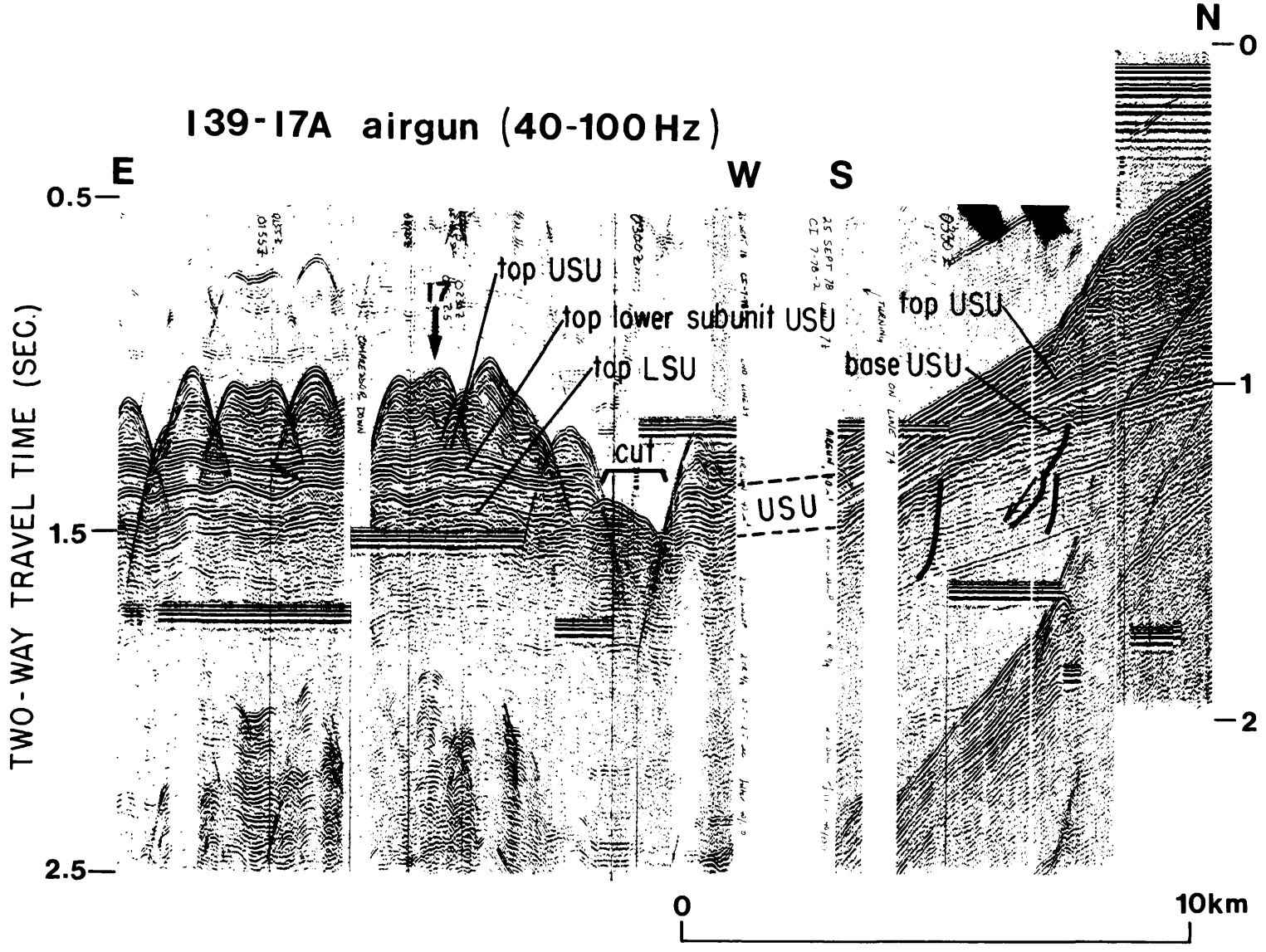

Figure 74. Profiles I39-I7A (airgun) show upper-slope unit (USU) on strike and downdip. Vertical exaggeration ~ 9:1.

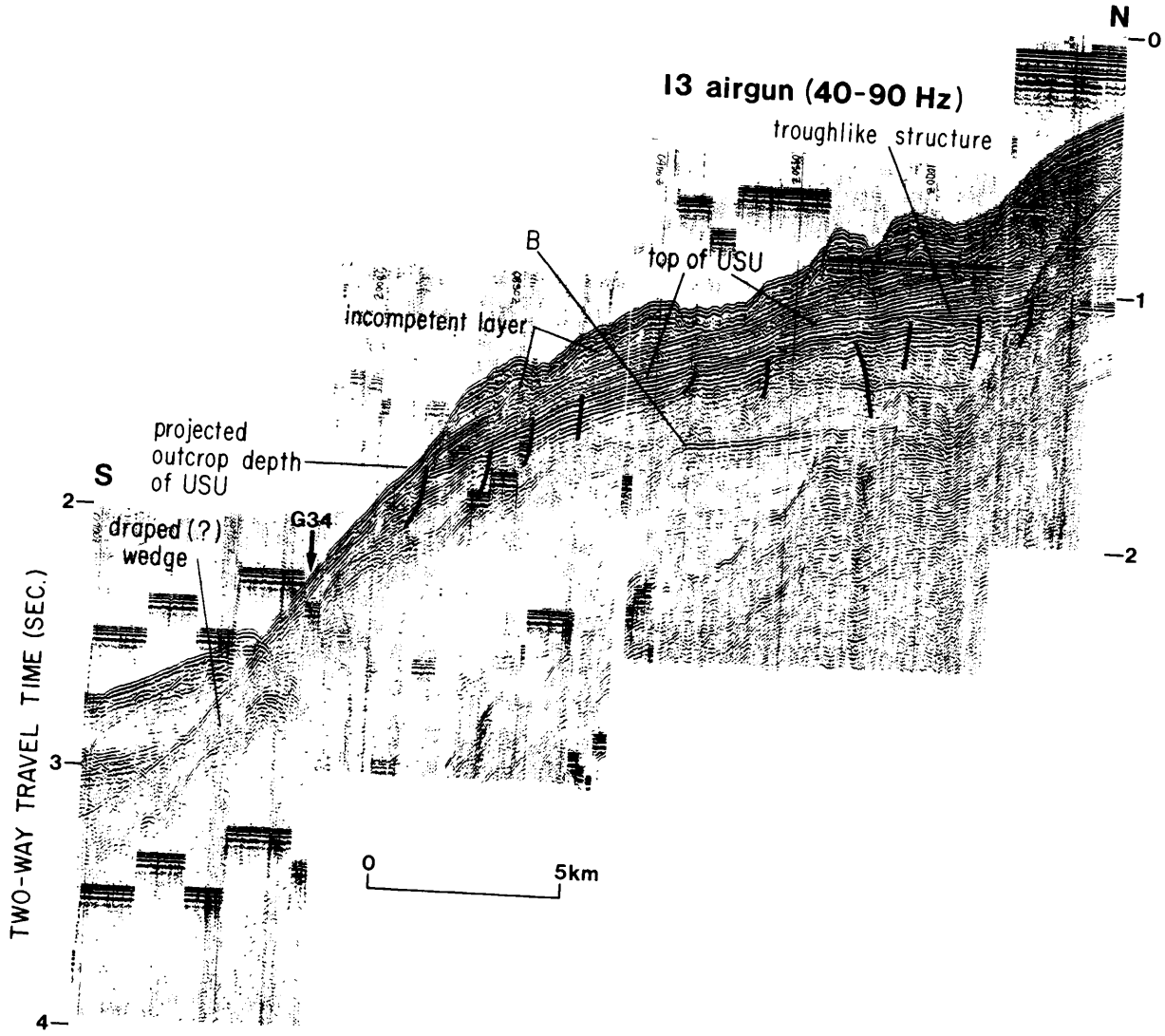

Figure 75. Profile I3 (airgun) shows structural features of the upper-slope unit (USU); vertical lines indicate locations of inferred fault traces. Vertical exaggeration ~ 9:1.

Beneath the outer part of the upper slope, the upper subunit of the upper-slope unit includes a peculiar shallow trough tens of kilometers long, oriented along strike (map G; fig. 9, I). The most pronounced feature of this depression is a sharp, shelf-facing surface on the seaward side, against which flatter, infilling updip layers onlap truncated downdip layers (figs. 75, 76). The updip side of the structure is less distinct and is represented by a slight monocline which accounts for the flattened dips within the trough. In places, the trough narrows to a distinct notch (fig. 73).

On the open slope the top of the upper-slope unit crops out at depths that vary from 1,000 m near the eastern end of the sector to less than 700 m toward the western end. In line I3 the top of the unit, obscured near the slope by acoustic interference, projects to outcrop at about 1,440 m (fig. 75). Elsewhere it extends, probably thinned, across the lower slope (fig. 77) and perhaps down to the rise. It is apparently exposed by erosion in many places across the lower slope and has been widely sampled (Stetson, 1949; Northrop and Heezen, 1951; Gibson, 1965, 1970).

In Veatch Canyon the upper subunit crops out below 425-m depth along a narrow dissected bench faced by steep, gullied cliffs. Upper middle Eocene argillaceous limestone has been reported cropping out at 950 m on the east wall of Veatch Canyon (Valentine, 1981). J. S. Schlee (pers. commun., 1982) observed a "large block of white chalk" (Eocene) at 1,034-m depth in the canyon.

The upper-slope unit thins and is increasingly broken and internally distorted downdip (fig. 75). It unconformably overlies the lower-slope unit, which has a regionally flatter dip; in places, the lower contact is a surface of some relief (figs. 74, 75). The contact of the upper slope with the lower-slope unit on strike is generally paraconformable, but locally the basal layers are draped or perhaps faulted down on depressions in the lower-slope unit (fig. 74).

The lower-slope unit shows weak layering on a scale and of a style similar to that of the overlying upper-slope unit, especially toward the eastern end of the sector (fig. 78). To the west, distinct subunits or acoustic intervals appear in the lower-slope unit (fig. 79): The uppermost subunit is a weakly parallel-layered, nearly transparent interval about 215 m thick that, east of 79°00'W., crops out between 1,125 m and 1,215 m. This interval rests on a rough, nearly horizontal reflector (A, fig. 79) which truncates locally more steeply seaward-dipping reflectors, evident toward the seaward edge of the upper slope (fig. 73), that comprise a less well-layered middle interval at least 150 m thick. The two intervals form steep slope segments that are deeply cut by Nantucket Canyon. They lie on a thin, seaward-thickening, strong reflector interval which, seaward of point B (figs. 75, 79), seems to have collapsed and splayed downdip, or to have been truncated and onlapped. The onlapped interval nowhere crops out, but seems to follow the dip of the slope. To the west, point B forms a distinct, acute shoulder.

The lower-slope unit is broadly and evenly layered on strike, but is disharmonically warped in relation to the suprajacent layers (fig. 80). Lensing and/or beveling of subunits on strike is also evident. Just west of G29 (fig. 80, map G) the broadly warped reflectors fade out in confusion in a

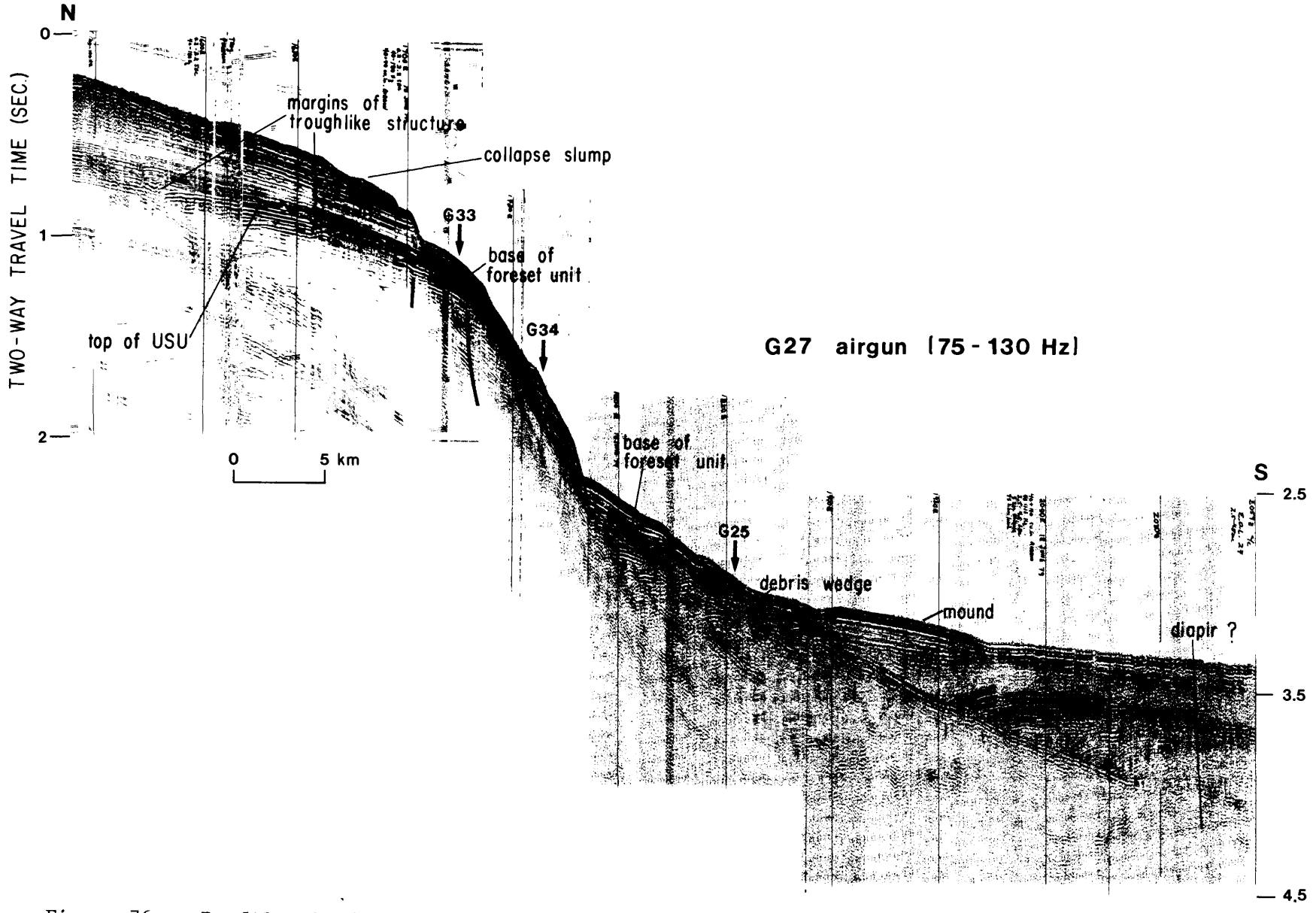

Figure 76. Profile G27 (airgun) across slope; heavy vertical lines indicate inferred fractures or faults. Vertical exaggeration ∿ 15:1.

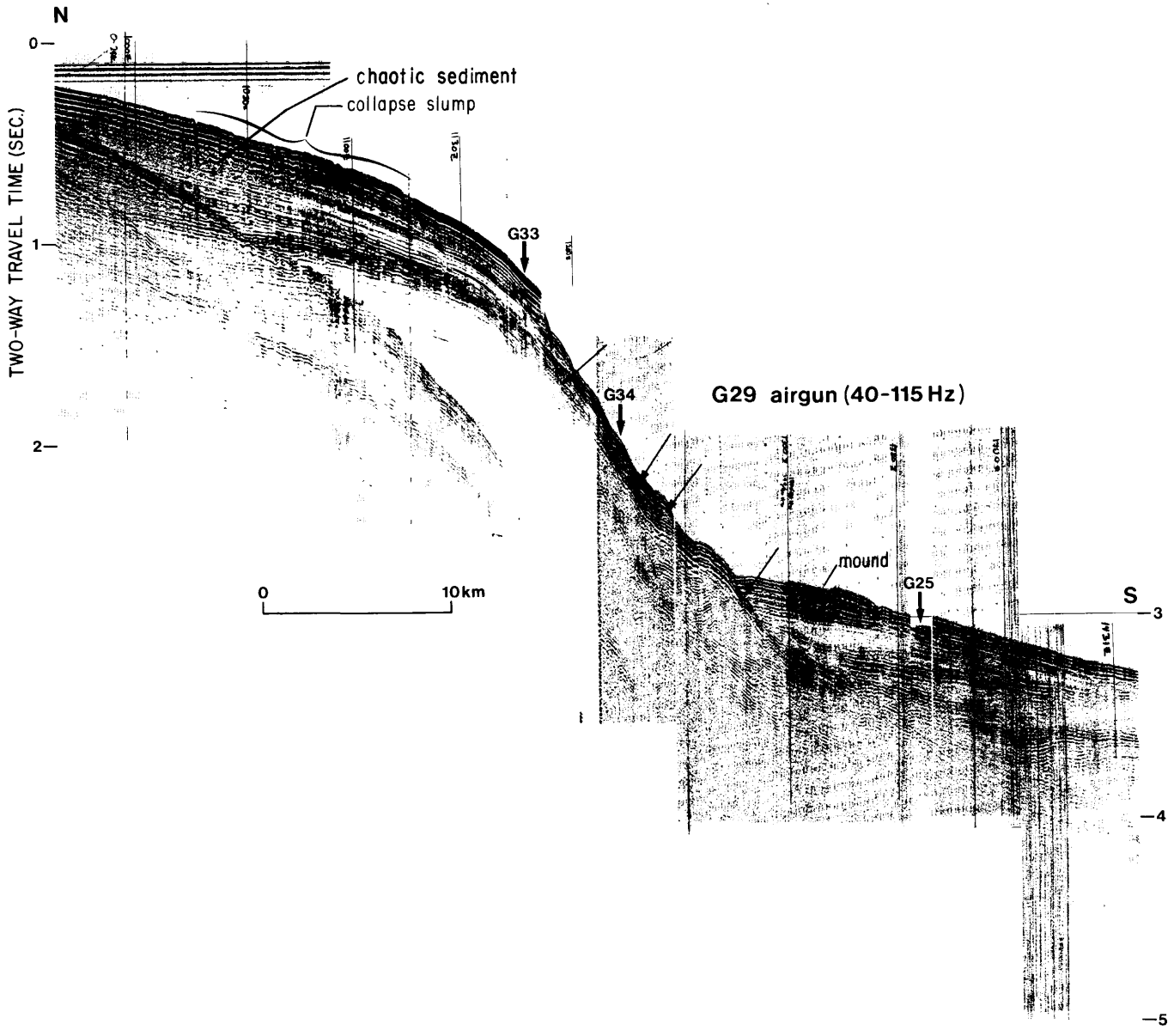

Figure 77. Profile G29 (airgun); arrows indicate top of upper-slope unit. Vertical exaggeration ~ 15:1.

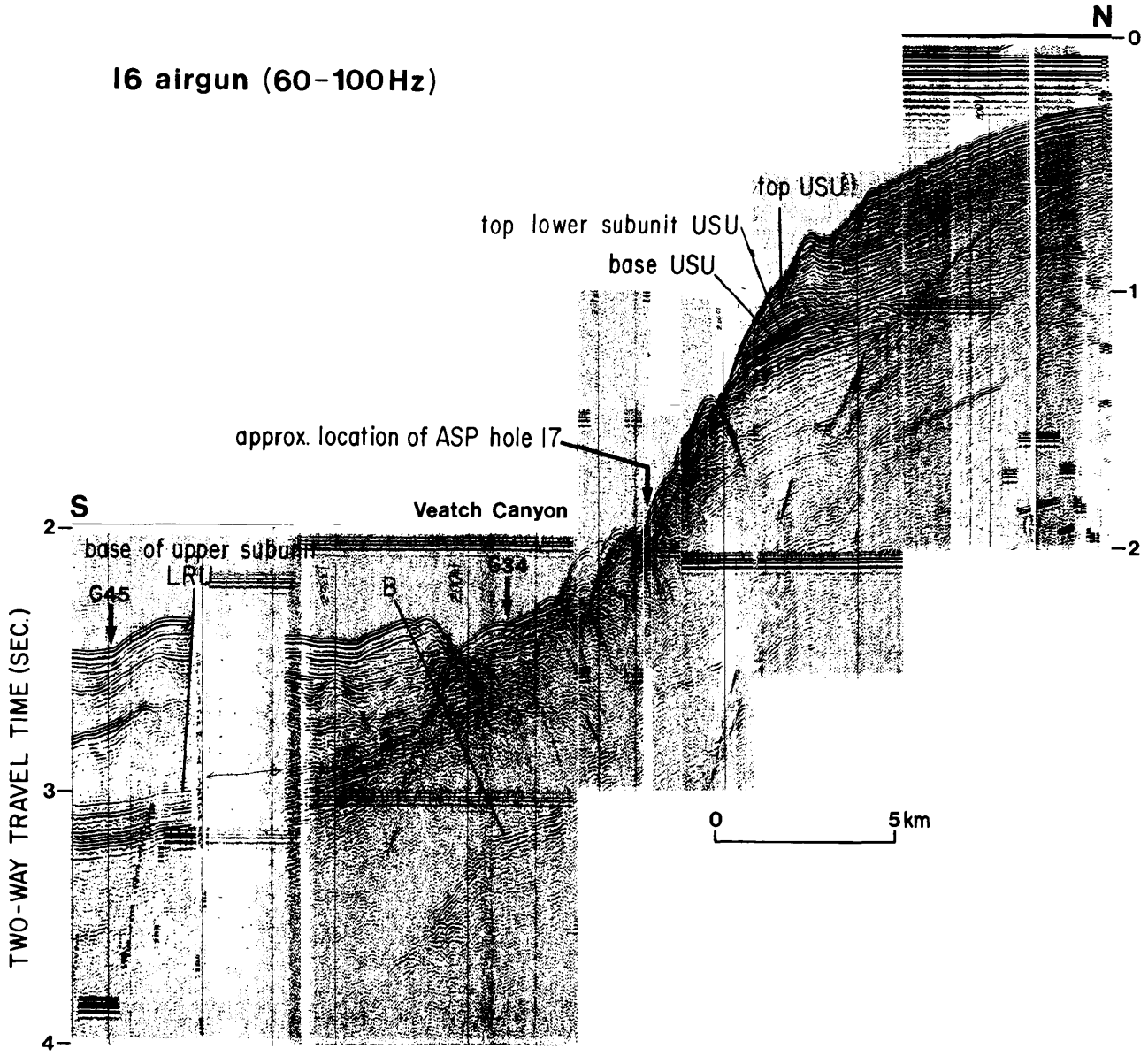

Figure 78. Profile I6 (airgun) obliquely crosses Veatch Canyon and shows stratigraphic position of upper-slope unit (USU). Vertical exaggeration ~ 10:1.

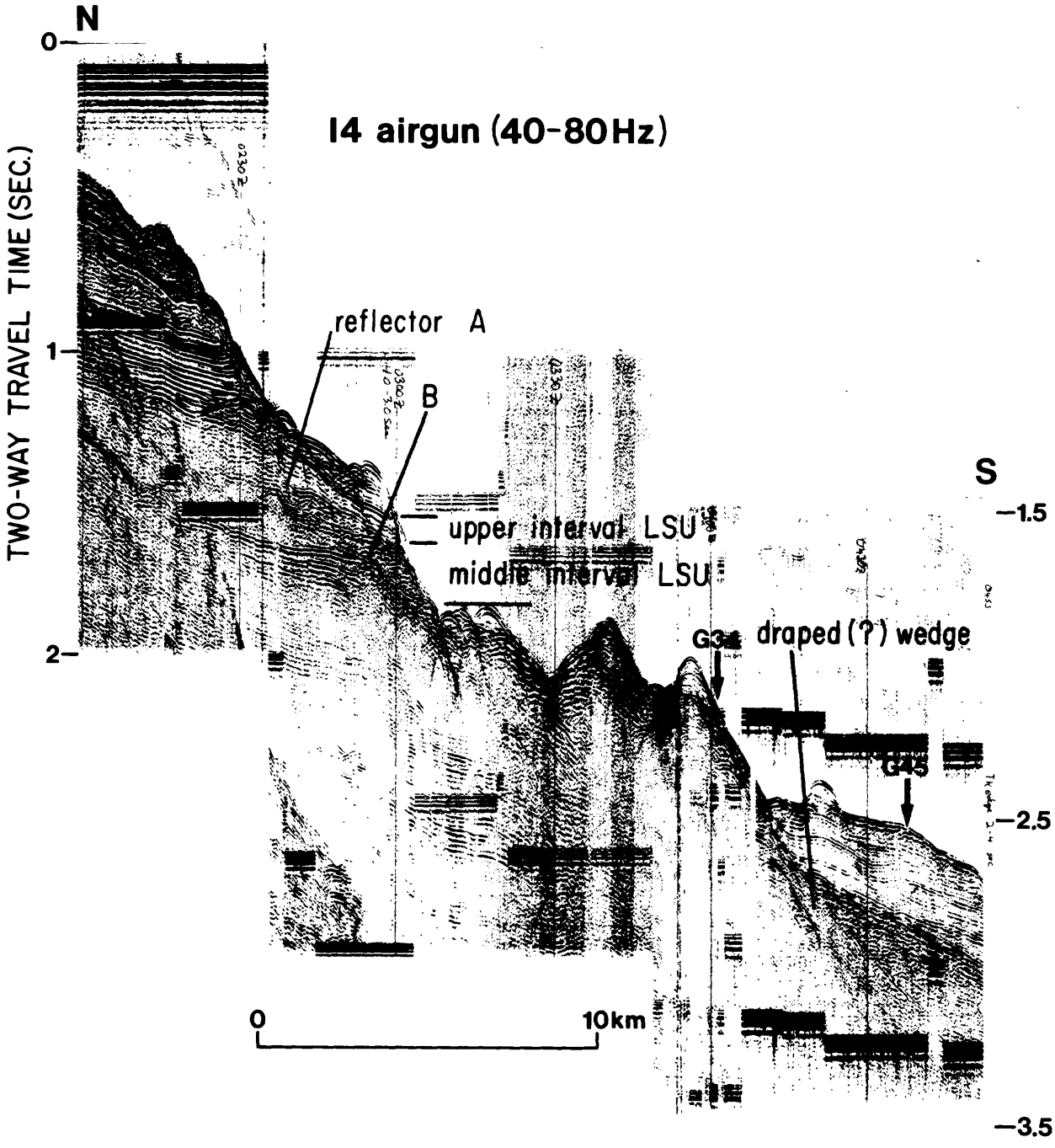

Figure 79. Profile I4 (airgun) shows subunits of lower-slope unit (LSU). Vertical exaggeration ∿ 12:1.

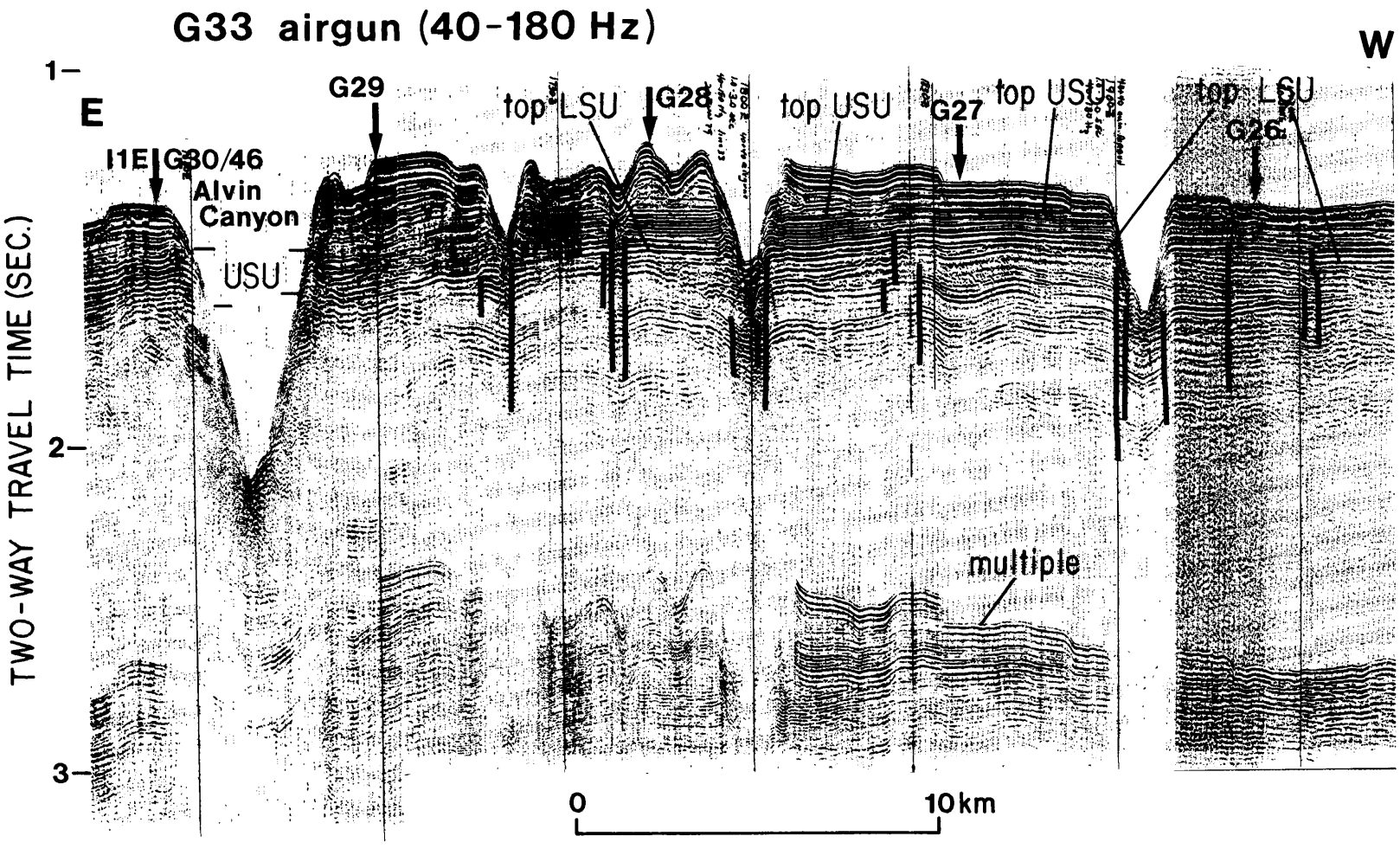

Figure 80. Profile G33 (airgun) along midslope at approximately 1,000 m depth shows relationship of upper-slope unit (USU) and lower-slope unit (LSU). Vertical lines show inferred faults or fracture-aligned flexures. Vertical exaggeration ~ 14:1.

zone that culminates at IlE, (fig. 80), just beneath the upper-slope unit. The confused zone is deeply cut by Alvin Canyon. The canyon also truncates thin, close, steeply dipping convergent reflectors flanking the confused zone just below the upper-slope unit; the canyon thus appears to have incised a previously cut-and-filled depression in the lower-slope unit (note also the subsurface structure adjacent to Alvin Canyon shown in fig. 81).

The upper levels of the lower-slope unit have been sampled in the eastern part of the sector. Below 1,200-m depth on the slope, on the east side of Veatch Canyon, ASP hole 17 penetrated Upper Cretaceous sediment (Manheim and Hall, 1976) including semi-indurated sandstone, bluish-gray mudstone, dark limey clay, and dark-gray compact silty micaceous clay. ASP hole 18, below 1,000-m depth on the west side of the canyon, encountered 58 m of lower Maestrichtian dark-olive gray to brownish gray laminated to massive siltstone with minor dark-olive-gray sand and medium-gray clay, from 1,154-1,212 m below sea level. Below 1,248 m, at least 128 m of indurated mudstone and siltstone of Santonian age was encountered (Poag, 1982).

At 1,288-m water depth in Veatch Canyon, J. S. Schlee (pers. commun., 1982) obtained olive-gray to very-dark-gray silty micaceous claystone and light-olive-gray hard glauconitic fine-to-medium-grained limestone (moderately well-sorted packstone) composed of foraminifera tests, glauconite, and scattered shell fragments in a calcareous matrix. P. C. Valentine (pers. commun., 1982) dates these as late Santonian-early Campanian. Schlee also collected lower Maestrichtian rock along the east wall of Veatch Canyon at 1,055 m (Valentine, 1981), 50 m below observed Eocene chalk. Valentine (1981) correlates the outcrop with the upper unit in the ASP 18 section. Line I6 (fig. 78) shows that the sampled interval is a thick, regular, evenly layered succession.

The layered rise unit comprises two distinct, slightly discordant subunits (figs. 79, 82). The upper subunit includes a relatively thick (170 m) transparent or very faintly layered onlapping interval capped by a locally unconformable layered interval (fig. 79) which, along strike, ranges in thickness from 170 m to 80 m and which is correlative with or coextensive with the foreset unit (fig. 73). The upper subunit attains a maximum thickness of about 300 m close to the slope and thins gradually seaward.

The lower subunit consists of a succession of continuous parallel layers, the base of which lies below the limit of acoustic penetration (fig. 83). At least the upper part of it is stratigraphically continuous with reflectors beneath the buried slope surface (figs. 77, cf., figs. 78, 83) which itself becomes a bedding plane at about 1 s beneath the rise, 4 s below sea level.

The layered rise unit thickens to the west. The uppermost layers pinch in and out and change markedly in acoustic aspect along strike; reflectors and reflector-bounded intervals vary in amplitude and thickness (figs. 82, 84); they are warped, folded, and possibly faulted on the mounded surface of the subjacent transparent interval. The lowermost reflectors of the uppermost layered interval fade in and out along strike, suggesting lateral gradation with the underlying transparent interval. Likewise, the uppermost reflectors of the lower subunit are interleaved with thin transparent layers, between which they are bowed up, rumpled, and cut out on strike.

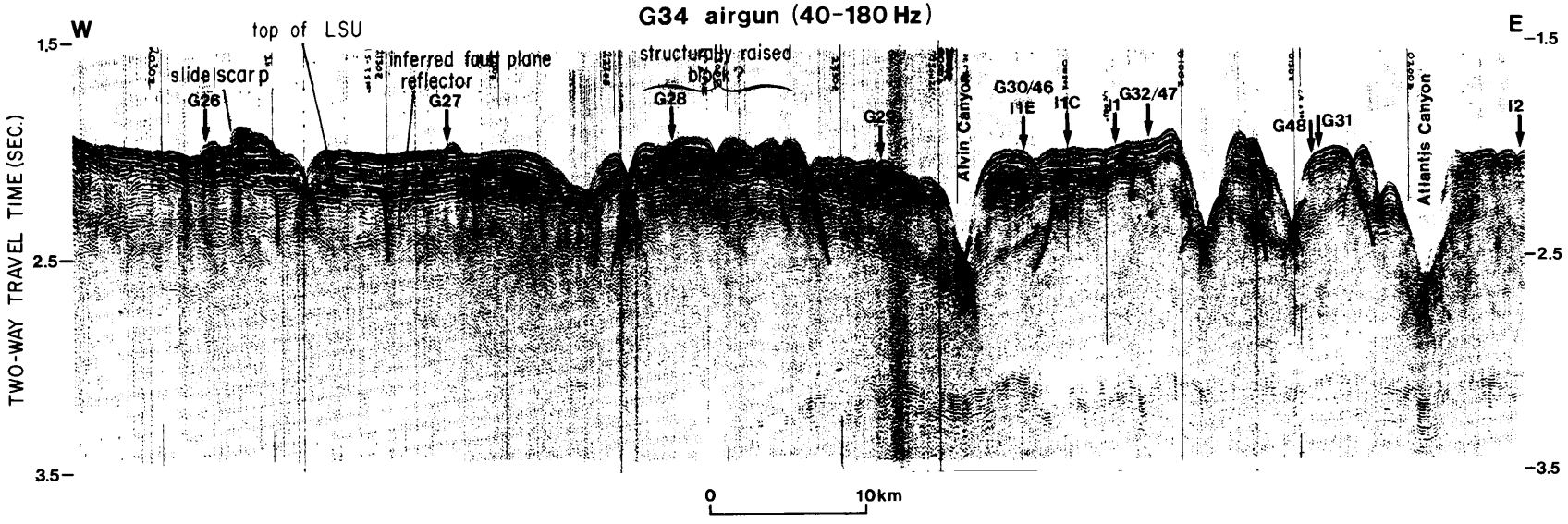

Figure 81. Profile G34 (airgun) along slope between approximately 1,500 m and 1,750 m depths; vertical lines indicate fracture traces. Vertical exaggeration ~ 19:1.

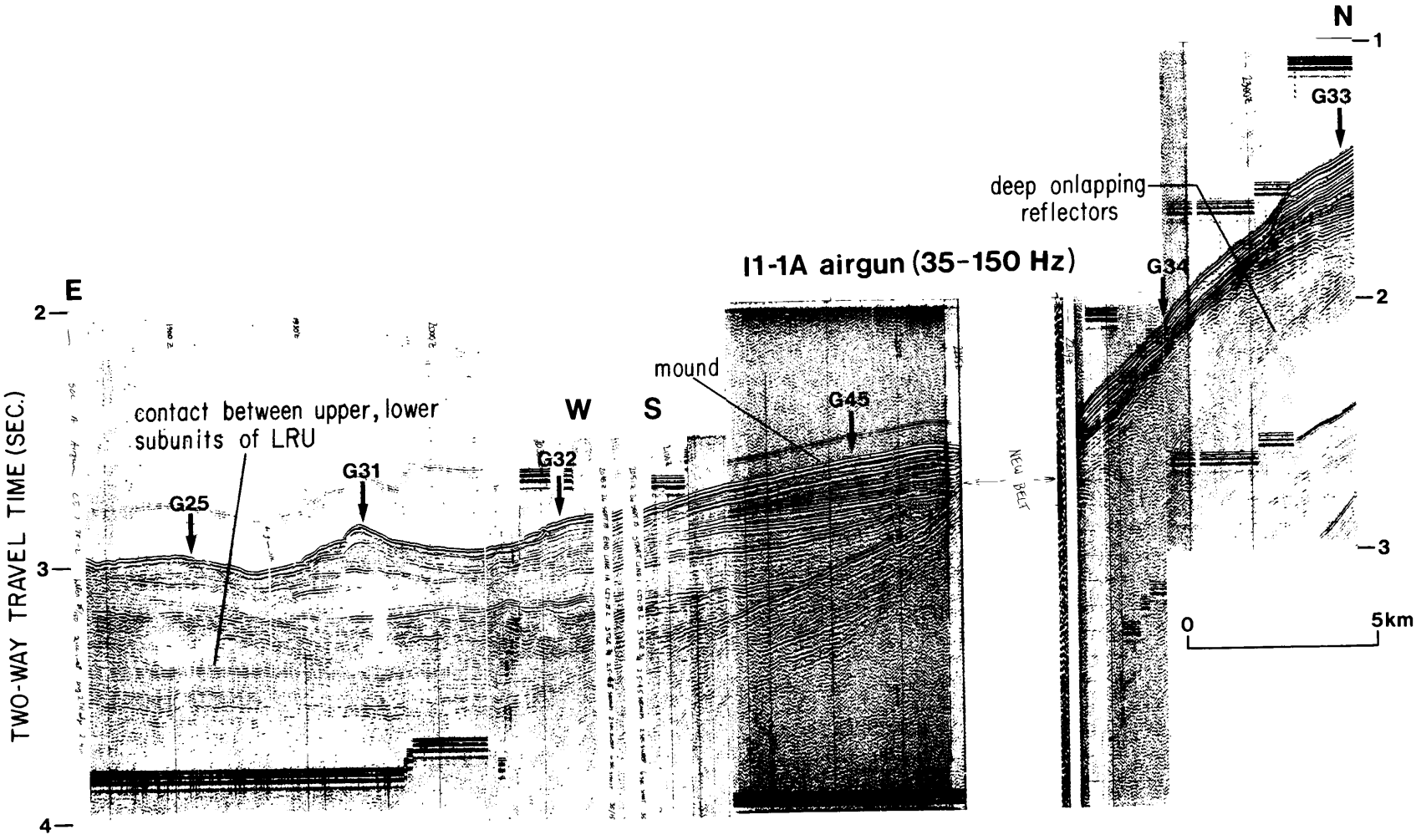

Figure 82. Profile I1-1A (airgun) shows features of the layered rise unit (LRU). Vertical exaggeration ~ 9:1.

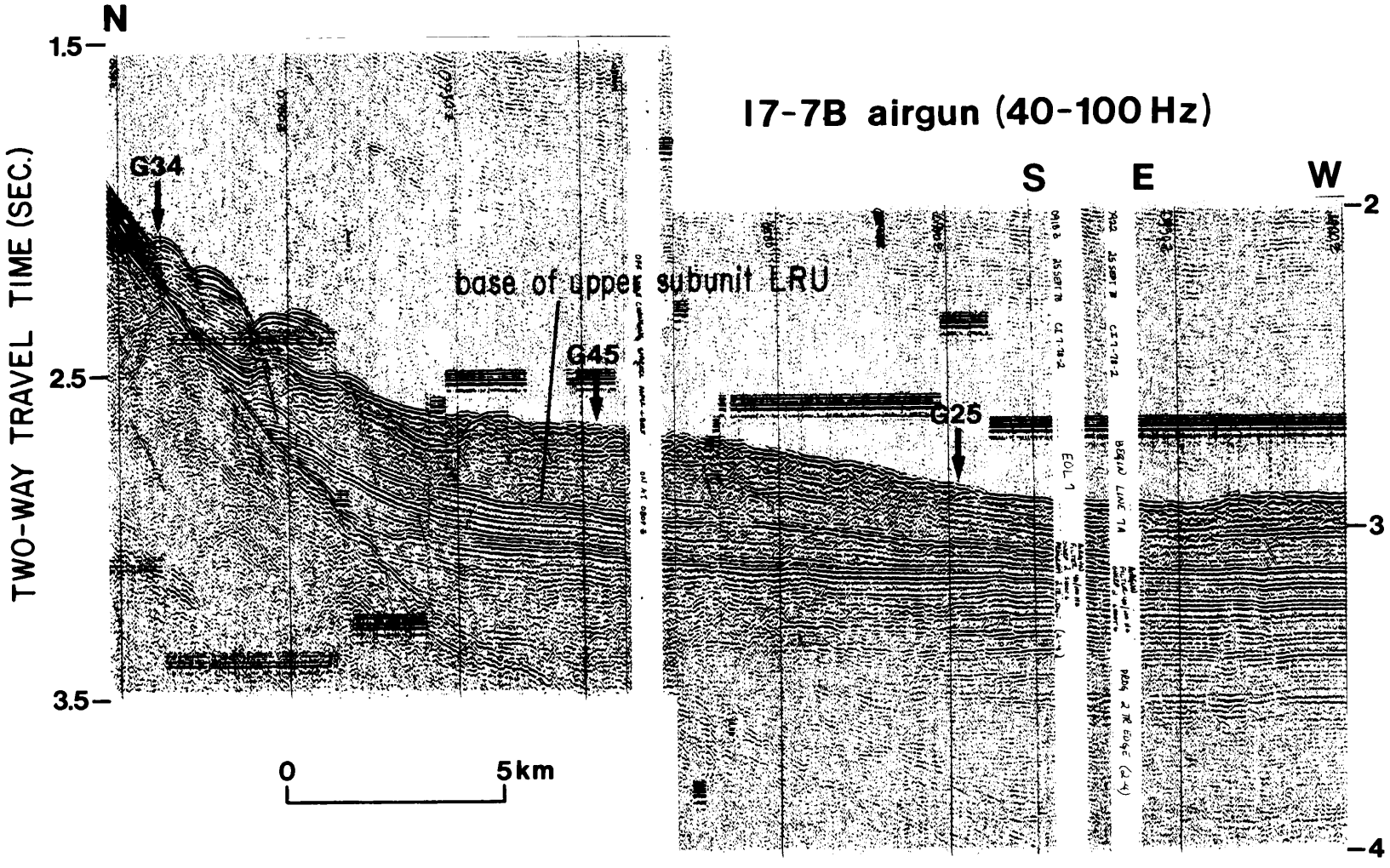

Figure 83. Profile I7-7B (airgun) shows features of the layered rise unit (LRU). Vertical exaggeration ~ 10:1.

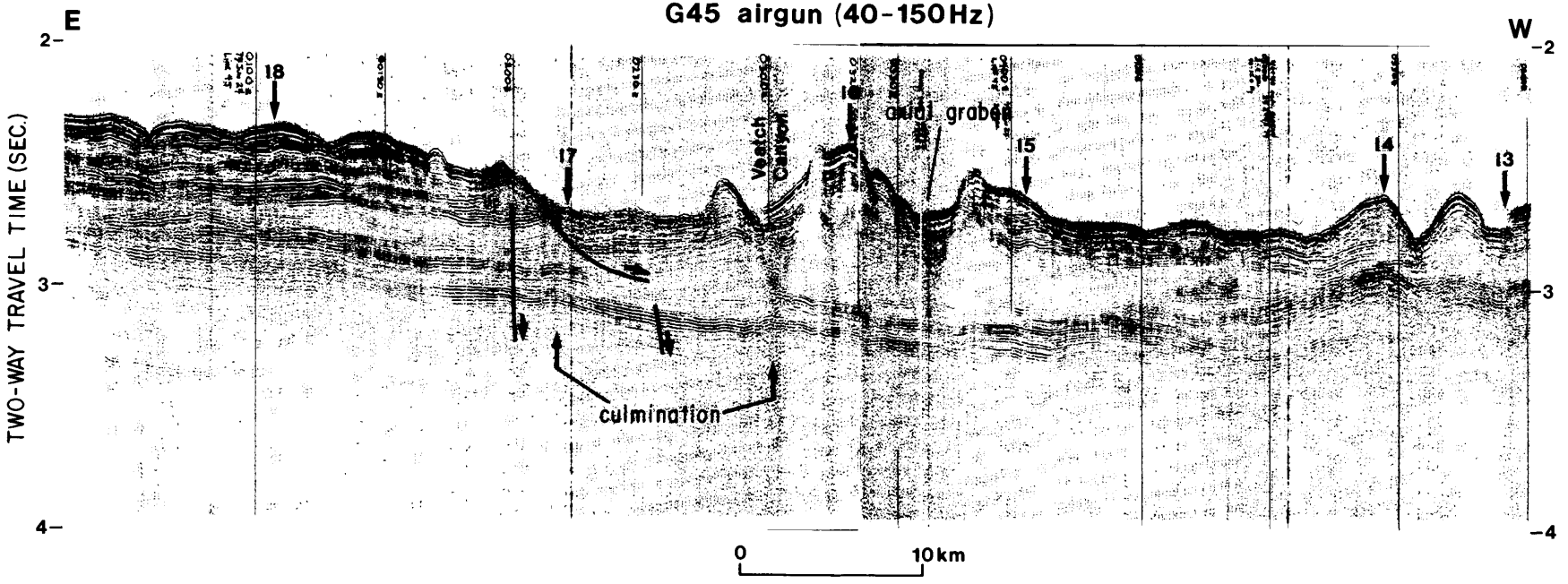

Figure 84. Profile G45 (airgun) along lower slope from aproximately 1,600 m to 2,000 m depths; arrow shows slip plane of displaced block. Vertical exaggeration ~ 18:1.

The age of the layered rise unit is unknown. Valentine (1981) considers the rise section to be formed of Pleistocene and Miocene sediment; the upper subunit would be entirely Pleistocene by his estimation, and the lower subunit would be Pliocene and Miocene.

Structure and mass movement

Extensive deformation, internal and surficial, has affected the foreset unit across the gently inclined upper slope west of 70°00'W. That flow is involved as shown in line G29 (fig. 77), where a broad, low-relief collapse slump is present over a thick interval of chaotic sediment. Such deformation is common along the upper slope in this sector.

Creep along the outer shelf may be indicated by convex forms such as those recorded in line I6 (fig. 85), but here, as to the east, the forms alternatively may represent relict wave-cut berms and shoreface bars.

In places along the upper slope, internal deformation seems to have been attended by layer thickening, probably due to downslope flow (fig. 86). A 136-m interval of internally deformed and flow-thickened sediment is present between Alvin and Atlantis Canyons (fig. 87). It is overlain by a 34-m-thick layer that is notched, sagged, and broken into variously tilted facets across the sea floor (fig. 86). Surficial deformation is diminished downdip as internal deformation is attenuated.

Internally deformed layers of the foreset unit on the upper slope have blunt, convex downdip terminations, possibly because they are the distal ends of sill-like intrusions (i.e., "mudflows": Coleman and Garrison, 1977). Typically, successive downdip terminations are marked by monoclinal folds in overlying layers. In line I1 (fig. 87) such flexures, originating from a subsurface depth of about 135 m, express a surface relief of as much as 23 m. Alternatively, the deep terminations could be old buried slide scars and the overlying folds may be an artifact of thick sediment drape (fig. 88); the weight of draped strata may have caused a basal incompetent layer to squeeze out, resulting in limited lateral injection, and pull-aparts in suprajacent layers, like the giant ball-and-pillow structures described by Howard and Lohrengel (1969).

Injections of incompetent sediment into vertical fractures have apparently attended block separation (fig. 89). Fracturing and displacement seem to be related to internal deformation as deep as 130 m. Where internally deformed layers are pinched out abruptly on strike, overlying strata are flexed all the way up the section to the sea floor (fig. 90). Vertical fractures probably pass along axes of some of the more acute flexures and control the position and shape of some slide troughs such as that shown in figure 90, adjacent to the position of G29, where a section of sediment about 22 m thick has slid away.

Breakup of competent layers over detachment zones (i.e., lateral spreads) is extensive in the western part of the sector and affects relatively thin intervals of strata. For example, along line G28 (fig. 72) the topmost 76 m of sediment - a distinct depositional unit - forms a broken layer terminated downslope by a tongue of debris; the broken layer extends about 5 km across the upper slope. Similar deformation is shown in figure 100.

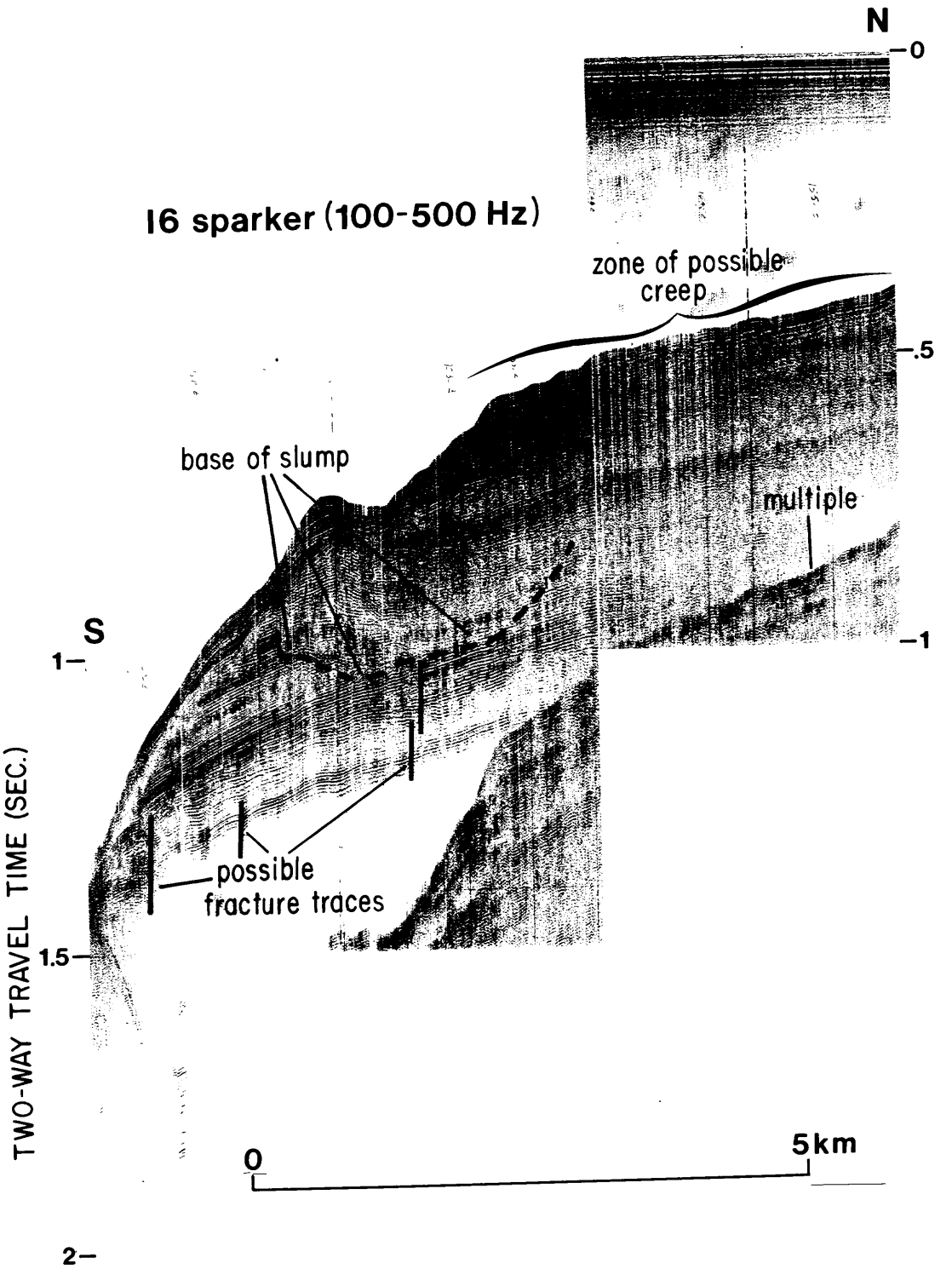

Figure 85. Profile I6 (sparker) shows deformation features along eastern wall of Veatch Canyon. Vertical exaggeration ~ 7:1.

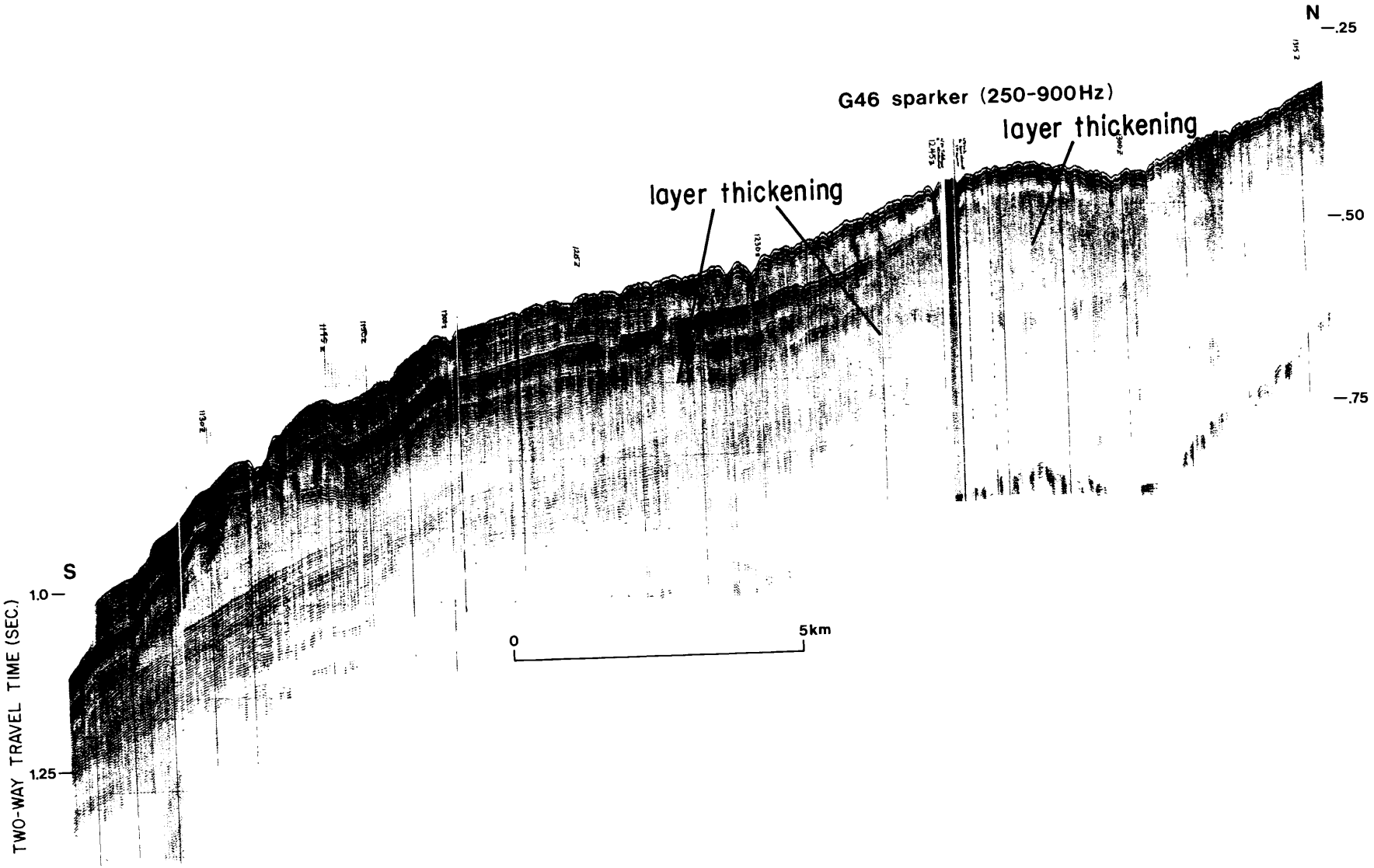

Figure 86. Profile G46 (sparker) shows internal deformation across upper slope along east side of Alvin Canyon. Vertical exaggeration ~ 18:1.

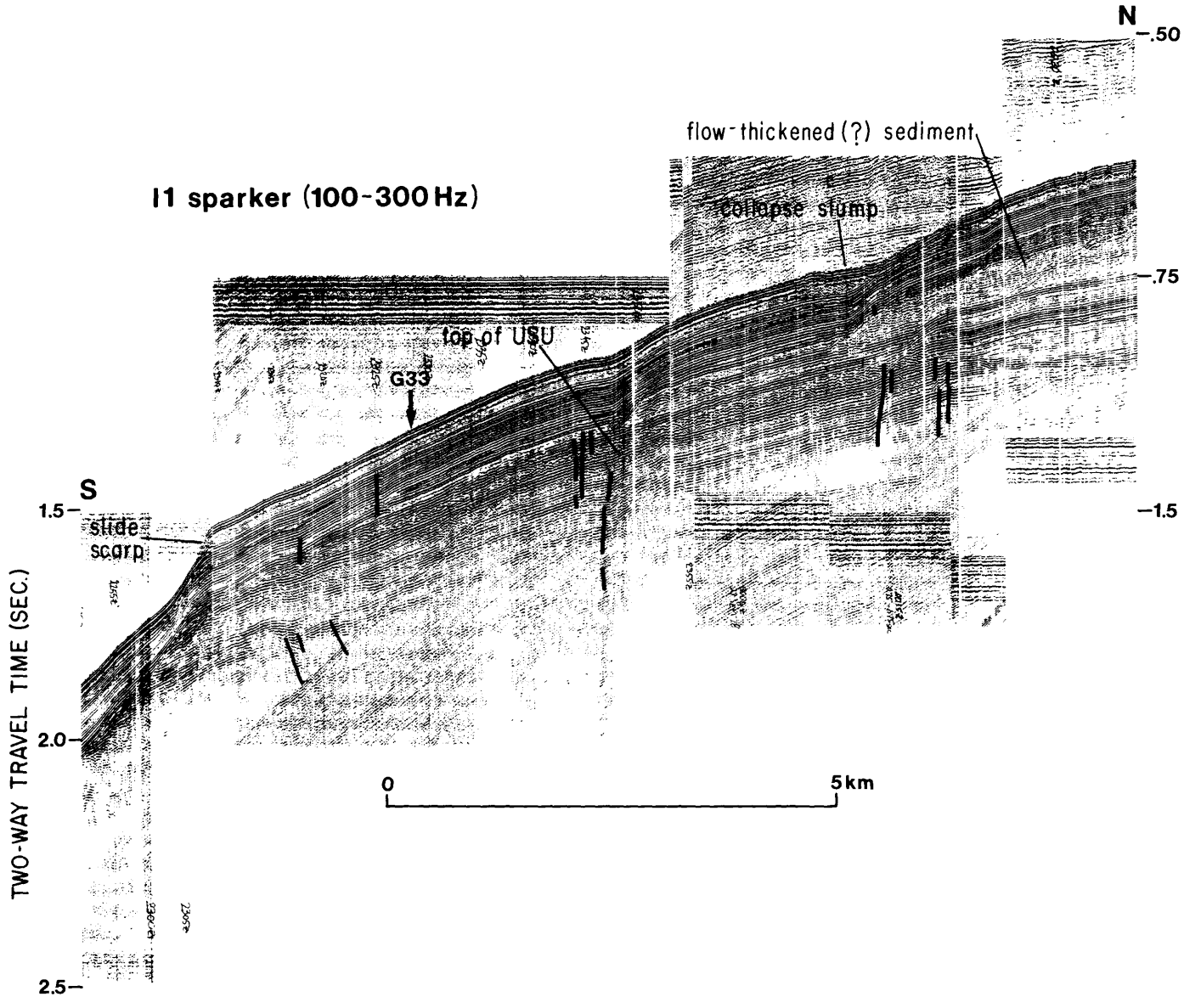

Figure 87. Profile I1 (sparker) shows deformation feature across upper slope; vertical lines mark inferred fractures in upper-slope unit (USU). Vertical exaggeration ~ 7:1.

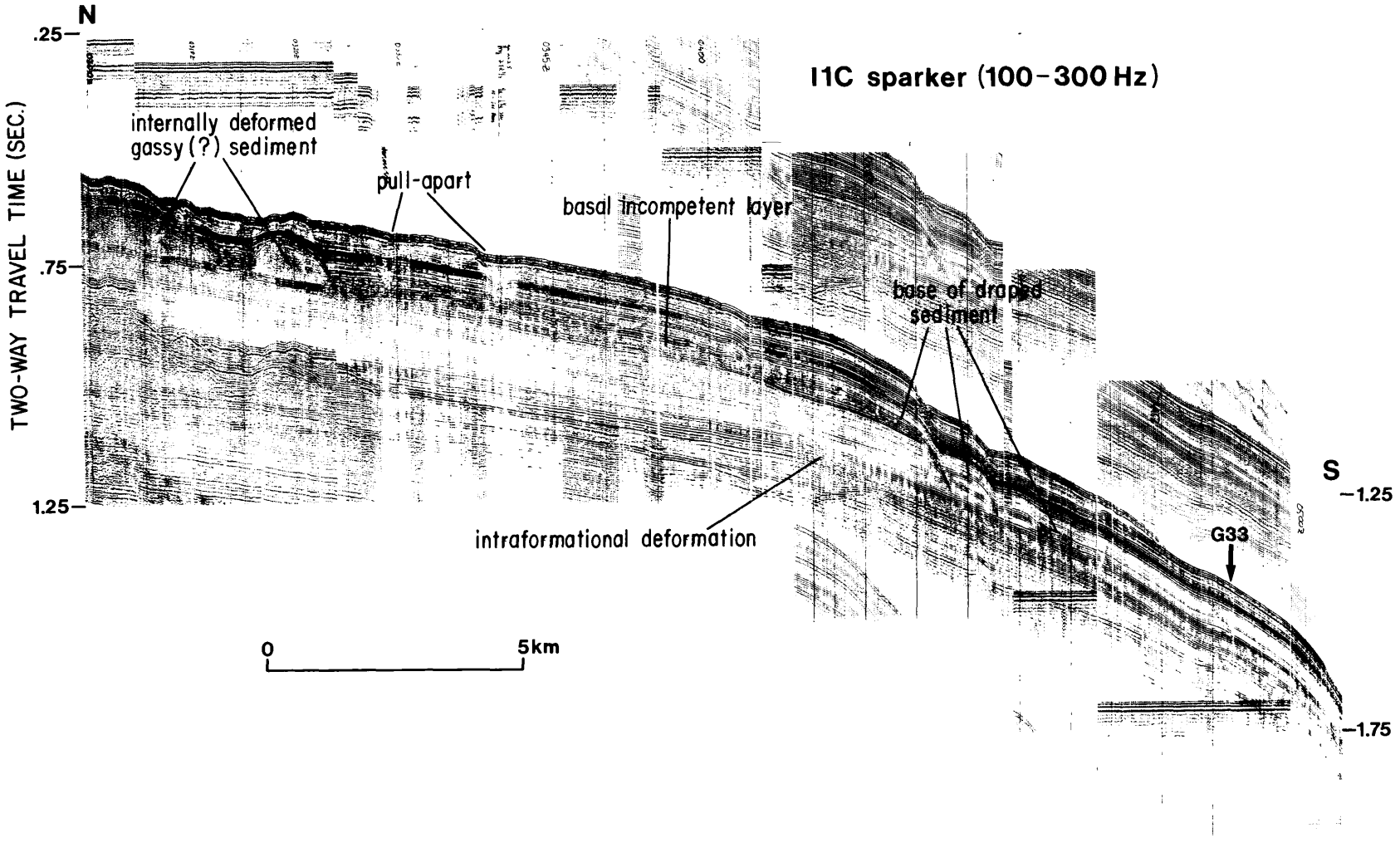

Figure 88. Profile I1C (sparker) shows internal deformation across upper slope. Vertical exaggeration ~ 13:1.

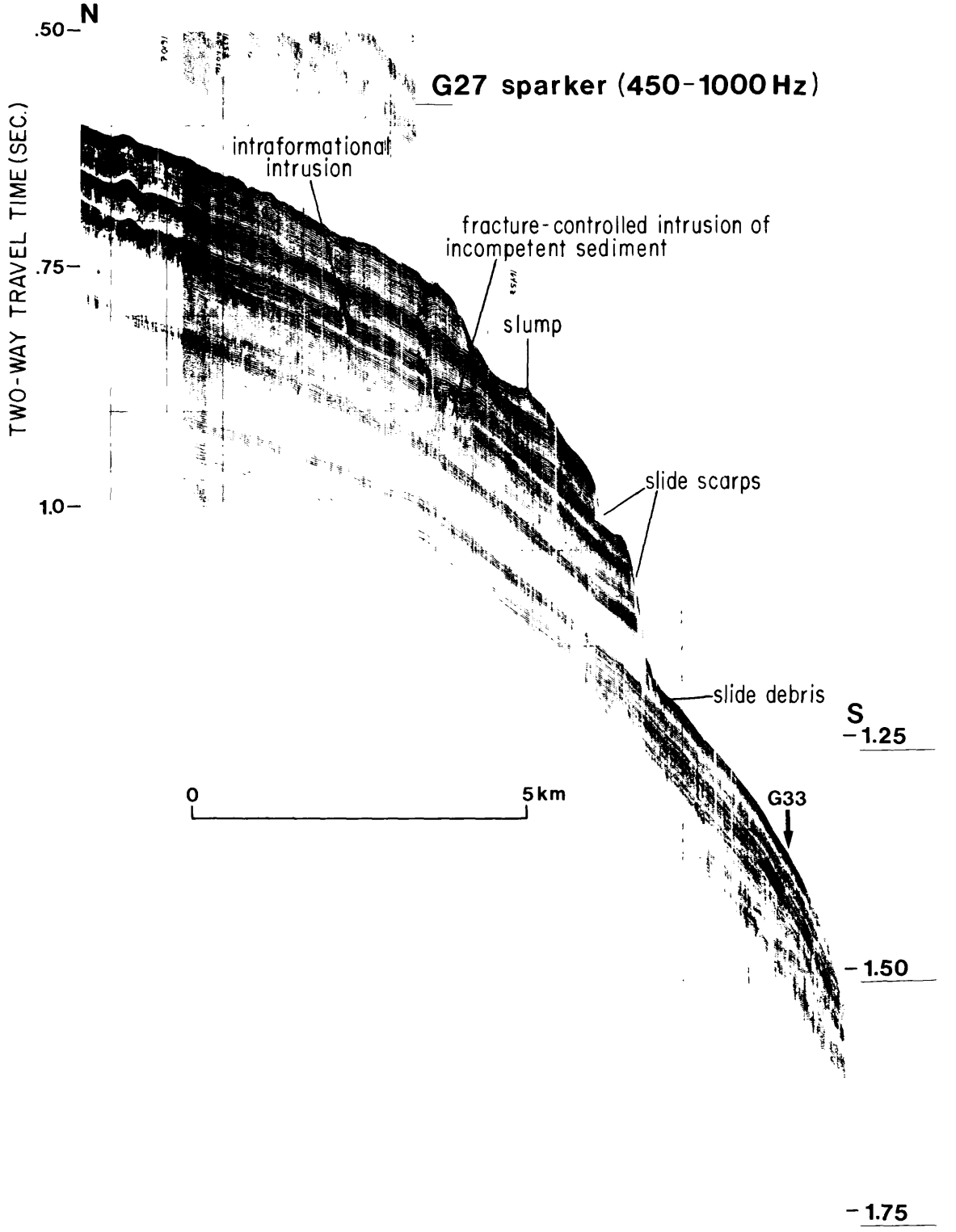

Figure 89. Profile G27 (sparker) shows mass-movement features at brow of lower slope. Vertical exaggeration ∿ 19:1.

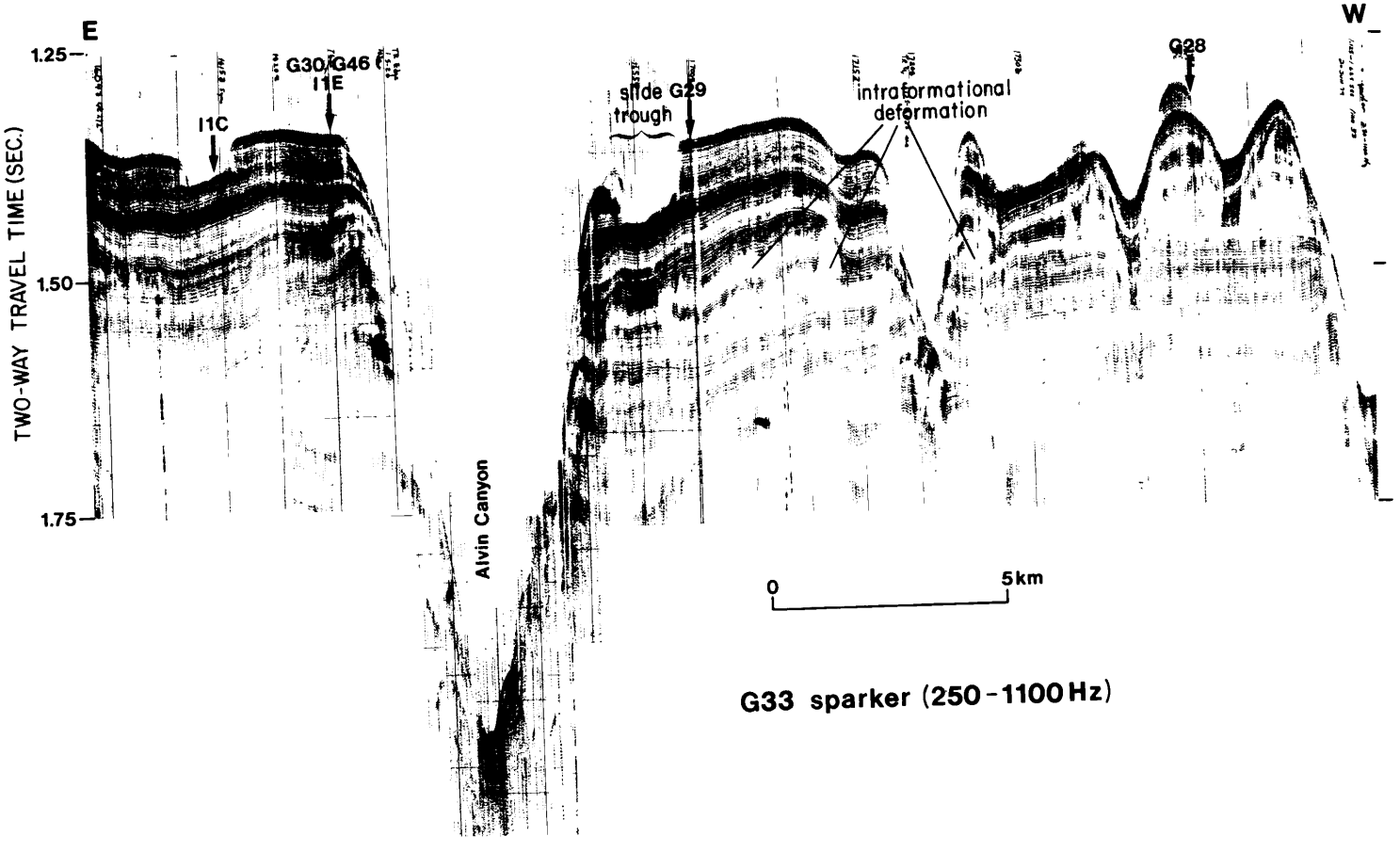

Figure 90. Profile G33 (sparker) shows intraformational deformation along midslope at about 1,000 m depth. Vertical exaggeration ~ 17:1.

In this sector some mass movement along the upper slope seems to be related to deformation in the upper-slope unit. For example, the upper subunit of the upper-slope unit recorded in line I7A (fig. 74) seems to be cut by listric faults. Following displacement, beds of the foreset unit were laid down on the uneven surface of the upper-slope unit. The upper part of the foreset unit seems to have subsequently collapsed and slid away, mainly along the rectangular cut at 0300 (fig. 74), which is about 195 m deep, well into the upper part of the upper-slope unit. A small amount of rubble is piled against the west side of the cut.

The structure immediately downslope from the zone of possible creep shown in figure 85 (cf. fig. 78) probably is a transverse section across a slump into Veatch Canyon at 525-m depth. Here, uniformly laminated sediment, possibly within the upper subunit of the upper-slope unit, has apparently slid along a concave slip surface in a direction nearly perpendicular to the profile. The displaced sediment is thoroughly deformed, but internal layering is preserved in the blocks. The slump may have been initiated by fractures extending up from an incompetent (transparent) zone low in the upper subunit of the upper-slope unit. The slump was subsequently beveled and eroded, and draped with sediment which seems also to have slid partly away, at the same site.

Impressive mass movements, marked by large filled depressions (perhaps slump bodies) have formed along the upper margins of Alvin and Atlantis Canyons. The dimensions and outlines of the depressions are unknown, although local bathymetry (map G) implies a general northeast elongation. Subjacent faulting of minor displacement seems to figure in their origin; some of the structures resemble "gravifossa" (Van Loon and Wiggers, 1976). A good example of such a filled depression (fig. 91) underlies a reentrant at the 500-m isobath on the east side of Atlantis Canyon. The depression, cut in the lower subunit of the foreset unit, is filled by about 240 m of well-layered sediment of the upper foreset subunit. The layered fill has been downfaulted and probably rotated out of the plane of the profile inasmuch as 40 m of displaced sediment cannot be accounted for in the profile. Faulting may have caused the uppermost 45 m of sediment to collapse (possibly later); as much as 20 m of this sediment was separately displaced out of the plane of the profile. A similar slumped depression is present along the northwest corner of Atlantis Canyon (fig. 92).

A rotated block forms the promontory along the east side of Nantucket Canyon at about 500-m depth (fig. 93). Here, internal deformation at or near the base of the foreset unit seems to have caused sag and rotation of relatively competent overlying beds. The uppermost layers of the foreset unit are affected, and a rough, concave depression at 405-m depth, possibly marked by tension cracks, defines the back side of the block. Much of the collapsed section seems to have slid down the steep facing slope, blanketing cliff outcrops of the upper-slope unit with debris (fig. 93).

The salients that are defined by the 1,000-m isobath on either side of Atlantis Canyon have been affected by and perhaps largely formed by mass movement. A 153-m-thick block slide (fig. 91) at 700-m depth forms the apex of the eastern salient. Acoustically, the block represents the same stratigraphic unit (upper foreset subunit) seen in the filled depression farther upslope. Although the block lies at the foot of a 90-m-high scarp, it

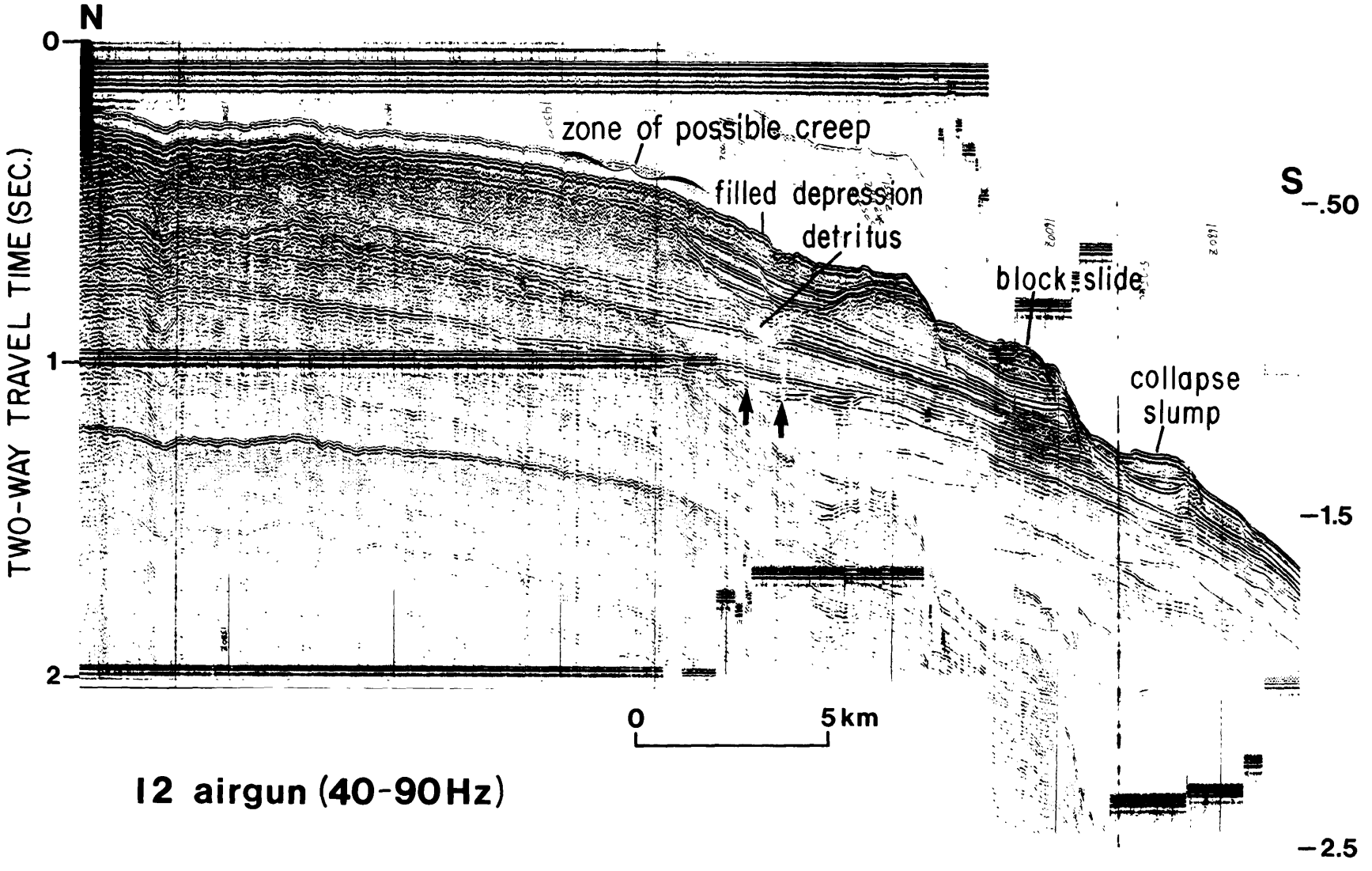

Figure 91. Profile I2 (airgun) shows mass-movement features across upper slope along east side of Atlantis Canyon; arrows indicate inferred graben. Vertical exaggeration ~ 11:1.

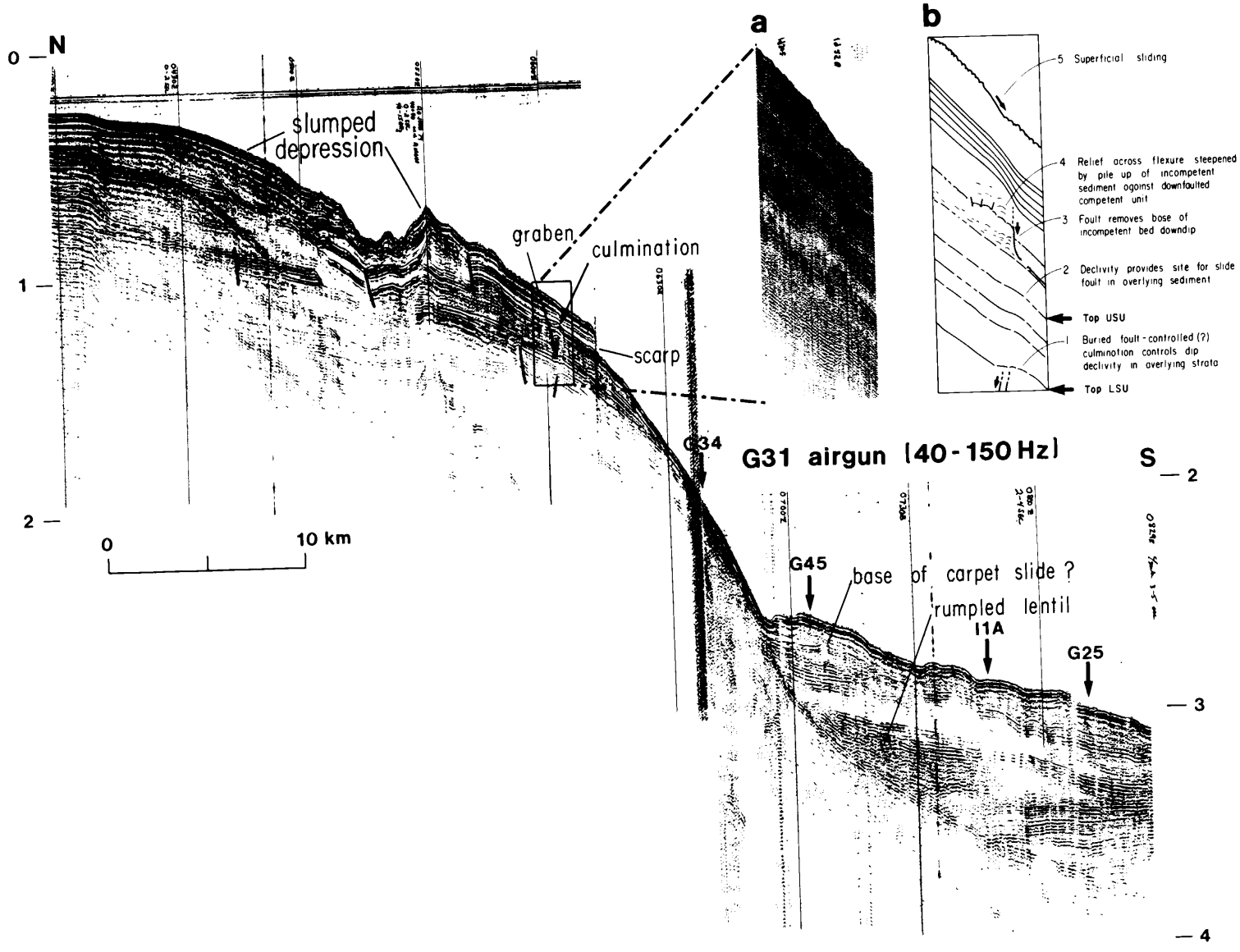

Figure 92. Profile G31 (airgun) along west side of Atlantis Canyon; vertical lines indicate faults. Inset a (from coincident sparker line G48) shows detailed internal deformation and suprajacent sliding; inset b shows diagrammatic relationship of structure (1-4) to mass movement (5). Vertical exaggeration ~ 16:1.

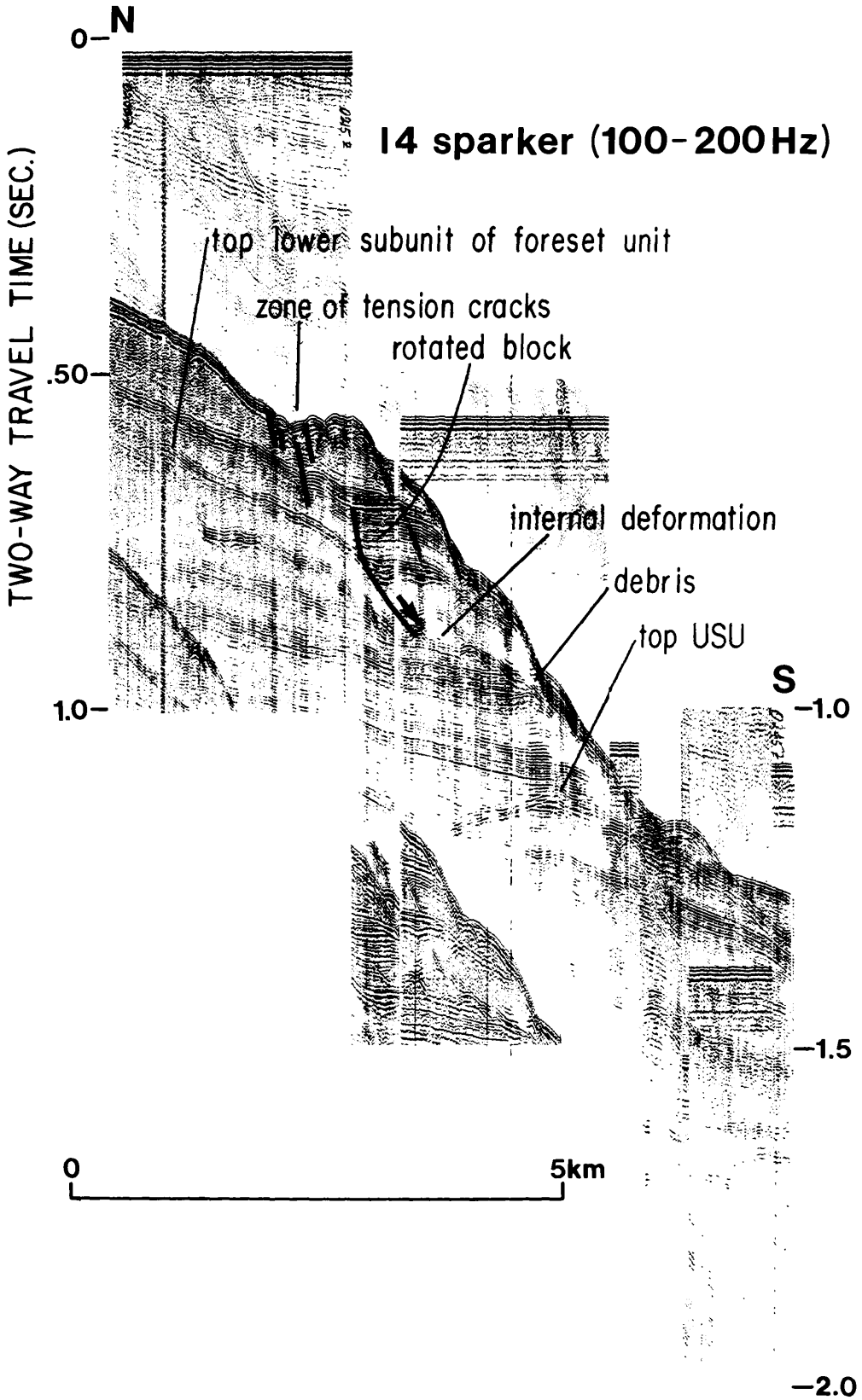

Figure 93. Profile I4 (sparker) shows deformation in upper-slope unit (USU) associated with collapse of the foreset unit. Vertical exaggeration ~ 9:1.

is difficult to account for substantial displacement because the block lies at the crest of the salient and the trace of the basal contact is nearly flat. A certain amount of lateral slip must have occurred during settlement of the block some 55 m below its inferred original position; the remaining displacement, about 34 m, is accounted for by separate collapse of the uppermost layer which probably originally draped down across the scarp brow.

A collapse slump, 3 km across, cuts the brow east of Atlantis Canyon (fig. 91). Transport was probably south-southwest toward the large embayment east of the canyon. The slump is approximately 125 m thick and is composed chiefly of strata of the foreset unit. It is probably derived from the large displaced block upslope at 750-m depth. The slip plane may be controlled by the contact with the upper-slope unit. If strata at the top of the slump are equivalent to strata at the top of the adjacent upslope block slide, then 125 m of section is missing from the profile; the profile must cross the relatively thin back end of the slump.

Normal faults, particularly a shallow graben, cut the upper-slope unit beneath a 9-km-long salient flanking the west side of Atlantis Canyon (fig. 92). Note that the flexures and the scarp in strata of the overlying foreset unit are on the downdip sides of slight culminations on the surface of the upper-slope unit. At a particular overburden load the culminations may focus stress sufficiently to cause failure. The inset in figure 92 illustrates how this might transpire.

The disposition of the scarp or major scarps along the brow of the steep lower slope seems to be controlled by orthogonal fractures (e.g., figs. 76, 80). In line G31, the length of the smooth lower-slope segment below the brow, measured with a rolling counter, is exactly equal to the length of the contorted, draped layer that blankets the upper rise (partly shown in fig. 92). It is tempting to see in this coincidence evidence for a detached slab of sediment having slid, intact, from the scarp at the slope brow completely across the lower slope and out across the rise as a great (15 km long) carpet slide. Figures 73 and 82 perhaps illustrate such a slide mass incompletely removed from the slope.

The upper-rise surface, just below the slope contact, is covered in places by broad, convex mounds of weakly layered sediment as much as 50 m thick (figs. 76, 77, 82). The mounds are remnants, isolated by erosion and mass wasting; they imply that a surficial blanket thicker than 50 m may once have covered wide areas of the upper rise. The remnants may represent the missing foreset-unit beds that have slid away from the brow scarp. The relict surficial blanket is shown on strike in figure 94 as an acoustically transparent, irregular, broken layer approximately 17 m thick, draped over a raised terracelike expanse of apparently faulted strata.

Toward the west end of the sector, a large complex debris wedge (fig. 76) forms a prominent rampart against the lower slope. Internally the wedge is chaotic; steplike reflector segments (fig. 73) indicate that in places along the slope the wedge includes large, jumbled blocks. Elsewhere (fig. 95) blocky structure is not evident. The strong reflector segments that indicate blocks in the wedge (fig. 76) resemble reflectors of the upper-slope unit, but the great mass of wedge debris is most likely derived from the Cretaceous strata immediately upslope.

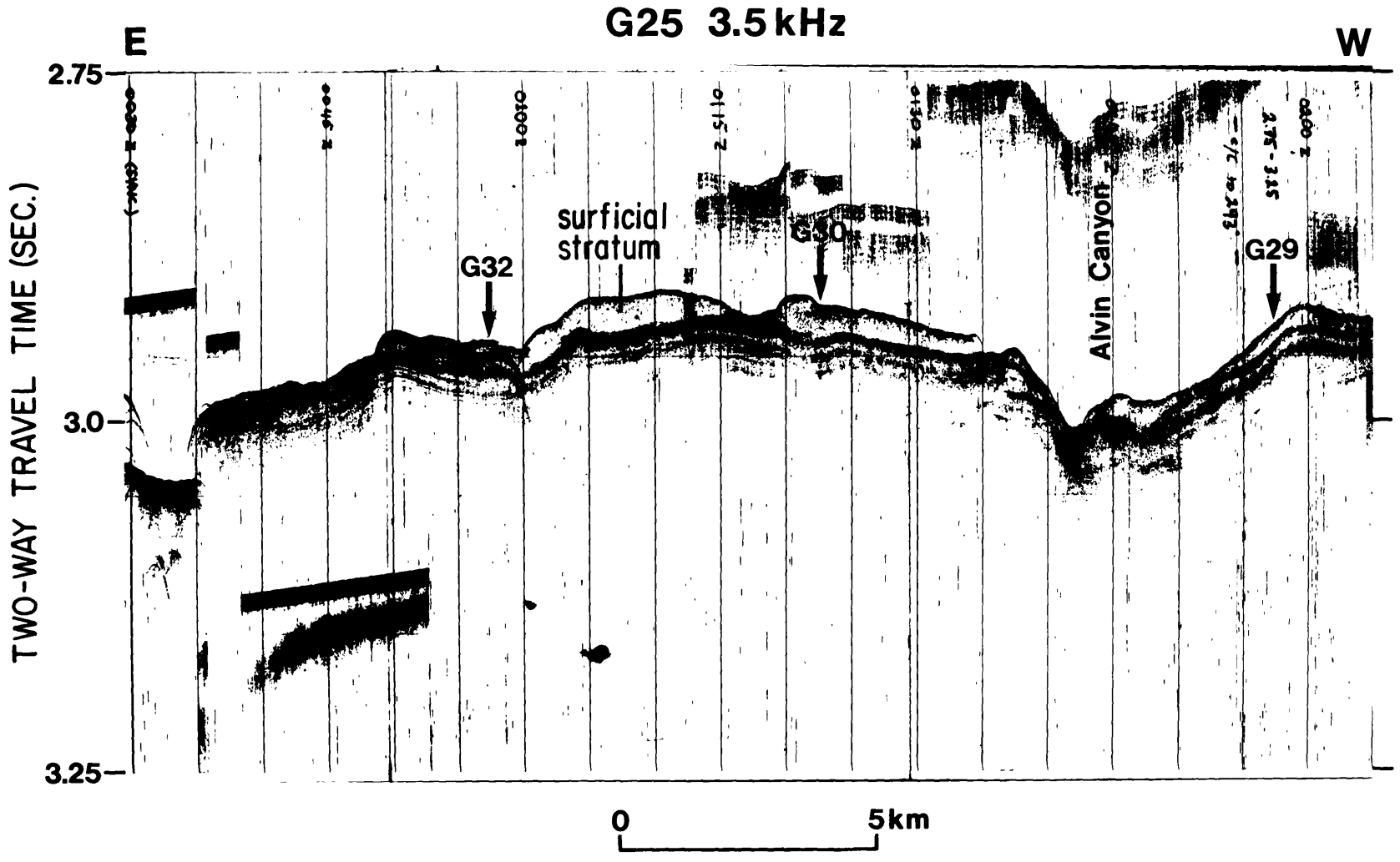

Figure 94. Profile G25 (3.5 kHz) shows deformation of surficial stratum along upper rise at about 2,200 m depth. Vertical exaggeration ~ 37:1.

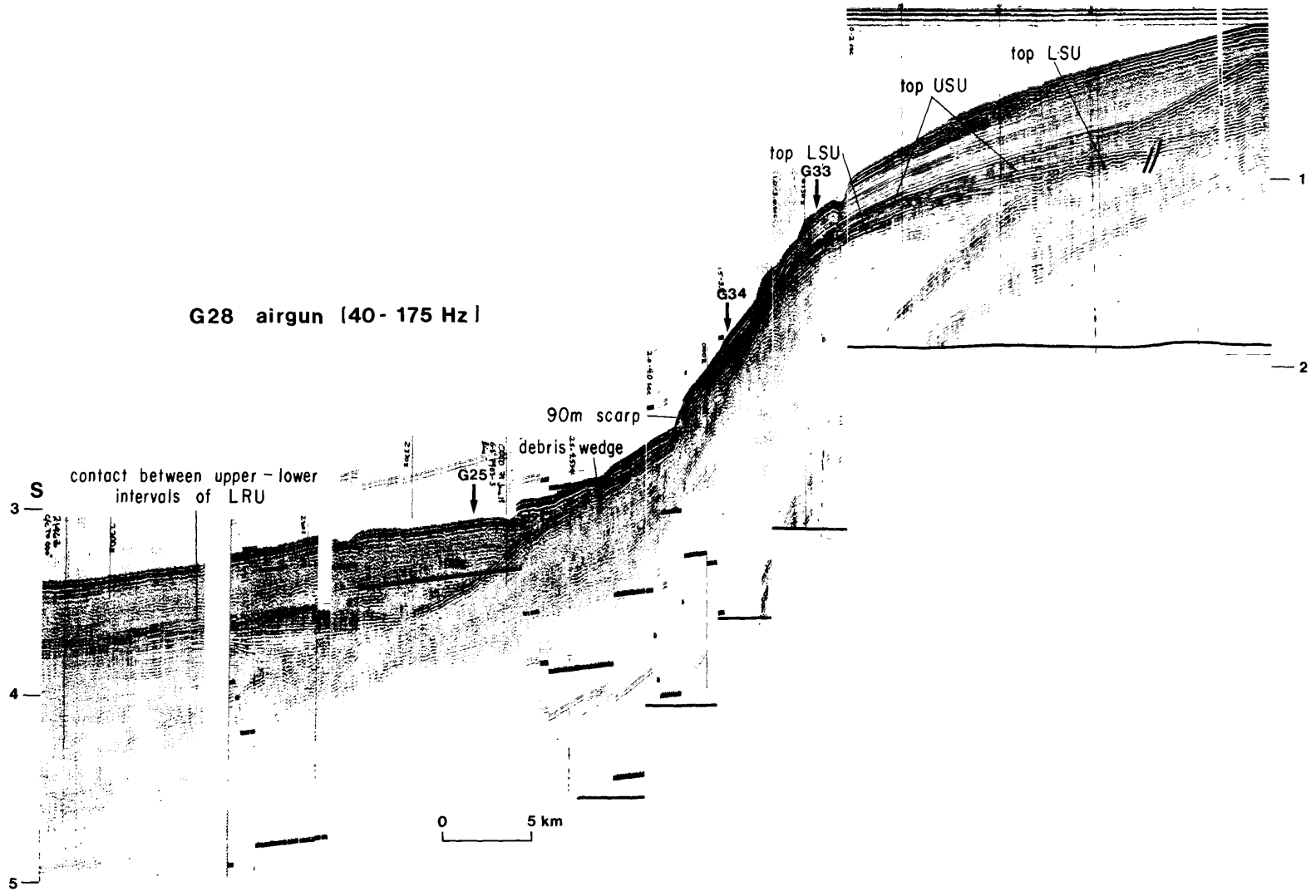

Figure 95. Profile G28 (airgun) shows relationships of upper-slope unit (USU) and lower-slope unit (LSU). Vertical exaggeration ~ 16:1.

Rotated internal dips suggest that the wedge is broken by, and perhaps rests on, listric faults. Figure 96 shows where faults probably are located, which have apparently propagated near to the surface and caused collapse of surficial sediment. In places (figs. 76, 95), the entire wedge seems to have rotated, producing a 90-m-high scarp in the foreset drape at the head. East of line I1E, where the debris wedge is thin or nearly absent, normal faults are perhaps indicated at the foot of the lower slope (fig. 97). The wedge is draped by as much as 120 m of sediment of the foreset group. The drape is thickened and thinned, flexed and distorted (fig. 76) across the wedge, implying postdepositional movement. Figure 98 implies that upper layers of the foreset unit have slid from the slope-brow scarp and accumulated at the top of the debris wedge.

The uppermost layers of the layered rise unit (correlative with the foreset strata) lap up over the wedge (fig. 99) and are thoroughly broken (fig. 100; cf. fig. 96). The deformed surficial layers have slid off the steepened foot of the debris wedge (fig. 101), exposing a deeper, rough surface that is abruptly flanked by the rubble-strewn rise. Along the buried wedge/layered rise unit contact, the deeper layers of the upper subunit of the layered rise unit are arched and possibly faulted (fig. 76). Reverse dips in these layers indicate a vertical displacement of nearly 90 m, roughly equivalent to the scarp height at the head of the debris wedge (fig. 76). These distortions may represent postdepositional rotation and seaward translation of the debris wedge (fig. 76). However, note the reverse dip of the lower member of the layered rise unit shown in figure 97. This implies deformation along the rise prior to deposition; all these features may indicate reactivation and toe bulge of the debris wedge.

West of Alvin Canyon the debris wedge thickens, flattens, and occupies an increasingly large portion of the lower slope. The depths bounding the debris wedge vary from as deep as 2,310 m to as shallow as 1,620 m, but total vertical extent increases from 375 m (G29) to 690 m (G26) to the west. Bathymetry (map G) of the slope west of line G26 suggests that the debris wedge extends at least as far west as 71°30'W. and becomes perhaps even wider toward the west. The bathymetry also suggests that slope canyons postdate the wedge complex, but that they may have been partly occluded by subsequent movement.

The two subunits of the layered rise unit are structurally disharmonic. Whereas the upper subunit shows discordant folding and gross lateral thickening and thinning on strike and downdip, the lower subunit, on strike, shows low-amplitude asymmetric flexures and smaller folds similar in style to kink folds, possibly broken by vertical fractures or faults of minor displacement (fig. 102). Buried supratenuous folds seen in line G25 (fig. 92) may indicate the influence of one or more deep (below acoustic penetration) incompetent units.

Line I7 (fig. 83) shows that nearly the entire upper subunit of the layered rise unit, approximately 220 m of section, is internally deformed. This deformed section represents the eastern edge of a large slab that has slid down toward the west (figs. 84, 102). Lateral movement seems to have been taken up by compression, rotation, and internal collapse of specific deep layers rather than by displacement along one or more shear planes.

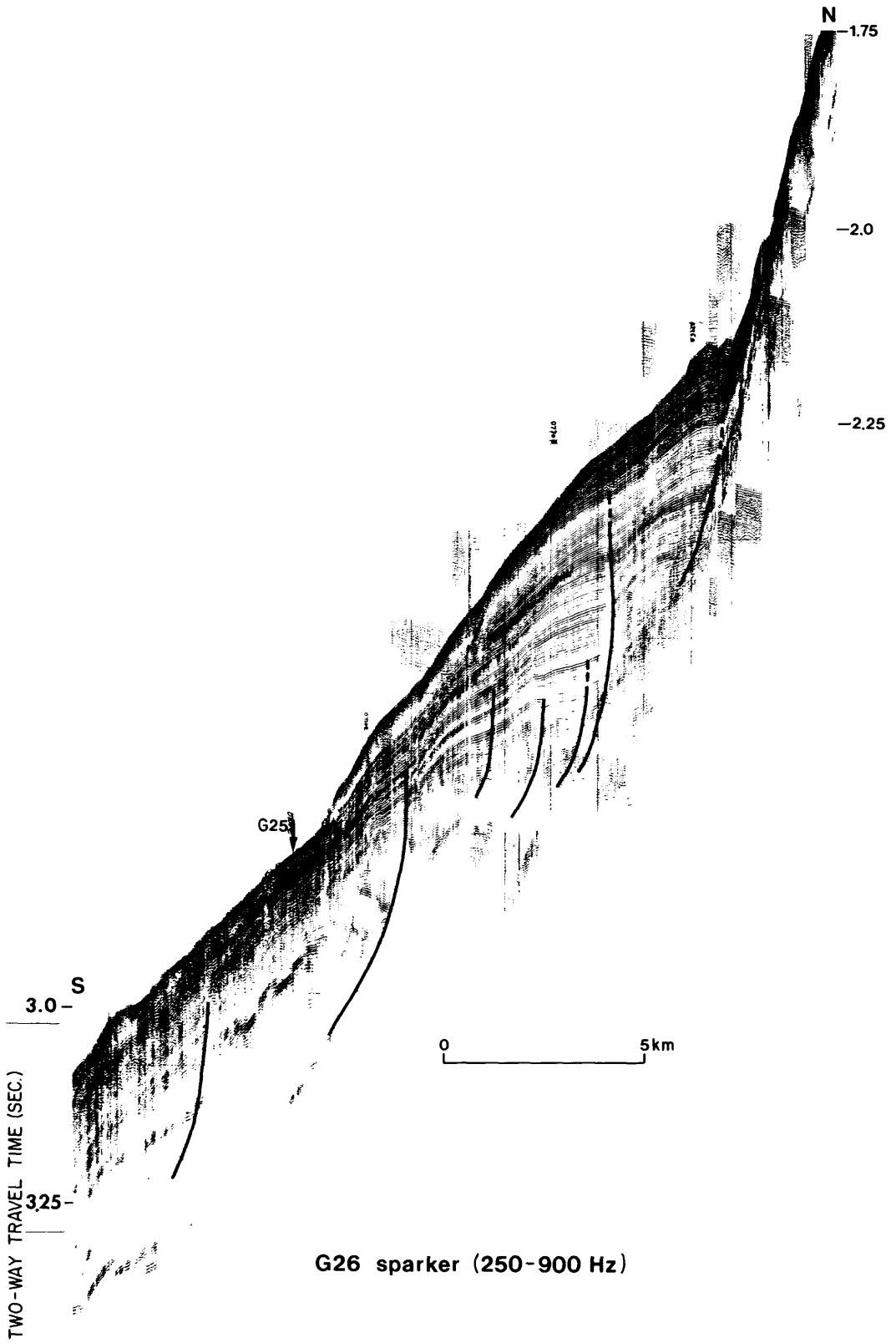

Figure 96. Profile G26 (sparker) across upper part of the debris wedge; curved lines indicate inferred faults. Vertical exaggeration ~ 26:1.

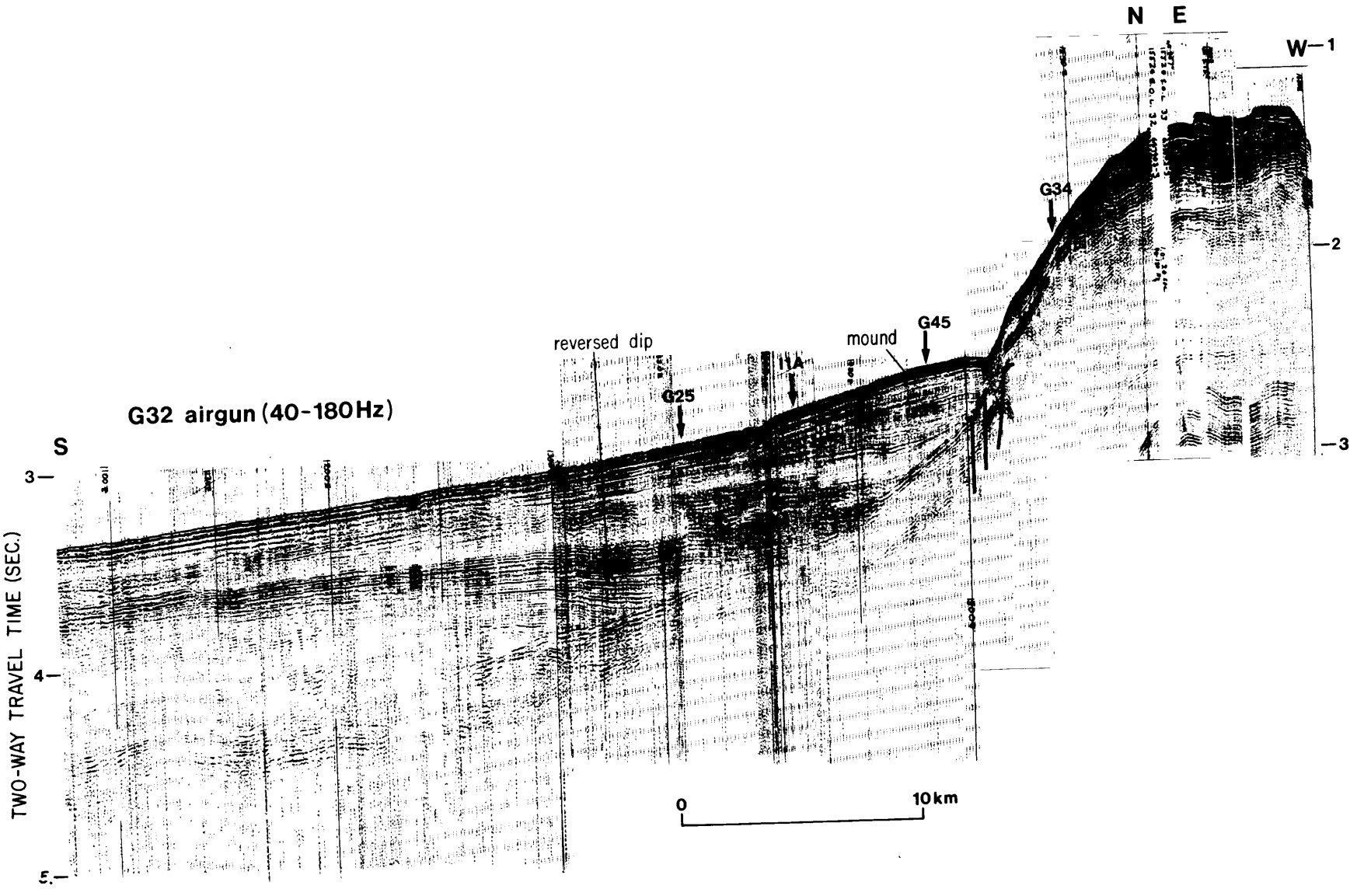

Figure 97. Profile G32 (airgun) and start of line G33 (airgun) shows stratigraphy of upper rise; heavy vertical lines indicate inferred faults. Vertical exaggeration ~ 23:1.

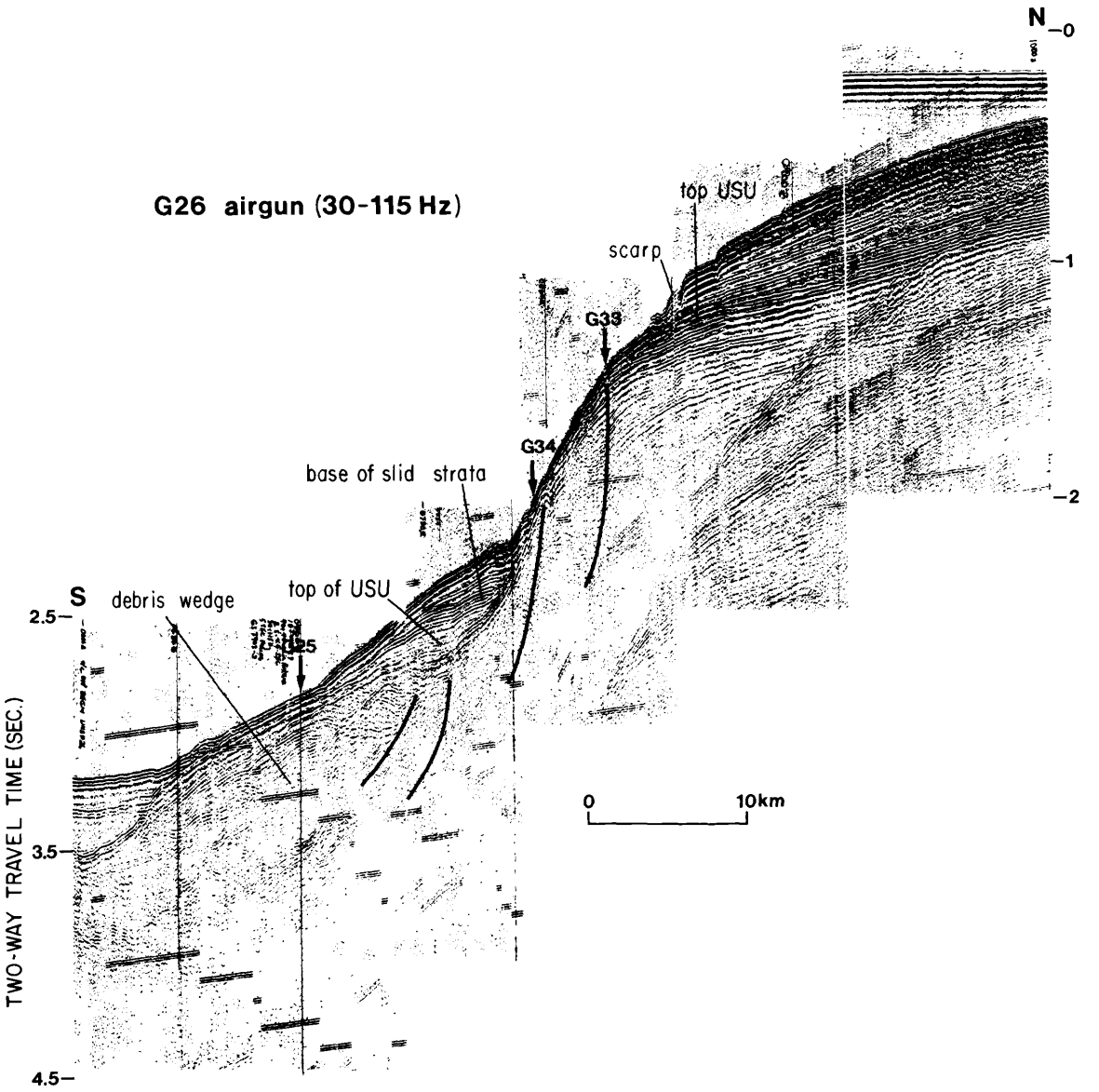

Figure 98. Profile G26 (airgun) shows debris wedge across lower slope (cf. fig. 96); heavy vertical (curved) lines indicate inferred faults. Vertical exaggeration ~ 19:1.

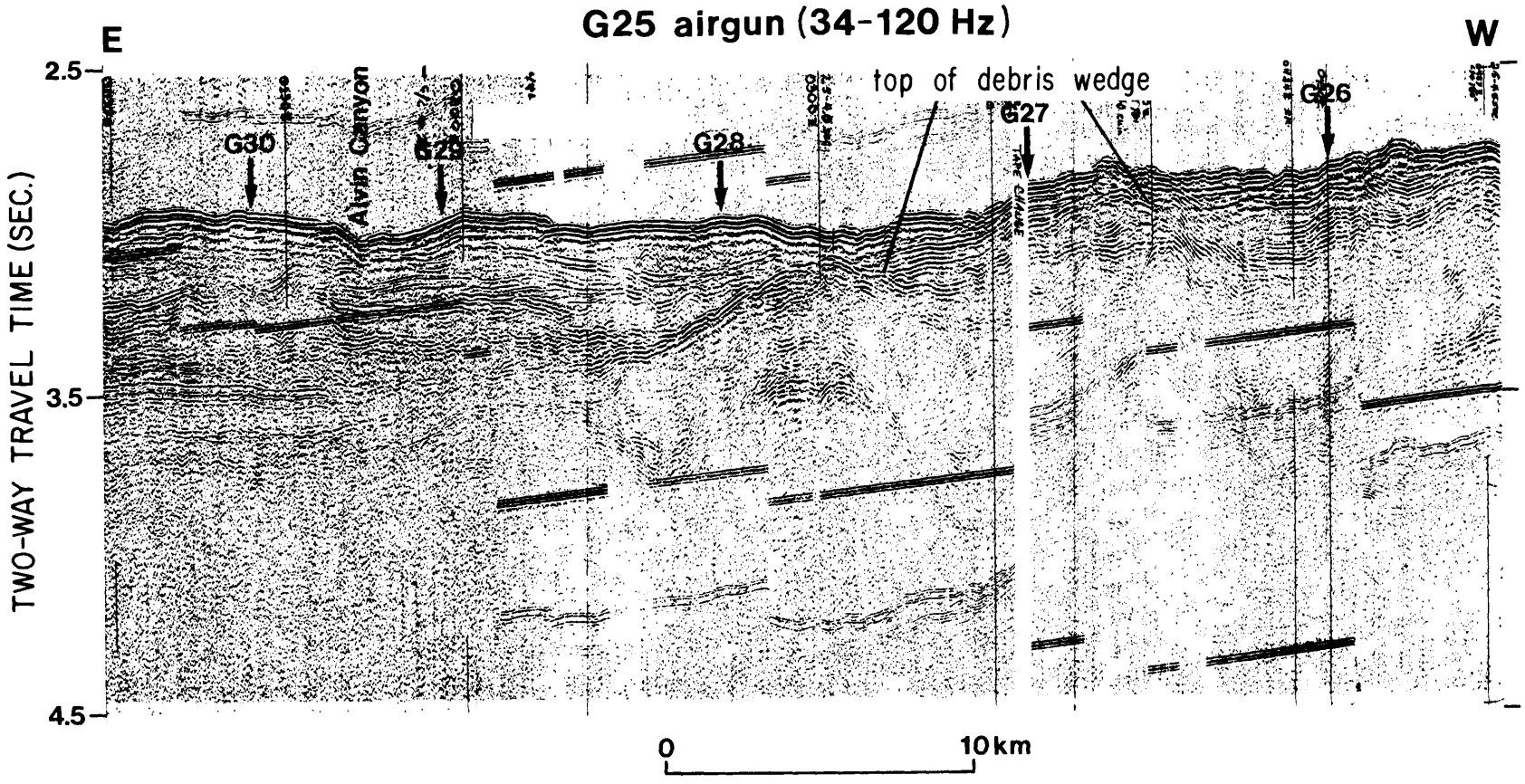

Figure 99. Profile G25 (airgun) along lower slope-upper rise from about 2,200 m to 2,100 m depths. Vertical exaggeration ~ 14:1.

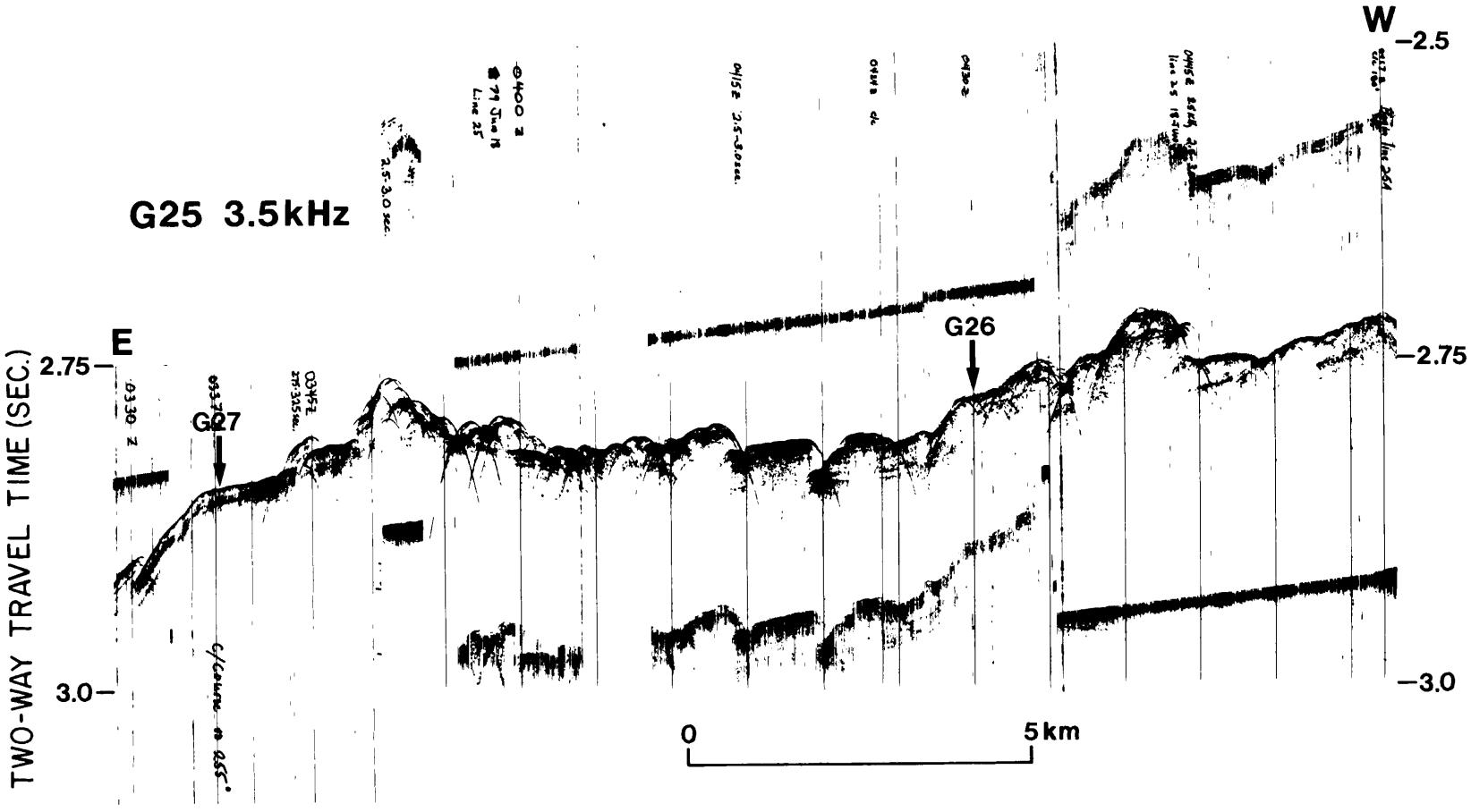

Figure 100. Profile G25 (3.5 kHz) along lower slope between about 2,100 m and 2,200 m depths. Vertical exaggeration ~ 25:1.

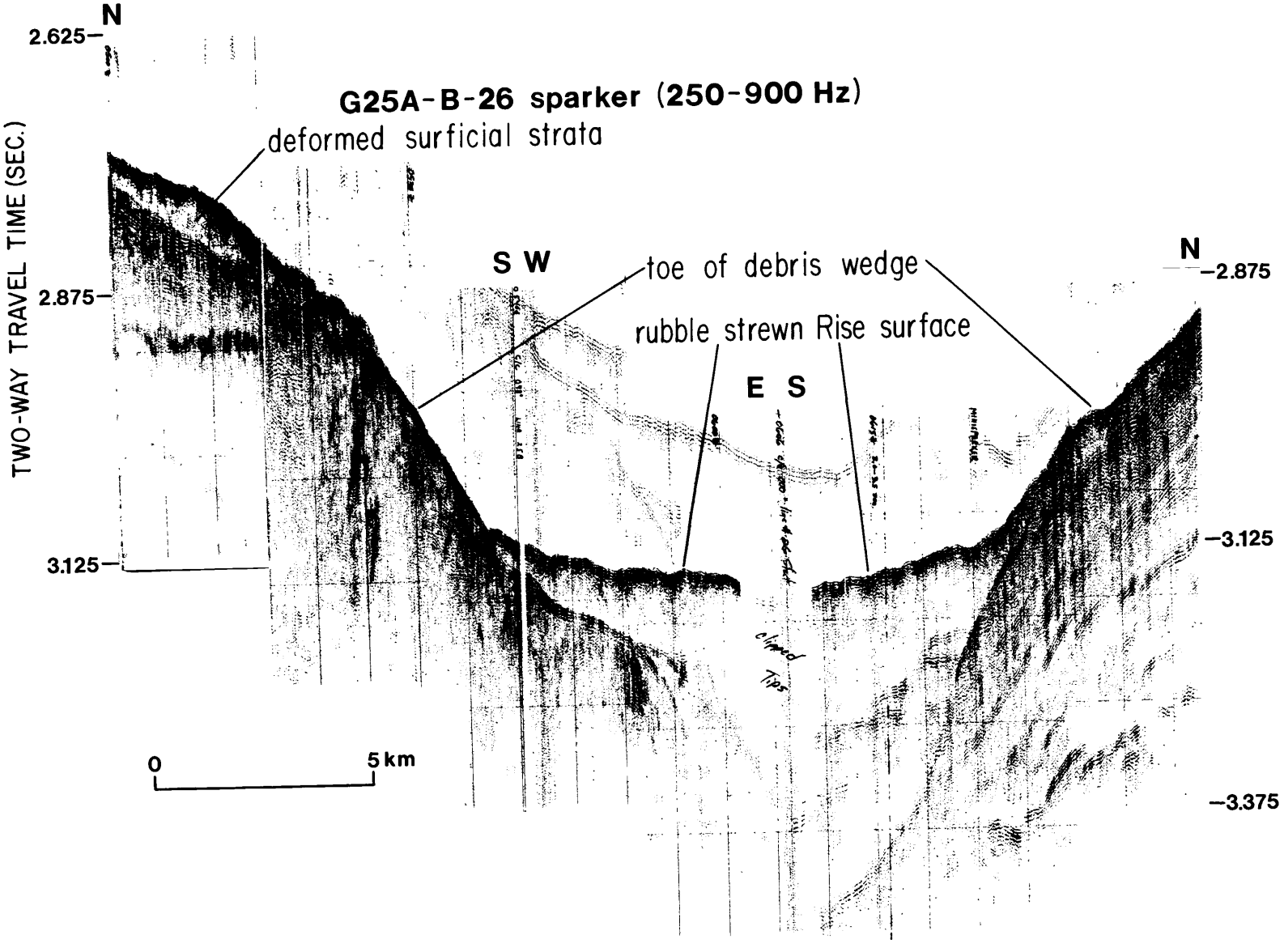

Figure 101. Profiles G25A-B-26 (sparker) along and across toe of debris wedge from 2,100 m to 2,250 m depths. Vertical exaggeration ~ 39:1.

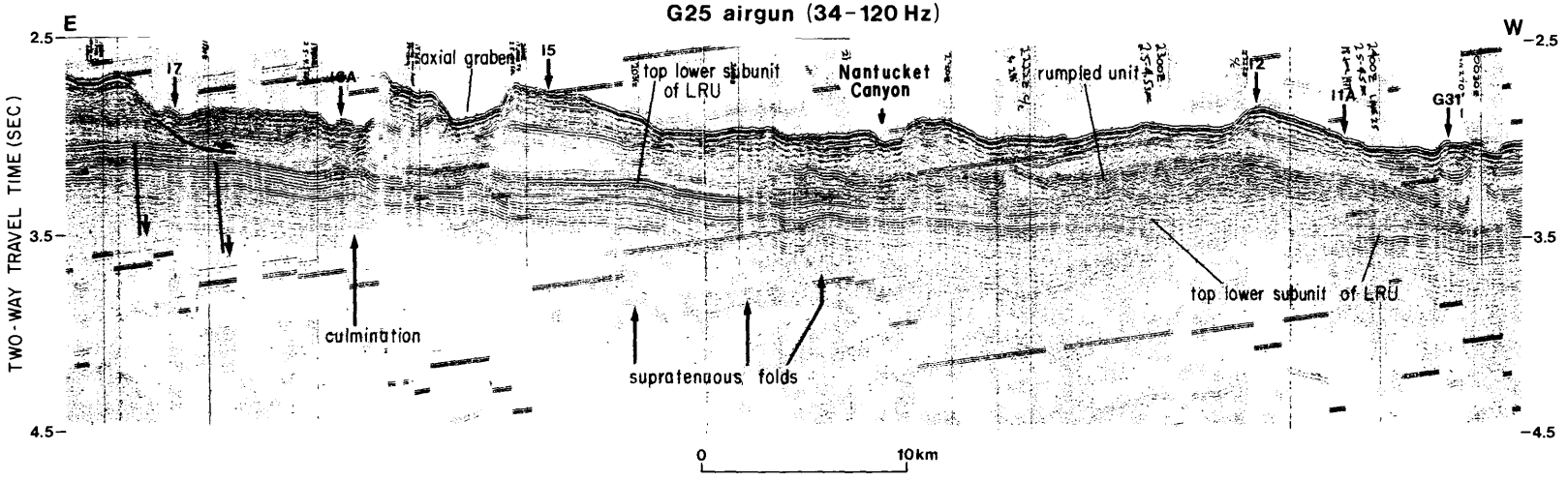

Figure 102. Profile G25 (airgun) along lower slope from approximately 2,100 m to 2,200 m depths shows features of the layered rise unit (LRU); curved arrow shows slip plane of displaced block. Vertical exaggeration ~ 13:1.

The upper 120 m of the displaced slab seems to have subsequently slid away. The slide scar is at least 17 km long and about 12 km across. The scarp profile shown in line G25 (fig. 103) includes a 50-m-thick cliff-forming section held up by a rubble-strewn ramp formed on an underlying transparent incompetent layer. Collapse of this incompetent layer was probably the immediate cause of the slide. Note the inferred graben shown in figure 103. This tensional structure suggests that further lateral detachment and collapse toward the west is possible. Note also that internal collapse along the margin of the slide has involved sediment within a meter or so of the sea floor (fig. 104, cf. fig. 84).

The western (downdip) end of the displaced slab lies over a slight culmination on the surface of the lower subunit (figs. 84, 102). The presence of normal (or at least high-angle) faults here suggests that differential uplift may have been a mechanism of disruption. Contours in the base map (map E) suggest that the block displacement has formed a broad embayment defined upslope by the 1,850-m contour. About one third of the missing section has probably slid downslope off the surface of the depressed block, inasmuch as thinning of the lower transparent interval is negligible, and fault displacement accounts for only about a quarter of the missing section.

The embayment cuts off a broad salient extending out from the slope from the northwest. The salient is a faulted ridge complex held up by perhaps incipient diapiric thickening of the underlying transparent layer. The complex is cut by an axial graben (figs. 84, 102, 105) and by a graben along the east flank within which Veatch Canyon appears as a 50-m-deep notch incised in graben fill (figs. 84, 106). The disrupted surficial strata west of the axial graben (fig. 105) appear to have been dropped into the trough, hence the graben is either of recent origin or it has been recently reactivated.

The western flank of the salient descends onto a broad, relatively depressed surface marked by complex surficial disruption, including graben and tilted, internally intact blocks adjacent to collapsed layers at and beneath the surface. At about the position of line I4 a series of broad ridges separated by graben troughs filled with 10-50 m of debris stand out from the slope. Nantucket Canyon occupies an inferred graben (fig. 107, cf. fig. 102) which seems to cut earlier surficial rubble, implying that the canyon is a recent feature.

The upper rise is broken into slabs on the order of 5 km across that have relief of about 50-100 m. Alvin and Atlantis Canyons are minor features in the blocky upper-rise terrain: Below 1,220 m depth, Atlantis Canyon is a notch less than 40 m deep in the floor of a wide trough; below 2,200-m depth Alvin Canyon is a notch about 23 m deep (fig. 99). The slabs are superficial features; they are not rooted in structure but result from diapiric mounding of the transparent layered rise interval between 100 and 200 m below the sea floor. The deformation is entirely confined to the upper member of the layered rise unit.

SYNOPSIS OF MASS-MOVEMENT PHENOMENA ALONG THE NEW ENGLAND CONTINENTAL MARGIN

Mass movement along the New England continental margin is evidenced by a hierarchy of forms ranging from barely discernable creep of surficial sediment

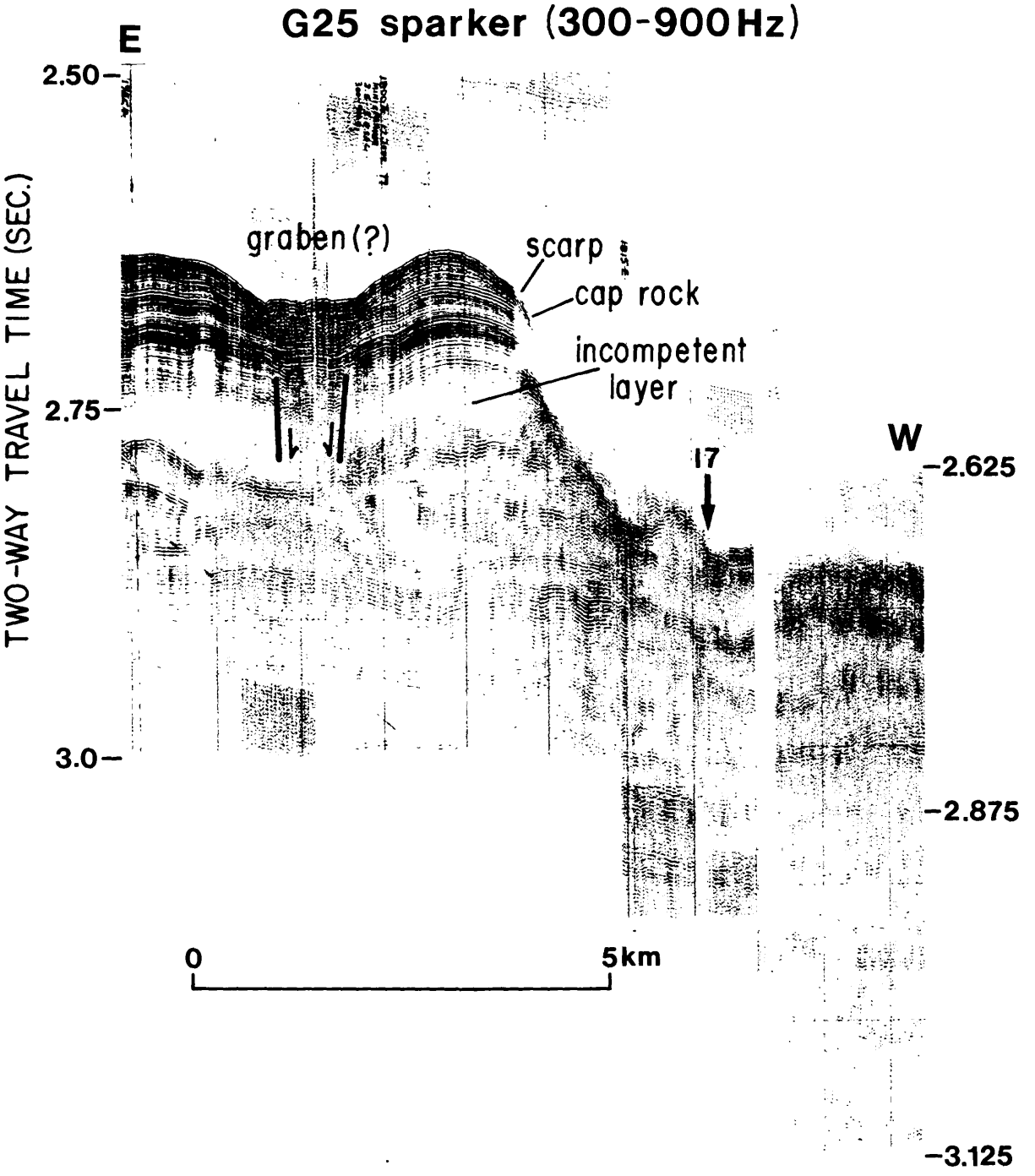

Figure 103. Profile G25 (sparker) across lower slope at about 2,050 m depth shows collapse of layered rise strata because of internal deformation (cf. fig. 84). Vertical exaggeration ~ 22:1.

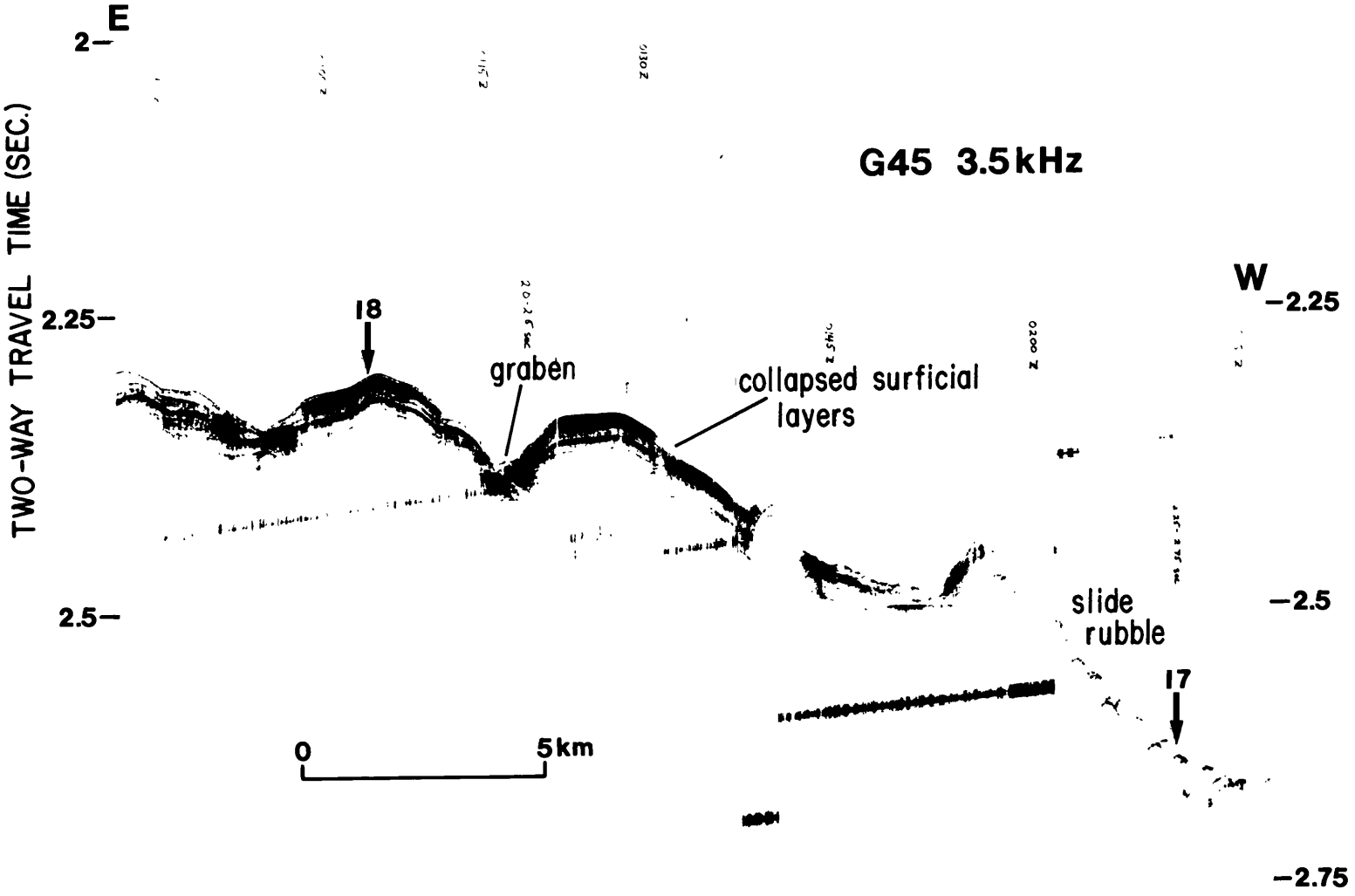

Figure 104. Profile G45 (3.5 kHz) along lower slope from about 1,750 m to 2,000 m depth shows collapse of surficial sediment along surface leading down to major slide excavation (cf. fig. 102). Vertical exaggeration ~ 32:1.

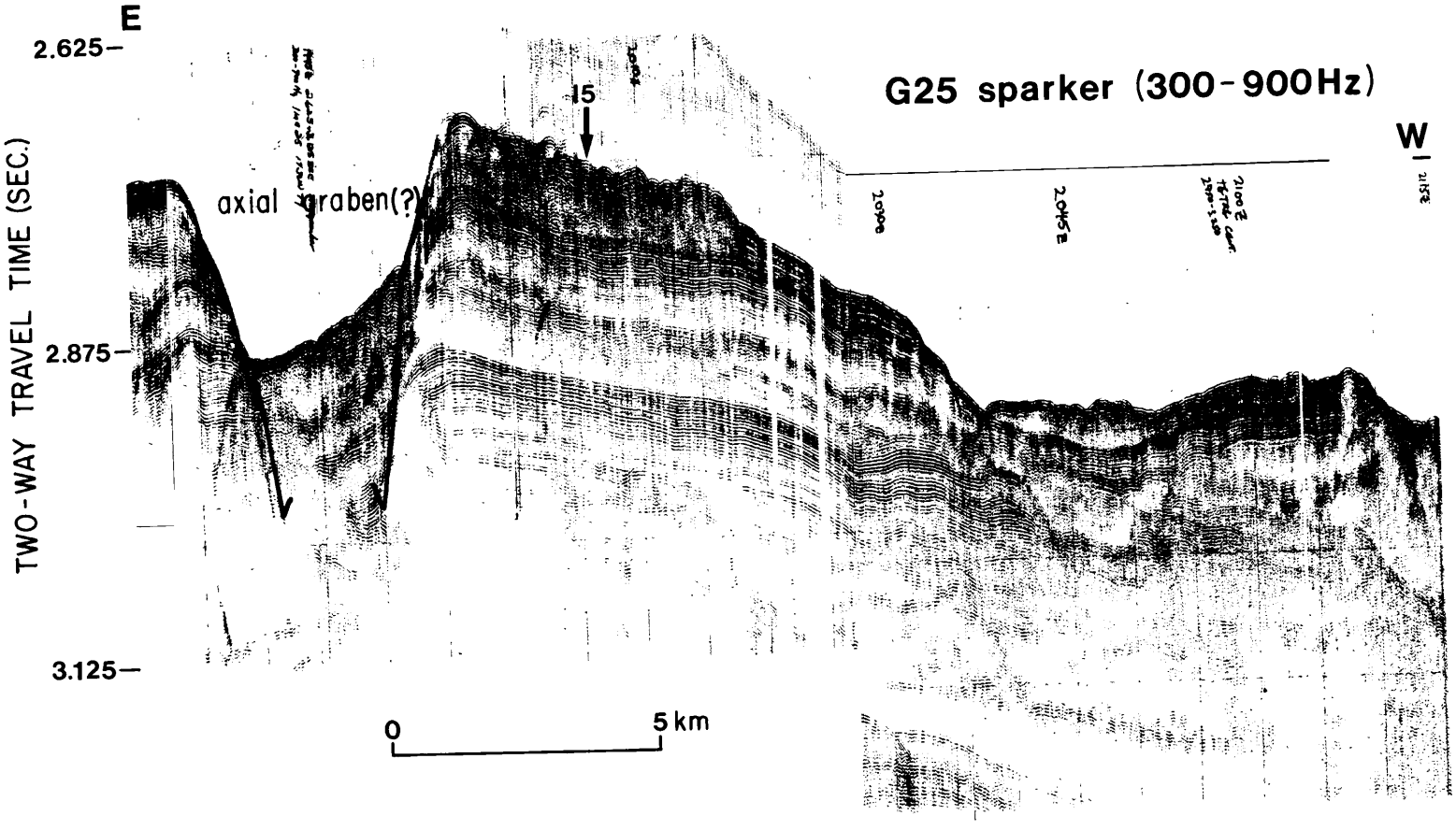

Figure 105. Profile G25 (sparker) across lower slope from approximately 2,000 m to 2,150 m depths (cf. fig. 84). Vertical exaggeration ~ 16:1.

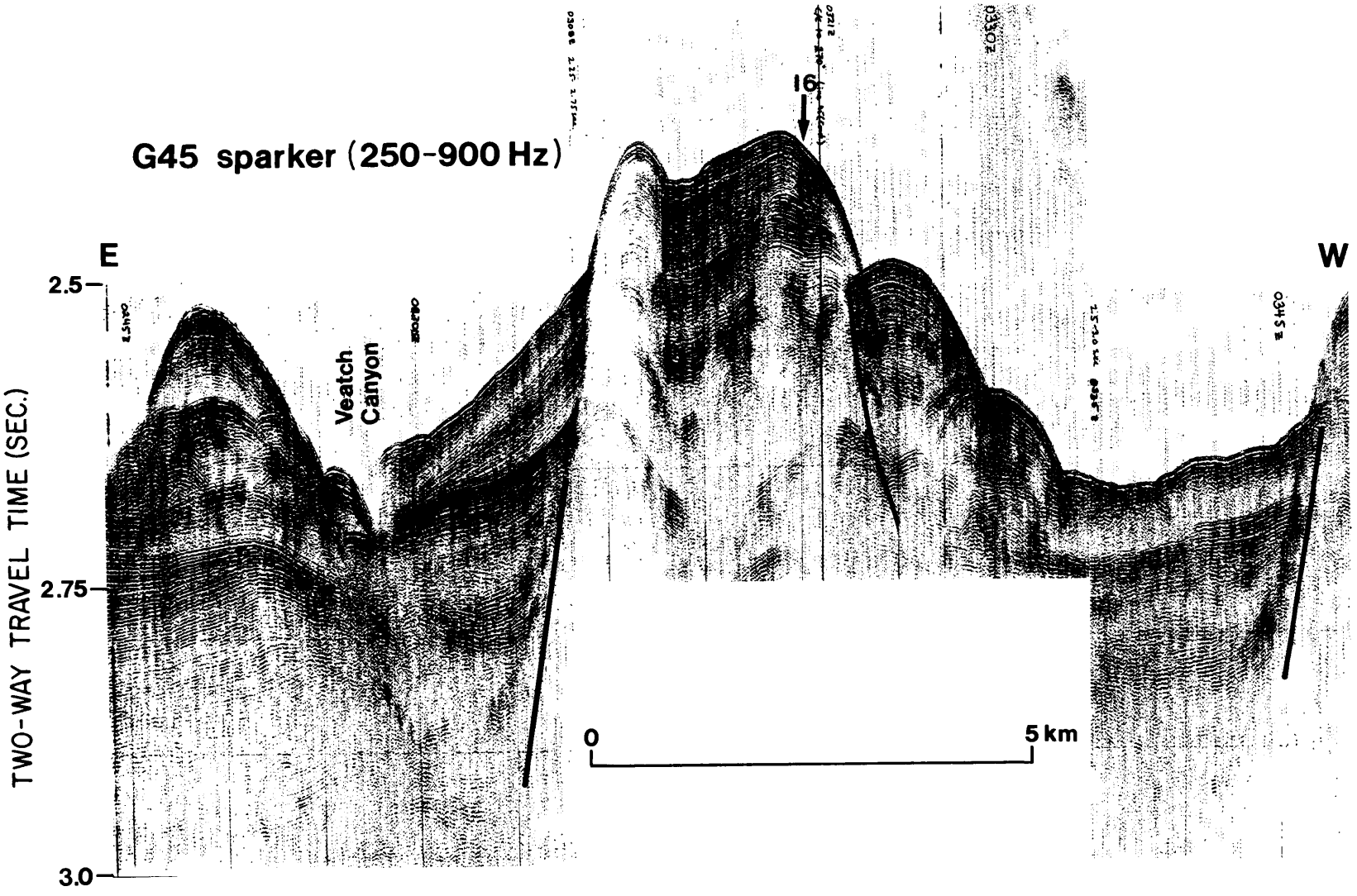

Figure 106. Profile G45 (sparker) shows graben along lower slope at about 2,000 m depth, including Veatch Canyon (cf. fig. 84). Vertical exaggeration ~ 18:1.

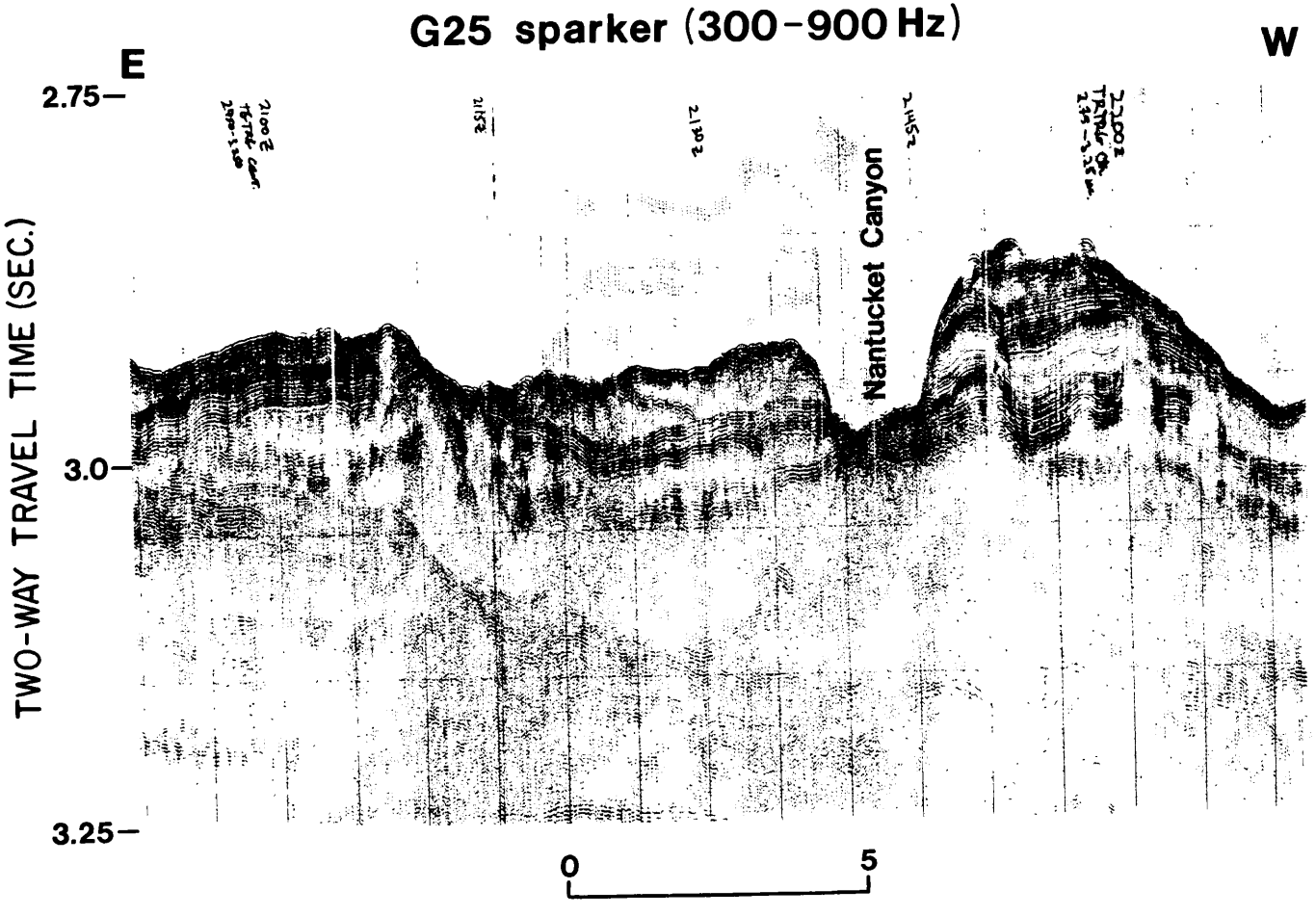

Figure 107. Profile G25 (sparker) along lower slope at about 2,200 m depth shows deformation of the layered rise unit. Vertical exaggeration ~ 33:1.

along the brow of the Continental Slope, to large slides, some encompassing hundreds of square kilometers of thick sediment, along the lower slope. Mass-movement features are typically best developed (or perhaps best recognized) in well-layered sediment with conformable surfaces; mass-movement features ranging in scale from the limit of acoustic resolution to hundreds of meters across and nearly as thick are associated with intraformational deformation and decollement structure. Decollement deformation is widespread in dipping strata along the New England margin. In places it occurs near the sea floor and is emphasized by a caprock effect, wherein a hard, thick, competent layer at the surface, in itself quite stable, breaks up and slides or subsides because of collapse of an underlying, less competent layer. In places, smaller debris flows and Toreva blocks are consequent to larger slides.

Along the New England shelf break and uppermost slope, mass-movement phenomena are sparse and obscure. West of Veatch Canyon (69°30'W.), surface relief near the 200-m isobath can be attributed to step faults, pull-aparts, and small tilted blocks, all of which are the result of internal deformation of one or more underlying beds. Low culminations and depressions of the incised upper slope, at a much broader scale, appear to be related to internal deformation, generally within 140 m of the sea floor. All this deformation resembles creep and/or deep plastic flow and is perhaps best categorized by the term lateral spread.

In places along the outer shelf, transverse fractures or normal faults of minor displacement break the upper-slope unit and perhaps cut the lower levels of the foreset unit. These faults are of uncertain origin. The presence, at the east end of Georges Bank, of a salt diapir intruded to the level of highest faulting, suggests that in this region deep salt flowage has caused differential subsidence, hence block faulting that penetrates high in the stratigraphic pile. Rare surficial faults, evidently due to differential compaction of sediment, cut some of the larger channel-fill deposits.

Filled channels that intercept the larger canyon heads may be sites of debris slides, where the unsupported, unconsolidated channel fill has partly collapsed into the canyon trough, causing a slight peripheral embayment at each such site (fig. 108, A; Laury, 1971). Large filled depressions that have undergone alternating periods of collapse and deposition apparently open into the heads of Alvin and Atlantis Canyons (fig. 109, A). These features are perhaps best described as sediment choked alcoves.

Along Georges Bank, shallow, concave depressions indicative of mass movement are cut in the upper part of the slope (fig. 108, B). A particularly good example, just east of Lydonia Canyon, indicates removal of a mass of sediment about 70-m thick from the foreset unit. These depressions seem to narrow down and feed into the deeply incised "erosional" surface of the midslope.

West of Veatch Canyon (69°30'W., fig. 7) the upper slope is terminated below 750-m depth by one or more longitudinal scarps sloping about 12° (MacIlvaine and Ross, 1979) from which layers of the foreset unit as much as 100-m thick have slid completely away (fig. 109, B). The scarps are indented by tabular cutouts (fig. 109, C) that imply fracture-controlled block detachment. Block segmentation in nondisplaced strata is indicated as far up on the slope as the 500-m isobath. The presence of thin, incompetent layers

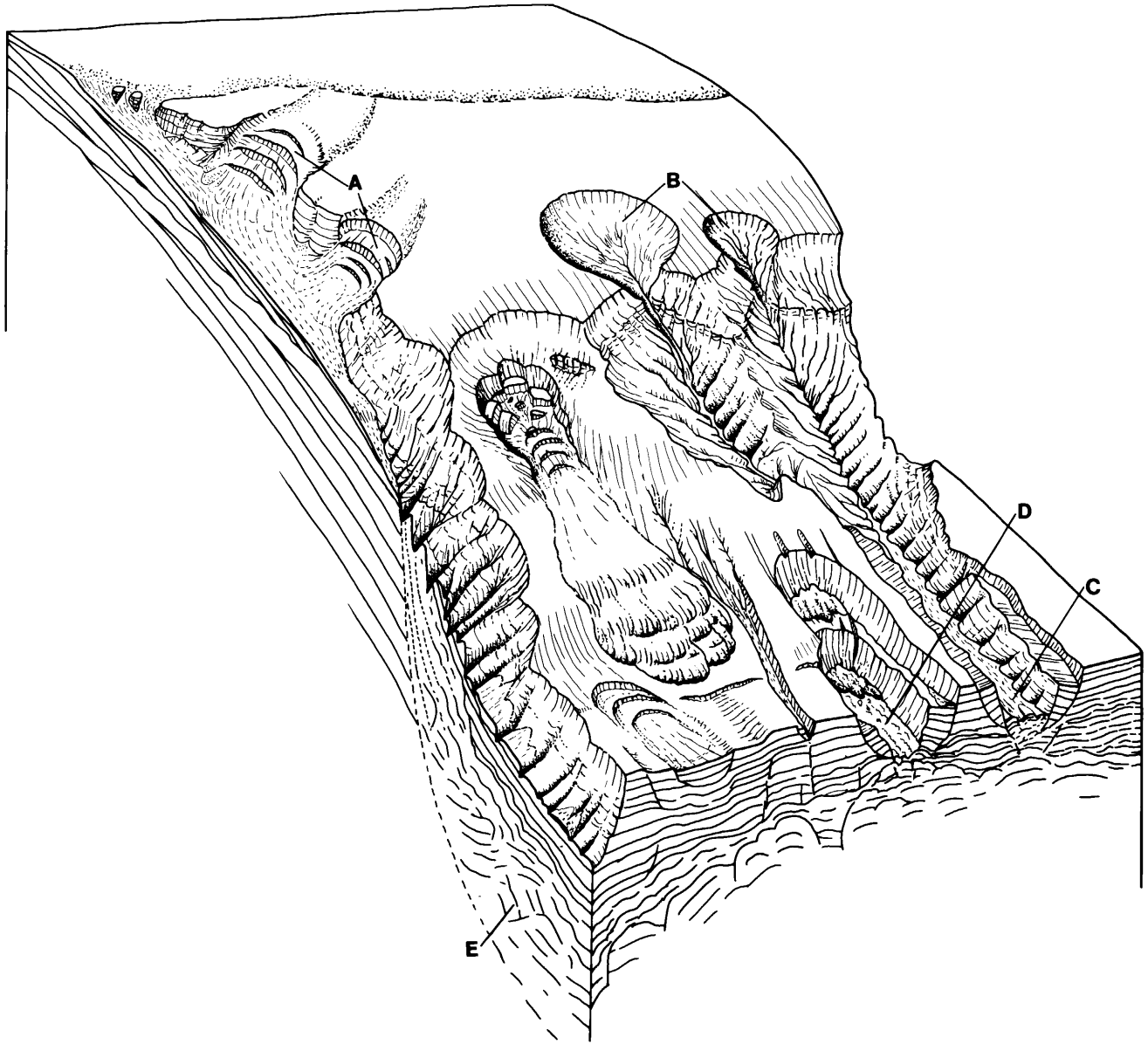

Figure 108. Schematic representation of styles of mass movement along the Continental Slope east of 69°30'W.

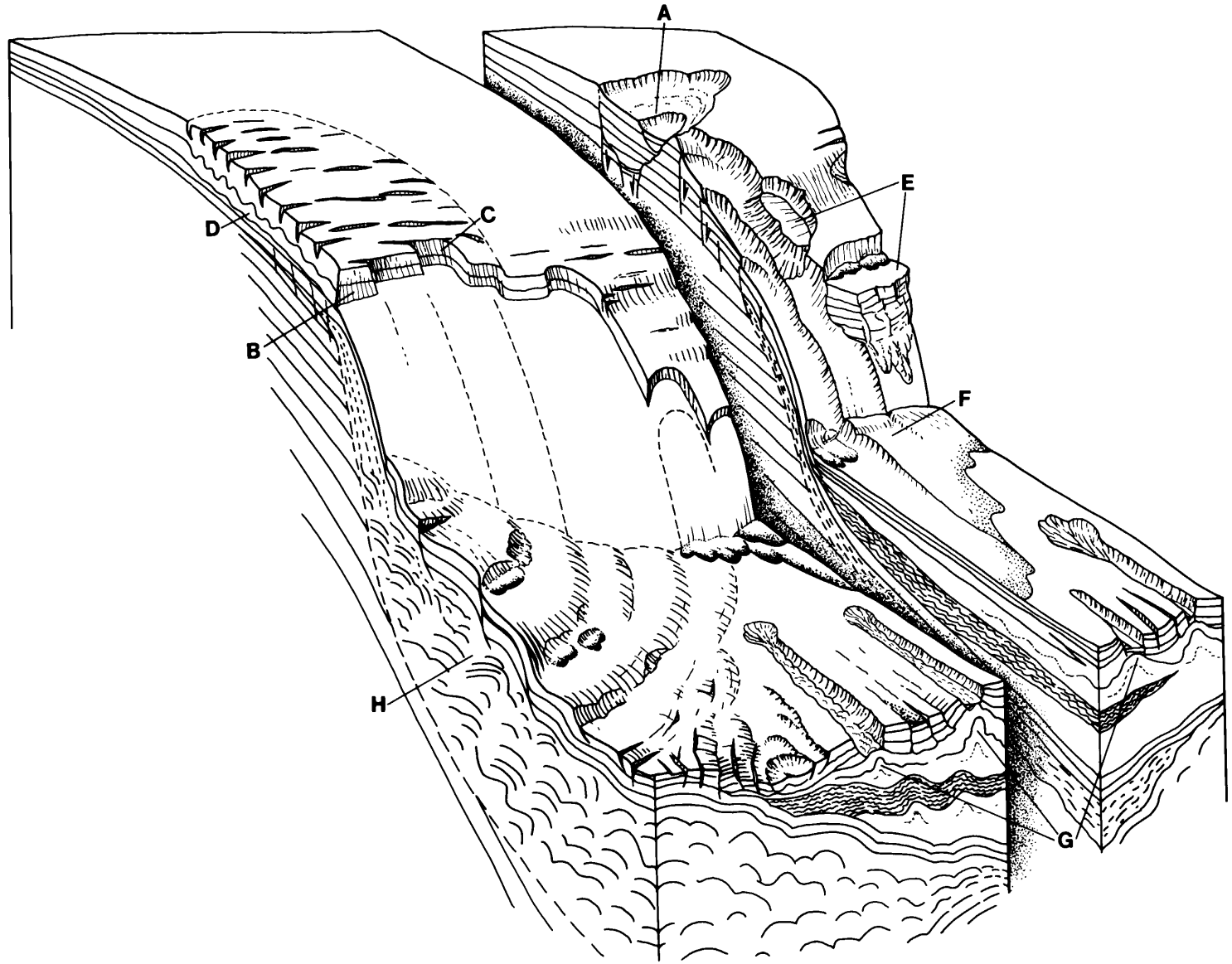

Figure 109. Schematic representation of styles of mass movement along the Continental Slope west of 69°30'W.

beneath the partly detached blocks and injected between them indicates that internal deformation accompanied sliding (fig. 109, D); internal deformation has occurred well updip from the zone of scarps and seems to be genetically related to the creep/deep-flow deformation described above. Block sliding along incompetent layers seems to have changed from a creep phenomenon to true translational sliding across a declivity of perhaps less than a degree along the outer edge of the upper slope.

The section susceptible to slab sliding has also undergone rotational displacement, at about the same bathymetric levels cited above, along salients bordering Atlantis and Alvin Canyons. Displaced, fractured blocks, apparently Toreva blocks more than 100-m thick, form parts of the canyon rims and the margins of adjacent slope depressions (fig. 109, E). These features evince a history of reactivation.

Beds of the foreset unit that blanket the steep lower slope are typically thinned, flexed, faulted, and cut out, phenomena that point to a history of surficial sliding. To the extent that the section includes incompetent layers, it manifests small slides, scarps, and general evidence of downdip translation of surficial layers.

There is evidence that slid layers of the foreset unit have disintegrated during transport and spread out across the upper rise as acoustically transparent debris as much as 50-m thick (fig. 109, F). There is even a hint, in one place, of a carpet slide - an olistostrome kilometers across - derived from the upper slope. At other sites plastic folding and internal thickening evince pileup of displaced strata at the base of the slope. Much of the debris seems to have ripped up sediment previously deposited on the upper rise, resulting in a confused melange of allochthonous and autochthonous debris on and adjacent to slabs of intact in situ sediment.

West of Dogbody Canyon (69°10'W.) the layered-rise unit is internally deformed at depths as shallow as a meter beneath the sea floor to as deep as 300 m in the inferred Miocene interval. Incompetent intervals several tens of meters thick are involved in the larger disruptions. In places the deformed section is greatly thickened by transverse diapiric structures which are overlain by graben and abutted by large broken blocks of more competent strata (fig. 109, G); along strike the upper rise is represented as a succession of transverse ridges, buttes, troughs, and terraces variously tilted and broken, having relief of 10-100 m, all controlled by deep internal deformation.

In transverse profile the same landforms have lower relief, and mass-movement features show the influence of regional dip: small slumps, surficial slides, and listric faults are typical longitudinal mass-movement features of the upper rise. Major surface deformation of the rise is terminated at the slope/rise contact or wherever the deep incompetent layers pass laterally into zones of intact stratification.

East of Dogbody Canyon (69°10'W.) incompetent intervals in the layered rise unit are thinned by onlap. The thinned section is preserved in broad, tilted, flexed, and finely fractured blocks separated by wide collapsed troughs floored or mantled by rubble including, rarely, large inliers (fig. 108, C). The troughs generally lie above culminations of the subjacent unconformity and thus supratenuous deformation is implied.

The pattern of transverse breakage and collapse extends along the rise east of Lydonia Canyon where the layered rise unit is relatively thick. Many troughs in the section here represent complex slides. For example, between Nygren and Munson Canyons a slide trough more than 100-m deep is present heading at about the 1,900-m isobath (fig. 108, D). It is bordered by large marginal blocks, displaced consequent to the main slide event, and by wide fields of collapsed surficial sediment. The slide excavation and the collapsed margins are 20 km across and at least 35 km long. The slide excavations widen and extend to unknown depths. This complex is probably typical of many less well-defined slide phenomena present along the lower slope/upper rise of the New England continental margin.

All along the lower slope there is evidence for a wedge of slide debris onlapped and partly buried by upper levels of the layered rise unit (figs. 108, E; 109, H). The wedge is a confused mass within which large, tilted reflector segments, evidently representing displaced blocks or slabs, are seen. The character of the reflectors suggests that the blocks were displaced from the upper-slope unit of inferred Eocene age. West of Alvin Canyon the wedge becomes a topographically impressive part of the lower slope, attaining a relief in excess of 300 m and a transverse dimension of more than 15 km. The wedge here is relatively flattened, with an average slope of 1.4^{o} (MacIlvaine and Ross, 1979). The part of the wedge lying beneath the layered rise onlap has dimensions probably nearly as great as those expressed above the onlap.

PROCESSES AND MECHANISMS OF MASS MOVEMENT

Along the New England Continental Slope mass wasting can be attributed to two fundamentally different processes: slope oversteepening due to removal of lateral support, and instability arising from sedimentological mechanisms, including possibly diagenesis. In the former case, destabilization of a mass of sediment occurs during or after deposition because lateral support is progressively or abruptly removed. Gravitational energy is thereupon released through a variety of related mass movements which have the ultimate effect of restabilizing the failed slope at a lower angle of inclination. In the latter case, shear strength of a thickening pile of sediment may be insufficient to support growing overburden or loading; too, shear strength may be decreased with time through such factors as progressive generation of excess pore pressure, strain weakening, or infusion of a fluid that dissolves cement or reduces grain cohesion.

A very large portion of mass movement in the New England region has affected sediment of Pleistocene age. Recognition of this has led to much speculation about the importance of rapid sedimentation along the slope and rise during periods of glacial wasting. Rapid sedimentation in fine-grained sediments is believed to lead to instability because of the generation of excess pore pressure and the associated abnormally low effective stress. Moore (1978) associated rapid sedimentation with contemporaneous sand or silt flows and with rotational slumps that have slip planes of about 2^{o} inclination, such as those found on the Mississippi Delta. Moore (1978) pointed out that slides of this type can be very large. Off the Rio Magdalena of Colombia a slide in 1935 exceeded 10^{7} m^{2} in area; deepening was as much as 60 m, and the volume of displaced material was at least $3x10^{8}$ m^{3}.

Data from DSDP holes low on the rise indicate that sedimentation rates for the Pleistocene interval were at least twice the rates for the Pliocene-Miocene interval (e.g., 5 cm/1,000 yrs vs. 2-3 cm/1,000 yrs at site 388 (Benson and others, 1978) 20 cm/1,000 yrs vs. 4.3 cm/1,000 yrs at site 106 (Hollister and others, 1972)). Rates of Pleistocene sedimentation on the slope would have had to have been more than an order of magnitude greater than the cited figures to have been instrumental in causing contemporaneous mass movement (J. S. Booth, pers. commun., 1984). The rate of Pleistocene deposition on the lower slope and upper rise in the survey area could have been greater than the cited figures, not only because of the contribution of distal outwash from directly upslope and melting of nearshore pack ice, but also because of local syndepositional sliding (Fairbridge, 1946), a source that cannot completely be ruled out on the lower slope. Nevertheless, only local intervals in the upper part of the foreset unit show distortion plausibly attributable to rapid sedimentation. On the other hand, there is good evidence everywhere for mass movement having occurred after most of the pre-Wisconsinan Pleistocene section was laid down.

Structures shown in seismic profiles imply that abrupt discontinuities of fundamental strength across layers in a section are important in controlling mass movement. This suggests that postdepositional internal deformation was instrumental in generating mass movement.

There are numerous ways in which intraformational deformation can lead to mass movement. In the simplest case, a rigid layer overlies a layer with low shear strength. Typically, weak and strong layers are interbedded in a thick pile, however, and failure can occur at more than one stratigraphic level. Such piles may be stable on a perfectly horizontal surface where quasi-lithostatic stress is maintained, but if the pile is laid over a culmination or small hill, or placed on a slope, a downslope shear-stress component is set up which may lead to plastic flow in the weakest layers (fig. 110) away from the high points. Plastic flow in incompetent layers sets up tensile stresses in overlying competent layers, by both removal of subjacent support and by imposition of tangential stress along bedding. Plastic deformation may proceed slowly for a long time before mass failure occurs; if the overlying competent bed eventually fails, accelerated downslope displacement may take place by means of "gravity slide faults" (Bruce, 1973) which combine normal faulting updip and bedding plane faulting downdip (i.e., listric faults). Following initial generation of the fault, subsequent displacement is parallel to bedding; hence, dilation occurs across the initial, steep segment of the fault plane (fig. 110) which becomes not only an area of dip reversal but also a site of keystone faulting. Seismic-profile data imply that such deformation began along the slope only after tens, perhaps a hundred or more, meters of sediment had been laid down (fig. 111).

Plastic flow of the incompetent layer may proceed very slowly and produce a surface characterized by dip-and-fault structure (fig. 112; Hollingworth and others, 1944; Judson, 1947). Such deformation might explain the broken surface over wide areas of the upper slope expecially in sector III (e.g., figs. 95, 76, 91), as well as the shallow scarps reported at the head of Lydonia Canyon (Slater, 1982).

A related type of deformation is valley bulge (Hollingworth and others, 1944; Judson, 1947), wherein an anticlinal welt or horstlike structure

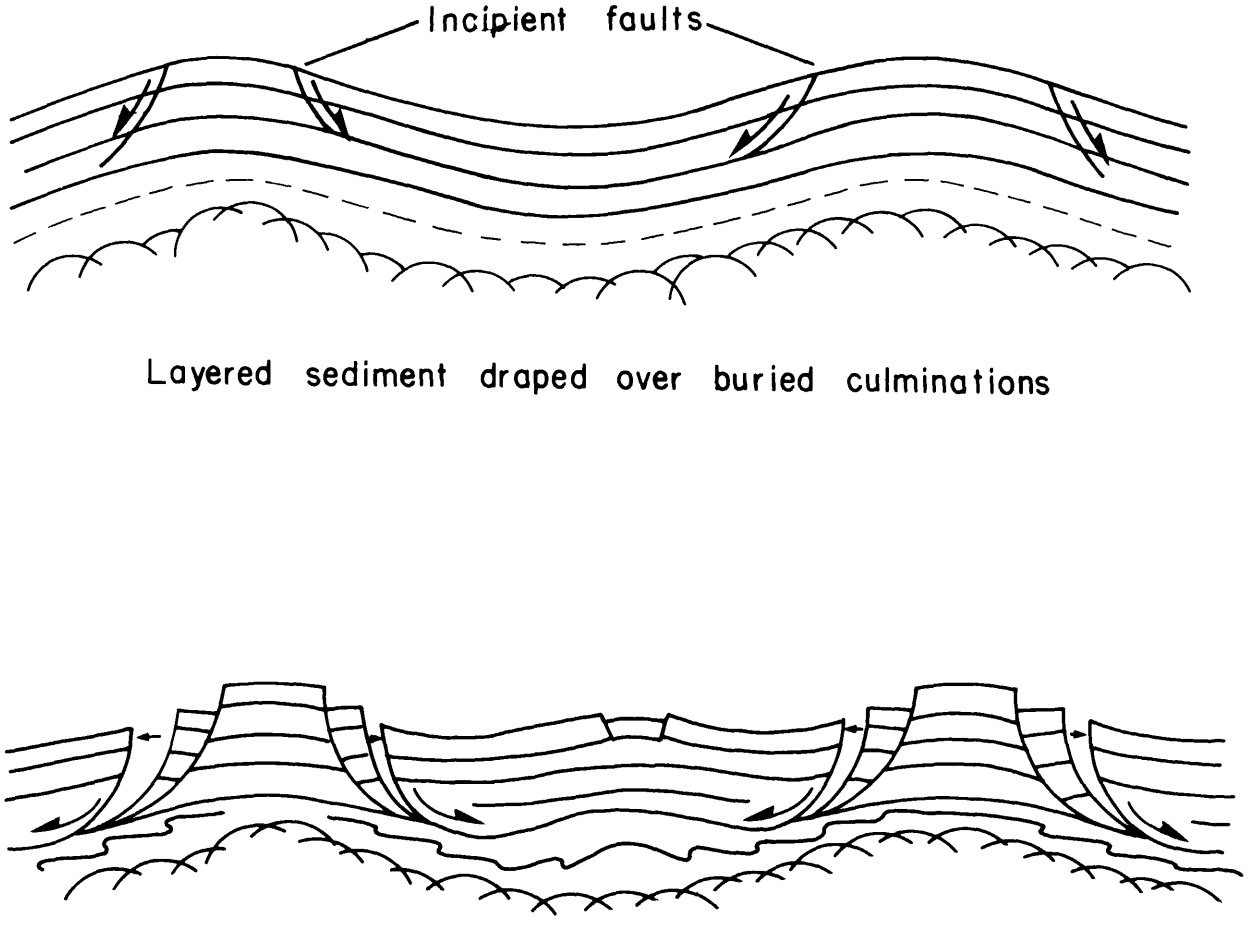

Figure 110. Diagrammatic representation of mass movement generated by plastic flow in incompetent sediment draped over culminations.

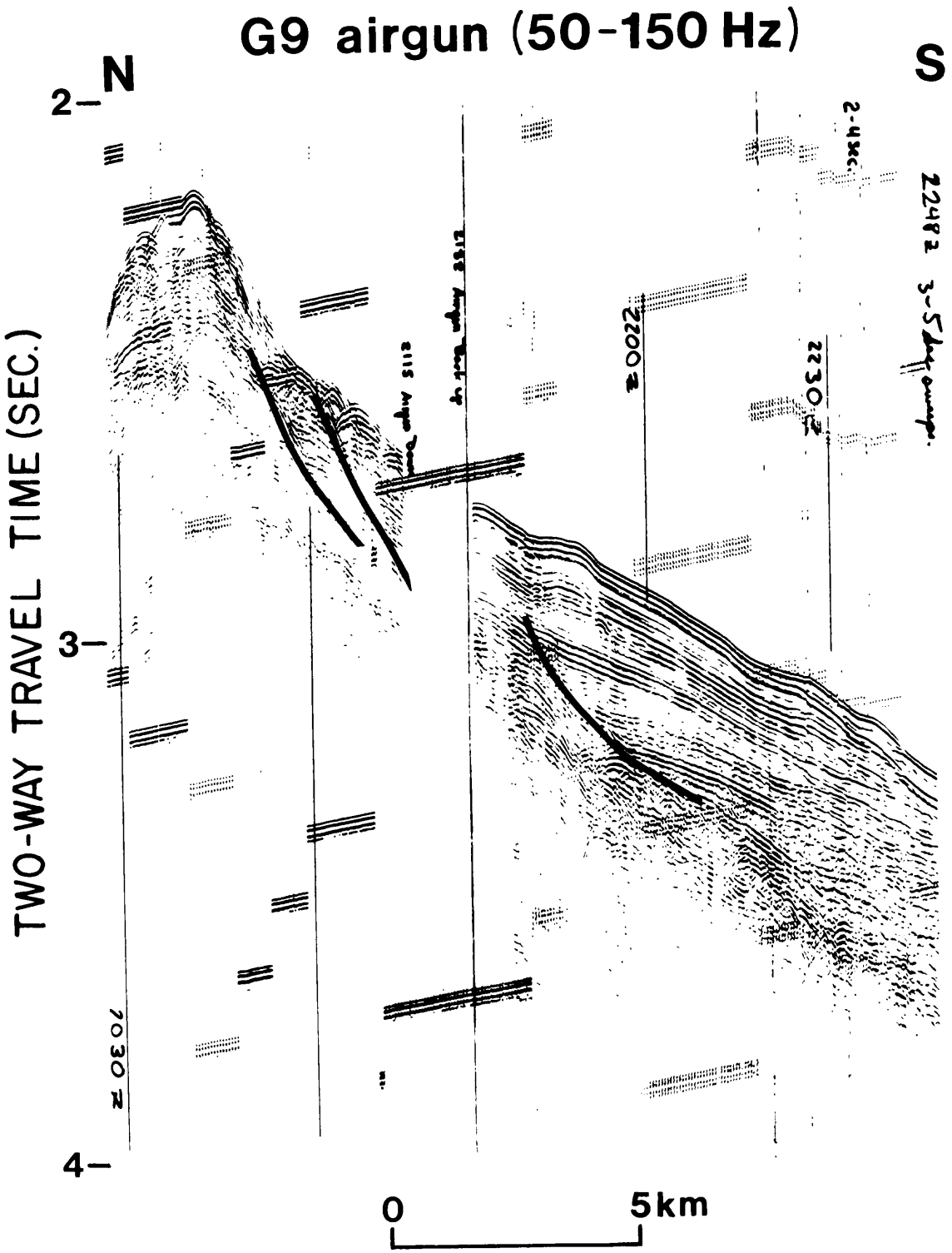

Figure 111. Profile G9 (airgun) shows deformation of layered sediment over a buried culmination along lower slope west of Corsair Canyon at about 2,000 m depth. Vertical exaggeration ~ 15:1.

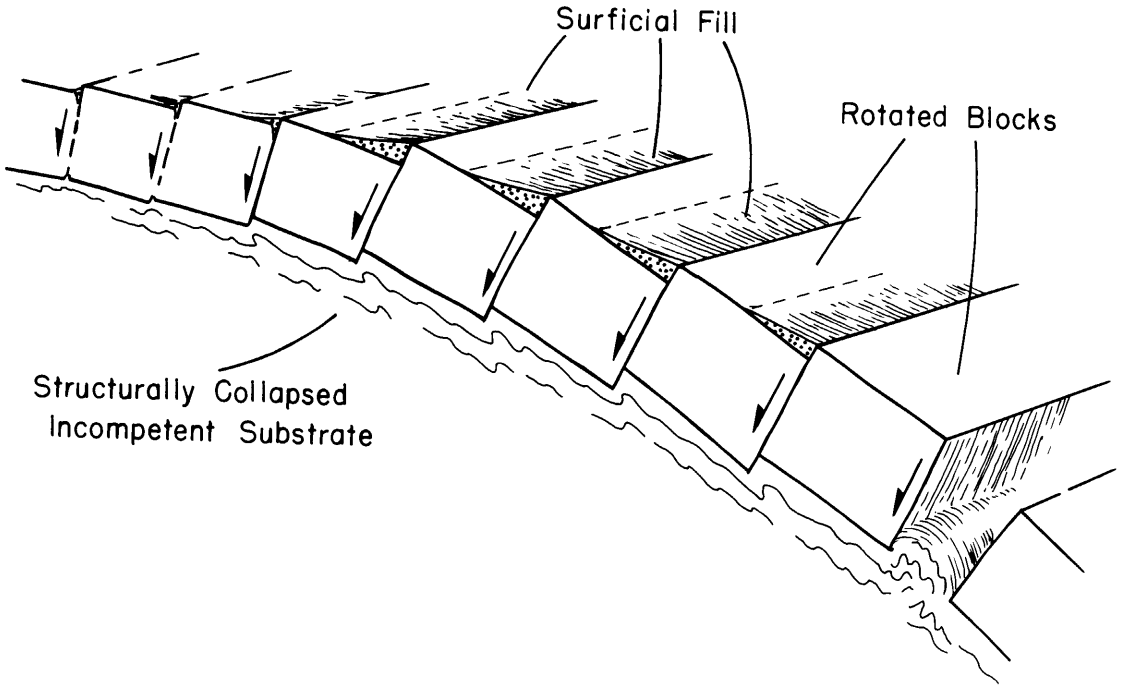

Figure 112. "Dip and fault structure" (from Hollingworth and others, 1944).

develops in incompetent strata along a valley axis that has been cut through a cap of competent strata (e.g., figs. 47, 82). Although upward movement of sediment may be driven by release of confining pressure, lateral movement appears to dominate in structures of this type (Judson, 1947); hence, the process leading to bulging is tensile and the intrusion is passive. Such bulges are a consequence of incision through overlying caprock and release of confining pressure; they are unrelated to either regional structure (except possibly a transverse fracture system) or to coexistent deformations arising from regional diastrophism (Hollingworth and others, 1944).

A peculiar type of decollement-related internal deformation involves thickening of an incompetent layer by downslope flow, somewhat like a sill intrusion. Coleman and Garrison (1977) describe this as one of the principal mechanisms of mass movement across low-gradient shelf surfaces off active deltas. They are presumably generated by overloading and are thus penecontemporaneous.

According to Coleman and Garrison (1977), most such "mudflows" are amorphous units characterized by a lobate, ramplike distal termination with an average slope of 2.3^{o}. The surfaces of "mudflows" are extremely irregular because the capping layer is broken into discrete blocks by the subjacent intrusion. Another characteristic feature is a tongue of amorphous material that extends seaward from the main mass of the flow, sandwiched between well-layered strata, for distances of up to 2.5 km. Coleman and Garrison (1977) describe a "mudflow" off the Mississippi Delta with a downdip extent of about 50 km, a thickness of up to 60 m, and an areal extent of 770 km^2. Comparable features in the foreset unit of sector III are shown in figures 94 to 96.

Decollement-generated folds can be described by a classic model of flexure folding (Billings, 1960), i.e., if a layer is arched by lateral stress, it undergoes tension on its convex surface and compression on its concave surface. Graben may result from crestal tension, and be propagated down to a surface of no strain (or detachment), below which compressional folds and reverse faults are generated (fig. 113, A). In this type of deformation incompetent layers tend to thicken beneath rising fold crests, even to the point of diapiric intrusion.

Folding and fracturing can also be caused by vertical uplift (fig. 113, B), for example by clay diapirism driven by overloading or gas generation (Colemen and others, 1974). Among the deformation features produced by clay diapirism are steep, narrow, faulted antiforms having structural relief as great as 200 m; they are separated by broad, flattened, subsided synforms in which syndepositional sediment may accumulate to thicknesses as great as 150 m (Coleman and others, 1974). If sufficiently steep slopes are formed by diapirism, sediment may slide off the anticlinal flanks into the subsiding synforms (Reading, 1978). This style of deformation is common along the New England Continental Slope and Rise. It has apparently been a major cause of graben structures and high-relief landforms along the upper Continental Rise and lower slope.

Many seismic profiles along and across the lower slope in the New England region show acoustic features attributable to gas (see appendix). Gas was detected deep in AMCOR holes 6012 and 6013 along the uppermost Continental Slope (Hathaway and others, 1976). In hole 6012 gas was found in gray clayey

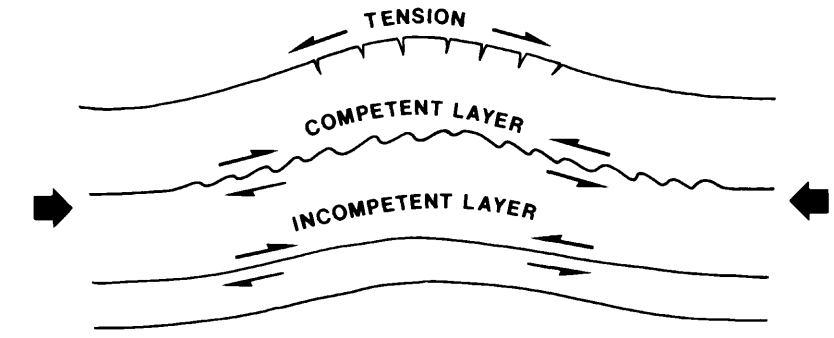

Flexure folding begins through lateral compression.

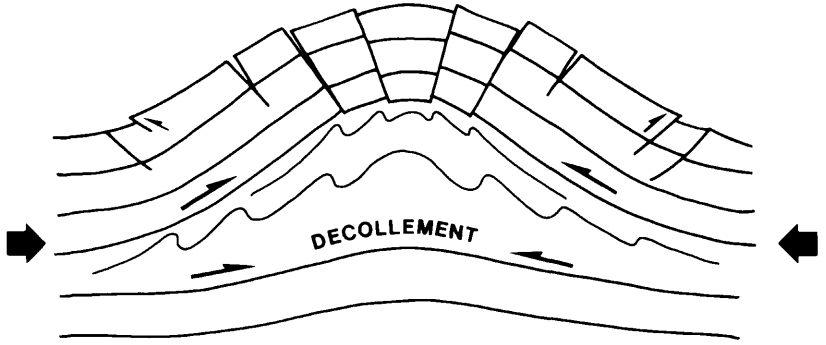

Advanced folding leads to decollement, core thickening of incompetent layer by flow folding, tensile failure and block faulting of suprajacent competent layer.

A

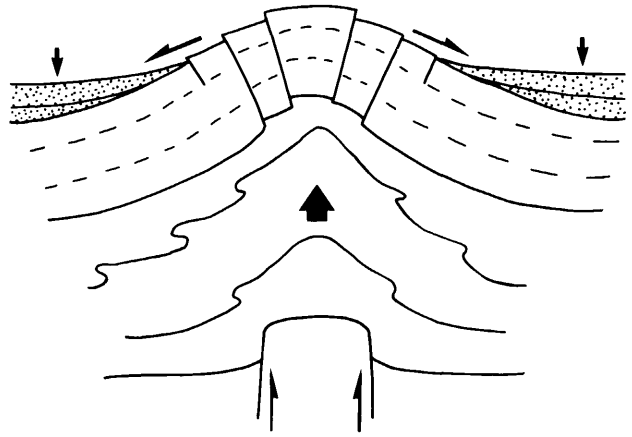

Uplift and flow – folding (accentuated by lateral sediment loading) leads to brittle failure of overlying competent layer and diapiric intrusion.

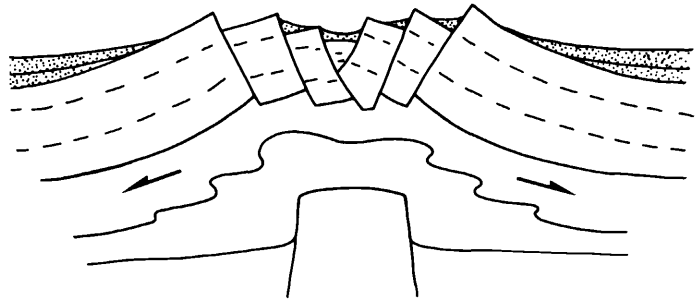

Relaxation of vertical stress is followed by flow of incompetent material away from fold crest, accompanied by graben collapse.

B

Figure 113. Diagrammatic representation of internal deformation caused by (A) flexure folding and (B) vertical uplift.

intervals above 240-m depth: CH_4>250,000 ppm; C_2H_6>2,000 ppm; C_3H_8>100 ppm. In hole 6013 gas was found in gray silty sand between 176-232-m depths: CH_4>315,000 ppm, C_3H_8>400 ppm.

Gas is commonly thought to contribute to low effective stress and low shear strength (Jerbo, 1967; Monroe, 1969; Roden, 1980). Gas-charged sediment is even capable of violent eruption (Hedberg, 1974; Bryant, 1980). In sediment samples from the Continental Rise, the recorded effects of gas expansion are spectacular. At DSDP site 106 on the lower rise, in stratigraphic intervals comparable to those of the deformed layered rise intervals, gas expansion was strong enough to cause extrusion of sediments from core liner and to produce sectioning of cores. The main gas component present throughout the sampled section was CH_4, with lesser amounts of CO_2, H_2S, C_2H_6 (Lancelot and Ewing, 1972). At DSDP site 388 a gas concentration of 390,000 ppm was recorded in the Miocene interval at 328 m subbottom depth. Silty clay was "highly disturbed" as high as 251 m in the cored section and sediment below 323 m was a slurry with soft clay fragments.

The weakening effects of gas on sediment strength have been surmised from "undrained" shear strength tests performed on shipboard samples. Expansion of gas that results from release of confining pressure on the samples leads to test results lower than those obtained in situ (Esrig and Kirby, 1977). The weakening effects of gas in sediment, as observed in laboratory tests, may be overestimated; it may not necessarily be true that the vapor phase in situ contributes to low shear strength. Esrig and Kirby (1977) calculated that gassy sediments with a (water) saturation of around 85 percent, tested onboard ship, are probably nearly fully saturated in situ. The effective stress in such sediment is determined by the pore fluid; the presence of gas bubbles in the pore fluid (and gas bubbles can be present even in a fully saturated sediment (Esrig and Kirby, 1977) would have essentially no effect on pore fluid pressure because a) gas pressure is in equilibrium with fluid pressure, b) changes in confining pressure do not greatly affect gas solubility; a ten-fold increase in gas solubility makes only a small difference in the calculated degree of soil saturation (Esrig and Kirby, 1977), and c) surface tension effects in small dispersed bubbles may lower maximum gas pressure (Whelan and others, 1978). Thus, despite gas in concentrations sufficient to obliterate acoustic reflections (>30 ml/l), low in situ shear strengths are not uniquely attributable to trapped gas (Whelan and others, 1977).

Nevertheless, gas is commonly associated with weak, overpressured sediment and gas must somehow play a part in strength reduction. If under normal confining conditions, gas-generating reactions are limited by the solubility of the gas and do not proceed much beyond the point of gas saturation, that is, the actual appearance of gas bubbles in the pore fluid, we must explain how abnormally high vapor pressures are generated. If dispersed gas bubbles in pore fluid were to coalesce and adhere to grain boundaries, surface tension effects might be reduced and elevated pore pressures could result. Pressure changes in overburden could result not only in bubble coalescence (Whelan and others, 1978), but in exsolution of dissolved gas, and perhaps even allow gas generation from remaining reactants to proceed. If a large enough volume of gas were to appear, it might form menisci between sediment grains as well as coalescent bubbles in pore fluid (Esrig and Kirby, 1977); the grain skeleton support might be weakened (Whelan and others, 1977) and sediment compressibility would be enhanced (Sangrey, 1977).

Generation of methane, a common gas in marine sediments, involves complex reactions, some of which produce H_2O as well as gas (Coleman and others, 1974). H_2O production in such reactions is favored owing to the large negative free energy of H_2O. Addition of H_2O to the pore fluid as a co-product of gas generation or even by osmotic migration may be a factor in reducing shear strength. A concomitant effect of pore-water generation is pore-water freshening, which could lead to structural weakening also. For example, dilution of a saline pore fluid could reduce electrostatic particle bonding, which would increase sensitivity (Embleton and Thornes, 1979).

A potentially important cause of pore-water freshening along the Continental Rise is the destruction of clathrates. Clathrates are crystal lattices composed of water molecules coordinated around large gas molecules and bound by weak electrostatic attraction. Clathrates can form below 1,500-m water depth within the upper 500 m of sediment, at temperatures below 20°C (Claypool and others, 1973), provided CH_4 is present in excess (Hesse and Harrison, 1981).

Crystallization of clathrates excludes monovalent and divalent cations. Thus, if a zone of clathrate in an interval of strata returns to solution as a result of the reduction of overburden pressure or a rise in temperature, the resultant pore water should be considerably fresher than the initial water of compaction and it should be capable of altering the chemistry and binding strengths of clay minerals (Hesse and Harrison, 1981).

It is thought that leaching of marine clays by fresh groundwater can lead to large mass movements (Bjerrum, 1954). The leaching of sediment along the upper slope by groundwater influx is moot. If groundwater piping or generation of seepage pressure (Terzaghi, 1956) were ever a process contributing to mass movement in strata of the foreset unit, it is certainly not active now and its effects are not distinguishable from those generated by other processes.

The textural character of the Pleistocene-Miocene interval suggests an inherent tendency toward instability. High porosities are typical of unsorted silt or silty sand (Terzaghi and Peck, 1948), especially those that contain a "slight" content of fines or organic matter (Andresen and Bjerrum, 1967). Liquefaction in such sediment could occur at overburden pressures equivalent to a 50-m-thick column, provided porosity is at least 44 percent (Andresen and Bjerrum, 1967); Andresen and Bjerrum (1967) note that the most unstable sand consists chiefly of rounded grains - a typical Miocene/Upper Cretaceous component along the New England margin.

Deep-seated slides can also occur in thick, relatively homogeneous deposits of clay or shale. This is possible in clayey sediment because a certain component of strength is provided by clay particle cohesion; therefore, if the rate of increase in shear strength with depth is less than the rate of increase in shear stress, at a certain depth (fig. 114) the pile is unstable (Carson and Kirkby, 1972). An increase in slope relief or slope angle (α, fig. 114) can thus lead to mass movement of relatively thick masses of such sediment.

The Pleistocene part of the foreset unit and the layered rise unit may be conducive to extreme mobility because of its composition. Cabrera and Smalley

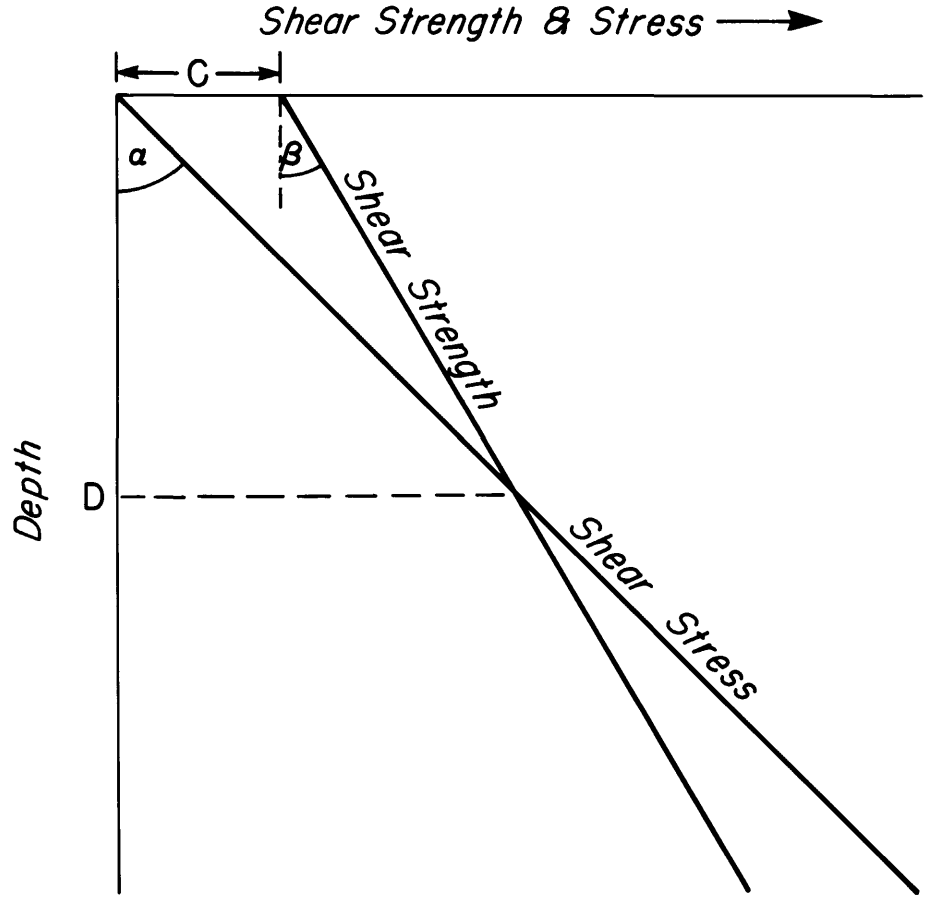

Figure 114. Relationships of shear strength and stress with depth in homogeneous fine sediment (from Carson and Kirkby, 1972).

(1973) demonstrated that in glacially derived sensitive clays, which include both silt and clay-sized quartz and feldspar particles that form inactive cohesive bonds among true crystallographic clay particles, the remolded strength is significantly reduced. They suggested that such sediment is capable of forming suspensions of particles in pore fluids when collapse occurs, producing very mobile debris.

The large slide scars along the lower slope show a puzzling lack of associated debris. This lack is generally attributed to the generation of turbidity currents which are purported to be highly efficient transport agents. However, there is very good observational evidence that large complex submarine mass movements do not degenerate into turbidity currents (D. Prior, oral commun., 1982) and there are important theoretical arguments against the supposition (Terzaghi, 1956). Embley (1976) noted the existence of "debris flows" on the North African Continental Rise several hundred kilometers from a likely source and considered this evidence for highly mobile material. Some sort of fluid flow is indicated, perhaps similar to that of snow slides or "retrogressive flow slides" (Andresen and Bjerrum, 1967).

Whatever the mechanism of large slide transport, it is capable of moving large amounts of sediment long distances and of leaving behind, in addition to a relatively clean, steep scarp, only a thin veneer of residuum that does not account for the displaced volume.

THE POTENTIAL FOR MASS MOVEMENT

Mass movement of considerable dimensions has occurred along the New England Continental Slope and Rise, and at a scale as to constitute major hazard to offshore engineering operations were it liable to be generated by historically observable natural stress, or man-induced stress. Is the slope presently stable or could the mass movements described in this report occur at this time?

The juxtaposition of fractured strata and flexures beneath mass-movement features along the New England margin implies that deeper displacement has triggered collapse in suprajacent incompetent layers. This brings up the possibility of earthquake shock as a triggering mechanism (Moore, 1978). In light of the great Cape Ann earthquake (est. MM 8) of 1755, the possibility of very large tremors in the New England region is not to be discounted. However, virtually nothing is known about offshore seismicity. The Northeastern U.S. Seismic Network (1978, 1980) has recorded only two minor tremors: a 2.4 nm earthquake on the rise (38°50'N., 70°41'W.) and a 2.8 nm earthquake on Georges Bank (41°40'N., 67°78'W.).

Along the New England coast tectonism is manifested by a gradual change in surface elevation, particularly by coastline subsidence (Gable and Hatton, 1983), punctuated by uncommon but historically large earthquakes (P. Barosh, oral commun., 1982). Subsidence may be continuous or incremental. We do not know whether contemporary tectonism affects the New England Continental Slope, but there is reason to surmise that differential uplift along the outer shelf of Georges Bank occurred by imposition of a glacial forebulge during advances of one or more continental ice sheets. If this is true, then slope steepening and induced strain due to ice loading may have greatly accelerated instabilities that result from tectonic subsidence along the upper rise. Many

of the larger mass-movement features must be relict Pleistocene forms. Along the outer margin of the upper slope there are lateral spreads, broken masses of strata tens of meters thick resting on internally deformed sediment, that await less than a degree of slope steepening to slide out of place. These deformed sediments may be presently advancing toward the slope brow by creep; in effect, they may be very slowly pouring off the upper slope in response to stress applied during Pleistocene ice/sediment loading, or in response to progressive tectonic subsidence. The presence of creep and deeper plastic flow in shallow-dipping strata along the upper slope and rise is important, because shear failure, particularly in stiff, fissured clay is often preceded by creep (Embleton and Thornes, 1979).

The presence of inherently weak layers buried deep in the stratigraphic pile is a potentially serious condition, as such layers could fail under earthquake or man-induced shock. Gas generated by diagenesis following the era of relatively rapid Pleistocene sedimentation may have played a part in the widespread surface collapse and mass movement along the lower slope/upper rise. The potential for large gas-enhanced failure in the upper 300 m of section may yet exist in masses of sediment metastable since Pleistocene time. Too, sediment which might have been in hydrostatic equilibrium may have subsequently become seriously overpressured because of sustained gas/pore water generation (Hedberg, 1974), or because of postdepositional infusion of gas from a deep artesian pressure source which could supply abnormally large volumes of gas into otherwise unpressured near-surface strata (Sangrey, 1977).

At present the question of stability cannot be resolved because of the unknown relationship between shear strength and stress at depth and because of the time-dependent nature of the deformation and slope failure. Geotechnical measurements of the upper several meters of strata indicate that slopes of around 30° would have to be attained before drained failure could occur (Moore, 1961; Keller and others, 1979). Keller and others (1979) and Moore (1961) believe that seismic shock is necessary to initiate mass movement under these conditions; Terzaghi (1956) believes seismic shock would have no effect. These conflicting conclusions and misleading observations do not take into account the structure and deformation history of the deep layers which I have presented in this report. The bottom line is that the sea floor, supposedly stable at slopes of less than 10°, has undergone prodigious collapse within the last 200,000 years; the potential for further collapse and for mass movement of great variety exists all along and across the New England Continental Slope.

SUMMARY AND CONCLUSIONS

The mass-movement features found along the New England Slope are of three general types: slides, slumps (including Toreva blocks), and flows (including creep deformation). Slides and flows are widespread, relatively young, and potentially active features. They range greatly in size and extent and possibly also in origin. Slumps are uncommon and their origin is enigmatic. They may result variously from rapid sedimentation, diagenesis, slope steepening, or previous mass movement. Toreva blocks and rockfalls are generally local secondary features that form consequent to mass movement away from culminations and along canyon walls or scarps because of removal of lateral support.

Surficial geologic characteristics of the slope vary along strike; a major transition occurs around 69°30'W. To the east, seaward of Georges Bank, the upper slope is steep, cut by coalescent, concave, broadly amphitheatric and notchlike depressions in which relief and dissection increase downslope. The lower slope is an incised cuesta or, more accurately, a series of narrow flatirons that project up between the amphitheatric depressions. The preserved strata are extensively tilted, broken and collapsed; mass movement is evidenced by decollements, slumps, and slab or block slides.

West of 69°30'W. the upper slope is a broadly convex, gently dipping surface much broken up by internal deformation and creep. It is abruptly truncated at around 1,000-m depth along a zone of scarps and large detached and translated blocks. The steeper lower slope is mantled by a wedge of ancient debris that thickens to the west and against which sediment of the rise is ponded. The layered rise strata are considerably deformed by internal folding and diapirism that has a strong transverse orientation.

The style and distribution of mass-movement forms along and across the slope suggest a pattern of deformation that includes a) strike-aligned scarps, faults, and major slides and slumps, b) transverse graben, block faults, and local slumps. Across the entire region these deformed strata, hundreds of meters thick, lie on a major post-Cretaceous(?) unconformity of high relief on strike.

The structural style and the stratigraphic and physiographic setting of mass-movement features are powerful clues to their origin. Two fundamental and unrelated processes seem to have generated the mass movements of the New England margin. Their main characteristics and likely products are summarized in table 1.

Widespread mass movement along the lower Continental Slope-upper rise was initiated in Late Cretaceous time. At least three erosional(?) unconformities occur in the Upper Cretaceous stratigraphic interval. During intervening periods of deposition terrigenous sediment was brought to the subsiding slope environment, and a wedge of slid debris, probably intercalated with primary deposits, accumulated against the steepening slope.

The uneven terrain of the Late Cretaceous debris wedge was partly covered by lower Eocene clastic sediment and by middle Eocene chalk and marl. Late Eocene through mid-Oligocene time seems to have been a period of widespread erosion, faulting, slope steepening, and perhaps general subaerial exposure of the shelf. Much of the Eocene section along the midslope was truncated and the debris incorporated into the lower-slope debris wedge.

Renewed mass wasting may have taken place during the early part of the Miocene epoch, but by latest early Miocene time marine transgression had spread a thin layer of glauconitic sediment across the shelf. Subsequently, deposition across the entire margin seems to have been fairly continuous and substantial through mid-Pleistocene time, probably because of nearshore glacial activity. Erosion and mass wasting in middle to Late Pleistocene time cut the slope into the gross forms we presently see.

Late Pleistocene glacially derived sediment was prograded across the truncated earlier Pleistocene upper-slope section and was draped over much of

Table 1. Primary processes inferred to have generated mass movement along the New England Continental Margin

Slope-steepening processes		Sedimentological processes
Superficial	Tectonic	
Slope steepening due to glacial forebulge(?). Possibly two major late Pleistocene events superposed on long-term or intermittent tectonic steepening; rapid sedimentation during glacial wasting may have accelerated and complicated effects of tectonic steepening and loaded the slope for mass wasting during a subsequent glacial forebulge steepening. Strain weakening of sediment may also have occurred. Features include slumping and sliding in the Pleistocene section; creep along upper slope, especially west of 70°00'W. Surcharge of sediment of glacial provenance on high pore-pressure sediment may have accelerated failure during one or two major late Pleistocene episodes of deformation.	Prolonged or intermittent subsidence of rise operative since Late Cretaceous time, possibly still active and strata being stressed by slope steepening. May involve many small, local, surficial slides; involves decollements, listric faults in deep, ancient rocks. Transverse fractures may control downslope incision including certain troughlike canyons.	Diagenetic gas generation and accessory effect of pore-water generation and freshening(?) could lead to weakening and failure of saturated sediment, especially if confining stress were released by fracturing; diagenetic gas generation may be diminishing but petrogenic gas infusion may occur. Features include diapiric deformation, internal collapse, major slides.

the middle and lower slope. A major period of mass movement and erosion, both of which formed the present slope terrain, followed deposition. Outwash of Wisconsinan age formed the present shelf surface, and a coeval veneer of ice-dropped sediment draped the slope and upper rise.

There remain some important questions about slope stability raised but not readily answered by the seismic-profile analysis:

1. Is the size or extent of mass movement proportional to magnitude of process? There may exist a population of small slides, perhaps related to creep, generated by progressive slope steepening, that could be forming at the present time or at intervals that are significantly short with respect to potential offshore oil-field development. The 3.5-kHz records show surficial mass movement at the limits of acoustic resolution, so the possibility that there exists a population of small, active slides amongst a field of huge, ancient relicts must be considered. Small slides can be important; vertical movements as small as 3 m in relief would drastically affect bottom-mounted structures and pipelines (Coleman and others, 1974). The presence of deep incompetent layers raises the possibility that very large blocks may be slowly settling in response to deep plastic deformation. If internal deformation proceeds in a Newtonian fashion, it may signal a serious potential hazard.

2. What spatial relations exist among mass-movement features? How laterally extensive are slides and is headward propagation common? Without answers to these questions, we cannot adequately outline zones of potentially unstable slope around the mass-movement features identified in this survey.

3. What is the relationship of erosion to mass wasting? Large parts of the slope, especially the flanks of the submarine canyons, are morphologically undecipherable because terrain features are masked by hyperbolic echoes. This rough terrain is generally attributed to erosion, but significant mass-movement features and shallow structure may be present. There is no doubt that some of the canyons are loci for mass movement, simply because they offer unsupported slopes. But the fundamental relationship of canyon genesis to mass-movement processes is essentially unknown.

REFERENCES CITED

Aaron, J. M., Butman, B., Bothner, M. H., and Sylwester, R. E., 1980, Environmental conditions relating to potential geologic hazards, U.S. Northeastern Atlantic Continental Margin: U.S. Geological Survey Miscellaneous Field Studies Map MF-1193, 3 sheets.

Almagor, G., and Wiseman, G., 1978, Analysis of submarine slumping in the Continental Slope off the southern coast of Israel: Marine Geotechnology, v. 2, p. 349-388.

Andresen, A., and Bjerrum, L., 1967, Slides in subaqueous slopes in loose sand and silt, in Richards, A. F., ed., Marine geotechnique: Urbana, Illinois, University of of Illinois Press, p. 221-239.

Bailey, N. G., and Aaron, J. M., 1982a, High-resolution seismic-reflection profiles from the R/V COLUMBUS ISELIN, cruise CI7-78-2, over the Continental Shelf and Slope in the Georges Bank area: U.S. Geological Survey Open-File Report 82-607.

_____1982b, High-resolution seismic-reflection profiles collected aboard R/V JAMES M. GILLISS, cruise GS-7903-3, over the Atlantic Continental Slope and Rise off New England: U.S. Geological Survey Open-File Report 82-718, 2 p.

Baldry, R. A., 1938, Slip-planes and breccia zones in the Tertiary rocks of Peru: Quarterly Journal of Geological Society, v. 94, pt. 3, p. 347-358.

Bennett, R. H., Lambert, D. N., and Hulbert, M. H., 1977, Geotechnical properties of a submarine slide area on the U.S. Continental Slope northeast of Wilmington Canyon: Marine Geotechnology, v. 2, p. 245-261.

Benson, W. E., Sheridan, R. E., and others, 1978, Initial reports of the Deep Sea Drilling Project, v. 44: Washington, U.S. Government Printing Office; Chpt. 3, p. 23-68.

Billings, M. P., 1960, Structural geology, 2nd ed.: Englewood Cliffs, N. J., Prentice-Hall, 514 p.

Bjerrum, L., 1954, Geotechnical properties of Norwegian marine clays: Geotechnique, v. 5, p. 101-119.

Bothner, M. H., and Spiker, E. C., 1980, Upper Wisconsinan till recovered on the Continental Shelf southeast of New England: Science, v. 210, p. 423-425.

Bothner, M. H., Spiker, E. C., Ferrebee, W. M., and Peeler, D. L., 1980, Texture clay mineralogy, trace metals, and age of cored sediments, in Aaron, J. M., ed., Environmental geologic studies in the Georges Bank area, United States northeastern Atlantic Outer Continental Shelf, 1975-1977: U.S. Geological Survey Open-File Report 80-240, chapter 3, p. 3-1 to 3-25.

Brown, C. B., 1938, On a theory of gravitational sliding applied to the Tertiary of Ancon, Ecuador: Quarterly Journal of Geological Society, v. 94, pt. 3, p. 359-368.

Bruce, C. H., 1973, Pressured shale and related sediment deformation: mechanism for development of regional contemporaneous faults: American Association of Petroleum Geologists Bulletin, v. 57, no. 5, p. 878-886.

Bryant, W. R., 1981, Gas charged sediments, in High resolution seismic profiling and sidescan sonar; short course notes: Corpus Christi, Texas, U.S. Geological Survey Office of Marine Geology, p. 139-162.

Cabrera, J. G., and Smalley, I. J., 1973, Quick clays as products of glacial action, a new approach to their nature, geology, distribution and geotechnical properties: Engineering Geology, v. 7, p. 115-134.

Carson, M. A., and Kirkby, M. J., 1972, Hillslope form and process: London, Cambridge University Press, p. 475.

Claypool, G. E., Kaplan, I. R., and Presley, B. J., 1973, Generation of light hydrocarbon gases in deep sea sediments (abs.): American Association of Petroleum Geologists Bulletin, v. 57, no. 4, p. 773.

Coffeen, J. A., 1978, Seismic exploration fundamentals; the use of seismic techniques in finding oil: Tulsa, OK, PPC Books, 277 p.

Coleman, J. M., and Garrison, L. E., 1977, Geological aspects of marine slope stability, northwestern Gulf of Mexico, in Richards, A. F., ed., Marine geotechnology: New York, Crane, Russak and Co., v. 2, p. 9-45.

Coleman, J. M., Suhayda, J. N., Whelan, T., and Wright, L. D., 1974, Mass movement of Mississippi River delta sediments: Transactions, Gulf Coast Association of Geological Societies, v. XXIV, p. 49-68.

Curray, J. R., 1965, Late Quaternary history, Continental shelves of the United States, in Wright, H. E., Jr., and Frey, D. G., eds., The Quaternary of the United States: Princeton, N. J., Princeton University Press, p. 723-735.

Dillon, W. P., and Zimmerman, H. B., 1970, Erosion by biological activity in two New England submarine canyons: Journal of Sedimentary Petrology, v. 40, no. 2, p. 542-547.

Doyle, L. J., Pilkey, O. H., and Woo, C. C., 1979, Sedimentation on the Eastern United States Continental Slope: Society of Economic Paleontologists and Mineralogists, Special Publication no. 27, p. 119-129.

Dott, R. H., Jr., 1963, Dynamics of subaqueous gravity depositional processes: American Association of Petroleum Geologists Bulletin, v. 47, no. 1, p. 104-128.

Embleton, C., and Thornes, J., 1979, Process in geomorphology: New York, John Wiley, p. 436.

Embley, R. W., 1976, New evidence for occurrence of debris flow deposits in the deep sea: Geology, v. 4, p. 371-374.

_____1980, The role of mass transport in the distribution and character of deep-ocean sediments with special reference to the North Atlantic: Marine Geology, v. 38, p. 23-50.

Embley, R. W., and Jacobi, R. D., 1977, Distribution and morphology of large submarine sediment slides and slumps on Atlantic Continental margins: Marine Geotechnology, v. 2, p. 205-228.

Emery, K. O., Uchupi, E., Phillips, J. D., Bowin, C. O., Bunce, E. T., and Knott, S. T., 1970, Continental rise off Eastern North America: American Association of Petroleum Geologists Bulletin, v. 54, no. 1, p. 44-108.

Emery, K. O., and Uchupi, E., 1972, Western North Atlantic Ocean - topography, rocks, structure, water, life, and sediments: American Association of Petroleum Geologists Memoir 17, p. 532.

Esrig, M. I., and Kirby, R. C., 1977, Implications of gas content for predicting the stability of submarine slopes, in Richards, A. F., ed., Marine geotechnology: New York, Crane, Russak and Co., v. 2, p. 81-100.

Fairbridge, R. W., 1946, Submarine slumping and location of oil bodies: American Association of Petroleum Geologists Bulletin, v. 30, no. 1, p. 94-92.

Feininger, T., 1971, Chemical weathering and glacial erosion of crystalline rocks and the origin of till: U.S. Geological Survey Professional Paper 750-C, p. C65-C81.

Gable, D. J., and Hatton, T., 1983, Maps of vertical crustal movements in the conterminous United States over the last 10 million years: U.S. Geological Survey Investigations Map I-1315, 2 maps, bibliography.

Gardner, G. H. F., Gardner, L. W., and Gregory, A. R., 1974, Formation velocity and density - the diagnostic basics of stratigraphic traps: Geophysics, v. 39, p. 770-780.

Garrison, L. E., 1970, Development of Continental Shelf south of New England: American Association Petroleum Geologists Bulletin v. 54, no. 1, p. 109-124.

Gibson, T. G., 1965, Eocene and Miocene rocks off the northeastern coast of the United States: Deep-Sea Research, v. 12, p. 975-981.

Gibson, T. G., Hazel, J. E., and Mello, J. F., 1968, Fossiliferous rocks from submarine canyons off the northeastern United States: U.S. Geological Survey Professional Paper 600-D, p. D222-D230.

Gregory, A. R., 1977, Aspects of rock physics from laboratory and log data that are important to seismic interpretation, in Payton C. E., ed., Seismic stratigraphy - applications to hydrocarbon exploration: American Association of Petroleum Geologists Memoir 26, p. 15-46.

Hathaway, J. C., Poag, C. W., Valentine, P. C., Miller, R. E., Schultz, D. M., Manheim, F. T., Kohout, F. A., Bothner, M. H., and Sangrey, D. A., 1979, U.S. Geological Survey core drilling on the Atlantic Shelf: Science, v. 206, no. 4418, p. 515-527.

Hathaway, J. C., Schlee, J. S., Poag, C. W., Valentine, P. C., Weed, E. G. A., Bothner, M. H., Kohout, F. A., Manheim, F. T., Schoen, R., Miller, R. E., and Schultz, D. M., 1976, Preliminary summary of the 1976 Atlantic margin coring project of the U.S. Geological Survey: U.S. Geological Survey Open-File Report 76-844, 218 p.

Hedberg, H. D., 1974, Relation of methane generation to undercompacted shales, shale diapirs, and mud volcanoes: American Association of Petroleum Geologists Bulletin v. 58, no. 4, p. 661-673.

Hess, R., and Harrison, W. E., 1981, Gas hydrates (clathrates) causing pore-water freshening and oxygen isotope fractionation in deep water sedimentary sections of terrigenous continental margins: Earth and Planetary Science Letters, v. 55, p. 453-462.

Heezen, B. C., and Drake, C. L., 1964, Grand Banks slump: American Association of Petroleum Geologists Bulletin, v. 48, p. 221-225.

Hollingworth, S. E., Taylor, J. H., and Kellaway, G. A., 1944, Large-scale superficial structures in the Northampton Ironstone Field: Quarterly Journal, Geological Society of London, v. C, p. 1-44.

Hollister, C. E., Ewing, J. I., and others, 1972, Initial Reports of the Deep Sea Drilling Project, vol. XI: Washington, D.C., U.S. Government Printing Office, Chpt. 6, p. 219-312; Chpt. 7, p. 313-350; Chpt. 8, p. 351-356.

Hoskins, H., 1967, Seismic reflection observations on the Atlantic Continental shelf, slope, and rise southeast of New England: Journal of Geology, v. 75, no. 5, p. 598-611.

Howard, J. D., and Lohrengel, C. F., II, 1969, Large non-tectonic deformational structures from upper Cretaceous rocks of Utah: Journal of Sedimentary Petrology, v. 39, no. 3, p. 1032-1039.

Jacobi, R. D., 1976, Sediment slides on the northwestern continental margin of Africa: Marine Geology, v. 22, p. 157-173.

Jerbo, A., 1967, Geochemical and strength aspects of Bothnian clay sediments, in Richards, A. F., ed., Marine geotechnique: Urbana, Ill., University of Illinois Press, p. 177-186.

Judson, S., 1947, Large-scale superficial structures - a discussion: Journal of Geology, v. LV, p. 168-175.

Kelling, G., and Stanley, D. J., 1970, Morphology and structure of Wilmington and Baltimore submarine canyons, eastern United States: Journal of Geology, v. 78, p. 637-660.

_____1976, Sedimentation in canyon, slope, and base-of-slope environments, in Stanley, D. J., and Swift, D. J. P., eds., Marine sediment transport and environmental management: New York, John Wiley, chpt. 17, p. 379-435.

Keller, G. H., Lambert, D. N., and Bennett, R. H., 1979, Geotechnical properties of Continental Slope deposits-Cape Hatteras to Hydrographer Canyon, in Doyle, L. J., and Pilkey, O. H., eds., Geology of continental slopes: Society of Economic Paleontologists and Mineralogists Special Publication no. 27, p. 131-151.

Knebel, H. J., and Carson, R., 1979, Small-scale slump deposits, Middle Atlantic Continental Slope, off eastern United States: Marine Geology, v. 29, p. 221-236.

Knott, S. T., and Hoskins, H., 1968, Evidence of Pleistocene events in the structure of the Continental Shelf off the northeastern United States: Marine Geology, v. 6, p. 5-43.

Krause, D. C., 1962, Interpretation of echosounding profiles: International Hydrographic Review, v. 39, p. 65-123.

Lancelot, Y., and Ewing, J. L., 1972, Correlation of natural gas zonation and carbonate diagenesis in Tertiary sediments from the North West Atlantic, in Hollister, C. D., Ewing, J. L., and others, Initial reports of the Deep Sea Drilling Project: Washington, U.S. Government Printing Office, v. XI, Chpt. 27, p. 791-800.

Laury, R. L., 1971, Stream bank failure and rotational slumping: Preservation and significance in the geologic record: Geological Society of America Bulletin, v. 82, p. 1251-1266.

Lewis, R. S., Sylwester, R. E., Aaron, J. M., Twichell, D. C., and Scanlon, K. M., 1980, Shallow sedimentary framework and related potential geologic hazards of the Georges Bank area, in Aaron, J. M., ed., Environmental geologic studies in the Georges Bank area, United States northeastern Atlantic Outer Continental Shelf, 1975-1977: U.S. Geological Survey Open-File Report 80-240, chapt. 5, p. 5-1 to 5-25.

MacIlvaine, J. C., 1973, Sedimentary processes on the Continental Slope off New England: MIT-WHOI, Woods Hole, MA, Ph.D. dissertation, 211 p.

MacIlvaine, J. C., and Ross, D. A., 1979, Sedimentary processes on the continental slope of New England: Journal of Sedimentary Petrology, v. 49, no. 2, p. 563-574.

Manheim, F. T., and Hall, R. E., 1976, Deep evaporitic strata off New York and New Jersey - evidence from interstitial water chemistry of drill cores: U.S. Geological Survey Journal of Research, v. 4, no. 6, p. 697-702.

McGregor, B. A., 1977, Geophysical assessment of submarine slide northeast of Wilmington Canyon: Marine Geotechnology, v. 2, p. 229-244.

McGregor, B. A., and Bennett, R. H., 1977, Continental Slope sediment instability northeast of Wilmington Canyon: American Association of Petroleum Geologists Bulletin, v. 61, no. 6, p. 918-928.

_____1979, Mass movement of sediment on the Continental Slope and rise seaward of the Baltimore Canyon trough: Marine Geology, v. 33, p. 163-174.

McIver, N. L., 1972, Cenozoic and Mesozoic stratigraphy of the Nova Scotia shelf: Canadian Journal of Earth Science, v. 9, no. 1, p. 54-70.

Middleton, G. V., and Hampton, M. A., 1976, Subaqueous sediment transport deposition by sediment gravity flows, in Stanley, D. J., and Swift, D. J. P., eds., Marine sediment transport and environmental management: New York, John Wiley, p. 197-218.

Mitchum, R. M., Jr., Vail, P. R., and Sangree, J. B., 1977, Stratigraphic interpretation of seismic reflection patterns in depositional sequences, in Payton, C. E., ed., Seismic stratigraphy-applications to hydrocarbon exploration: American Association of Petroleum Geologists Memoir, v. 26, p. 117-133.

Monroe, J. M., 1969, Slumping structures caused by organically derived gases in sediments: Science, v. 164, p. 1394-1395.

Moore, D. G., 1961, Submarine slumps: Journal of Sedimentary Petrology, v. 31, no. 3, p. 343-357.

_____1978, Submarine slides, in Voight, B., ed., Rockslides and avalanches, 1, Natural phenomena: Amsterdam, Elsevier Press, chapt. 16, p. 564-604.

Moore, D. G., Curray, V. R., and Emmel, F. J., 1976, Large submarine slide (olistostrome) associated with Sunda area subduction zone, northeast Indian Ocean: Marine Geology, v. 21, p. 211-226.

Mountain, G. S., 1981, Stratigraphy of the western North Atlantic based on the study of reflection profiles and DSDP results: New York, N. Y., Columbia University, Ph.D. dissertation, 260 p.

Nardin, T. R., Hein, F. J., Gorsline, D. S., and Edwards, B. D., 1979, A review of mass movement processes, sediment and acoustic characteristcs, and contrasts in slope and base-of-slope systems versus canyon-fan-basin floor systems, in Doyle, L. J., and Pilkey, O. H., eds., Geology of continental slopes: Society of Economic Paleontologists and Mineralogists Special Publication no. 27, p. 61-73.

Neurauter, T. W., 1981, Geophysical fundamentals and instrumentation, in High resolution seismic profiling and sidescan sonar; short course notes: Corpus Christi, Texas, Office of Marine Geology, August 1981, p. 11-33.

Nichols, R. L., 1953, Marine and lacustrine ice-pushed ridges: Journal of Glaciology, v. 2, no. 13, p. 172-175.

Northeastern U.S. Seismic Network, 1979, Bulletin no. 12., Seismicity of the Northeastern United States: Boston, Weston Observatory, Boston College, 5 p.

_____1981, Bulletin no. 20, Seismicity of the Northeastern United States: Boston, Weston Observatory, Boston College, 7 p.

Northrop, J., and Heezen, B. C., 1951, An outcrop of Eocene sediment on the Continental slope: Journal of Geology, v. 59, p. 396-399.

Offield, T. W., 1975, Line-grating diffraction in image analysis; enhanced detection of linear structure, Colorado Front Range: Modern Geology, v. 5, p. 101-107.

Poag, C. W., 1982, Foraminiferal and seismic stratigraphy, paleoenvironments and depositional cycles in the Georges Bank basin, in Scholle, P. A., and Wenkam, C. R., eds., Geological studies of the COST Nos. G-1 and G-2 wells, United States North Atlantic Outer Continental Shelf: U.S. Geological Survey Circular 861, p. 43-91.

Pohn, H. A., 1971, Analysis of images and photographs by a Ronchi grating, Part 1, Remote sensor application studies progress report, 1968-1969: National Technical Information Service, PB197 101, 9 p.

Poppe, L. J., 1981, Data file Atlantic Margin Coring Project (AMCOR) of the U.S. Geological Survey: U.S. Geological Survey Open-File Report 81-239, 96 p.

Quinlan, G., and Beaumont, C., 1981, A comparison of observed and theoretical postglacial relative sea level in Atlantic Canada: Canada Journal of Earth Sciences, v. 18, p. 1146-1163.

Randall, R. G., 1981, Seismic stratigraphy in marine engineering geology, in High resolution seismic profiling and sidescan sonar; short course notes: Corpus Christi, Texas, U.S. Geological Survey Office of Marine Geology, p. 117-138.

Reading, H. G., ed., 1978, Sedimentary environments and facies: New York, Elsevier, 569 p.

Renz, O., Lakeman, R., and Van der Meulen, E., 1955, Submarine sliding in western Venezuela: American Association of Petroleum Geologists Bulletin, v. 39, no. 10, p. 2053-2067.

Roberson, M. I., 1964, Continuous seismic profiler survey of Oceanographer, Gilbert and Lydonia submarine canyons, Georges Bank: Journal of Geophysical Research, v. 69, no. 22, p. 4779-4789.

Roden, R., 1981, Interpretation of apparent geological features, in High resolution seismic profiling and sidescan sonar; short course notes: Corpus Christi, Texas, U.S. Geological Survey Office of Marine Geology, p. 97-116.

Ryan, W. B. F., Cita, M. B., Miller, E. L., Hanselman, D., Nestroff, W. D., Hecker, B., and Nibblelink, M., 1978, Bedrock geology in New England submarine canyons: Oceanologica Acta, v. 1, no. 2, p. 233-254.

Sangree, J. B., and Widmier, U. M., 1977, Seismic interpretation of clastic depositional facies, in Payton, C. E., ed., Seismic stratigraphy-applications to hydrocarbon exploration: American Association of Petroleum Geologists Memoir 26, p. 165-184.

Sangrey, D. A., 1977, Marine geotechnology - state of the art, in Richards, A. F., ed., Marine geotechnology: New York, Crane, Russak and Co., v. 2, p. 45-80.

Scanlon, K. M., 1982, GLORIA sidescan and seismic data collected by the DESV STARELLA along the Continental Slope and upper Continental Rise of the eastern United States: U.S. Geological Survey Open-File Report 82-1095, 3 p.

Shepard, F. P., 1933, Depth changes in Sagami Bay during the great Japanese earthquake: Journal of Geology, v. 41, p. 527-536.

Sheriff, R. E., 1977, Limitations on resolution of seismic reflections and geologic detail derivable from them, in Payton, C. E., ed., Seismic stratigraphy-applications to hydrocarbon exploration: American Association of Petroleum Geologists Memoir 26, p. 3-14.

_____1978, A first course in geophysical exploration and interpretation: International Human Development Corp., Boston, Mass., 313 p.

Slater, R. A., 1982, Submersible observations of the sea floor near the proposed Georges Bank lease sites along the North Atlantic outer Continental Shelf and upper Slope: U.S. Geological Survey Open-File Report 81-742, 65 p.

Stetson, H. C., 1936, Geology and paleontology of the Georges Bank Canyons, 1, Geology: Geological Society of America Bulletin, v. 47, p. 339-366.

_____1949, The sediments and stratigraphy of east coast continental margin - Georges Bank to Norfolk Canyon: Massachusetts Institute of Technology and Woods Hole Oceanographic Institution Papers in Physical Oceanography and Meterology, v. 11, no. 2, p. 1-60.

Stuart, C. J., and Caughey, C. A., 1977, Seismic facies and sedimentology of terrigenous Pleistocene deposits in northwest and central Gulf of Mexico, in Payton, C. E., ed., Seismic stratigraphy-applications to hydrocarbon exploration: American Association of Petroleum Geologists Memoir 26, p. 249-176.

Summerhayes, C. P., Bornhold, B. D., and Embley, R. W., 1979, Surficial slides and slumps on the Continental Slope and rise of southwest Africa: a reconnaissance study: Marine Geology, v. 31, p. 265-277.

Terzaghi, K., 1956, Varieties of submarine slope failures: Proceedings, eight Texas conference on Soil Mechanics and Foundation Engineering, University of Texas Bureau of Engineering Research, Austin, Texas, 41 p.

Terzaghi, K., and Peck, R. B., 1948, Soil mechanics in engineering practice: New York, Wiley and Sons, 566 p.

Trumbull, J. V. A., and Hathaway, J. C., 1968, Further exploration of Oceanographer Canyon: Woods Hole Oceanographic Institution, Summary of Investigations no. 68-32, p. 57.

Twichell, D. C. 1981, Bed-form distribution and inferred sand transport on Georges Bank, United States Continental Shelf: U.S. Geological Survey Open-File Report 81-764, 35 p.

Uchupi, E., 1967, Slumping on the Continental margin southeast of Long Island, New York: Deep-Sea Research, v. 14, p. 635-639.

_____1968, Atlantic Continental Shelf and Slope of the United States - physiography: U.S. Geological Survey Professional Paper 529-C, 30 p.

Uchupi, E., Ballard, R. D., and Ellis, J. P., 1977, Continental Slope and upper rise off western Nova Scotia and Georges Bank: American Association of Petroleum Geologists Bulletin, v. 61, no. 9, p. 1483-1492.

Vail, P. R., Todd, R. G., and Sangree, J. B., 1977, Chronostratigraphic significance of seismic reflections, in Payton, C. E., ed., Seismic stratigraphy-applications to hydrocarbon exploration: American Association of Petroleum Geologists Memoir 26, p. 99-116.

Valentine, P. C., Uzmann, J. R., and Cooper, R. A., 1980, Geology and biology of Oceanographer Submarine Canyon: Marine Geology, v. 38, p. 282-312.

Van Loon, A. J., and Wiggers, A. J., 1976, Metasedimentary "graben" and associated structures in the lagoonal Almere Member (Groningen Formation, the Netherlands): Sedimentary Geology, v. 16, p. 237-254.

Varnes, D. J., 1978, Slope movement types and processes, in Schuster, R. L., and Krizek, R. J., eds., Landslides analysis and control: Washington, D.C., Transportation Research Board Special Report 176, National Academy of Science, p. 11-33.

Whelan T., III, Coleman, J. M., Suhayda, J. N., and Roberts, H. H., 1977, Acoustical penetration and shear strength in gas-charged sediment, in Richards, A. F., ed., Marine geotechnology: New York, Crane, Russak and Co., p. 147-160.

Whelan, T., III, Ishmael, J. T., and Rainey, G. B., 1978, Gas-sediment interactions in Mississippi delta sediments: Proceedings, 10th Offshore Technology Conference, Houston, Texas, OTC #3166, p. 1029-1033.

Woodbury, H. O., 1977, Movement of sediment on the Gulf of Mexico, Continental Slope and upper Continental Shelf: Marine Geotechnology, v. 2, p. 263-273.

APPENDIX: SEISMIC DATA AND CHARACTERISTICS

During ISELIN cruise 7-78-2 and GILLISS cruise 7903-3 three kinds of high-resolution seismic-profile were obtained simultaneously, generated by airgun, sparker, and tuned (3.5-kHz) transducer. Airgun data were acquired by means of acoustic energy supplied by a 5-in^3 or 40-in^3 airgun (Pneumatic Acoustic Repeater) fired at four- or six-second intervals. Return signal was filtered generally between 35 and 200 Hz with a band pass width ranging from 30 to 70 Hz (set in response to character of subbottom reflectors). The return signal was recorded on a paper recorder generally at a two-second sweep rate.

The sparker data were acquired with an 800-joule Teledyne minisparker signal source fired at one or two-second intervals, depending on water depth. Return signal was filtered between 200-1,000 Hz. The band pass width generally ranged from 200 to 500 Hz. Filters were set to maximize fine reflector contrast. Return signal was recorded on a paper recorder at a one-half- or a one-second sweep rate depending on bottom relief.

The ORE 3.5-kHz ship-mounted transducer return signal was recorded on a paper recorder at a one-half-second sweep rate.

All profiles were annotated at synchronized 15 or 30 minute intervals. The paper records were subsequently photographically reduced to half-scale reproductions which were examined line by line for this report. The airgun records were overlaid with clear acetate on which the sea floor and principal subbottom reflectors were traced. Time marks were also traced as these allow the profiles to be keyed to the trackline charts and the 1:250,000 NOS bathymetric maps used for regional correlation.

The airgun records with their deep penetration and relatively coarse resolution provide the physiographic and stratigraphic context for analysis of various features identified in the other records. The airgun records also provide the physiographic control for regional geomorphic characterization. The sparker records have suitable resolution to provide for identification and analysis of forms and structures indicative of potential geological hazards. The 3.5-kHz records are very useful for observing detailed morphology and surficial stratigraphy critical to the estimation of potential geological hazards, particularly where these phenomena are obscured in the sparker records.

The following discussion is provided so that the reader can more fully understand and appreciate the difficulties of interpreting structures and stratigraphy from seismic-reflection records. The profile data are obscured and complicated by a variety of phenomena of which geological features are only a part. The validity of seismic interpretation is strongly constrained by these phenomena. Among the variables that shape a profile are velocities of sound in different media, signal frequency (including filtering), signal source/receiver configuration, configuration of reflecting surfaces, layer discontinuities, and local and transitory field conditions. Of these variables we are most interested in contributions from the configuration of reflecting surfaces and from subsurface layer discontinuities. It must be fully appreciated that the geologic interpretation of seismic profiles depends entirely on the way sound waves behave as they travel through or reflect off

geologic materials. We can narrow the uncertainties of interpretation appreciably by first considering those acoustic variables over which we have some control or which are distinctly nongeologic contributions.

The fact that the velocity of sound varies with the density of the material through which it passes gives rise to interesting distortions in the seismic records. The most important velocity distortion is shown in the apparent conformity of subsurface reflectors to the contours of the ocean bottom; not only do the subsurface strata look folded but the ocean bottom conforms to the apparent fold surfaces. This effect comes about because the seismic profiler records events vertically according to the times successive reflected signals are detected from below the recorder. Thus, the faster the return signal passes through the combined water-sediment transmission column (i.e., the shallower the water), the sooner it is recorded and the higher up the reflecting layers seem to be in the column. And because sediment density increases with depth, so does acoustic velocity. The result is that the record also shows greater apparent vertical compression with depth than is actually present. These phenomenan become more pronounced as survey speed is increased because vertical exaggeration is increased.

It is important, then, to have at least a "rule of thumb" estimate of the depths of sediment layers beneath the sea floor, as depicted in seismic profiles. Depths can be estimated directly from seismic profiles if the velocities of sound through the sediment are known. In the area of the survey, AMCOR logs (Hathaway and others, 1979) show that to depths of approximately 300 m sediment consists of compact fine sand and silty clay. According to Gregory (1977), shale at 61 m subbottom depth has an acoustic propagation velocity of 1,524 m/s; at 305 m depth the velocity is 1,890 m/s. Within this depth range sand has an appreciably higher propagation velocity than shale (Gardner and others, 1974). Therefore, on the basis of the AMCOR logs, we can assume that in the survey area - at least on the shelf and upper slope - velocities range from 1,600 m/s to 1,900 m/s in the upper 300 m interval.

In an earlier survey of the Lydonia-Oceanographer Canyons area, Roberson (1964) used a geometric technique to calculate interval velocities. At 300-m subbottom depth he obtained an average velocity of about 1,900 m/s. His lowest calculated velocity was 1,700 m/s at about 150-m subbottom depth. Below about 300 m Roberson's calculated velocities are notably higher than those we estimate on the basis of well log data. The highest velocity Roberson (1964) obtained is 2,500 m/s at about 350-m subbottom depth.

Probably the most important variable governing the appearance of a seismic record is signal frequency. The relationship of velocity and frequency determines depth of signal penetration and vertical and spatial resolution of the signal. Effective resolution is generally considered to be about 1/4 wavelength (λ) at the fundamental signal frequency. Wavelength (λ) is related to frequency (f) and velocity (v) according to:

$$\lambda = v/f \qquad (1)$$

The 40-in^3 airgun has a fundamental frequency of about 20 Hz. Using the previously estimated acoustic velocities in the frequency-velocity relation, and calculating for 1/4 λ, the resolutions obtainable with the 40-in^3 airgun are:

at the sea floor: 20 m
at 300 m subbottom: 23.75 m
at 1,000 m subbottom: 28.75 m

Hence, the 40-in^3 airgun signal, at its maximum penetrating frequency, is capable of resolving units ranging from 20 to 30 m thick. Note that resolution decreases with depth. The 20-in^3 airgun, with a fundamental frequency of about 40 Hz, offers twice the resolution of the 40-in^3 gun. In general, the airgun system offers relatively low resolution and deep penetration - a bit more than 1/2 s (or 1,000 m, assuming an average propagation velocity of 1,950 m/s).

The sparker, with a fundamental frequency of about 1 kHz, has a resolution potential less than that of the 3.5-kHz echo sounder. In practice it is filtered back (generally below 500 Hz) so that reflectors on the order of 2.5-3 m apart are recorded. This is because the sparker has a penetration of about 1/4 s (250 m); a record depicting a 250-m interval with reflectors closer than 3 m apart would be too dense to interpret easily.

The 3.5-kHz echo sounder has a short pulse at nearly a single frequency. Because of this, resolution is approximated by the product of pulse length x propagation velocity (Neurauter, 1981) or, 0.0005 s x 1,600 m/s = 0.8 m. Penetration is within the top 80 m of sediment, depending on character of the sea floor and near-subsurface sediment.

The vertical resolving power of the seismic systems is realized only where a stratigraphic interval provides surfaces spaced an appropriate distance apart and which bound layers of sufficient acoustic impedance contrast to reflect the signals. During seismic profiling a number of inevitable acoustic phenomena occur which tend to degrade the vertical resolution. In water the outgoing signal is objectionably prolonged due to oscillating bubbles generated by the initial acoustic pulse. This problem is greatest with the airgun (signal pulse length is at least 20 ms), least with the 3.5-kHz transducer (0.5 ms). The problem comes about because during the time that near-subbottom reflectors are being recorded, stronger sea-floor reflections are also being recorded from signals sent out by the oscillating bubbles generated by the main pulse. Twenty milliseconds worth of signal return at 1,500 m/s results in a stack of repeated bottom reflections over a vertical interval equivalent to 30 m of subbottom record. By the time the last bubble-pulse return has been received reflections from 30 m down in the section are being simultaneously recorded. Furthermore, the bubble-pulse pattern is regenerated at every prominent subbottom reflector, but to decreasing degrees as pulse energy is attenuated with depth. Whenever possible, then, we use the 3.5-kHz record to investigate the profile interval wiped out by bubble pulse in the records of the other systems.

The sea-floor-reflected signal is not only received by the seismic recorder, it is echoed back to the bottom from the water-air interface with enough strength to be re-reflected and re-recorded at later times as "multiples". The delay in reception of the echoed bottom signal means that it is recorded simultaneously with later (deeper) subbottom reflectors. And below the first multiple are re-recorded the more prominent subbottom reflectors that were echoed back after the initial sea-floor return signal. Thus, below the first multiple the record tends to be confused and it is not

always easy to trace primary reflectors, particularly in recordings made in shallow water.

Depending on frequency, the acoustic signal may cause certain reflecting units to resonate, a phenomenon called "ringing". A resonating layer propagates a diminishing succession of pulses recorded as faint parallel reflectors that tend to blur the primary reflector. Another phenomenon that tends to degrade vertical resolution is "ghosting": Not only does the acoustic signal propagate downward from the source, it propagates upward and is reflected from the water-air interface as a slightly delayed, slightly weaker, slightly noisier secondary signal which generates its own reflections which appear on the record as a faint "ghost" of the primary pattern. Thus, within limits, the deeper the signal source, the more out of focus the seismic record.

As with vertical resolution, spatial resolving power of the acoustic signal is a function of constructive interference of the reflected acoustic pulse, which occurs within 1/4 λ. This takes place within an area of beam impingement called the fresnel zone, the size of which is related to wavelength, velocity, and distance from source to reflector, according to the relation

$$r_f \cong \frac{v}{4}\sqrt{t/f_c}$$

where, r_f = radius of fresnel zone; t = 2-way travel time; v = acoustic velocity; f_c = signal frequency

Thus, the 40-in^3 airgun, operating in 1 second (2-way) water depth (750 m), provides a sea-floor resolution element 168 m in diameter. In 1/2-s water depth the resolution element diameter is 120 m. If, within 1 s, subbottom is penetrated to a depth of about 300 m where we assume a velocity of 1,900 m/s, the spatial resolution element at that depth has a diameter of 208 m. In general, for any given frequency, the higher the propagation velocity the wider the zone of constructive interference, hence the poorer the spatial resolution. At t = 1/2 s the sparker resolves an area of sea floor about 17 m in diameter; for the 3.5-kHz echo sounder the resolution element at t = 1/2 s is about 9 m.

Because the profiler records discrete areas of reflection at each shot, it is clear that the profile-depicted surfaces are moving averages of relatively large repetitive areas (e.g., the center point of each resolution cell is displaced 2.8 m per 1 s shot interval, 10.3 m per 4 s shot interval, assuming a ship speed of 5 kns). Thus, in order to maintain resolution as water depth increases it is neccessary to increase the signal or shot rate.

A consequence of fresnel-zone reflection and overlap is that slopes steeper than 20^o are not recorded, and surface irregularities smaller than the resolution cells are smoothed in the record due to scattering or diffraction, depending on the dimensions of the irregularities. Irregularities with a relief or spacing or lateral dimension on the order of an acoustic wavelength diffract the signal, as do corners and edges; for some distance before and after they are crossed they produce reflections which are recorded as hyperbolic echo traces. Only the vertex of each hyperbola represents the

bottom directly below the source-receiver along the trackline. (The position of the point along a line normal to the trackline is less certain).

The 40-in^3 airgun will generate hyperbolic echoes from features with a lateral dimension of about 75 m or less; the sparker will do the same for features approximately 1.5 m across. For the 3.5-kHz echo sounder, diffraction is generated by irregularities with a lateral dimension or spacing of about 0.45 m. Krause (1962) gives a graph for finding the maximum width of features which would be hidden beneath hyperbolic echoes generated by their peaks. For example, in 1,000 m water on a slope of 6^{o}, a hyperbolic echo can hide a feature approximately 100 m across.

The geometry and distributions of hyperbolic reflections can be complex and our treatment of the data does not include the deciphering of hyperbolic echoes. Suffice it to say that hyperbolic reflections indicate surface complexities beyond the resolving capacity of the acoustic profiling system and that other means of surface discrimination are called for.

Vertical exaggeration and distorted slope angles are characteristic of seismic profiles. The fact that sound propagates in a spherical wave front from a point source and is returned from a reflecting surface in the same fashion means that the detected fresnel zone is centered on a line extending perpendicular from the sea floor to the receiver, which line represents the acoustic ray path, the shortest distance between the nearest reflecting surface and the receiver.

Thus, if the sea floor is horizontal, the point of initial reflection is directly beneath the receiver, but if the sea floor slopes, that point is displaced upslope from the receiver to a point closest to the source. The reflected signal is from a shallower point upslope but it is recorded as though it were directly beneath the ship. Not only does this phenomenon appear to flatten slopes, it tends to compress the record horizontally in the upslope direction. The problem is further complicated in that it is the apparent dip that is distorted. The relationship of true slope to echo trace is given by

$$\sin \theta = \tan \partial$$

where $\tan \theta$ = angle of true slope, $\tan \partial$ = slope of echo trace (Krause, 1962). For slope angles as great as 15^{o} the differences in $\tan \theta$ and $\tan \partial$ are not very great (Krause, 1962). In areas of sloping sea bottom, we can assume that the seismic profile will show the bottom as shallower than it actually is.

Beam dispersion is another result of the spherical propagation of the signal wavefront. Because of this phenomenon, only a relatively small part (defined by the fresnel zone) of the wavefront that hits the sea floor directly beneath the ship is reflected back. The effective signal beam is actually defined by a cone subtending about a 30^{o} angle from the vertical. Beyond the area of effective beam impingement, reflection ordinarily is lost because of signal attenuation and destructive interference. However, this apparently simple geometry can lead to complicated results where the sea floor is uneven enough to provide more than one surface capable of reflecting a single acoustic pulse.

Thus, if the survey line is parallel to a dipping surface the return signal will indicate an essentially flat reflector, but one apparently shallower than is truly the case. But a still deeper slope, say the opposite side of a valley, optimally oriented toward the receiver, will return a later reflection which will thereupon be recorded beneath the first as though it were a deeper stratigraphic horizon. Reflections that originate from surfaces perpendicular to the ray path but at different elevations or slopes than that directly beneath the survey track are called side echos. Side echos that fade in and out of the record or overlap (produced by rough terrain) add considerable confusion to the stratigraphic record depicted in seismic profiles.

Vertical exaggeration is primarily a function of ship speed, though recording speed and sweep rate are also factors. Because ship speed is so much slower than acoustic wave velocity, any given vertical interval on the chart represents much less distance than a like horizontal interval. An interval of chart representing 500 m horizontally is a tiny fraction of the interval which represents 500 m vertically, hence the vertical exaggeration. Unless recorder speed is accelerated, increased ship speed results in increased horizontal compression because more shot data are crowded into a fixed horizontal interval. And because ship speed is ordinarily poorly regulated with respect to recorder speed, vertical exaggeration varies to a greater or lesser extent from place to place during a survey. Also, vertical exaggeration decreases with subbottom depth because propagation velocity increases. It is apparent that any quantitative geomorphic analysis of seismic data requires that slopes be reconfigured on a spatially accurate base map, and that bottom surface positions be adjusted or "migrated" to their true configuration.

The ISELIN 2-second airgun records generally have a vertical exaggeration of about 11:1; the GILLISS 2-second airgun records have a vertical exaggeration of as much as 20:1. This is because the GILLISS logged a slightly higher average survey speed, nearly 6 kns, than did the ISELIN which logged about 5 kns. The GILLISS 3.5-kHz echo sounder records have a vertical exaggeration of about 20:1. ISELIN sparker records have a vertical exaggeration of about 22:1; GILLISS sparker records range in vertical exaggeration from 19:1 to 23:1. Unless the point is geologically significant, all records discussed in this report are assumed to have vertical exaggerations of 20:1.

Vertical exaggeration further complicates the impression of a sloping surface. For example, at a vertical exaggeration of 20:1, a 2^{o} slope appears to have declivity of 35^{o}. True apparent dips can be calculated from the records according to the relation

$$\theta = \tan^{-1} (\tan \partial / V.E.)$$

where, θ = angle of true apparent dip
∂ = recorded angle
V.E. = vertical exaggeration

Noise is contributed to the records directly by the systems used to record them. Because the seismic systems were run simultaneously each of the records carries to a greater or lesser extent the acoustic imprint of the

other. The 3.5-kHz frequency is so far removed from the sparker/airgun frequencies that crosstalk is not a problem in the echo-sounder records. A particular problem with crosstalk has to do with the recording of the signal pulse from the complementary system. Since the systems are fired at different intervals the non-keyed signal pulse records tend to march across the profiles. There is little that can be done to alleviate this during a survey except to manually rephase the records as often as possible. More insidious and confusing is the superimposition of the entire sparker record on the airgun record and vice versa.

The records are also marred by late time-delay shifts, changes in filter setting, changes of record paper and recording belts, and mechanical/electrical problems in the system. Periodic down-time due to the necessity to trim sparker electrodes results in sometimes critical sparker record gaps. Rough seas degrade the records by producing incoherent wave noise. Cavitation at relatively low sea states particularly affects the quality of the 3.5-kHz echo-sounder records. These various deficiencies are partly compensated for by scrupulous record annotation.

A final factor in geologic interpretation of seismic records is navigation accuracy. During the ISELIN cruise, navigation was performed from Northstar Loran-C fixes. During the GILLISS cruise, a Teledyne Loran-C receiver and a satellite receiver were used. Positions from satellite fixes averaged about 92 m difference from those received from the Teledyne Loran-C unit; discrepancies of as much as 400 m were recorded under adverse conditions (J. Dodd, USGS, pers. commun.). The ISELIN track positions are much less accurate than the GILLISS track positions and much less precise. Position discrepancies of as much as 1.6 km were obtained with the Northstar receiver. We assume a navigational precision of approximately 1,600 m in the ISELIN data and 400 m in the GILLISS data. Comparison between the two tracks probably involves a precision error of as much as 2 km.

Probably the most important source of geological information recorded in seismic profiles is the acoustic effects of subsurface layer discontinuities. Acoustic reflection occurs within the subsurface at those bedding planes, unconformities, or other geological discontinuities characterized by a high-reflection coefficient. The reflection coefficient (R) is the ratio of the amplitude of the reflected wave to the amplitude of the incident wave of an acoustic signal (Sheriff, 1978); it is a function of the contrast in density times propagation velocity (acoustic impedance) on either side of a contact: the greater the contrast, the stronger the reflection. A reflection is recorded provided (a) the density contrast across the boundary is great enough to ensure a return signal of sufficient amplitude, (b) layer spacing is great enough to prevent destructive interference, (c) signal frequency is sufficient to resolve the layers.

It is important to realize that not all geologically important discontinuities in a section may be recorded, that the conditions for acoustic detection of geologic contacts may be effective in complex ways. In the simplest case, acoustic reflection can occur at the top and/or bottom of a resolvable layer if there is an appropriate reflection coefficient at each surface (Coffeen, 1978). In this case a reflector couplet on the record would then define a stratigraphic unit. However, many reflections are actually the result of constructive interference arising from the geometry and acoustic

impedances of relatively thin layers relative to signal wavelength (Sheriff, 1977). As the acoustic impedances of the layers vary laterally and vertically, the composite reflection will rise or fall in response, or it will vary in definition, fade in and out, or disappear.

In fact, the interaction of acoustic wavefronts and subsurface layer discontinuities results in a variety of ambiguities. It is uncommon that the initial reflection point can be determined on the basis of maximum composite wave amplitude (as indicated by the recorded reflection) because reflected waves have composite shapes. Coffeen (1978) notes that the delay from initial reflection to maximum amplitude construction is about 30 ms. This means that reflecting surfaces within a 50- to 70-m vertical interval (depending on frequency and propagation velocity) may contribute to a single strong echo. Because of the complex interaction of acoustic wavefronts, layer thickness, facies changes, propagation velocities, signal frequency, and wavelength, the true apparent dip in a section may be shallower than is depicted in the seismic record, and the true character of the stratigraphy may be obscured (fig. 115).

In general, reflections are considered to represent chronostratigraphic surfaces rather than facies boundaries (Sheriff, 1977; Vail and others, 1977). Vail and others (1977) state that chronostratigraphic correlations from seismic data are accurate only to ± 1/2 wavelength because of the possible variations in reflection character caused by changes in bed spacing and reflection coefficients. Seismic profiles provide very little geological information such as age, composition, depositional facies, sedimentological features, secondary internal structure; all these must be inferred from reflector patterns which are represented according to their acoustic properties in the record.

In our data there is no question that reflectors in the 3.5-kHz records represent bedding planes. In the sparker records individual reflectors of great lateral extent, uniform linearity, and in high contrast to adjacent intervals are taken to represent bedding planes, but in intervals of abundant, closely stacked, discontinuous, somewhat curvilinear reflectors we assume that facies transitions are an important part of the stratigraphic section. In the airgun records we assume that only the most prominent laterally continuous reflectors represent chronostratigraphic surfaces of regional extent (except, of course, for cross-cutting horizons).

In light of the stratigraphic ambiguities presented in seismic profiles, some discussion of terms is called for. In this report a continuous reflector is an echo trace taken to represent a surface which can be followed laterally for a considerable distance such that a characteristic stratigraphic or structural contour is expressed, or reflectors above or below are seen to vary or terminate. A discontinuous reflector is one that can be traced intermittently along a single horizon, the continuity of which is expressed by the parallelism of higher and lower reflectors. Discontinuity implies variation in reflection coefficient along a horizon, or variations in constructive/destructive interference, possibly due to reflector spacing. A horizon is a line, presumed to represent a bedding plane, defined in the record by a single reflector. A continuous reflector and a horizon are synonymous; segments of a discontinuous reflector fall on a single horizon. All reflections represent horizons, but not all horizons are represented by reflections.

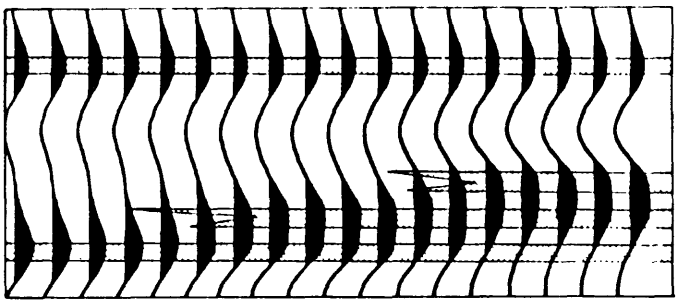

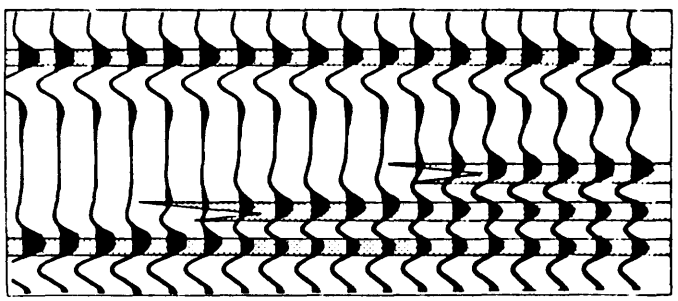

Figure 115. Variations in seismic stratigraphy according to signal frequency; the higher frequency obtains greater resolution (from Vail and others, 1977, fig. 17, p. 115).

Continuous and discontinuous reflectors form seismic units, which are vertical intervals in which reflectors of distinctive character are recorded. The units presumably represent stratigraphic intervals of distinctive contrasting acoustic impedance and may thus include reflections caused by "ringing". Unit refers, then, to a vertical record interval of distinct, laterally traceable acoustic character or pattern such that the top and bottom can each be traced along a horizon for an appreciable distance. A unit may be characterized by a succession of notably parallel reflectors of similar or contrasting character, or by discontinuous reflectors of distinct and similar form.

Reflections are discerned in acoustic backgrounds, the simplest type of which is transparent, in which weak or no reflections are recorded due to nearly uniform acoustic impedance. There is a good deal of published opinion on the geologic meaning of acoustic transparency. Stuart and Caughey (1977) describe a "weak-reflector facies" as characterized by weak or no internal reflectors in an interval bounded by parallel, flat boundaries. Borehole evidence suggests to them that at least some such intervals are caused by massive shale or massive sand units. Mitchum and others (1977) describe "reflection-free areas" as expressions of "homogeneous, non-stratified, highly contorted, or steeply dipping geologic units, for example, thick seismically homogeneous shales or sandstones" (p. 128). Stratigraphic units consisting mostly of soft clay are "acoustically transparent" (Randall, 1981).

An important secondary cause of acoustic transparency is interstitial gas. Dispersed gas bubbles in sediment can cause acoustic effects ranging from "wipeout" (total transparency) to blurring or "hazy" shadowing (Roden, 1981). Gas features show as nonstructural dark patches, isolated "pockets", dispersed throughout an interval, or associated with particular features such as gas-vent zones with sharp, vertical boundaries (Roden, 1981). Dark blurring or "adumbration" is diagnostic in lower frequency records (Bryant, 1981). Here, the gas effect partially obscures what may be a distinctly layered background. Gas-charged sediments on the Continental Slope may show as well-layered intervals over a "chaotic" interval. Bryant (1981) opines that the chaotic interval may represent internally deformed sediment from which dispersed gas has collected in coherent overlying sediment.

Seismic records commonly manifest a kind of fine, nearly homogeneous "test pattern" background, which we here call opaque, consisting of subparallel, irregular reflector segments interleaved on a fine scale. In most sedimentary sections sufficient contrasts in acoustic impedance exist on a bed-to-bed scale that seismic reflections of low amplitude are inevitable. Seismic recorder automatic gain control (AGC) make these low amplitude reflections visible, particularly at high pass filter settings (Vail and others, 1977). Sangree and Widmier (1977), Mitchum and others (1977) attribute such patterns to complex cut and fill intervals or "small, interfingering clinoform lobes". Randall (1981) states that "closely-spaced, prominent reflections arranged in short, discontinuous segments are characteristic of many sandy units" (p. 128).

The opaque background is a record of low-level, pervasive fine-scale reflections, reverberations and, probably acoustic interference patterns. It contains subtle geological information, some of which may be retrieved by analysis of line pattern continuity. This study is conveniently carried out

by use of the Ronchi grating (Offield, 1975). The Ronchi grating is a diffraction grating consisting of fine parallel lines drawn on a sheet of clear plastic. Used in the way described by Offield (1975) or Pohn (1971) it serves as an optical filter, enhancing linear features oriented perpendicular to the grating lines, diffusing all others. Thus, depending on the orientation of the grating with respect to the viewer, lines in the opaque background are made to stand out. In this way horizons are discerned, sets of discordant lines are identified, subtle reflector groups are brought out. The diffraction effect also produces the visual impression of a color contrast of red and green on opposite sides of strongly defined reflectors. This effect facilitates the tracing of continuous reflectors which pass through opaque backgrounds.

Many marine geologists recognize a distinct variety of opaque background characterized by hyperbolic echo traces. The term "chaotic" is used to describe this type, and it is thought to indicate sediment disrupted by mass movement. Mitchum and others (1977) describe "chaotic reflection configuration" as "discontinuous, discordant reflections suggesting a disordered arrangement of reflection surfaces" which they interpret as either "strata deposited in a variable, relatively high-energy setting, or as initially continuous strata which have been deformed so as to disrupt continuity. Penecontemporaneous slump structures, highly faulted, folded, or contorted zones may have chaotic seismic expression" (p. 128). Sangree and Widmier (1977) describe a "chaotic-fill" seismic facies characterized by "mounded external form, by location in topographic lows, and by an internal pattern of contorted and discordant to wavy subparallel reflections" (p. 183). Mass-transport, slump and creep, and high-energy turbidity current processes are thought to be responsible. Contorted internal reflections of chaotic fill units originate from bent and folded beds that have retained some coherence during downslope transport. Diffraction traces originating from these segmented masses are common. Chaotic intervals which represent slide deposits, according to Sangree and Widmier (1977), form irregular zones characterized by broken chaotic reflectors or by no coherent reflectors. The upper boundary of these units is hummocky and the lower contact is commonly flat and sharp. Small diffractions are concentrated along the hummocky upper surface but are common throughout the unit. Interpretation of a mass-transport origin for a chaotic fill unit is strengthened by recognition of up-dip detachment scars and "erosional gouge" below the unit (Sangree and Widmier, 1977). Tight "folds" in strong reflectors of the upper slope may indicate creep or closely spaced slump blocks with small vertical offsets (Stuart and Caughey, 1977).